Adenosine 2A receptor signalling as a key mechanism of stabilization of newly formed GABAergic synapses

Ferran Gomez Castro

Université Pierre et Marie Curie

Ecole doctorale n°158

- Cerveau Cognition Comportement -

Institut du Fer à Moulin, équipe « Plasticité des réseaux corticaux et épilepsie »

La signalisation du récepteur d'adénosine 2A comme mécanisme clé de la stabilisation des synapses GABAergiques nouvellement formées

Adenosine 2A receptor signalling as a key mechanism of stabilization of newly formed GABAergic synapses

Par Ferran Gomez Castro

Thèse de doctorat de Neurosciences

Dirigée par Dr Sabine Lévi

Présentée et soutenue publiquement le 28 setembre 2017

Devant un jury composé de :

Dr Pascal Legendre	Président du jury
Dr Corette Wierenga	Rapporteur
Dr David Blum	Rapporteur
Dr Cécile Charrier	Examinateur
Dr Eric Boué-Grabot	Examinateur
Dr Sabine Lévi	Directeur de thèse

ABSTRACT

In the adult brain, adenosine signaling facilitates or inhibits neurotransmitter vesicular release mainly through activation of type 2A or 1 adenosine receptors ($A_{2A}R$ or A_1R), respectively. However, its role in development remains to be elucidated. During my PhD, I addressed the role of $A_{2A}R$-mediated signalling in GABAergic synaptogenesis in the hippocampus.

We found (i) a larger activity-dependent release of ATP and adenosine during the period of synaptogenesis in the hippocampus, (ii) a peak of expression of the ecto-5'-nucleotidase, the rate-limiting enzyme for the formation of adenosine from extracellular ATP in synapses during this critical period, and (iii) a peak of peri/post-synaptic expression of $A_{2A}R$ concomitant with the period of synaptogenesis. This developmental expression of the key molecules of the adenosine $A_{2A}R$ signalling pathway correlated with a role of $A_{2A}R$ in the stabilization of nascent GABA synapses, a regulation restricted to the period of synaptogenesis. Furthermore, suppressing $A_{2A}R$ with a shRNA approach in isolated neurons led to a loss of synapses equivalent to that seen upon $A_{2A}R$ activity blockade, reporting that the $A_{2A}R$-mediated synapse stabilization is a cell autonomous process that requires $A_{2A}R$ activation in the postsynaptic cell.

ATP/adenosine can be secreted by both glia and neurons; however, we found that activity-dependent release of neuronal adenosine is sufficient to stabilize newly formed GABA synapses *in vitro*. Using live cell imaging, we showed adenosine signalling stabilizes active synapses. We then characterized the molecular mechanism downstream postsynaptic $A_{2A}R$. We report the contribution of adenylyl cyclase/cyclic adenosine monophosphate/protein kinase A signalling cascade and we identified a key target, the postsynaptic scaffolding molecule gephyrin. We further showed the $A_{2A}R$-mediated stabilization of the presynaptic compartment most probably requires the trans-synaptic Slitrk3-PTPδ complex.

Since GABA exerts a similar function during development and GABA and adenosine are co-released at some synapses, I further investigated the interplay between these two pathways. My results support the hypothesis that GABA signalling converge onto the adenosine signalling pathway by potentiating calcium-sensitive adenylyl cyclases through the activation of calmodulin.

Altogether these results let us propose that, during a key developmental period, postsynaptic $A_{2A}Rs$ act as sensors of the activity of GABAergic presynaptic terminals to stabilize active nascent GABAergic synapses. In absence of activity and therefore secretion of adenosine/ATP, synapses will be eliminated.

RESUMÉ

Dans le cerveau adulte, la signalisation liée à l'adénosine facilite ou inhibe la libération vésiculaire de neurotransmetteurs suite à l'activation des récepteurs de l'adénosine de type 2A ou 1 ($A_{2A}R$ ou A_1R), respectivement. Cependant, son rôle dans le développement est mal connu. Au cours de ma thèse, j'ai étudié le rôle de la signalisation adénosine dans la synaptogenèse GABAergiques de l'hippocampe.

Nous avons mis en évidence (i) une sécrétion activité-dépendante accrue d'adénosine et d'ATP pendant la période de synaptogenèse, (ii) un pic d'expression de l'enzyme limitant la formation de l'adénosine à partir de l'ATP extracellulaire, l'ecto-5'-nucleotidase, aux synapses pendant cette période critique, et (iii) un pic d'expression péri/post- synaptique du $A_{2A}R$ concomitant de la période de synaptogenèse. Cette expression développementale des molécules clés de la signalisation adénosine dépendante du $A_{2A}R$ corrélait avec un rôle de ce récepteur dans la stabilisation des synapses GABAergiques naissantes, une régulation restreinte à la période de synaptogenèse. De plus, la suppression de $A_{2A}R$ par une approche shRNA dans des neurones isolés conduisait à une perte de synapses GABAergiques équivalente à celle observée après un blocage pharmacologique de l'activité du $A_{2A}R$, signifiant que la stabilisation synaptique médiée par le $A_{2A}R$ est un processus « cellule autonome » indépendant de l'activité du réseau neuronal et qu'elle requiert l'activation du $A_{2A}R$ dans la cellule post-synaptique.

L'ATP et l'adénosine sont secrétés par la glie et les neurones ; cependant, nous avons montré *in vitro* que la libération neuronale activité-dépendante suffit à stabiliser les synapses GABAergiques naissantes. En utilisant la vidéomicroscopie sur cellules vivantes, nous avons montré que la signalisation adénosine stabilise les synapses actives. Puis, nous avons caractérisé le mécanisme moléculaire sous-jacent. Nous rapportons la contribution de la cascade adénylate cyclase/adénosine monophosphate cyclique/protéine kinase A et nous avons identifié une ciblé clé, la géphrine, la molécule d'ancrage postsynaptique des récepteurs $GABA_A$. Enfin, nous avons mis en évidence que la stabilisation de l'élément présynaptique requiert probablement le complexe trans-synaptique Slitrk3-PTPδ.

Puisque le GABA exerce une fonction similaire au cours du développement et que le GABA et l'adénosine sont co-libérés à certaines synapses, j'ai étudié l'interaction entre ces deux voies de signalisation. Mes résultats favorisent l'hypothèse que la signalisation GABA, en activant la calcium-calmoduline, converge vers la signalisation adénosine en potentiant les adenylates cyclases sensibles au calcium.

Mon travail m'a permis de proposer que, au cours d'une période clé du développement, les A_{2A}Rs postsynaptiques agissent comme des senseurs de l'activité des terminaisons présynaptiques GABAergiques pour stabiliser les synapses actives. En absence d'activité et donc de libération d'adénosine/ATP, les synapses seraient éliminées.

ACKNOWLEDGEMENTS

My first acknowledgments go to the jury who has accepted to review my PhD manuscript and discuss my results during the defence. I hence warmly thank Dr Pascal Legendre, Dr Corette Wierenga, Dr David Blum, Dr Cécile Charrier and Dr Eric Boué-Grabot. A special thanks thereby to Dr Cécile Charrier who accepted also to follow my PhD project during the annual PhD committes.

Mes plus grands remerciements sont pour toi Sabine. Pour le support continu tout au long de ma thèse, pour ta patience et ta motivation. Dans les moments de découragement de ma thèse je me suis toujours senti soutenu et ta vision positive m'a beaucoup aidée. Merci pour ton investissement et toutes les heures passées ensemble : soit en réunion, soit les plus excitantes au microscope et d'autres moins au Metamorph ! J'espère avoir retourné l'effort et l'implication que j'ai toujours senti de ta part dans ce projet. Merci pour toutes les connaissances que tu m'as appris, des présentations orales à la rigueur scientifique en passant pour des expressions en français.

Un grand merci aussi à Jean Christophe pour apporter sa vision de physiologiste sur mon travail. Merci encore pour chacune des leçons d'électrophysiologie dans les réunions d'équipe et pour toujours essayer de nous ouvrir vers vision plus globale de la science.

À tous les membres de l'équipe Marie, Eric, Marion, Jessica, Sana, Clémence, Yo and Marianne. Merci à tous pour les pauses-détente mais aussi pour la passion que vous éprouvez tous dans vos projets tout comme dans la vie. J'espère vous avoir retourné un peu de cette passion et vous avoir appris un peu d'espagnol! Je ne peux pas oublier non plus le temps passé avec les gens qui sont passés par le 1er étage et qui ont aussi marqué ma thèse : Sereina, Manuel, Frank, *Mágico* Salvatore, Kristina et Anna.

Merci aussi pour toutes les autres personnes au sein de l'institut qui ont contribué à la bonne atmosphère de l'IFM. Merci à tous qui ont passé même si c'était un peu de temps avec moi en analysant des images, surtout Richard et Emily. Muchas gracias también a Jimmy, Ana y María por tanto apoyo. A Mariano por las asistencias en la ciencia (¡y en el fútbol!).

Merci encore à mes amis à Paris: Mariangela, Stefania, Pietro, Federica, Giulia, Rodrigo, Pedro, Ángel, Ana Ruiz, Dani (gracias muy fuerte). Et courage pour vos thèses aussi! A la gent de casa, per fer que quan torni tot segueixi igual malgrat la distància.

A mi familia a quién se lo debo todo. A la Marta, pel teu amor incansable.

TABLE OF CONTENTS

Table of contents **1**

Table of figures **4**

Abbreviations **5**

INTRODUCTION **8**

1. The purinergic system **8**

1.1 Overview on purinergic system 8

1.2 Purinergic signalling 9

1.2.1 P2 receptors 9

1.2.2 Adenosine receptors 10

1.2.3 Source and metabolism of ATP and adenosine 13

1.3 Multiple functions of adenosine signalling 16

1.3.1 Physiology: at the cellular level 16

1.3.1.1 Adenosine in neurons 16

1.3.1.2 Adenosine in glia 18

1.3.2 Physiology: at the behavioural level 18

1.3.3 Adenosine in pathology 22

1.4 Impacts of caffeine intake during gestation and lactation in the offspring 24

1.5 Spatiotemporal expression of $A_{2A}R$ 26

1.5.1 Cellular and subcellular expression of $A_{2A}R$ 28

1.5.2 Ontogenic development of $A_{2A}R$ 29

2. Synapse formation **30**

2.1 The inhibitory synapse: an overview 30

2.2 Introduction to synapse formation 35

2.3 Timing of hippocampal synaptogenesis 37

2.4 Synapse formation is a dynamic process 39

2.5 Building a synapse 42

2.5.1 Generation of specificity 42

2.5.1.1 Positive cues 42

2.5.2.2 Inhibitory cues 46

2.5.2.3 Other factors regulating neuronal specificity 46

2.5.2 Recruitment of synaptic elements 46

2.5.2.1 Bidirectional organizers 47

2.5.2.2 Anterograde organizers 49
2.5.2.3 Retrograde organizers 50
2.5.2.4 Glia-secreted organizers 50
2.5.3 Activity-dependent regulation of synaptic contacts 51
2.5.4 Synapse elimination 53
2.5.5 Transcription factors regulating synapse formation 55
2.6 Current knowledge of mechanism of synaptogenesis at the inhibitory synapse 57
2.6.1 Trans-synaptic adhesion proteins 57
2.6.2 Secreted factors 60
2.6.3 Intracellular submembranous scaffold 62
2.6.4 Synapse specificity 64
2.7 Defects in synapse formation: implications in pathology 66
2.7.1 Epilepsy 66
2.7.2 Psychiatric disorders 67
MATERIALS AND METHODS 70
Neuronal culture 70
DNA constructs 70
Neuronal transfection 70
Pharmacology 71
Immunocytochemistry 71
Fluorescence image acquisition and analysis 72
Immunohistochemistry 72
In vivo pentylenetatrazole injection 73
Calcium Imaging 73
cAMP Imaging 74
Statistics 75
RESULTS 78
1. Adenosine A_{2A} receptor: a key sensor of synaptic activity to stabilize/eliminate GABAergic synapses during development 78
Abstract 81
Introduction 82
Results 82
References 87
Figures 89

Materials and methods 95
Supplementary material 106
2. Adenosine A_{2A} receptor and $GABA_A$ receptor signaling pathways converge to stabilize nascent GABAergic synapses 116
Abstract 118
Introduction 118
Material and methods 119
Results 123
Discussion 133
References 136
DISCUSSION 142
1. Spatiotemporal expression and synapse stabilization function of $A_{2A}R$ 143
2. $A_{2A}R$-mediated molecular pathway leading to the stabilization of synapses 148
3. Signalling at the developing inhibitory synapse 153
4. Pathological implications for the $A_{2A}R$-mediated stabilisation of synapse 156
General conclusions 158
ADDITIONAL PUBLICATIONS 162
1. $GABA_A$ receptor dependent synaptic inhibition rapidly tunes KCC2 activity via the Cl^--sensitive WNK1 kinase 162
REFERENCES 214

TABLE OF FIGURES

Figure 1: Notable purines 8
Figure 2: Adenosine receptors can modulate adenylate cyclase activity 10
Figure 3: Extracellular metabolism of ATP and adenosine 15
Figure 4: Different molecular targets of caffeine 19
Figure 5: Roles of adenosine in the brain in physiology and pathology 20
Figure 6: $A_{2A}R$ expression in the postnatal hippocampus. 27
Figure 7: Ontogenic expression of $A_{2A}R$ 29
Figure 8: Structure of $GABA_AR$ 31
Figure 9: Interneurons in CA1 hippocampus 36
Figure 10: Development of GABAergic innervation in hippocampus 38
Figure 11: Synaptic boutons: persistent and non-persistent 40
Figure 12: Inhibitory synapse formation model 41
Figure 13: Subregion-specific expression of the LRR proteins 45
Figure 14: Different nature of synapse organizers 47
Figure 15: Examples of synaptogenic activity by neuroligins and neurexin 48
Figure 16: Schematic representation of the trans-synaptic proteins of the GABAergic synapse and their intracellular interactors 60
Figure 17: Intracellular scaffolds of the inhibitory synapse 64
Figure 18: Inhibitory synapse organizers act on different synapses 64
Figure 19: Acute $A_{2A}R$ blockade does not affect VGLUT1 and PSD95 clustering 145
Figure 20: $A_{2A}R$ is expressed is expressed in the hippocampus, cortex and cerebellum at P16 146
Figure 21: Acute A_1R blockade does not affect VGAT nor GABAARγ2 clustering 147
Figure 22: P2 receptors can modulate PSD95 clustering in young neurons 148
Figure 23: Functional model of adenosine via $A_{2A}R$ stabilizing the nascent GABAergic synapses 159

ABBREVIATIONS

A_1R	Adenosine 1 receptor
$A_{2A}R$	Adenosine 2A receptor
$A_{2B}R$	Adenosine 2B receptor
A_3R	Adenosine 3 receptor
ACh	Acetylcholine
aCSF	Artificial cerebrospinal fluid
ADP	Adenosine diphosphate
AIS	Axon initial segment
AKAP	A-kinase anchoring proteins
AKT/PKB	Protein kinase B
AMPA	α-amino-3-hydroxy-5-methyl-4-isoxazolepropionic acid
araC	cytosine -D-arabinofuranoside
ASD	Autism spectrum disorders
ATP	Adenosine triphosphate
BDNF	Brain derived neurotrophic factor
C. elegans	Caenorhabditis elegans
CA1/2/3	Cornu Ammonis 1/2/3
CaM	Calmodulin
CAM	Cell adhesion molecule
cAMP	Cyclic adenosine monophosphate
CB	Calbindin
CB1	Cannabinoid receptor type 1
CCK	Cholecystokinin
CNS	Central nervous system
CNTN	Contactin
D_2R	Dopamine D_2 receptors
DG	Dentate gyrus
DGC	Dystroglican complex
DIV	Days in vitro
ENT	Equilibrative transporter
ERK	Extracellular signal-regulated kinases
GABA	γ-aminobutyric acid
GAD	Glutamic acid decarboxylase
GARLH	$GABA_AR$ regulatory Lhfpl
GFP	Green fluorescent protein
GL	Granular layer
GPCR	G-protein coupled receptor
GSK3β	Glycogen synthase kinase 3β
IGHMBP2	Immunoglobulin mu binding protein 2
InSyn1-2	Inhibitory Synapse Protein 1 and 2
IPT	Infrapyramidal tract
JNK	c-Jun N-terminal kinases

Lhfpl	Lipoma HMGIC fusion partner- like
LTP	Long term potentiation
MAGI-2	Membrane associated guanylate kinase inverted-2
MAPK	Microtubule-associated protein kinases
MDGA	MAM domain-containing GPI anchor proteins
mEPSC	Miniature excitatory postsynaptic current
mGluR5	Metabotropic glutamate receptor 5
mIPSC	Miniature inhibitory postsynaptic current
ML	Molecular layer
NA	Noradrenaline
NARP	Neuronal activity regulated pentraxin
NMDA	N-methyl-D-aspartate
NMJ	Neuromuscular junction
NP1	Neuronal pentraxin 1
Npas4	Neuronal PAS domain protein 4
NTD	N-terminal domain
NTRK1	Neurotrophic tyrosine kinase receptor type 1
Nxph	Neurexophilins
O-LM	Oriens lacunosum moleculare
PCL	Purkinje cell layer
PI-3K	Phosphoinositide 3-kinase
PKA	Protein kinase A
PKC	Protein kinase C
PKG	Protein kinase G
PLC	Phospholipase C
PNS	Peripheral nervous system
PPARγ	Peroxisome proliferator-activated receptor
PSD95	Postsynaptic density protein 95
PTZ	Pentylenetatrazole
PV	Parvalbumin
Px	Postnatal day
RGC	Retinal ganglion cell
Src	Sarcoma kinases
SRGAP2	Slit-Robo Rho-GTPase activating protein 2
S-SCAM	Synaptic scaffolding molecule
STORM	Stochastic Optical Reconstruction Microscopy
trkB	Tyrosine receptor kinase B
TTX	Tetrodotoxin
UDP	Uridine diphosphate
UTP	Uridine triphosphate
VGAT	Vesicular GABAergic transporter
VGLUT	Vesicular glutamate transporter
VIP	Vasoactive intestinal polypeptide
VNUT	Vesicular Nucleotide Transporter
WRP	WASP family veprolin-homologous protein

INTRODUCTION

INTRODUCTION

1. The purinergic system

1.1 Overview on purinergic system

The purinergic system is composed of several types of ligands and its corresponding receptors, as well as enzymes and transporters which are responsible for the production and/or reuptake of purines that mediate intra/intercellular physiological events.

Chemically, a purine is a heterocyclic aromatic organic compound that consists of a pyrimidine ring fused to an imidazole ring (Figure 1). Purines are fundamental molecules of life as they are key components of nucleic acids (RNA and DNA) that constitute the basic forms of life (Burnstock and Verkhratsky, 2012). They include the nucleobases adenine and guanine, with other notable purines being adenosine triphosphate (ATP), adenosine, cyclic adenosine monophosphate (cAMP), and caffeine (Figure 1). Through evolution, a multitude of roles have emerged for purines ranging from energy metabolism, transduction of intracellular signals, fatty acid metabolism, and epigenetic control. Although purines can be found all throughout an organism, the scope of this thesis will cover purinergic signalling in the brain.

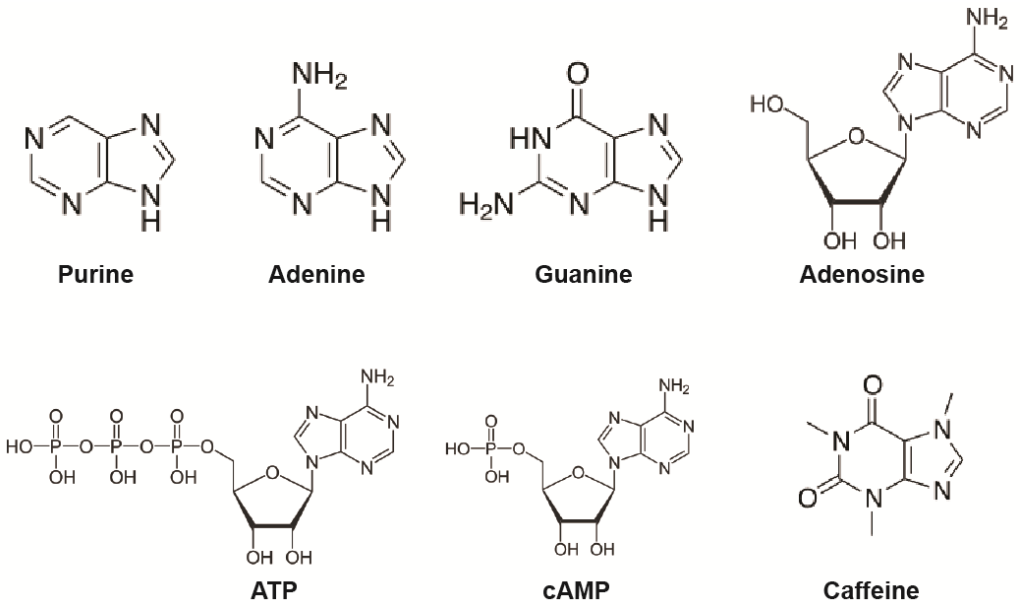

Figure 1: Notable purines
Structure the most important purines and caffeine

1.2 Purinergic signalling

Purinergic signalling is a type of extracellular/intracellular signalling mediated by purine nucleotides and nucleosides such as adenosine and ATP. It involves the activation of purinergic receptors thereby regulating cellular functions. The existence of this signalling implies the existence of ligands and receptors. The family of purines is diverse and as such was divided into two primary groups in 1978 by Geoffrey Burnstock (Burnstock, 1978). Based on several criteria he established two types of receptors: P1 and P2 receptors. The P1 receptors, later renamed into **adenosine receptors, are responsive to adenosine** and are selectively and competitively antagonised by methylxanthines. They modulate the adenylate cyclase activity, resulting in changes in intracellular levels of cAMP (van Calker et al., 1979; Jacobson and Gao, 2006) and downstream activation/inhibition of protein kinase A (PKA). **The P2 receptors are responsive to ATP and ADP**. They are not antagonised by methylxanthines (Abbracchio and Burnstock, 1994).

1.2.1 P2 receptors

Even before the subdivision of adenosine and P2 receptors, Burnstock proposed ATP as a possible neurotransmitter (Burnstock, 1972) and later it was proposed as a ligand for the P2 receptors. However, it was not until 1994, after the accumulation of many studies that Burnstock and Abbracchio (Abbracchio and Burnstock, 1994) proposed a classification of the P2 receptors based on the structure and function of the receptor: **P2X family consisting of ligand-gated cation channels and a P2Y family consisting of G protein-coupled receptors**.

P2X receptors are ionotropic receptors. These ligand-gated channels are the only ones in the mammals/human body to be trimeric, the others being tetrameric (glutamate receptors) or pentameric (GABA, glycine, serotonin receptors) (Burnstock and Verkhratsky, 2012). Upon binding of ATP, they open and they are **permeable to Na^+, K^+ and Ca^{2+}**. Until now, seven receptor subtypes have been characterized: P2X1 to P2X7 (North, 2002). Every P2 receptor has its own regional and cell-type pattern of expression (Burnstock and Verkhratsky, 2012). **All the P2X receptors are present in the hippocampus.**

P2Y receptors are metabotropic receptors. They can be sub-classified depending on the G-protein they bind. P2Y1, P2Y2, P2Y4, P2Y6, P2Y11 bind to G_q to activate phospholipase C (PLC) while P2Y11, P2Y12, P2Y13, P2Y14 bind to G_i to inhibit adenylate cyclase (Abbracchio et al., 2006). P2Y receptors can be activated by other purines such as adenosine diphosphate (ADP), uridine triphosphate (UTP), uridine

diphosphate (UDP), UDP glucose and other nucleotide sugars. Some P2Y receptors show higher affinity for other purines than for ATP itself (Abbracchio et al., 2006). As for P2X receptors, the expression of P2Y is region and cell-type dependent. **In the adult hippocampus we can find P2Y1, P2Y2, P2Y4, P2Y6 and P2Y12 receptors** (Burnstock and Verkhratsky, 2012).

In total, there are fifteen P2 receptors displaying different pharmacological properties, region and cell specific expression, making the ATP signalling a complex system. **ATP signalling has multiple roles in the brain i) acting as neurotransmitter ii) as a paracrine modulator of glial cells iii) as synaptic neuromodulator with an impact in synaptic plasticity iv) controlling inflammation v) regulating oligodendrocyte maturation** (Rodrigues et al., 2015; Cunha, 2016).

1.2.2 Adenosine receptors

The first description of adenosine receptors function was performed by van Calker and colleagues when they showed that adenosine could inhibit the accumulation of cAMP (van Calker et al., 1978). They later discovered that other adenosine receptors can increase the intracellular cAMP level (van Calker et al., 1979). This finding, in addition to biochemical, pharmacological and molecular cloning studies showed that there are in fact **four subtypes of adenosine receptors: A1, A2A, A2B and A3 receptors** (Maenhaut et al., 1990; Libert et al., 1991; Stehle et al., 1992; Zhou et al., 1992). All four subtypes were found to be members of the superfamily of G-protein-coupled receptors (GPCRs). The adenosine receptors share a high degree of homology resulting in all of the receptor subtypes forming a seven transmembrane helices (as all other GPCRs), with the N-terminus facing the extracellular space and the C-terminus in the intracellular milieu (Jacobson, 2009). Classically, **A1 (A_1R) and A3 (A_3R) receptors activate $G_{i/0}$ and $G_{i/q}$ respectively to inhibit adenylate cyclase (AC), while A2A ($A_{2A}R$) and A2B ($A_{2B}R$) receptors activate adenylate cyclase** via G_s/G_{olf} –A_{2A} receptors- or G_s/G_q –A_{2B} receptors (Figure 2, Jacobson and Gao, 2006).

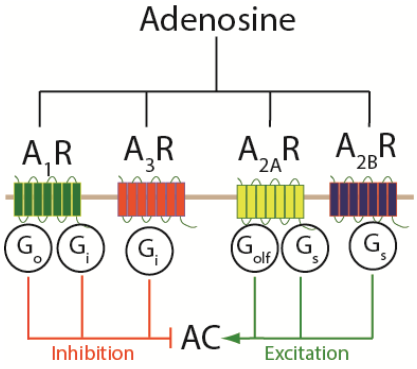

Figure 2: Adenosine receptors can modulate adenylate cyclase activity
A_1R activate $G_{i/0}$ while A_3R activate $G_{i/q}$ to inhibit adenylate cyclase. $A_{2A}R$ and $A_{2B}R$ activate G_s to further activate adenylate (Jacobson and Gao, 2006).

Regulation of adenylate cyclases

AC activation leads to the production of cAMP signalling modulates a set of developmental processes such as cell differentiation, axon outgrowth and response to guidance molecules (Nicol and Gaspar, 2014). The unique combination of regulations, tissue-specific regulation and subcellular localization of ACs concedes them a key role in cAMP signalling (Cooper and Tabbasum, 2014). To date, ten isoforms of AC have been described. Molecular cloning studies showed that ACs have a highly conserved catalytic domain, however the non-catalytic displays more differences to permit different regulatory features (Willoughby and Cooper, 2007). As observed in Table 1, the regulators of AC are multiple allowing them to integrate the activity of many cellular signalling pathways (Cooper and Tabbasum, 2014).

Regulator		AC isoform	effect
G-protein	$G_s\alpha$	All	Stimulation
	$G_i\alpha$	AC1, AC3, AC5, AC6,AC8, AC9	Inhibition
	$G\beta\gamma$	AC1, AC8	Inhibition
Forskolin		All	Stimulation
Ca2+		AC1, AC8 (via calmodulin)	Stimulation
		AC9, AC5, AC6	Inhibition
Kinase	CaMKII	AC3	Inhibition
	CaMKIV	AC1	Inhibition
	PKA	AC5, AC6, AC8	Inhibition
	PKC	AC2, AC4, AC5, AC6, AC7	Stimulation
		AC6, AC9	Inhibition
	RTK	AC1, AC5, AC6	Stimulation
RGS		AC3, AC5, AC6	Inhibition

Table 1: Regulation of the adenylate cyclases
Reproduced from (Cooper and Tabbasum, 2014)

Of special interest for my studies are the Ca^{2+}-stimulated ACs. AC1 and AC8 are both stimulated through calmodulin upon intracellular Ca^{2+} rise. In hippocampal neurons, AC1 and/or AC8 are stimulated by Ca^{2+} entry mediated by NMDAR activation (Chetkovich et al., 1991) or through Ca^{2+} L-type channels (Ferguson and Storm, 2004). Interestingly, $GABA_AR$ activation in young neurons leads to membrane depolarization inducing Ca^{2+} influx via the activation of L-type Ca^{2+} channels (Perrot-Sinal et al., 2003).

The cAMP responses are different in the different cellular compartments, showing thus that ACs and/or their regulators are targeted to different cell microdomains (Nicol et al., 2011). All Ca^{2+} sensitive ACs are enriched in lipid rafts, where also calmodulin and phosphodiesterases (enzymes that catabolize

cAMP) are present (Willoughby and Cooper, 2007). Interestingly, $A_{2A}R$ is also in lipid rafts (Charalambous et al., 2008).

Both AC1 and AC8 are expressed in the brain. The expression of AC1 is higher during embryonic and early postnatal life but decreases in mature neurons (Nicol et al., 2005). Conversely, AC8 expression is low in development but increases in mature neurons. It is mostly expressed in CA1 region (Nicol et al., 2005). This explains why AC1 has been involved in the developmental processes such as axon guidance (Nicol and Gaspar, 2014) and AC8 in modulation of LTP in adult neurons (Wang et al., 2003). However, these ACs have never linked to synaptogenesis.

Multiple pathways activated by adenosine receptors

The concept of adenosine receptors modulating adenylate cyclase only has proved to be oversimplified as later studies have shown that adenosine receptors are capable of activating additional signalling pathways. Apart from the inhibition of adenylyl cyclase, A_1R can increase the activity of phospholipase C (PLC) (Rogel et al., 2005). In cardiac muscle and neurons, A_1R can activate K^+ channels and inhibit Q, P- and N-type Ca^{2+} channels (Jacobson and Gao, 2006).

As mentioned earlier, $A_{2A}R$ activation leads to the activation of adenylate cyclase but can also modulate other pathways. **The complete list of pathways recruited by $A_{2A}R$ can be found in Table 2**.

Pathway	Reference
Adenylate cyclase	(van Calker et al., 1979)
PPARγ (peroxisome proliferator-activated receptor)	(Nayeem et al., 2013)
MAPK (microtubule-associated protein kinases)	(Canas et al., 2009; Li et al., 2015)
JNK (c-Jun N-terminal kinases)	(Genovese et al., 2009)
PI-3K (phosphoinositide 3-kinase)	(Ahmad et al., 2013)
Protein phosphatases	(Murphy et al., 2003)
protein kinase C (PKC)	(De Ponti et al., 2007)
Src (acronym for sarcoma) kinases	(Che et al., 2007)
N- and P- type calcium channels	(Gubitz et al., 1996)

Table 2: Summary list of all the pathways activated by $A_{2A}R$

As $A_{2A}R$ has been linked to several pathways has prompted studies to unravel the reason of this pleiotropy. First, **$A_{2A}R$ can form homo/heterodimers** with numerous GPCRs and enzymes (Canals et al., 2004) that can modulate the signalling (Table 3). This is achieved through $A_{2A}R$ long C-terminal tail which expands 122 aminoacids, for the 36-40 residues of the C-terminus of the other adenosine

receptors (Klinger et al., 2002). Second, the lipid microenvironment of the cell is also important as **$A_{2A}R$ is enriched in lipid rafts**. Its delocalization from these microenvironments by cholesterol depletion selectively hampers their ability to recruit AC rather than MAPK (Charalambous et al., 2008). Third, $A_{2A}R$ can activate different transducing pathways in different brain regions: while $A_{2A}R$ activates AC in hippocampus; in basal ganglia it mainly activates MAPK pathway. This region-dependent modulation could be caused by the presence/absence of interactors of $A_{2A}R$ in different regions. There are six G-protein interacting proteins that interact with $A_{2A}R$; actinin, calmodulin, Necab2, translin- associated protein X, ARNO/cytohesin 2, ubiquitin-specific protease-4, that can bias the signalling in a cell-specific manner (reviewed in Keuerleber et al., 2011).

Molecule	Type of molecule	Reference
Dopamine D2 receptors (D2R)	GPCR	(Canals et al., 2003)
A_1R	GPCR	(Ciruela et al., 2006)
$A_{2B}R$	GPCR	(Moriyama and Sitkovsky, 2010)
Cannabinoid receptor type 1 (CB1)	GPCR	(Carriba et al., 2007)
Glutamate metabotropic group 5 receptors (mGluR5)	GPCR	(Ferre et al., 2002)
G protein-coupled receptor 37 (GPR37)	GPCR	(Lopes et al., 2015)
Adenosine deaminase	Enzyme	(Gracia et al., 2011)
Ecto-5'-nucleotidase	Enzyme	(Augusto et al., 2013)

Table 3: Proteins forming heterodimers with $A_{2A}R$

The other two adenosine receptors are also coupled to other pathways than adenylyl cyclase. $A_{2B}R$ is positively coupled to PLC, and the same is observed for A_3R. The latter has also been shown to stimulate release from intracellular calcium stores (Jacobson and Gao, 2006)

1.2.3 Source and metabolism of ATP and adenosine

ATP and adenosine the main ligands for P2 and adenosine receptors respectively, are found in all the cells of the human body. Adenosine comes mostly from the catabolism of ATP (discussed later). The major source of ATP is the mitochondria that keeps the cytosolic ATP in a low millimollar range (3-10mM), while in the extracellular space ATP is in the range of low nanomolar (Burnstock and Verkhratsky, 2012).

Release of ATP

ATP release involves two major pathways, regulated vesicular exocytosis and diffusion through various plasmalemmal channels. Both mechanisms can work in isolation or in concert, depending on the physiological context.

ATP can be loaded in synaptic vesicles through Vesicular Nucleotide Transporter (VNUT) (Sawada et al., 2008). Alternatively, ATP may enter vesicles by passive diffusion through non-specific anion channels (Lange and Brandt, 1993). ATP can be co-stored and co-released with glutamate, noradrenaline (NA), γ-aminobutyric acid (GABA), or acetylcholine (ACh) (Pankratov et al., 2003, 2006; Cunha, 2016); however, the presence of ATP-only sets of vesicles in the medial habenula has been suggested (Pankratov et al., 2006). Regarding cell types, ATP can be stored in synaptic vesicles in neurons (Pankratov et al., 2003, 2006) and in astrocytes (Parpura and Zorec, 2010). Exocytic ATP release can occur through lysosomes in astrocytes (Oya et al., 2013) and microglia (Dou et al., 2012), as observed in *in vitro* preparations. Neuronal lysosomal ATP release has also been observed but only in the peripheral nervous system (Jung et al., 2013).

ATP can also diffuse into the extracellular space via different plasmalemmal channels such as i) anion channels ii) P2X7 receptors (seen in spinal cord astrocytes) iii) connexin-43 hemichannels iv) pannexin channels (Stout et al., 2002; Suadicani et al., 2006; Iglesias et al., 2009; Burnstock and Verkhratsky, 2012). This is an exhaustive list of all the currently described ways of ATP secretion, excluding cell damage that can induce a discontinuity of the plasma membrane leading to release of intracellular content.

Some of these ATP secretion pathways have been observed in pathological scenarios, it is known that physiological ATP release occurs through tonic release and upon electrical stimulation in neurons (Cunha et al., 1996; Lazarowski et al., 2000). Different molecules such as thrombin, lysophosphatidic acid and UTP induce ATP release from astrocytes (Blum et al., 2008; Parpura and Zorec, 2010). ATP can also be secreted in response to mechanical stress from almost all cell types (Darby et al., 2003).

Metabolism of ATP

Once in the extracellular space, the ATP concentration is regulated by enzymes called **ectonucleotidases that metabolize ATP into other molecules belonging to the purinergic system** (Figure 3). There are three families of enzymes that metabolize ATP: nucleoside triphosphate diphosphohydrolases (NTPDases) (Robson et al., 2006); nucleotide pyrophosphatases/phosphodiesterases (NPPs) (Stefan et al., 2006); alkaline and acid phosphatases

(ALP and ACP, respectively) (Millán, 2006; Burnstock and Verkhratsky, 2012). At last, the activity of the **ecto-5'-nucleotidase (CD73) will hydrolyse AMP into adenosine** (Colgan et al., 2006; Kulesskaya et al., 2013).

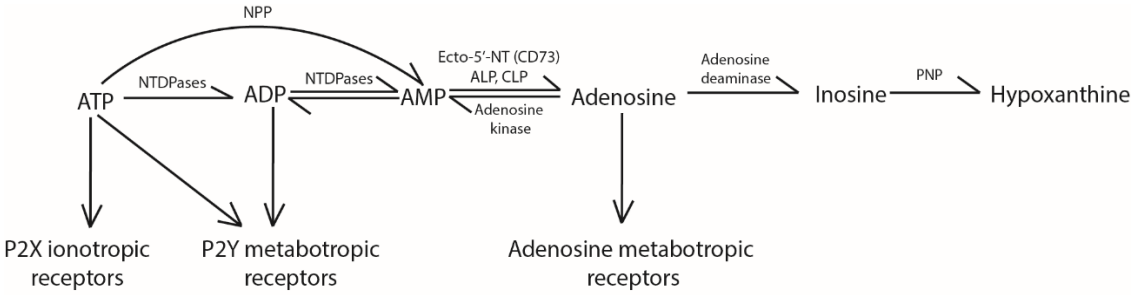

Figure 3: Extracellular metabolism of ATP and adenosine
ATP can be transformed into adenosine by different pathways, and adenosine can be degraded by adenosine deaminase to terminate its actions on the adenosine receptors. From (Jacboson, 2009)

Source of adenosine

Adenosine can be found in the extracellular milieu after the transformation of ATP by ectonucleotidases, being the main source of extracellular adenosine in the brain (Kulesskaya et al., 2013). Otherwise, the presence of **equilibrative transporters (ENTs) permeable to adenosine has also been observed in all the CNS cell types** (Parkinson et al., 2011; Wall and Dale, 2013). In physiological conditions, the adenosine concentration gradient is always inward because cytosolic adenosine concentrations are very low (Wall and Dale, 2007). Some authors (Wall and Dale, 2007; Klyuch et al., 2012) **suggest a vesicular release of adenosine**. In these works, in the cerebellar parallel fibres to Purkinje cell synapses they detected an increase in extracellular adenosine levels by adenosine biosensors, this increase was independent of ENTs and blocked when preventing action potential dependent vesicular release, thus suggesting that there might exist subpopulations of neurons that release adenosine directly (Wall and Dale, 2008). In other cell types and in pathological scenarios, adenosine can be formed from *S*-Adenosyl-L-homocysteine (SAH), but the contribution of this pathway in the brain is negligible (Latini et al., 1996).

Metabolism of adenosine

The actions of adenosine are terminated upon the action of another ecto-nucleotidase, **adenosine deaminase (ADA) that catalyses conversion of adenosine into inosine** (Nofech-Mozes et al., 2007). Inosine will be further metabolised to hypoxanthine by yet another ecto-nucleotidase, the purine nucleoside phosphorylase (PNP) (Figure 3, Burnstock and Verkhratsky, 2012).

1.3 Multiple functions of adenosine signalling

The different pattern of expression of receptors, ligands and metabolic enzymes related to the purinergic system depicts a complex picture, conferring a wide range of roles in physiology and pathology in different tissues. The P2 receptor-mediated signalling system, expressed all throughout the body is really complex, but more is known regarding the adenosine functions, because the pharmacology of adenosine receptors is more developed. If we focus our attention on the adenosine receptors many efforts have been done to treat pathologies using this system, these were recently reviewed (Jacobson and Gao, 2006; Burnstock et al., 2011). Therapies blocking adenosine receptors, or increasing/decreasing the adenosinergic tone have been tried in cardiovascular disease (arrhythmia, ischemia), renal disorders (ischemia-induced kidney injury and fluid retention disorders), pulmonary disorders (asthma), inflammatory disorders, nervous systems disorders, endocrine disorders and cancer amongst others (Jacobson and Gao, 2006)

I am only going to review the roles regarding adenosine in the brain in this section. Adenosine is present all throughout the brain so its effects are linked to the expression pattern of the receptors. Of the four adenosine receptors it is mostly A_1R and $A_{2A}R$ that are responsible for the effects of adenosine in the brain (Fredholm et al., 2005). Whereas A_1R are the most abundant and widespread (they are the second most abundant metabotropic receptor in the brain), $A_{2A}R$ are more abundant in the basal ganglia as compared to the rest of the brain (Fredholm et al., 2005). In fact, both A_1R and $A_{2A}R$ are mostly located in synapses and have been found in glutamatergic synapses, GABAergic, cholinergic, dopaminergic, serotoninergic or noradrenergic synapses (Cunha, 2016).

1.3.1 Physiology: at the cellular level

Adenosine is a well-known synaptic modulator but extracellular adenosine can also play multiple physiological roles in the brain parenchyma. Their function will be determined by the subtype of receptor expressed, the cell type and brain region, amongst other factors. To classify the effects of adenosine, I will distinguish between effects on neurons and on glial cells.

1.3.1.1 Adenosine in neurons

The modulatory effect of adenosine in neurons is the best described role for adenosine in the brain. Adenosine can modulate synaptic transmission directly via presynaptic A_1R, presynaptic $A_{2A}R$ or indirectly modulating the effect of neurotrophins (Cunha, 2016).

A_1R -mediated tonic inhibition

Adenosine is considered an inhibitory neuromodulator responsible for a feedback decrease in the activity of excitatory synapses in basal transmission (Cunha, 2016). The increased activity of a glutamatergic synapse leads to an increase in energy consumption, forcing a greater use of ATP, which subsequently leads to greater formation intracellular adenosine that will be released via ENTs. In hippocampal excitatory synapse at steady state adenosine acts on **presynaptic A_1R** to decrease calcium influx through presynaptic voltage-dependent Ca^{2+} channels (Gundlfinger et al., 2007) therefore controlling vesicular glutamate release (Barrie and Nicholls, 1993). **Postsynaptic activation of A_1R** decreases the activation of ionotropic glutamate receptors (Klishin et al., 1995) and hyperpolarizes principal neurons through a control of K^+ channels (Kim and Johnston, 2015). Interestingly, **A_1R-mediated inhibition becomes less efficient the more intense the recruitment of neuronal circuits** is, as we observe a modest effect of A_1R in long term plasticity (LTP) paradigms (Costenla et al., 2011). However, the A_1R has been implicated in other plasticity paradigms such as the heterosynaptic depression (Manzoni et al., 1994; Pascual et al., 2005) and short-term plasticity (George et al., 2016).

$A_{2A}R$ -mediated facilitation

$A_{2A}R$ has an opposite role to A_1R, it has a **facilitatory role in the glutamatergic neurotransmission**. $A_{2A}R$ has a discrete role in basal neurotransmission but its function is more evident in LTP paradigms (Costenla et al., 2011; Viana da Silva et al., 2016). The activation **of presynaptic $A_{2A}R$** leads to i) increased calcium entry through voltage-sensitive calcium channels thereby increasing the release of glutamate (Gubitz et al., 1996; Matsumoto et al., 2014) ii) enhanced the activity of AMPA receptor by PKA-dependent phosphorylation of serine 845 (Dias et al., 2012), iii) decreased the efficiency of cannabinoid CB1 receptors (CB1Rs) by direct interaction, thereby facilitating synaptic vesicle release (Martire et al., 2011).

The facilitatory effect of $A_{2A}R$ was found at the excitatory glutamatergic Schaffer collateral synapses to CA1 pyramidal cells, but not on synapses formed on GABAergic inhibitory interneurons (Rombo et al., 2015). Furthermore, $A_{2A}R$ has no effect on GABAergic synapses formed on pyramidal cells, but it boosts GABAergic inhibitory transmission between CA1 interneurons leading to disinhibition of pyramidal cells (Rombo et al., 2015).

These roles of adenosine in synaptic transmission, i.e. inhibitory in A_1R and facilitatory in $A_{2A}R$, go in opposite directions therefore this might be counterintuitive. The switch from the A_1R-tonic inhibition

to the $A_{2A}R$ facilitation that can be explained by the rapid desensitization of A_1R plus the shutdown of CB_1 receptor, shifting the synaptic modulation from inhibitory to facilitatory.

Modulating the effect of neurotrophins

The actions of brain derived neurotrophic factor (**BDNF**) in the brain are multiple ranging from the survival of differentiated neuron, to synapse formation and maturation, refinement of developing circuits and beyond (Park and Poo, 2013). Activation of $A_{2A}R$ can regulate BDNF production (Tebano et al., 2008; Jeon et al., 2011), and that $A_{2A}R$ can transactivate the BDNF receptor tyrosine kinase B (trkB) even in the absence of BDNF (Lee and Chao, 2001). Furthermore, the effect of BDNF on synaptic strengthening (LTP) has been shown to depend on $A_{2A}R$ activation (Diógenes MJ et al. 2004, Tebano et al., 2008). These evidences show a close link between $A_{2A}R$ and BDNF and raises the possibility that some **effects of BDNF might be mediated by $A_{2A}R$**.

1.3.1.2 Adenosine in glia

The adenosine system is emerging as a master regulator of the glial function. Adenosine can regulate astrocytic metabolism (via $A_{2B}R$) and frequency of the calcium waves (via $A_{2A}R$) (Allaman et al., 2003; Kanno and Nishizaki, 2012). Interestingly, **$A_{2A}R$ in astrocytes can modulate the synaptic transmission by inhibiting glutamate uptake and increasing GABA uptake, while A_1R blocks GABA uptake** (Matos et al., 2012; Cristóvão-Ferreira et al., 2013).

Oligodendrocyte maturation has been shown to be modulated by A_1R and $A_{2A}R$ (Coppi et al., 2013, 2015). Proliferation and motility in microglia are also dependent on adenosine receptor function (Orr et al., 2009; George et al., 2015).

The adenosine receptors are present in all cell types in the brain and they have the ability to modulate synaptic transmission. The majority of studies show that **A_1R activation in neurons and glia has an inhibitory role on synaptic transmission, while $A_{2A}R$ facilitates it**.

1.3.2 Physiology: at the behavioural level

The behavioural effects of adenosine have been assessed in animal models. Many studies were performed to examine the effect of caffeine intake, a natural A_1R and $A_{2A}R$ antagonist. Caffeine is a

compound that can cross both the placental barrier and the blood brain barrier, and has various molecular targets (Fredholm et al., 1999). Caffeine is able to block signalling of $A_{2A}R$ (most potent) and A_1R at micromolar concentrations achieved after a single cup of coffee. At millimolar concentrations, caffeine can inhibit phosphodiesterases, and at even higher concentrations it can block $GABA_A$ receptor activation and induce intracellular calcium release from calcium stores (Figure 4, Fredholm et al., 1999). Upon the drinking of coffee and/or caffeinated beverages, the only mechanism affected would be the $A_{2A}R$ and A_1R (Fredholm, 1995). Subsequent studies using pharmacological agents blocking/stimulating A_1R or $A_{2A}R$ were used to determine if the effects induced by caffeine were A_1R or $A_{2A}R$ -mediated.

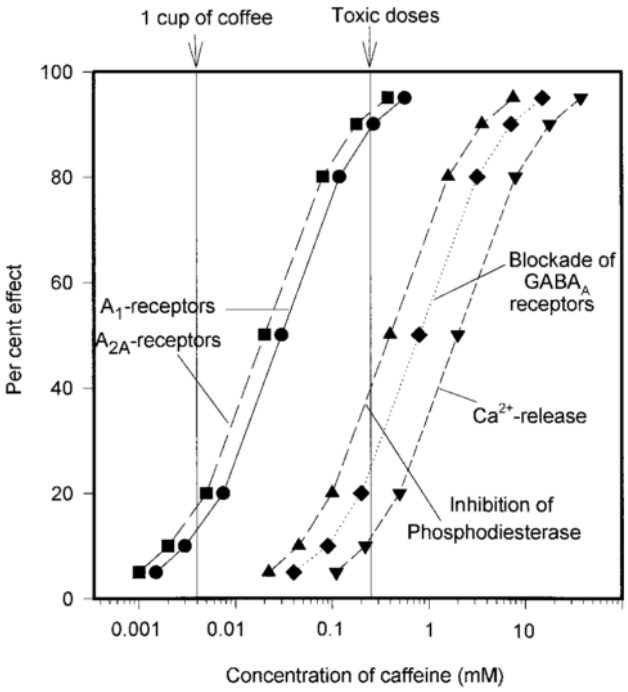

Figure 4: Different molecular targets of caffeine

Caffeine blocks adenosine effects on $A_{2A}R$ and A_1R receptors at concentrations resulting after the intake of a single cup of coffee. At higher concentrations it can also block phosphodiesterases, block $GABA_A$ receptors and mobilize intracellular calcium release from calcium stores (Fredholm et al., 1999).

Another tool to study the relation between receptors and behaviour are the genetically modified animals. Two constitutive, global A_1R knockout mouse lines (gb-A_1R KO) from similar mixed genetic backgrounds, 129sv/C57BL/6J or 129/ OlaHsd/C57BL backgrounds have been generated. Regarding $A_{2A}R$, four constitutive, global $A_{2A}R$ knockout mouse lines (gb-$A_{2A}R$ KO) from different genetic backgrounds, CD1, mixed Sv-129-C57BL/6, Sv-129 or C57BL/6, have been generated (Wei et al., 2011). All the gb-A_1R-KO and all the gb-$A_{2A}R$ KO mice lines were viable, without gross anatomic abnormalities, and fertile (Wei et al., 2011). Brain-regional deletion of $A_{2A}R$ has been performed in the forebrain

(striatum, cortex, and hippocampus) or striatum only. The animals have no gross anatomic abnormalities, they are viable and fertile. At last, transgenic rats over-expressing human A_{2A}Rs have been generated. An overview of the roles of adenosine in physiology and pathology in shown in Figure 5.

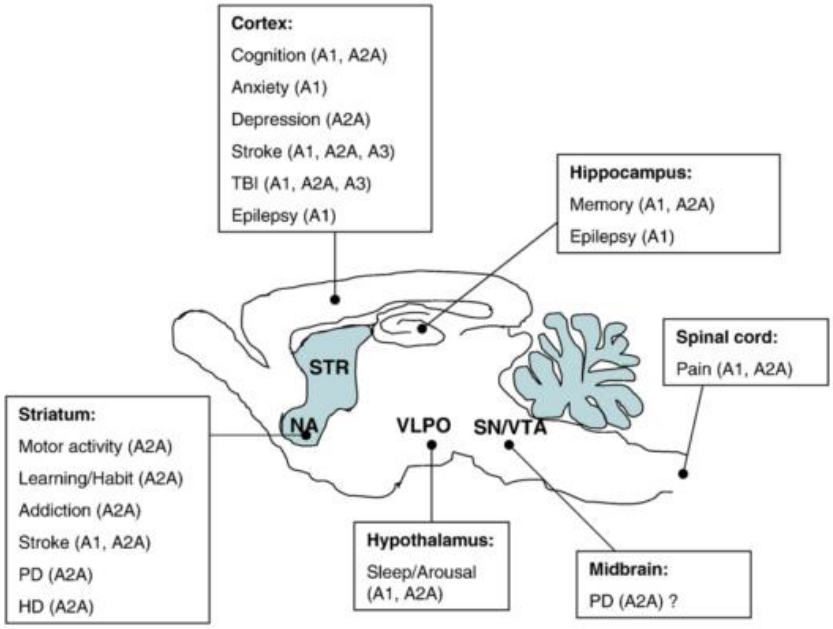

Figure 5: Roles of adenosine in the brain in physiology and pathology
See the implication of adenosine in physiology and pathology linked to a brain region as suggested by pharmacological and knock-out studies. From (Wei et al., 2011).

Learning and memory

The neurophysiological basis for learning and memory involves activity dependent changes in the strength of synaptic transmission mostly in hippocampus and cortex. As adenosine is a neuromodulator expressed in these areas, it was postulated to regulate learning and/or memory processes. It is difficult to draw clear conclusions on the effect of adenosine on learning and memory, due to the multiplicity of types of memory and different paradigms studied. Furthermore, the effects of adenosine could involve different types of memory or memory-related processes (acquisition, consolidation, retention and retrieval).

The evidence points that activation of **A_1R tends to impair learning and memory function**, as it worsens the performance in different memory-related tasks (fear conditioning, 3-panel runway, passive avoidance task amongst others) (Normile and Barraco, 1991; Corodimas and Tomita, 2001; Pereira et al., 2002). On the other hand, **acute A_{2A}R blockade improve the learning and memory performance** in social recognition memory, eye blink conditioning test (Prediger and Takahashi, 2005)

(Fontinha et al., 2009). In line with this evidence, the gb-A_{2A}R -KO show enhanced working memory (Zhou et al., 2009), while this type of memory was impaired in rats overexpressing A_{2A}R (Gimenez-Llort et al., 2007). Thus, the stimulation of A_1R impairs while the blockade of A_{2A}R improves memory-related processes.

Sleep and arousal

Regulation of arousal/sleep and circadian rhythms implies the complex regulation of many nucleus in the brain, all of them endowed with adenosine receptors (Burnstock et al., 2011). Adenosine accumulation triggers a response to initiate sleep (Strecker et al., 2000) and mutations increasing the adenosinergic tone lead to increased total sleep time (Rétey et al., 2005); thus **adenosine is a somnogenic agent**.

It is widely accepted that caffeine intake leads to an arousal state. This caffeine-induced wakefulness is still present in gb-A_1R-KO but blunted in gb-A_{2A}R -KO (Huang et al., 2005), but stimulation of A_1R in rat preoptic area increased total sleep time (Ticho and Radulovacki, 1991). Overall, **the adenosinergic system can modulate sleep but the direct contribution of A_1R and A_{2A}R is probably region-dependent**.

Locomotor activity and exploration

The knock-out animals for the adenosine receptors do not have any motor impairment, but regarding spontaneous activity gb-A_{2A}R -KO display hypolocomotion when compared to control littermates or gb-A_1R-KO (Wei et al., 2011a). Surprinsingly, the spontaneous activity of the double knock-out for A_1R and A_{2A}R is even more reduced than in the gb-A_{2A}R -KO (Yang et al., 2009). This suggests that **A_{2A}R is the most important adenosine receptor subtype when it comes to modulation of spontaneous motor activity; but A_1R exert an effect that is only revealed when A_{2A}Rs are also eliminated**.

Feeding

Adenosine receptors can modulate food intake as shown in studies performed after food deprivation: food intake was not changed upon A_1R stimulation; reduced upon A_1R blockade or A_{2A}R stimulation and increased upon A_{2A}R blockade (Burnstock et al., 2011).

Anxiety and mood

Adenosine receptors are enriched in the basal ganglia. The basal ganglia connect with the nucleus accumbens, which is highly implicated in mood, motivation and reward-seeking behaviour. This has

poised studies that concluded that the A_1R stimulation is anxiolytic in different paradigms (Zangrossi et al., 1992; Florio et al., 1998; Prediger et al., 2004, 2006), which correlates with the elevated anxiety described in the gb-A_1R-KO. The pharmacological studies revealed no modulation of anxiety by $A_{2A}R$, however, the $A_{2A}R$ -KO mice have been shown to be more anxious (Ledent et al., 1997; Giménez-Llort et al., 2002). (Prediger et al., 2006). This anxiety level of both gb-A_1R-KO and gb-$A_{2A}R$ -KO could lead to more aggressivity as observed in a resident intruder test (Ledent et al., 1997; Giménez-Llort et al., 2002).

1.3.3 Adenosine in pathology

Adenosine signalling has been implicated in many brain pathologies and many treatments have tried to modulate the adenosine signalling to improve the symptomatology of a given disease. A summary of all the treatments and observations made on different diseases linked to adenosine receptors is found in Table 4.

Pathology	Brain region	Adenosine receptor	Treatment/ Modulation	Effect	Outcome
Trauma, ischemia, stroke	All	A_1R	Stimulation	Decrease glutamate release	Reduced brain damage after ischemia (Von Lubitz et al., 1994, 1996; Monopoli et al., 1998; Chen et al., 1999)
		$A_{2A}R$	Blockade		
		$A_{2A}R$	Deletion		
Parkinson's Disease	Basal ganglia	$A_{2A}R$	Blockade	Increase dopamine release	Improves motor function and reduces memory impairment (Hauser et al., 2008; Armentero et al., 2011; Uchida et al., 2014)
Alzheimer's Disease	Hippocampus and cortex	A_1R	Stimulation	Increased PKC, p21, Ras and ERK1/2 signalling	Increase formation of soluble β-amyoloid fragments (Angulo et al., 2003)
		$A_{2A}R$	Blockade	Unknown	Revert the LTP impairments in a mice model of AD (Viana da Silva et al., 2016)
		$A_{2A}R$	Blockade	Blockade of MAPK pathway	Reduced neurodegeneration induced by exposure to β-amyloid peptides (Canas et al., 2009)
		A_1R + $A_{2A}R$	Blockade	Unknown	Decreases incidence of AD in humans (Barranco-Quintana et al., 2007). In rodents but not in humans, caffeine prevents AD-induced memory impairment(Arendash et al., 2006; Carman et al., 2014)
Hungtinton's Disease	Basal ganglia	$A_{2A}R$	Deletion	Unknown	Worse motor performance and survival (Mievis et al., 2011).
Schizophrenia	Basal ganglia	$A_{2A}R$	Stimulation	Reduced dopamine release	Improves symptomatology either when administered alone or as a co-medication to haloperidol (Akhondzadeh et al., 2000; Lara et al., 2001)
Depression	Cortex	$A_{2A}R$	Blockade	Unknown	Reverses depressive behaviour in mice (El Yacoubi et al., 2001; Yamada et al., 2014)
Epilepsy	Hippocampus	A_1R	Stimulation	Reduced glutamate release?	(Dunwiddie and Worth, 1982; Avsar and Empson, 2004)
Migraine	Unknown	Unknown	Stimulation	Unknown	Extracellular adenosine augmentation leads to migraine (Hawkes, 1978)
Pain	All	A_1R	Stimulation	Unknown	Acute treatments led to antinociception (Johansson et al., 2001)
	All	$A_{2A}R$	Stimulation	Unknown	Acute treatments led to antinociception (Suh et al., 1997)

Table 4: The adenosine signalling is involved in many pathologies

1.4 Impacts of caffeine intake during gestation and lactation in the offspring

The roles of adenosine in the adult brain have been described extensively, however the roles of adenosine in the developing brain are starting to be unravelled. Some studies have shown that exposure to drugs (cocaine, nicotine, alcohol amongst others) during pre- and peri-natal development have a deleterious effect for the offspring (Thompson et al., 2009).

The fact that caffeine is the most widely consumed psychoactive drug in the world and is permeable to placental and blood brain barrier (Fredholm et al., 1999), prompted studies about the impact of caffeine on early life development. Upon the drinking of coffee and/or caffeinated beverages, the only mechanism affected would be $A_{2A}R$ and A_1R (Figure 4, Fredholm, 1995). It was demonstrated that if a human mother drinks 3 cups of coffee per day, the caffeine blood levels in umbilical cord are between 0.5-2 mg/L (Nehlig et al., 1992). Similar caffeine levels were found in breast-fed babies of caffeine-consuming mothers (Adén et al., 2000); and in line with these observations it is was observed that a mother who drinks 3 cups of coffee in 1 hour has breast milk caffeine levels of 0.32-1.15 mg/L over 10 hours (Bailey et al., 1982).

Studies in humans show that caffeine consumption (>200mg/day, 3-4 cups of coffee per day) during pregnancy may increase the risk of miscarriage (Weng et al., 2008). Another study points that maternal caffeine intake during pregnancy is not associated with changes in gestational length but with lower birth weight (Sengpiel et al., 2013). Lower weight at birth correlates with higher seizure susceptibility (Sun et al., 2008) and cognitive deficits (Jefferis et al., 2002). High caffeine consumption has been associated with fetal death specially after 20 weeks of pregnancy (Bech et al., 2007);however and although many meta-analysis have been performed with analysis dating from 1970s the studies contemplating moderate doses of caffeine remain inconclusive (de Mérici Domingues Paula et al., 2017).

Studies in rats about the effects of caffeine administered in early life intake (between P2-P6) were reported to upregulate A_1R over adulthood (Etzel and Guillet, 1994); however the dose used (80mg/kg/day) results in caffeine blood levels too high to compare with patterns of human caffeine consumption. This point was raised by a later study in which they administered caffeine during pregnancy and early postnatal life through drinking water (0.3g/L, giving rise to blood concentrations between 0.4-2mg/L) and it did not modify mRNA nor protein level of $A_{2A}R$, A_1R nor $GABA_AR$ at any stage

of development checked (from E14 to P21) (Adén et al., 2000). To avoid mixing the effects of the different molecular targets of caffeine, I will only describe here the studies that have used concentrations that will block only the $A_{2A}R$ and A_1R and thus are relevant in terms of human caffeine consumption. Most of the studies studying the effect of caffeine on development, they choose to administer the caffeine in the drinking water of the mother (Adén et al., 2000; León et al., 2005; Silva et al., 2013; Mioranzza et al., 2014; Ardais et al., 2016). Concentrations of 0.3g/L mimic correctly the pattern of caffeine human consumption, while 1g/L is too high resulting in blockade of phosphodiesterases (Ardais et al., 2016).

Recently, a study in rats has shown how caffeine intake during pregnancy affects proteins levels in the offspring. It was found an increase in Sonic Hedgehog and a decrease of the axonal marker GAP-43 both in the hippocampus at E18 in offspring whose mother was drinking 0.3g/L of caffeine (Mioranzza et al., 2014). In another study, treating the pregnant dams from gestation until weaning with the same amount of caffeine they report some changes in synaptic proteins (neurotrophin trkB receptor and the glial marker GFAP) of the offspring at adult stages (Ardais et al., 2016). The offspring whose mother was treated with caffeine displayed behaviour changes in recognition memory and in locomotion. This study showed the impact of caffeine on synaptic proteins, memory performance and locomotion and confirms that caffeine exposure during brain development can cause long-term effects in both memory performance and locomotor behaviour (Ardais et al., 2016).

Interestingly, another paper looked at the effects of caffeine intake during gestation and lactation (the first 3 postnatal weeks). Upon treatment with caffeine (0.3g/L) or an $A_{2A}R$ selective antagonist (KW6002), the migration and insertion of GABA neurons in cortical and hippocampal layers was impaired, leading to anatomical alterations and subsequently to hippocampal hyperactivity accompanied by a shift in the balance between the GABAergic and glutamatergic synaptic inputs in CA3 pyramidal cells. There was also a cell loss observed at 3 months in different hippocampal layers. Behaviourally, the animals were more susceptible to induced epilepsy (at young stages) and showed some cognitive deficits regarding spatial hippocampal-dependent memory in adult life (Silva et al., 2013). In continuing with the described roles of $A_{2A}R$ in development, in young primary cortical cultures that stimulation of **$A_{2A}R$ enhances axonal elongation** via 3-kinase (PI3K) , mitogen-activated protein kinase (MAPK) and phospholipase C (PLC) and **augments dendritic branching**, facilitating the action of BDNF (Ribeiro et al., 2015). The fact that **$A_{2A}R$ is implicated in multiple roles during development (interneuron migration, axonal elongation, dendrite branching) questions a possible role in the formation of synapses *per se***.

1.5 Spatiotemporal expression of $A_{2A}R$

I studied the role of $A_{2A}R$ on synaptogenesis. It is of crucial importance to assess its spatial and temporal expression. Both questions are of the same importance to try to better understand the regulation occurring through $A_{2A}R$.

Early studies studying the brain localization of $A_{2A}R$ were done with autoradiography techniques with the $A_{2A}R$ selective agonist CGS21680. The first studies in adult rat (Jarvis and Williams, 1989) and adult human (Martinez-Mir et al., 1991) suggested that the $A_{2A}R$ was restricted to striatum (caudate nucleus, putamen, nucleus accumbens, olfactory tubercle) and the lateral segment of the globus pallidus.

Later, studies using different techniques demonstrated that $A_{2A}R$ is expressed outside the striatum and expression of $A_{2A}R$ was observed in the hippocampus (Cunha et al., 1994; Johansson and Fredholm, 1995), cortex (Fink et al., 1992; Johansson and Fredholm, 1995) and midbrain (Fink et al., 1992). Dixon and colleagues (Dixon et al., 1996) performed *in situ* hybridisation showing expression of $A_{2A}R$ mRNA in striatum, nucleus accumbens and olfactory tubercle despite the functional evidence for the presence of this receptor in other regions. When using retro-transcriptase-PCR, a technique that is much more sensitive they could show that $A_{2A}R$ is expressed in striatum, olfactory bulb, nucleus accumbens, hippocampus, hypothalamus, thalamus and cerebellum thus showing that $A_{2A}R$ has a broader pattern of expression than previously thought. The most comprenhensive study on the expression of $A_{2A}R$ in brain was performed by Rosin and colleagues (Rosin et al., 1998) where they purified an $A_{2A}R$ antibody and performed immunohistochemistry in 20µm-thin adult rat all throughout the brain. They described $A_{2A}R$ dense immunoreactivity in striatum, nucleus accumbens, olfactory tubercles, and areas of amygdala, globus pallidus and nucleus of the solitary tract. Lighter staining was found in the cortex, hippocampus, thalamus, cerebellum, and regions of the hindbrain.

The first observation of $A_{2A}R$ in the hippocampus was done by Rodrigo Cunha (Cunha et al., 1994). In this study they used adult rats to show that adenosine $A_{2A}R$ mRNA is expressed in the hippocampal CA1, CA3 and dentate gyrus and they confirm this observation using in situ hybridization to show that $A_{2A}R$ was mainly localized in the pyramidal and granular cells. By autoradiography they show how the density of [^{3}H]CGS21680 binding was greatest in the stratum radiatum of the CA1 area, followed by the stratum oriens of the CA1, stratum radiatum of the CA3 area and supra-granular layer of the dentate gyrus. Finally, they confirm its presence by electrophysiological studies at the Schaffer collateral to CA1 pyramidal synapse. This information can be complemented with the one from the study of Rosin and colleagues in which they reported the presence of $A_{2A}R$ in the rostral hippocampus

and dim staining was observed in CA1, CA2, and CA3 pyramidal cells (Rosin et al., 1998). Images taken in our laboratory by Jessica Pressey show that $A_{2A}R$ is expressed in the adolescent hippocampus of mice (Figure 6) in dentate gyrus, CA3 and CA1.

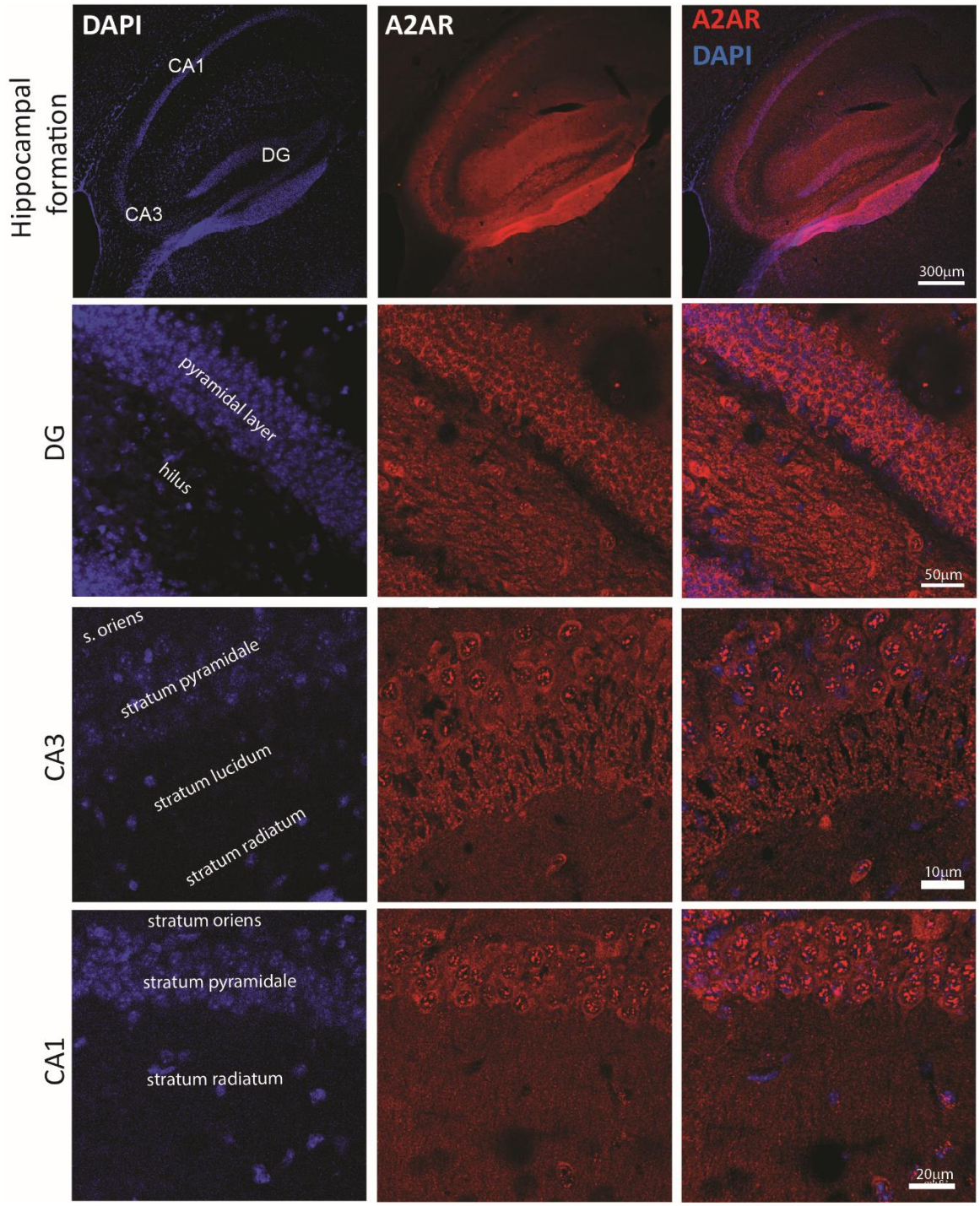

Figure 6: $A_{2A}R$ expression in the postnatal hippocampus.

Top, $A_{2A}R$ is expressed in the hippocampal formation at P16. In the dentate gyrus (DG), see the presence of $A_{2A}R$ in the granule cell layer and in the hilus. In CA3, $A_{2A}R$ is present in pyramidal cells and stratum lucidum. In CA1, $A_{2A}R$ is found in stratum pyramidale and stratum radiatum.

1.5.1 Cellular and subcellular expression of $A_{2A}R$

$A_{2A}R$ have been found in adult hippocampal glutamatergic synapses (Cunha et al., 1994; Rebola et al., 2005b), adult hippocampal GABAergic synapses (Cunha and Ribeiro, 2000; Rombo et al., 2015), adult globus pallidus GABAergic synapses (Shindou et al., 2002), hippocampal cholinergic (Cunha et al., 1995), striatal dopaminergic (Garção et al., 2013) hippocampal sertoninergic (Okada et al., 1999), nucleus tractus solitarius serotoninergic and noradrenergic (Barraco et al., 1995, 1996) or hippocampal noradrenergic synapses (Jackisch et al., 1985). From now on, I will focus my study in the hippocampus, sometimes comparing to the striatum where the $A_{2A}R$ has been mostly studied.

In the hippocampus of adult rats (6-8 weeks) the binding of a radioactive selective antagonist of $A_{2A}R$ ([^{3}H]SCH 58261) is higher in nerve terminals than in total membranes. Subcellular fractionation showed that **$A_{2A}R$ is enriched in the presynaptic active zone in hippocampus** (Rebola et al., 2005a). This contrasts with its expression in the striatum where it is predominantly expressed in the postsynaptic density. This suggests different roles of $A_{2A}R$ in striatum (signal processing) and in hippocampus (control of neurotransmitter release) (Rebola et al., 2005a). Immunocytochemistry on hippocampal synaptosomes from adult rats, revealed that $A_{2A}R$ colocalizes with 29.2±6.2% of the Vesicular glutamate transporter (VGLUT, marker of excitatory neurons) 1/2-positive terminals. Moreover, they show that in hippocampus A_1R and $A_{2A}R$ are expressed by the same neuron in a subpopulation of pyramidal cells (Rebola et al., 2005b). However, these data must be interpreted with caution, because the sub-synaptic localization of $A_{2A}R$ can vary depending on the synapse. Contrasting with the data of (Rebola et al. 2005a) which described a presynaptic localization of $A_{2A}R$ in the hippocampus, electronic microscopy studies showed that $A_{2A}R$ are postsynaptic in the mossy fiber to CA3 pyramidal cells synapse in adult mice (Rebola et al., 2008).

Less is known about the presence of $A_{2A}R$ in hippocampal interneurons although functional studies show how $A_{2A}R$ regulates GABA release (Cunha and Ribeiro, 2000) and modulates BDNF effects in these cells (Fernandes et al., 2008). $A_{2A}R$ is also expressed in glial cells. The presence of $A_{2A}R$ has been demonstrated in astrocytes (Cristóvão-Ferreira et al., 2013; Orr et al., 2015), oligodendrocytes (Coppi et al., 2015) and microglia (Orr et al., 2009; George et al., 2015).

1.5.2 Ontogenic development of $A_{2A}R$

The ontogenical expression of $A_{2A}R$ in rat brain has been studied using radioligand and in situ hidrization assays (Johansson et al., 1997; Adén et al., 2000). The earliest detection of $A_{2A}R$ mRNA was found at E14 by *in situ* hibridization, it was diffusely distributed all over the brain. However it was not detected by any of the radioligand assays at this age. From E18, $A_{2A}R$ mRNA was found in the caudate putamen. The first signal detected by the radioligand assays is at E21 in the caudate putamen. Both signals increase from then on until P14.

Data from the Allen Brain Atlas (Figure 7) show that $A_{2A}R$ is detected at E18.5 as the earliest timepoint in the midbrain and medullary hindbrain. $A_{2A}R$ is starting to be expressed in the late embryonic stages, increasing during infancy (P4-P14) and adolescence (P28), then decreasing in adulthood (P56) and then increases again in old animals (P18 months).

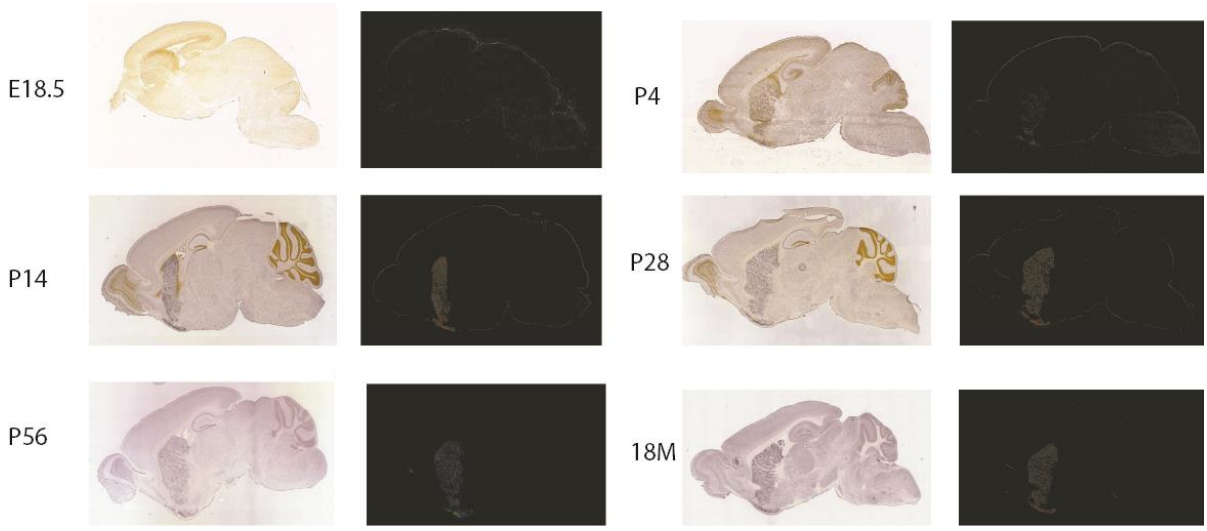

Figure 7: Ontogenic expression of $A_{2A}R$
See the in situ hybridization of $A_{2A}R$ over time (E18.5, P4, P14, P28, P56, 18 months) in the left panel, in the right panel the expression mask displays those cells with a probability of gene expression (from low/blue to high/red). Data extracted from Allen Brain Atlas

The peak of expression of $A_{2A}R$ in early life is concomitant with the period of synaptogenesis. This prompted me to study the role of $A_{2A}R$ in GABAergic synapse formation in the hippocampus.

2. Synapse formation

2.1 The inhibitory synapse: an overview

In the mammalian central nervous system, **GABA is the main inhibitory neurotransmitter**. GABA synthesis occurs by the enzyme L-glutamic acid decarboxylase (GAD) that catalyses decarboxylation of glutamic acid to form γ-aminobutiric acid (GABA)(Erlander et al., 1991). After being released from the presynaptic neuron, GABA will be rapidly removed from the synaptic cleft by GABA transporters (GAT1-4) (Minelli et al., 1995). In the synaptic cleft, GABA can bind either $GABA_A$ or $GABA_B$ receptors.

$GABA_A$ receptors ($GABA_AR$) are ionotropic while $GABA_B$ are metabotropic receptors. $GABA_B$ receptors are GPCRs that activate second messenger systems such as PLC and AC and activate K^+ and Ca^{2+} ion channels via G-coupled proteins to hyperpolarize the neuron (Chebib and Johnston, 1999). $GABA_AR$ are ligand-gated ion channels. Upon binding of GABA a conformational change opens the channel leading to chloride influx/efflux depending on the electrochemical gradient of the ion. During early development, $GABA_AR$ are depolarizing because the intracellular chloride is high; in adult neurons, intracellular chloride is lower and GABA is hyperpolarizing (Rivera et al., 2005). In the developing brain, GABA depolarization leads to calcium entry via L-type voltage-gated calcium channels (Perrot-Sinal et al., 2003) which in his turn will activate different pathways, modulating neurite outgrowth and synapse formation (Spoerri, 1988; Barbin and Pollard, 1993; Represa and Ben-Ari, 2005; Oh et al., 2016). In the adult brain, $GABA_AR$ are the major source of inhibition (Comenencia-Ortiz et al., 2014).

Molecular structure of $GABA_AR$ and subcellular distribution

$GABA_AR$ are organized as heteropentamers. To date, twenty-one $GABA_AR$ subunits have been identified and classified into eight classes based on sequence identity: α(1–6), β(1–3), γ(1–3), δ, ε(1–3), π, θ and ρ(1–3) and π (Olsen and Sieghart, 2009). All the $GABA_AR$ subunits present four transmembrane domains, a long N-terminal extracellular domain and a short C-terminal extracellular domain (Figure 8). The extracellular N-terminal sites are important for the oligomerization of the protein and for subunit– subunit interactions. The intracellular domains contains a critical site for cytoplasmic protein interactions with regulatory and signalling molecules (Jacob et al., 2008). Between the third and fourth transmembrane domains there is a long intracellular loop with multiple sites for post-translational modifications (Jacob et al., 2008).

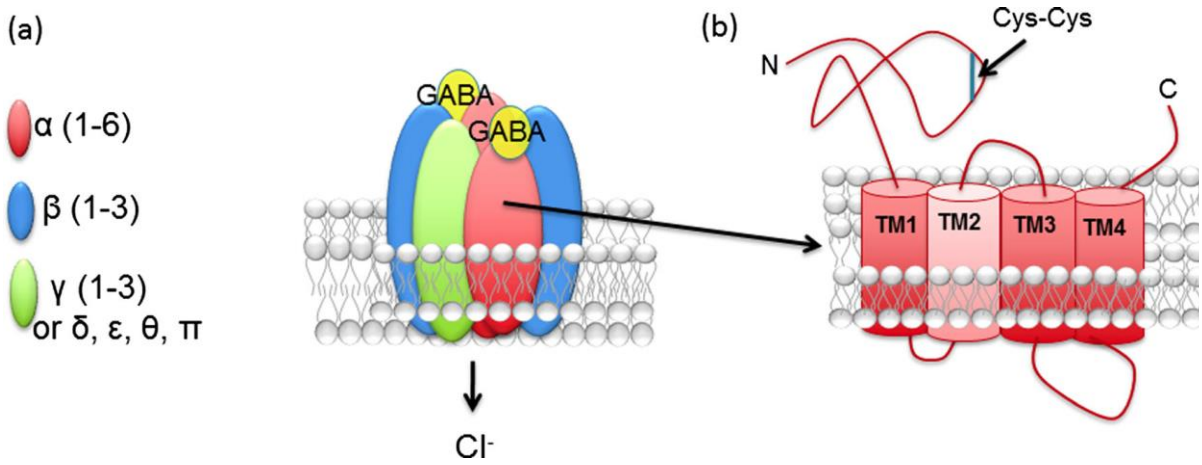

Figure 8: Structure of $GABA_AR$

(a) $GABA_AR$ are composed of five subunits assembled as a heteropentamer. The prototypical $GABA_AR$ is composed of two α, two β, and one γ or δ. (b) The common molecular $GABA_AR$ subunit structure is composed of a large N-terminal extracellular domain, four transmembrane domains, a short C-terminal extracellular domain, and a long intracellular loop domain between TM3 and TM4. From (Comenencia-Ortiz et al., 2014)

The different $GABA_AR$ subtypes have different subcellular localization (Connolly et al., 1996). **$GABA_ARs$ composed of the α1–3, β1–3, and γ2 are predominantly synaptic** and mediate phasic inhibition (Comenencia-Ortiz et al., 2014). The majority of $GABA_AR$ subtypes in the brain are composed of 2α:2β:1γ (Vithlani and Moss, 2009). The synaptic $GABA_AR$ are activated transiently after an exposure to high GABA release from the presynaptic membrane, leading to a rapid chloride influx resulting in hyperpolarization of the plasma membrane (Jacob et al., 2008). I have focused my studies on the $GABA_ARγ2$ subunit. The $GABA_ARγ2$ subunit is highly expressed in the developing and adult brain and forms part of almost 60% of all $GABA_ARs$ (De Blas, 1996). It is found at synaptic and extrasynaptic sites (Bannai et al., 2015). **Importantly $GABA_ARγ2$ expression is required for the synaptic clustering of $GABA_ARs$** (Essrich et al., 1998; Crestani et al., 1999; Li et al., 2005). *In vivo* and *in vitro* studies knocking down this subunit show a loss of $GABA_ARs$ clustering and a loss of the GABAergic innervation was reported, without any change in excitatory synapse markers (Li et al., 2005).

Null mice for $GABA_ARγ2$ were generated but they were lethal in the perinatal period (Günther et al., 1995). In this model, no compensation by other $GABA_AR$ subunit was observed. Although no major abnormalities were observed at birth, they developed sensorimotor abnormalities. The heterozygous mice from this line was used to study the function of $GABA_ARγ2$ *in vivo*. This $GABA_ARγ2^{+/-}$ mice presents a ~50% reduction in γ2 protein levels and reduced synaptic $GABA_AR$ clustering (Crestani et al., 1999). Normal life span, social behavior, motor coordination, memory and reproduction were reported but an elevated anxiety was found (Crestani et al., 1999). The elevated anxiety phenotype was also

described in another mice whose $GABA_AR\gamma2$ mRNA levels were reduced by ~35% compared to control levels (Chandra et al., 2005).

$GABA_ARs$ composed of the α4-6, β2/3, and δ subunits are primarily localized at extrasynaptic sites where they mediate tonic inhibition. When activated, the extrasynaptic $GABA_ARs$ reduce the cell input resistance resulting in a reduction in both size and duration of excitatory post-synaptic potentials (Farrant and Nusser, 2005).

Scaffolding molecules

The subcellular distribution between synaptic and extrasynaptic $GABA_AR$ is mediated by the interaction with scaffolding molecules. The $GABA_A$ receptors containing α5-subunits **($GABA_AR$ -α5) have been shown to interact with the scaffolding molecule radixin**. Suppression of radixin abolishes the membrane clustering of α5-containing $GABA_AR$; however, has no effect on GABA-mediated currents (Loebrich et al., 2006; Hausrat et al., 2015).

The synaptic $GABA_AR$ are first targeted to the extrasynaptic sites and then laterally diffuse to synaptic sites (Bogdanov et al., 2006), where they interact with **gephyrin, the main intracellular scaffolding protein of the inhibitory synapse**. The interactions between the **$GABA_ARs$** and gephyrin are crucial in terms of lateral diffusion. $GABA_AR$ can enter and escape the synapse by diffusion and thus regulating receptor number at synapses and ultimately the synaptic transmission (Bannai et al., 2009; Choquet and Triller, 2013)

Gephyrin has a key role regulating the clustering of synaptic $GABA_ARs$ at inhibitory synapses (Choii and Ko, 2015). Gephyrin forms an hexagonal lattice underneath the cell membrane forming a two-dimensional scaffold that anchors postsynaptic receptors (Specht et al., 2011)and interacts with different proteins such as the $GABA_AR$, GARLH, neuroligin-2 and collysbistin. Gephyrin interacts directly with the synaptogenic organizer neuroligin-2. This interaction would activate collybistin that binds to both of them to initiate the formation of GABAergic synapses and recruit the postsynaptic elements to these sites (Poulopoulos et al., 2009). Recently, $GABA_AR$ regulatory Lhfpl (GARLH) proteins were described as putative auxiliary subunits of GABAARs. GARLHs were identified and showed to form a complex with $GABA_ARs$ and neuroligin-2, and are required for the synaptic localization of $GABA_ARs$ and inhibitory synaptic transmission in the hippocampus (Yamasaki et al., 2017).

Gephyrin scaffolding properties are mediated by its interaction with the cytoskeleton. Gephyrin interacts with microtubules (Kirsch et al., 1995). Microtubule disruption in spinal cord neurons (where $GABA_AR$ and glycine receptors are present) led to reduction of gephyrin clusters (Charrier et al., 2006). However, the postsynaptic density is mostly formed of actin microfilaments. Gephyrin has been shown to interact with actin-binding proteins (profilin 1 and profilin 2), and profiling 2 colocalizes with gephyrin at postsynaptic sites in cortical cultured neurons (Murk et al., 2012). Yet, disruption of the tubulin or actin cytoskeleton did not affect gephyrin clustering in mature cultured hippocampal neurons (Allison et al., 2000). It has been suggested that the gephyrin-profilin interaction regulates dynamic modifications of the postsynaptic actin cytoskeleton, and thus actin polymerization could tune $GABA_AR$ stability through gephyrin (Tyagarajan and Fritschy, 2014).

Post-translational modifications at the inhibitory synapse

Cell surface stability, receptor activity and trafficking of $GABA_AR$ can be modulated by protein interactions and post-translational modifications, that occur in the intracellular loop of the different $GABA_AR$ subunits. Palmitoylation, ubiquitination and phosphorylation have been described to occur in different $GABA_AR$ subunits (Vithlani et al., 2011). I will only describe in this section the post-translational modifications that modify GABAergic synapse number.

The **mutations of palmitoylation sites in GABAARγ2 subunit resulted in a loss of $GABA_AR$ clusters** at the cell surface (Rathenberg et al., 2004). Preventing the GABAARγ2 subunit palmitoylation led to a decreased amplitude of mIPSC attributed to a decrease in postsynaptic $GABA_AR$ number (Fang et al., 2006).

Phosphorylation of $GABA_AR$ subunits has been implicated in channel gating, conductance and/or kinetics, sensitivity of the receptors to pharmacological agents, protein-protein interactions and membrane trafficking (Vithlani and Moss, 2009). Phosphorilation sites are present in different $GABA_AR$ subunits (β1, β2, β3, γ2) and are mediated by an array of kinases (CAMKII, PKA, PKC, PKG, AKT, Src). The phosphorylation of the same residue in different $GABA_AR$ subunits can have different effects, as shown by the phosphorylation of serine 408/409 on β1 shows a depression of GABA-activated currents and in β3 subunit-expressing cells a potentiation was observed (Moss et al., 1992; Mcdonald et al., 1998). Importantly, phosphorylation of $GABA_AR$ subunits can also modulate the protein-protein interactions and indirectly the density of $GABA_AR$ synapses: the phosphorylation of either tyrosine 365 or tyrosine 367 in GABAARγ2 subunit hamper the interaction with AP2 adaptor protein, thus

preventing the endocytosis, hence it was accompanied by an increased number of receptor on the cell surface (Vithlani and Moss, 2009).

Gephyrin can also undergo many post-translational modifications: twenty-two phosphorylation sites, two SUMOylation sites, one palmytoilation sites and one acetylation can occur in gephyrin (Choii and Ko, 2015; Ghosh et al., 2016). These **post-translational modifications might induce conformational changes thereby altering the clustering, trafficking and binding properties of gephyrin**. Tyagaran and colleagues have performed many studies to understand the posttranslational modifications on gephyrin. They described two phosphoresidues serine 270 and serine 268 targeted by GSK3β and ERK1/2 respectively with the ability to modulate gephyrin cluster density and impact the inhibitory synaptic transmission as observed in mIPSC recordings (Tyagarajan et al., 2011; Tyagarajan and Fritschy, 2014). In another study from the same laboratory, they demonstrated the importance of other two phosphoresidues: serine 303 (phosphorylated by PKA) and serine 305 (phosphorylated by CAMKII) in the activity dependent formation of new gephyrin clusters (Flores et al., 2014).

This non-exhaustive list of studies shows how the posttranslational modification can dynamically regulate the efficacy of neuronal inhibition by controlling the accumulation of $GABA_A$Rs at the postsynaptic membrane. All the posttranslational modification and protein interaction act in concert to regulate the function of the inhibitory synapse.

2.2 Introduction to synapse formation

Synapses are cell to cell connections allowing the controlled transfer of an electrical or chemical signal between a presynaptic neuronal cell and a postsynaptic cell. Correct synapse function is essential for neuronal processing from synaptic transmission to higher cognitive functions such as learning and memory.

At electrical synapses transmission of an electrical signal occurs through gap junctions (Pereda et al., 1998); while at chemical synapses the signal is a neurotrasmitter. In the latter case, the presynaptic neuron releases a neurotransmitter into the synaptic cleft that in turn binds and activates the receptors in the postsynaptic cell. In many animals, both electrical and chemical synapses co-exist. From now on, I will only discuss about chemical synapses.

Ultrastructurally, chemical synapses are morphologically classified as either type I (asymmetric; mainly on dendritic spines) or type II (symmetric; mainly on soma and dendritic shafts) (Harris and Weinberg, 2012). Type I synapses mediate excitatory synaptic transmission by the use of glutamate, whereas type II synapses use GABA and glycine to mediate inhibitory synaptic transmission (Harris and Weinberg, 2012).

In the hippocampus, the principal cells mediating excitation are pyramidal neurons. The pyramidal neurons form type I synapses and represent 89-93% of neurons in the hippocampus, while the remaining 7-11% are interneurons and mediate the inhibition using GABA as a neurotransmitter (Bezaire and Soltesz, 2013). The interneuron function is crucial for the correct functioning of the hippocampus, as it was pharmacologically demonstrated that reducing the strength of GABAergic inhibition leads to epileptiform activity (Miles and Wong, 1999), while an increase in GABA release impairs hippocampal dependent memory tasks (McNaughton and Morris, 1987).

The GABAergic interneurons are a diverse population of cells. They display a wide range of different morphological, molecular and physiological features. This has prompted many attempts of classification of the interneurons (Markram et al., 2004; Kepecs and Fishell, 2014) and a criteria to classify and name all the interneurons has been established (Ascoli et al., 2008). Some years ago it was believed that the classification by six neuronal markers (parvalbumin, somatostatin, vasoactive intestinal peptide, nitric oxide synthase, reelin and calretinin) could divide most interneurons within the forebrain. However, within the hippocampus there are four or five somatostatin-expressing cell types and at least three parvalbumin-expressing types of interneurons (Kepecs and Fishell, 2014). The

complexity of the interneuron classification can be grasped when we observe that in hippocampal CA1 region alone there are 21 different types of them (Klausberger and Somogyi, 2008, Figure 9).

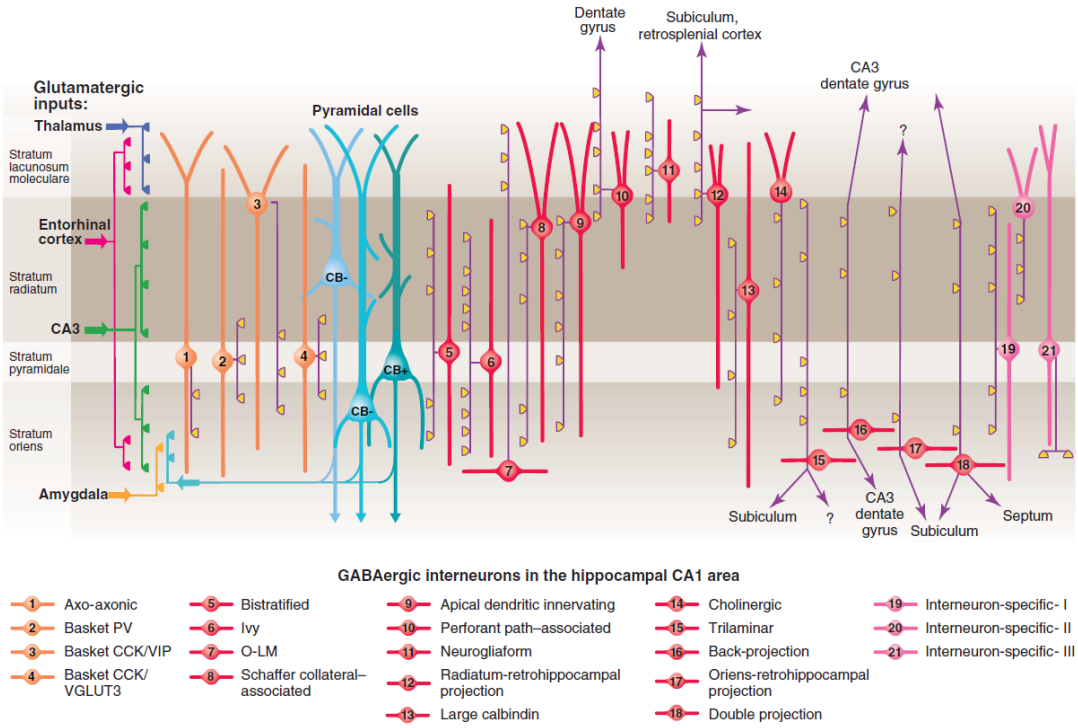

Figure 9: Interneurons in CA1 hippocampus

See the three types of pyramidal cell (in blue) and the 21 types of interneuron. For all interneurons, axons are purple, the main synaptic terminals are yellow. In orange, the interneurons whose somata and dendrites innervate pyramidal cells. In red, interneurons whose axons project to pyramidal cells. In pink, interneurons that mainly innervate other interneurons. From (Klausberger and Somogyi, 2008).

As observed in Figure 9, interneurons establish synapses on principal cells and interneurons. Interneurons forming inhibitory synapses on the perisomatic region of principal cells control the initiation of action potentials, while inhibitory synapses on distal dendrites of pyramidal neurons modulate dendritic calcium spikes (Miles et al., 1996). Thus it is of crucial importance where are the synapses formed but as well when are they formed as a defect in any of these points can have pathological implications.

2.3 Timing of hippocampal synaptogenesis

Synapses are formed throughout the lifetime of an organism, but it is especially important during the early development of the nervous system. Although the GABAergic synapses in hippocampus represent only 5% of the total synapses on a CA1 pyramidal cell (Megías et al., 2001), they control the proper functioning of the hippocampus.

Hippocampal GABAergic synapses form earlier than excitatory ones (Tyzio et al., 1999; Hennou et al., 2002). As (Hennou et al., 2002) some authors have detected GABAergic currents in late embryonic stages, but the GABAergic synaptogenesis is mostly a postnatal process. Recordings from both pyramidal neurons and interneurons in hippocampal rat foetuses (E18-20) revealed that the majority of interneurons (95%) receive functional synapses whereas nearly 90% of pyramidal neurons are quiescent (Tyzio et al., 1999; Hennou et al., 2002). Therefore, interneurons are the source and the targets of the first functional synapses (Gozlan and Ben-Ari, 2003). This is also the case in other brain regions such as the brain stem (Varoqueaux et al., 2006).

Immunohistochemical studies to study GABA innervation onto pyramidal cells were performed in the late 1980s, however the low amount of GABA (earliest detection at P4) and GAD (earliest detection at P6) do not really match the electrophysiological studies that observe presence of GABA much earlier (Ben-Ari, 2001). The GABA and GAD immunoreactivity around pyramidal cell bodies were shown to increase dramatically between P4 and P18, timepoint where they reached levels similar to the ones observed in adulthood (Seress and Ribak, 1988). Similarly, vesicular GABAergic transporter (VGAT) also accumulates over time and increases between P7 and P21 in the stratum pyramidale of CA3 and CA1 (Figure 10, Marty et al., 2002). These immunohistochemical studies correlate with mIPSCs recordings in CA1 pyramidal neurons showing an immature profile of mIPSC kinetics (large in amplitude, slow and infrequent) during the first two post-natal weeks (Cohen et al., 2000). By the third postnatal week, the kinetics of mIPSC are mature but respond different to modulatory drugs, probably due to a certain immaturity in synaptic structure and function persisting through adolescence (Cohen et al., 2000).

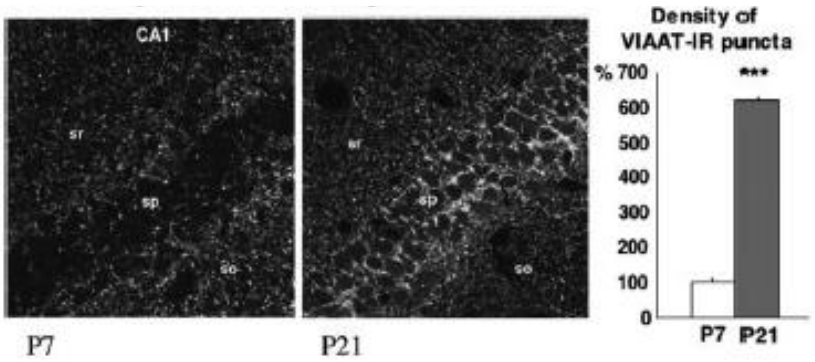

Figure 10: Development of GABAergic innervation in hippocampus
(Left) Immunostaining of VGAT in hippocampal CA1 at P7 and P21. See the increased expression at P21 as compared to P7. (Right) Quantification of VGAT in stratum pyramidale at the mentioned ages. so, stratum oriens; sp stratum pyramidale; sr, stratum radiatum. From (Marty et al., 2002)

The development of the GABA innervation is not homogenous throughout the hippocampus. As an example, in the dentate gyrus the first GABAergic synapses form at the border of the molecular layer, where the granule cells are more mature and increases during the first 10 postnatal days; while at the hilar border the number of synapse starts to increase after the second postnatal week (Danglot et al., 2006).

Altogether these studies indicate that **synaptogenesis is a post-natal process occurring mostly during the first two post-natal weeks**, although the maturation of the synaptic circuits continues during adolescence. As shown in different studies, the development of the GABAergic innervation occurs previous to the glutamatergic innervation.

2.4 Synapse formation is a dynamic process

Synapses are dynamic entities that can appear and disappear. This concept was grasped upon live imaging studies in cell cultures, slices and even *in vivo* animals to understand how synapses are formed and eliminated. It was early observed that the neuronal arbors are highly dynamic with synapses appearing and disappearing at the same time, thus we cannot talk of separate phases of synapse formation and synapse elimination (Hua and Smith, 2004; Wierenga, 2017). Both the pre- and post-synaptic specialization can undergo structural changes in shape and size (Wierenga, 2017), and move coordinately (Dobie and Craig, 2011). **This allows a rapid response to synaptic strength and connectivity of the neuronal circuitry and are believed to be very important for experience-dependent circuit adaptations** (Chen et al., 2012; Villa et al., 2016).

Glutamatergic synapses are mostly formed on dendritic spines (Prange and Murphy, 2001); while the majority of **GABAergic synapses are found on the dendritic shaft**, but some have been found in spines where there are excitatory synapses as well (Villa et al., 2016). Within a neuron some compartmentalization of inhibitory synapses has been observed at least in cortical V1 layer II/III neurons. In the Nedivi laboratory they could show that inhibitory synapses on the dendritic shaft were equally distributed between apical and basal dendrites; however, the inhibitory synapses on spines were enriched on apical dendrites. Upon monocular deprivation the inhibitory synapses on the shaft are much more dynamic showing a different implication in experience-dependent structural plasticity in the visual cortex (Chen et al., 2012). The spatial separation between glutamatergic/GABAergic synapses suggested that different mechanisms organize excitatory/inhibitory synapses, although there are some common mechanisms. Accumulating evidences show that cell adhesion molecules (CAM) are key for both excitatory and inhibitory synapse development, but **the sets of molecules are different between excitatory and inhibitory synapses** (Shen and Scheiffele, 2010).

Inhibitory synapses have been shown to be highly dynamic (Wierenga et al., 2008; Dobie and Craig, 2011; Keck et al., 2011), even more than excitatory ones and this has been suggested to serve as a gating mechanism for plasticity at nearby excitatory synapses (Villa et al., 2016). Live imaging studies of inhibitory synapses have enabled to see that two different pools of presynaptic boutons (the pre-synaptic element) co-exist: the persistent and the non-persistent ones (Figure 11). The persistent boutons are of large size and are continuously present and immobile during hours. Their shape and size can change over time (Matz et al., 2010). They represent *bona fide* inhibitory synapses as revealed by post-hoc analysis by immunostaning or electronic microscopy (Wierenga et al., 2008; Mullner et al., 2015). The non-persistent boutons are smaller and they can appear *de novo* or from the division of a

persistent bouton. Those are incipient synapses being formed or dismantled that can release neurotransmitter supposedly to signal to glial cells (Wierenga et al., 2008; Schuemann et al., 2013).

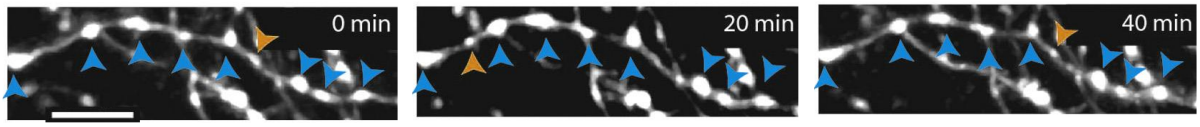

Figure 11: Synaptic boutons: persistent and non-persistent
Magnification of GFP-labelled inhibitory axons from an organotypic slice from a GAD65-GFP mouse. See the persistent boutons in blue (present all throughout the images) and the non-persistent in orange (they appear and disappear). Scale bar, 5µm. From (Wierenga, 2017).

Recordings for several hours indicated that inhibitory synapses appear and disappear at specific locations (Wierenga et al., 2008; Villa et al., 2016a). The presence of pre- and/or post-synaptic proteins at these locations act as triggers to construct a synapse (Schuemann et al., 2013). **Non-persistent boutons can form persistent boutons and persistent boutons can be dismantled showing that these boutons are simply inhibitory synapses at different stages of development**.

Packets of synaptic vesicles can travel along the axon (Wierenga, 2017) and they can stop and form a synapse. The signal triggering the stop of the vesicular packets has not been described in mammals, but studies in *C. elegans* demonstrate that the locations where the future synapses will be formed are enriched with adhesion molecules (Shen and Bargmann, 2003; Shen and Scheiffele, 2010). In mammals, the contact between the dendrite and axon is required to form an inhibitory synapse, but we do not know the molecular composition at the site of contact (Wierenga et al., 2008). However, not all contacts will give rise to a bouton which suggests that the presence/absence of cell adhesion molecules or other scaffolding molecules could also play a role in determining the formation or not of the synapse.

Once the contact is **established and somehow validated, recruitment of pre- and post-synaptic molecules occurs rapidly by the fusion of large vesicles that contain preassembled active zone protein complexes** (Ziv and Garner, 2004). The exchange of synaptic vesicles in boutons observed during development is also observed in mature formed synapses (Darcy et al., 2006; Fernandez-Alfonso and Ryan, 2008). The fact that presynaptic material is moving in and out of the synapse enables rapid changes in synaptic strength; and if necessary, dismount or mount a synapse in the course of hours (Frias and Wierenga, 2013). As mentioned before, a persistent bouton can split giving rise to other boutons. Splitting of the postsynaptic element has also been observed (Dobie and Craig, 2011).

When recording *de novo* synapse formation, **the presynaptic element arrives before the postsynaptic counterpart** (Dobie and Craig, 2011; Schuemann et al., 2013). The time it takes to form a *de novo* synapse was estimated in (Dobie and Craig, 2011) in hippocampal neurons labelled for VGAT and transfected with gephyrin-YFP. In these recordings VGAT appears two hours before gephyrin and the fluorescence of both markers increases in the following eight hours. After the recruitment of pre- and post-synaptic compartments**, the maturation of the synaptic bouton continues during the following 1–2 days** (Nägerl et al., 2007) (Figure 12).

To conclude, the live imaging experiments show that the synapse formation is a multistep process, which can be regulated at multiple levels, **allowing an activity-dependent regulation of the synaptic connections**.

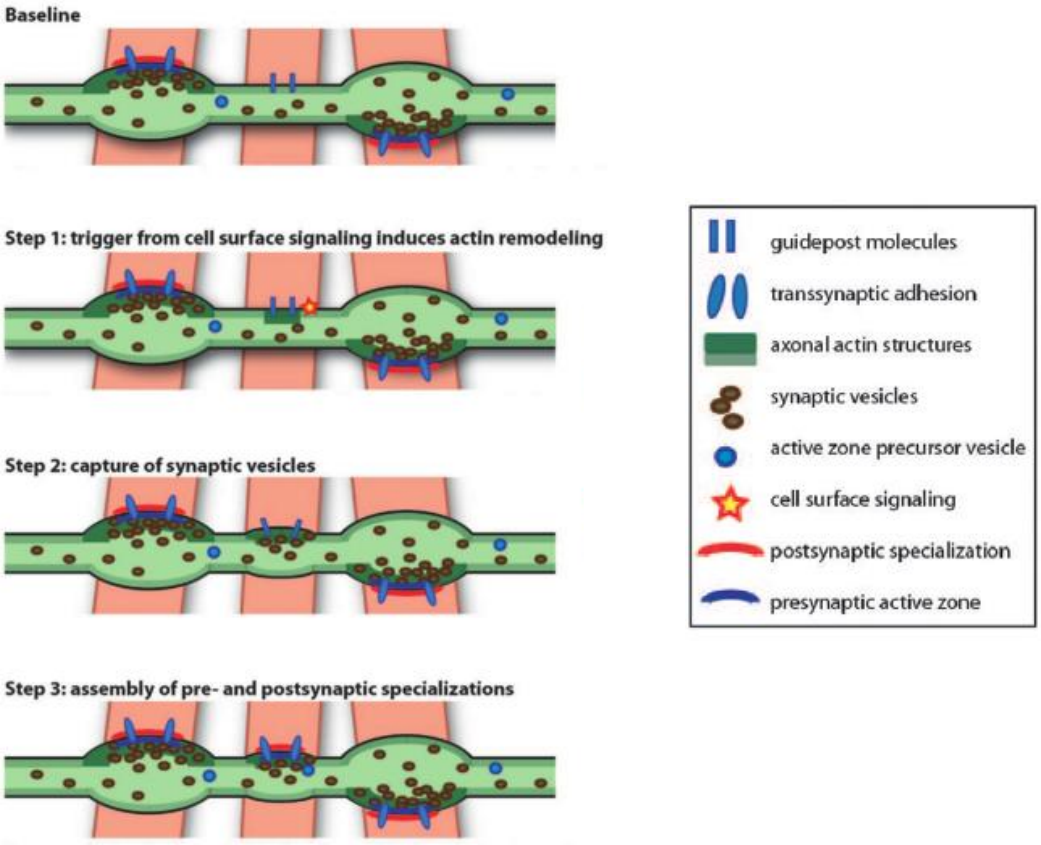

Figure 12: Inhibitory synapse formation model

Baseline. See inhibitory axons (green) making synapses (corresponding to persistent boutons in Figure 11) with multiple dendrites (red, left and right dendrite). Synaptic vesicles and larger vesicles containing components of the presynaptic compartment are transported along the axon. Step 1: In the middle dendrite, an unknown signal triggers the remodelling of the cytoskeleton to attract recruit vesicles. Step 2: capture of synaptic vesicles. Step 3: assembly of pre- and postsynaptic specializations. From (Wierenga, 2017)

2.5 Building a synapse

The correct wiring of the brain is vital, as shown by the fact that some knock-out animals of proteins implicated in synapse formation are lethal in the perinatal period (Varoqueaux et al., 2006; Missler et al., 2012). The structural organization of neuronal circuitry results from a complex set of developmental events that include cell fate determination, cell migration, axon guidance, axonal and dendritic branch layer formation, synapse formation, and the activity-dependent maturation of synaptic circuits (Shen and Scheiffele, 2010). My study will be circumscribed to the period of formation of synapses *per se*, but I will give an overview on all the elements concerning the process of synapse formation. We can subdivide the process of synapse formation in four different stages:

1. **Generation of specificity**: involves the molecular mechanisms of recognition between cells.
2. **Recruitment of synaptic elements**: the process by which synapse organizers recruit molecules to the pre- and post-synaptic membrane.
3. **Activity-dependent maturation of synaptic circuits**
4. **Synapse elimination**

All of the above stages are **under control of transcriptional programs**, which I will describe later. I will give a brief overview of these different points focusing specially on the inhibitory synapse.

2.5.1 Generation of specificity

The connection specificity is critically important for the function of neuronal circuits. We define synapse specificity as the process that enables pre- and post-synaptic cells to select each other as synaptic partners among the surrounding cells thus allowing synapses to form at particular subcellular locations (Shen and Scheiffele, 2010). This initial contact precedes the mechanisms of synaptogenesis *per se.* To achieve this specificity a set of cues have to be expressed at the correct spatiotemporal scale in order to form or not the initial contact. These cues are mostly **cell adhesion molecules (CAMs)** that can either promote or inhibit the contact between the future pre- and/or post-synaptic compartments.

2.5.1.1 Positive cues

The specificity of attachment of the pre- to the post-synaptic membrane is mediated by CAMs. The coordinated expression of adhesion molecules by the pre- and post-synaptic membrane leads to an initial contact at the site of the future synapse (Fannon and Colman, 1996; Shapiro et al., 2007). The initial molecular assembly stage includes the recruitment of different pre- and post-synaptic elements to a developing synaptic contact, resulting in an **anatomically identifiable synapse, but this does not in itself produce a functional synapse**. Functionality of a synapse is achieved in a subsequent step with

the organization of its molecular components during the functional specification stage (Missler et al., 2012).

Some of this CAMs have synaptogenic activity (molecules that have the ability to drive the pre- and post-synaptic recruitment of molecules) while others have not, but their loss-of-function leads to a synapse loss due to the lack of formation of the initial contact. A great number of CAMs can be found at the synapse and an initial classification of these CAMs can be made by their extracellular domains. There are five domains that can be found in these CAMs: i) Laminin A, neurexin, and sex hormone-binding protein (LNS) domains ii) cadherin domains iii) Immunoglobulin-(Ig-)domains iv) leucin-rich repeats (LRRs) v) integrins (Table 5).

Domain	Relevant molecules	Function
LNS	Neurexin1-3 Neuroligin1-4	Synapse formation (Gokce and Südhof, 2013)
Cadherin	N-cadherin	Plays broad modulatory roles in synapse development (Jungling et al., 2006)
Immuno-globulin	SynCAM	Promote excitatory but not inhibitory synapse number (Stagi et al., 2010; Missler et al., 2012).
	Nectins	Participation in synapse unknown
	Receptor phospho-tyrosine phosphatases (RPTPs): the LAR (leukocyte- associated receptor) family, RPTPσ, and RPTPδ	Synapse formation (Takahashi and Craig, 2013).
	Contactins	Inhibitory synapse development (Chen et al., 2011)
	NCAM/L1	Post-synaptic NCAM clustering influences the assembly of cytoskeletal scaffolds (Sytnyk et al., 2006)
	Dscam	Ensure proper lamina connectivity in the retina (Yamagata and Sanes, 2008; Krishnaswamy et al., 2015)
LRR	LRRTMs	Synapse formation (de Wit and Ghosh, 2014)
	Netrin-G ligands (NGL1-3)	Suggested modulatory signaling system for synapses (Zhang et al., 2008)
	Synaptic adhesion-like molecules (SALMs/Lrfn)1-5	Unknown. Described interaction with AMPAR AND NMDAR (de Wit and Ghosh, 2014)
Integrins	Integrins β1, β3	Regulate glycine clustering in hippocampus (Charrier et al., 2010)

Table 5: CAMs found at synapses

Some of these **CAMs are able to generate a unique signature per cell**. From the three neurexin genes, up to 3,000 splice variants are predicted to arise as a result of two alternative promoters and five

alternatively spliced segments. Decreasing the number of splice variants in a neurexin knockout mice lead to impaired synapse function, while synapse ultrastructure and numbers seemed essentially unaltered (Ullrich et al., 1995; Missler and Südhof, 1998). This ability of neurexin to create a multiplicity of isoforms has been shown in other CAMs, such as dsCAM1 in *Drosophila melanogaster* (Neves and Chess, 2004) and protocadherins in vertebrates (Esumi et al., 2005). The molecular diversity of these CAMs is restricted to the extracellular domain; thus connecting different extracellular interactions into a common intracellular signalling pathway (Missler et al., 2012). Not all the CAMs can undergo alternative splicing, some of them achieve their specificity by displaying a certain number of repeats of their binding domains, matching the number of domains present in the synaptic counterpart (Missler et al., 2012).

Another feature of the CAMs is their synapse-dependent or region-dependent expression. Neuroligins are specifically enriched in particular synapses: neuroligin 1 is only present at excitatory synapses (Song et al., 1999), neuroligin 2 and neuroligin 4 at inhibitory synapses (Varoqueaux et al., 2004; Hoon et al., 2011), whereas neuroligin 3 is present at both excitatory and inhibitory synapses (Budreck and Scheiffele, 2007). If we take now the example of the LRR-containing surface proteins, we see a subregion-dependant pattern of expression in the hippocampus (Figure 13)

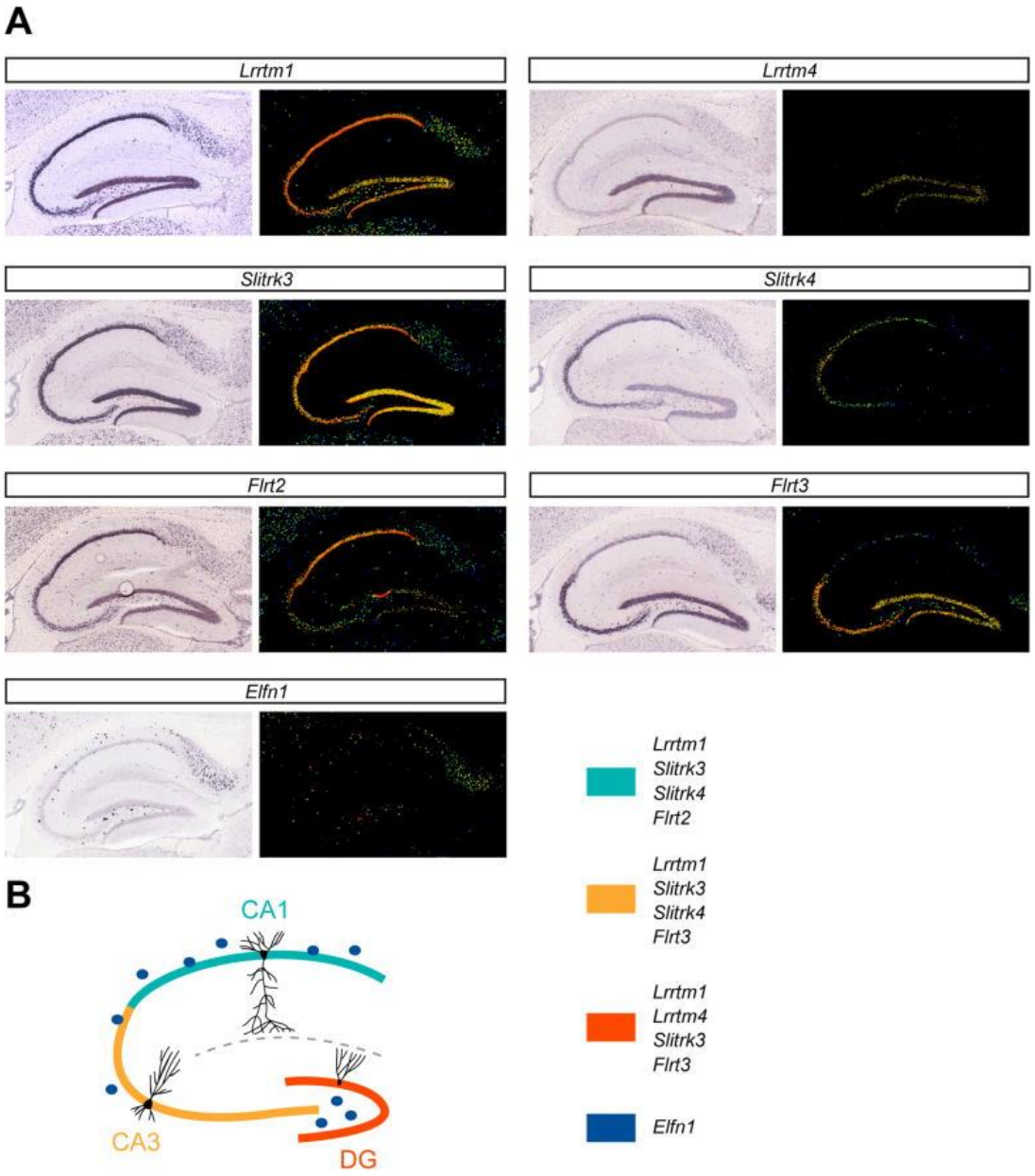

Figure 13: Subregion-specific expression of the LRR proteins

A. See the hippocampal region-specificity of LRR proteins in in-situ hibridization and expression data from the Allen Brain Atlas. B. Representation of the expression of the different LRR proteins in the hippocampus. From (de Wit and Ghosh, 2014)

This overlapping pattern of proteins is found as well within the RPTPs, which demonstrates that the system for the formation of synapses is redundant but at the same time there is a competition for the binding between the pre- and post-synaptic partner (Takahashi and Craig, 2013). This is better observed in individual glutamate synapses that contain multiple neurexins, neuroligin, LRRTM and RPTPs, suggesting a cooperative function in synapse development (Takahashi and Craig, 2013). This cooperation has been suggested to increase the number and diversity of component recruited to the forming synapses.

2.5.2.2 Inhibitory cues

At the neuromuscular junction (NMJ) of *Drosophila melanogaster* the presence of a semaphorin (SemaII, a CAM) prevents the axonal growth cone from forming a synapse (Winberg et al., 1998). In the same system it was observed that others CAMs lead the attraction of the axonal growth suggesting that growth cones assess the balance of attractive and repulsive forces to define what synapses to eestablish (Shen and Scheiffele, 2010). Although a molecule doing the same role in mammalian synapses has not been described, a molecule of the same family, Sema5B reduces the synapse number probably by synapse elimination (O'Connor et al., 2009), (discussed later in 2.2.6). This suggests the appearance of a different mechanism during evolution but with the same outcome.

2.5.2.3 Other factors regulating neuronal specificity

During development, neurons establish many transient contacts and these contacts could impact formation of synapses occurring later. Cajal-Retzius (CR) cells are a type of cell present in the developing hippocampus that will create transient contacts before undergoing cell death. However the ablation of them prevents layer-specific innervation by entorhinal axons, thus suggesting that CR cells are required for the layer-specific innervation of these axons (Del Río et al., 1997). CR cells have been suggested to impact synapse formation in the cortex as well (Frotscher, 1998).

Glial cells can secrete critical axon guidance molecules and serve as intermediate targets to specify axon trajectory. In the cerebellum, where Bergmann glial cells secrete the close Homologue of L1 (**CHL1**, an immunoglobulin protein), which is required for the association between stellate axon and the Bergmann glial cells, without L1, there is mistargetting of stellate axons, which leads to atrophy of them (Ango et al., 2008). This has also been shown in epithelial cells in *C. elegans* through the release of two transmembrane immunoglobulin superfamily proteins (SYG-1 and SYG-2)m regulating the subcellular localization of a subtype of motoneurons (Shen and Scheiffele, 2010)

Importantly, **all the above mentioned CAM-mediated mechanisms are not mutually exclusive. Multiple strategies are likely used by the same neuron at different stages of development to form, establish, maintain or remodel its synaptic connectivity.**

2.5.2 Recruitment of synaptic elements

Once the initial contact is formed the synapse organizers will drive the differentiation of the pre- and post-synaptic membrane. The synapse organizers are molecules that have synaptogenic activity, this means that when expressed in heterologous systems (fibroblasts, COS cells) they are able to recruit

pre- or post-synaptic components at the site of contact (Scheiffele et al., 2000; Takahashi et al., 2012; Pettem et al., 2013a). As mentioned before, some CAMs can promote the formation of contacts, but only a subset of them show synaptogenic properties. The synapse organizers can be classified in i) bidirectional organizers ii) anterograde organizers iii) retrograde organizers and iv) glial-derived organizers (Figure 14).

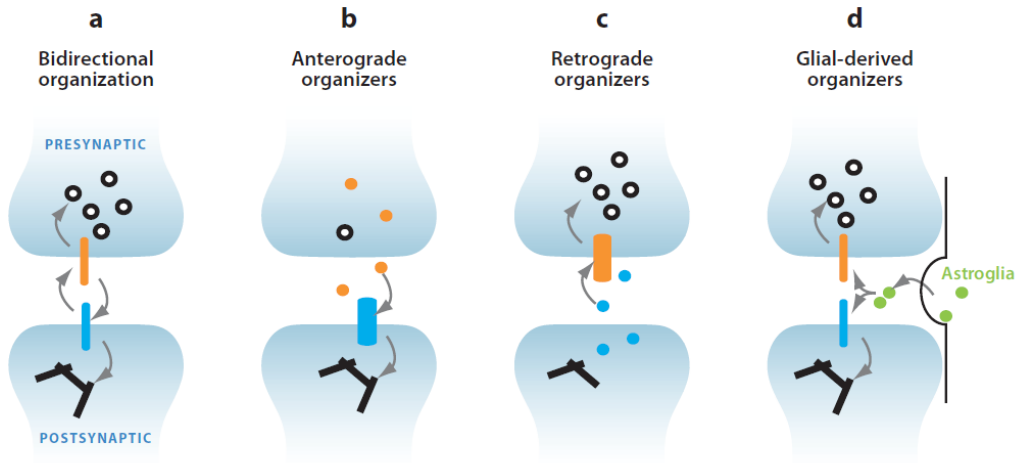

Figure 14: Different nature of synapse organizers
The synapse organizers can work bidirectionally (a), as anterograde organizers (b), as retrograde organizers (c) and as glial-derived organizers (d). From (Shen and Scheiffele, 2010)

2.5.2.1 Bidirectional organizers

From the discovery of the synaptogenic properties of neuroligin (Scheiffele et al., 2000) many studies have followed to find synaptogenic molecules. The use of bioinformatics tools and unbiased expression screening libraries for synaptogenic proteins has led to an explosion of the number of synaptogenic proteins. They are bidirectional organizers: neurexins, neuroligins, the family of LRRTM1-4, the family of Slitrk1-6, family of NGL 1-3, TrkC, IL1RAPL1, PTPδ and calsyntenin-3 amongst others (Scheiffele et al., 2000; Graf et al., 2004; Chih et al., 2005; Takahashi et al., 2012; Takahashi and Craig, 2013; de Wit and Ghosh, 2014).

The best known example of **bidirectional organizers molecules are the paired presynaptic neurexin and postsynaptic neuroligin**. The contact of dissociated neurons with neuroligin-expressing non-neuronal cells leads to recruitment of presynaptic markers (Scheiffele et al., 2000), while contact of the neurons with non-neuronal cells expressing neurexin recruits post-synaptic markers (Graf et al., 2004, Figure 15).

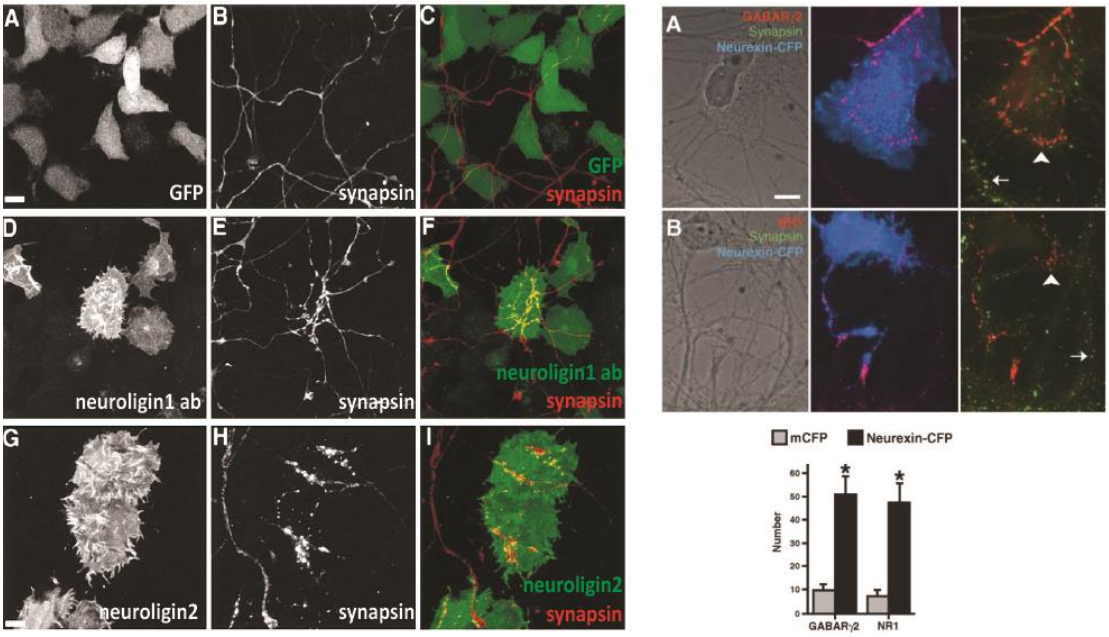

Figure 15: Examples of synaptogenic activity by neuroligins and neurexin

(Left) HEK293 cells transiently transfected with GFP (A–C), neuroligin-1ab (D–F) and neuroligin-2 (G-I) and cocultured with pontine explants. Neuroligin induces presynaptic accumulation in HEK293 transfected with neuroligin1-ab or neuroligin2. Adapted from (Scheiffele et al., 2000). (Right). Fibroblasts transfected with neurexin-1β-CFP cocultured with hippocampal neurons induced clusters of $GABA_AR\gamma2$ (A) and NR1 (B). In the bottom, the quantification shows that neurexin Clusters GABA and NMDA Glutamate Receptors. From (Graf et al., 2004).

To recruit the post-synaptic elements, the **neuroligins** have a PDZ-domain that can bind synapse scaffolding proteins and a gephyrin binding motif (Irie et al., 1997; Poulopoulos et al., 2009). **Neurexins** also have a PDZ-domain binding sequence to bind presynaptic scaffolding proteins such as CASK (Missler et al., 2012).

The discovery of the neurexin-neuroligin pair ***in vitro*** suggested that these molecules where the key molecules to form synapses. The first experiments showed that neuroligin-1 is only present at excitatory synapses (Song et al., 1999) and neuroligin-2 at inhibitory synapses (Varoqueaux et al., 2004). Coherent with these observations, the single knock-down of neuroligins in cultures, led to synapse loss, with a selectivity of neuroligin-1 for excitatory synapses and neuroligin-2 for inhibitory synapses. Overexpression of neuroligins in cultures increased neuronal synapse density, with specific effect of neuroligin-1 at excitatory and neuroligin-2 at inhibitory synapses (Chih et al., 2005; Chubykin et al., 2007).

Surprinsingly and contrasting with in vitro data, ***in vivo*** **triple knock-out of neuroligin-1,-2-,3 exhibit only a 15% decrease in synapse density** in the brainstem (Chih et al., 2005; Varoqueaux et al., 2006). However, this mice line exhibit more severe reductions in synaptic transmission due to defects in the recruitment of postsynaptic neurotransmitter receptors (Varoqueaux et al., 2006; Chubykin et al.,

2007). This means that although synaptogenic adhesion complexes can drive pre- and post-synaptic differentiation *in vitro*, only certain aspects of these functions are essential for synapse formation *in vivo*. The loss-of-function phenotypes in *Drosophila melanogaster* are more dramatic, as it was shown that the loss of neurexin reduces greatly the number of synaptic boutons and pre- and post-synapses detach (Li et al., 2007). This evidence compared to the mild phenotypes in vertebrates, shows the complexity of the vertebrate system where there are multiple, partially redundant parallel trans-synaptic pathways. For example, neurexin can bind to other synapse-organizing proteins, such as the LRRTM family in hippocampus (Wit and Ghosh, 2015), dystroglycan (Früh et al., 2016) and to cerebellins implicated in synapse formation in cerebellar Purkinje cells (Uemura et al., 2010). These multiple possible connections facilitate the maintenance of the overall function even with the loss of an individual synapse organizer (Takahashi and Craig, 2013). However, this might alter the excitation/inhibition ratio and stability/plasticity of a subset of synapses leading to pathological states (discussed in Section 2.7)

Molecules blocking the process of synapse formation have also been described. In the inhibitory synapse, neurexins can also bind MDGA1 preventing the neurexin-neuroligin2 interaction therefore **acting as a molecular brake** (Lee et al., 2013; Pettem et al., 2013b). Excitatory molecular brakes such as Nogo and MHCI have also been described but the underlying molecular mechanism are still unknown (Glynn et al., 2011; Wills et al., 2012). Thus, **the regulation by bidirectional synaptogenic organizers is an important step in synapse formation, regulated by molecular brakes and with redundancy** in vertebrates.

2.5.2.2 Anterograde organizers

Anterograde organizers are the factors secreted by the presynaptic element to drive the postsynaptic maturation. In this category, the best known molecule is **agrin.** Agrin is an extracellular matrix protein found at the neuromuscular junctions which is required for the clustering of postsynaptic acetylcholine receptor at the postsynaptic membrane (Shen and Scheiffele, 2010).

At central synapses, the family of neuronal **pentraxins can be secreted and act as synapse organizers**. Pentraxins bind to the extracellular N-terminal domain (NTD) of postsynaptic ionotropic glutamate receptors. In the family of pentraxins, neuronal activity regulated pentraxin (NARP) and neuronal pentraxin 1 (NP1) have been shown to be sufficient and necessary for GluA4 subunits clustering specifically at glutamatergic shaft synapses formed on GABAergic interneurons (Sia et al., 2007). This NTD domain is also present in GluN1 and GluN2 subunits of NMDA receptors. Furthermore, EphB-

receptor tyrosine kinase interact with these subunits and Ephrins can modulate spinogenesis (Henkemeyer et al., 2003). EphB receptors knockout has lower synapse density and the spines are under-developped (Kayser et al., 2008), suggesting a possible involvement of ephrins in the formation of NMDAR containing synapses.

A whole set of anterograde synapse organizer belong to the C1q/tumor necrosis factor (C1q/TNF) superfamily proteins. These **proteins are related to the C1q complement component cascade** and are highly expressed in the CNS (Matsuda, 2017). The first molecule discovered of this family was **cerebellin-1. It is secreted from cerebellar granule cells to form a bridge** between post-synaptic Gluδ2 and presynaptic neurexin. Gluδ2 expression by postsynaptic Purkinje cells, combined with exogenously applied Cbln1, was necessary and sufficient to induce new synapses *in vitro* and in the adult cerebellum *in vivo* (Matsuda et al., 2010; Uemura et al., 2010). Other proteins from the same family, **C1ql2** and **C1ql3**, are produced by hippocampal mossy fibers to recruit functional postsynaptic kainate glutamate receptors complexes at the mossy fiber to CA3 synapse via binding to the NTD of GluK2 and GluK4 subunits. (Matsuda, 2017).

2.5.2.3 Retrograde organizers

Retrograde organizers are factors secreted post-synaptically to influence the differentiation and maturation of pre-synaptic terminals. In the vertebrate NMJ, **laminin β2** is an extracellular matrix protein secreted by the muscle that extends through the synaptic cleft. Its loss leads to multiple presynaptic defects, suggesting that laminin β2 is essential for the maturation of presynaptic terminals (Noakes et al., 1995).

At mammalian central synapses, in the cerebellar glomerular rosette, **Wnt7a** and **FGF22**, are released by the postsynaptic granule cells during synapse formation. In culture, blocking either Wnts or FGF22 inhibits the maturation of the rosette. In Wnt7a knockout or the genetic inactivation of the receptor of FGF22, FGFR2c, leads delayed rosette formation (Hall et al., 2000; Umemori et al., 2004).

2.5.2.4 Glia-secreted organizers

Glial cells also play a role in synapse formation. Pure neuronal cultures supplemented with astrocyte-conditioned medium show increased number of synapses. (Mauch et al., 2001; Christopherson et al., 2005; Hughes et al., 2010). In retinal ganglion cell cultures, astrocyte-derived **cholesterol complexed to apolipoprotein E** increases the number of functional glutamatergic presynaptic terminals (Mauch

et al., 2001). In the same system, **thrombospondins** expressed by immature astrocytes increase the number of glutamatergic synapses (Christopherson et al., 2005). TGFβ1 secreted from astrocytes also increases glutamatergic synapses by modulating the levels of **D-serine** in cortical neurons (Pereira Diniz et al., 2012). GABAergic synaptogenesis has been shown to be increased upon secretion of a protein by astrocytes, but this factor has not been identified yet (Hughes et al., 2010). The underlying mechanism regulating the secretion of these molecules by the glia or the pathways activated in the neuron have not been assessed in any of these studies.

Recently it has been discovered that **hevin**, a protein secreted by astrocytes forms a bridge between two neurexin-1α and neuroligin-1β, two isoforms that do not interact directly with each other. The role of hevin is reminiscent of the roles C1q proteins (mentioned in 2.5.2.2). The role of hevin is crucial for the formation and plasticity of the thalamocortical connections in the developing visual cortex (Singh et al., 2016).

A clear role for glia in synapse formation has been found and probably involves different mechanisms, from bridging between transsynaptic molecules (Singh et al., 2016) to a possible activation of intracellular pathways in neurons.

2.5.3 Activity-dependent regulation of synaptic contacts

The first works studying the effect of activity modulation in the CNS were performed by Hubel and Wiesel. In this classical study they show that the visual experience is necessary for the formation of ocular dominance columns in the visual cortex (Le Vay et al., 1980), and since then many studies have followed. From the NMJ to the visual system, activity (spontaneous or driven by sensory experience) plays a role in refinement and maintenance of circuits in different systems and at different stages (Le Vay et al., 1980; Lichtman and Colman, 2000; Andreae and Burrone, 2014).

Most of the studies have been performed in the visual system, due to the simplicity of blocking the activity by visual deprivation. **Activity-dependent competition between the ipsi- and contra-lateral retinal axons is crucial for the correct establishment of the retinotopic maps by acting on the refinement of axon arborisation** (Penn et al., 1998; Stellwagen and Shatz, 2002). The activity-dependent competition has also been described in other systems such as the NMJ (discussed in 2.5.4). In the visual system as well, studies from the Yamamoto laboratory show how **the importance of activity in axon branch formation**. In the long-range axon collaterals that run in layer II/III of the visual

cortex, the absence of activity resulted in reduced axonal branching (Uesaka et al., 2005). Using pharmacology they identified netrin-4 and showed its expression in an activity-dependent fashion and that it can regulate axon branching (Hayano et al., 2014). These two examples of the role activity are restricted to a developmental period, but it is known that synapse formation and the regulation by activity occurs all throughout life in vertebrates. **Synaptic activity is crucial in all paradigms of plasticity**, as exemplified in long term potentiation protocols (Toni et al., 1999).

Activity in synapse formation

In the absence of synaptic vesicle release in mice deleted for a SNARE protein, Munc13-1 or Munc18-1, **there is no activity but morphologically normal synapses were formed** (Verhage et al., 2000; Varoqueaux et al., 2002). In Munc18-1 KO mice the synapse loss was massive in the cortex (Bouwman et al., 2004). In the NMJ, the deletion of the acetyl transferase completely abolishes the cholinergic transmission and show smaller motor nerve terminals that make fewer synapses (Brandon et al., 2003). In principal neurons of the visual cortex, the innervation pattern persists even in the absence of sensory inputs, suggesting that the subcellular specificity created by the homophillic interactions is encoded genetically (Cristo et al., 2004). Contrasting with these experiments, blockade of neuronal activity prevents the increased number of synapses induced by the overexpression of neuroligin-1 or neuroligin-2 (Chubykin et al., 2007). **Thus, activity is not necessary for synaptogenesis *per se*, but the number of synapses is reduced in absence of activity**.

This reduced number of synapses due to a defect in synapse formation or an increase in synapse elimination. Time-lapse imaging of hippocampal neurons showed that a high turnover of PSD95 (>20% of the PSD-95 clusters over 24 hours), could be inhibited by either blocking all activity or excitatory activity, showing thus that activity promotes synapse formation (Okabe et al., 1999). In line with this finding, it was shown in the mice retina that the activity-dependent glutamate release regulates the formation but not the elimination of synapses between the basket and retinal ganglion cells (Kerschensteiner et al., 2009). However, more recent studies demonstrated that in the visual system, monocular deprivation (a model for reduced activity of one eye) leads to a reduction in inhibitory synapse formation and to an increase in excitatory synapses **showing that the effect of activity in synapse formation can be cell-type dependent** (Andreae and Burrone, 2014).

In organotypic cerebellar cultures, neuronal activity exerts its effects by **increasing the number of inhibitory synapses** but with no change in excitatory ones (Seil and Drake-Baumann, 1994), and **this**

regulation seems to be mediated by BDNF (Seil, 1999). Control of the number of inhibitory synapses by neuronal activity has also been shown in the somatosensory cortex *in vivo* (Micheva and Beaulieu, 1995). In line with these studies showing that activity leads to increased inhibitory synapse formation, Marty and colleagues showed that in hippocampal organotypic slices from a P7 brain, thirteen days of the pharmacological blockade of $GABA_AR$ with bicuculine leads to an increase density of GABA synthethizing enzyme (GAD65), GABA and gephyrin immunoreactivity (Marty et al., 2000, 2004). In bicuculine-treated slices the application of an antibody blocking BDNF blunted the increased density of the GABAergic markers (Marty et al., 2000), **showing that the effect of activity could be mediated by BDNF.**

Hence, the effect of activity on synapse formation is cell-type dependant and in hippocampus and cerebellum the effect of activity increasing the inhibitory synapse number might be mediated by BDNF.

2.5.4 Synapse elimination

During development, an excess of synapses is formed and they will be removed to prevent excessive connections. Synapse elimination differs from pruning, but they refer to two different concepts that can be mixed. Pruning is a strategy to selectively remove excessive neuronal branches and connections in the immature nervous system to ensure the proper formation of functional circuitry; while synapse elimination is the process of removal of a synapse (Low and Cheng, 2006).

Often pruning is preceded by synapse elimination. For example, during the pruning of the infrapyramidal tract (IPT) of the hippocampus, distal infrapyramidal synapses are eliminated prior to IPT axonal retraction (Liu et al., 2005). It is not yet known, whether synapse elimination and axonal pruning within these tracts are separate, sequential, cellular events, or if both developmental processes are intrinsically connected and controlled by the same molecular mechanisms (Riccomagno and Kolodkin, 2015). Some authors suggest that synapse elimination is always the first step in the pruning process (Lin and Koleske, 2010). However, in the androgen-dependent pruning of the male mammary gland, it is likely not preceded by synapse elimination, suggesting that in this system there is a mechanistic separation between these developmental processes (Riccomagno and Kolodkin, 2015).

The molecular mechanisms mediating the synapse elimination are multiple. Here is a brief description of those mechanism based on the classification by (Riccomagno and Kolodkin, 2015):

1) **Self-destruction**: observed in the peripheral nervous system, in the mammillary gland of the rodent. Upon hormonal stimulation, a truncated form of trkB receptor leads to reduced neurotrophin signalling, leading to axonal pruning followed by apoptotic cell death (Liu et al., 2012).
2) **Transcriptional control of axon pruning**: in the dorsal root ganglion cells, the absence of neurotrophin leads to the activation of transcriptional factors (tbx6 and dleu2) and further signalling to axon pruning (Riccomagno and Kolodkin, 2015)
3) **Repulsive guidance cue signalling**: observed in the hippocampal IPT upon the expression of Sema3F. **Sema3F negatively regulates the number and size of dendritic spines in different hippocampal layers** possibly by promoting the loss of spines and synapses (Tran et al., 2009). **Sema5B in hippocampal cultures reduces synapse numbers**, possibly by destabilizing presynaptic terminals associated with a Sema5B-expressing postsynaptic cell (O'Connor et al., 2009).
4) **Neuronal activity**: In the vertebrate immature NMJ each myotube is multiinervated, and during development the most active will be selected and the rest will be eliminated, giving rise to monoinervation (Lichtman and Colman, 2000). Manipulations with activity show that we can bias the outcome of the selected axon (Buffelli et al., 2003). In the CNS, a similar case is found in the climbing fiber that innervates the Purkinje cell (PC). Early in development the PC is polyinnervated to give rise to a mature monoinnervation, where only the strongest connection kept (Riccomagno and Kolodkin, 2015). In this system, activity activates a metabotropic glutamate receptor 1 (mGluR1) signaling cascade in PCs that drives the perisomatic elimination of climbing fiber synapses (Hashimoto et al., 2001).

A summary of all the synapse elimination mechanisms observed in the vertebrate nervous system is found in Table 6.

Synapse (system)	Signal mediating the elimination	Reference
Motor axons to muscle fiber (Neuromuscular junction)	Unknown (regulated by activity)	(Lichtman and Colman, 2000)
Climbing fiber to Purkinje neuron connections (Cerebellum)	mGluR1 (regulated by activity)	(Hashimoto et al., 2001)
Thalamocortical axon to layer IV stellate neurons (mouse barrel cortex)	Suggested to occur via NMDA receptors	(Mizuno et al., 2014)
Infrapyramidal mossy fiber axon to CA3 synapses (hippocampus)	Sema3F binding to plexin-A3 and neuropilin-2 → modulation of actin citoskeleton	(Liu et al., 2005)
Corticospinal tract axons to layer V (visual and motor cortex)		(Low et al., 2008)
Retinal ganglion cell to dorsolateral geniculate nucleus (visual system)	C1q and C3 (complement pathway proteins regulated by activity)	(Bialas and Stevens, 2012; Schafer et al., 2012)

Table 6: Synapse elimination mechanisms in the vertebrate nervous system

As discussed, glia controls the formation of synapses but it plays also a role in synapse elimination. Microglia can phagocyte cellular debris or cellular compartments upon injury, and recent studies showed an implication in synapse elimination (Kettenmann et al., 2011). The works of Paolicelli showed that the neuronal release of fractalkine (CX3CL1), a chemokine that binds microglial CX3CR1, is a signal for **microglia to engulf synapses**. Mice knockout for CX3CR1 results in synaptic pruning defects in the hippocampus and cortex, and these defects correlate with changes in social behaviour (Paolicelli et al., 2011; Bilimoria and Stevens, 2015). Recently, **astrocytes were reported also to engulf synapses** (Chung et al., 2013).

Synapse elimination is a process that involves different mechanisms and different cell types in different systems to ensure correct synapse function.

2.5.5 Transcription factors regulating synapse formation

The expression of all the proteins described above must be controlled somehow during development. The spatiotemporal control of wiring specificity has been shown to be regulated by transcription factors (Shen and Scheiffele, 2010)

Transcriptional programs can control the expression of receptors that influence migration, axon guidance and synaptic partner selection therefore biasing wiring specificity (Polleux et al., 2007; Shen and Scheiffele, 2010). Transcription can also regulate common programs that drive the formation or

elimination of synapses in a population of cells, thus regulating synapse number. Examples of this transcriptional programs are MEF2A-D and Npas4.

The family of transcription factors **MEF2A-D are negative regulators of glutamatergic synapse** *In vitro* and *in vivo* data shows that MEF-2 supression leads to increase in glutamatergic synapse numbers, while its activation reduces synapse number (Pulipparacharuvil et al., 2008).

The neuronal PAS domain protein 4 (Npas4) is increased with neuronal activity, stimulating the formation of GABAergic synapses on Npas4-expressing cells (Lin et al., 2008). **Npas4 knockdown selectively reduces the number of inhibitory synapses** formed on both the soma and dendrites, suggesting that Npas4 may regulate the development of inhibitory synapses originating from multiple interneurons. The downstream targets of Npas4 are multiple including BDNF but others targets controlling inhibitory synapse number have been suggested (Bloodgood et al., 2013).

2.6 Current knowledge of mechanism of synaptogenesis at the inhibitory synapse

The new technical advances have made it possible to obtain a catalog of proteins present at inhibitory synapses. Here I describe in detail all the molecules found in the inhibitory synapse: (i) trans-synaptic adhesion (Figure 16) (ii) secreted factors and (iii) intracellular submembranous scaffolds (Figure 17). I will describe the impact of its deletion and the synapse/region specificity if it is known.

2.6.1 Trans-synaptic adhesion proteins

Neuroligin-2 (NL-2) was the first adhesion molecule and synapse organizer reported to be selectively present at inhibitory synapses (Varoqueaux et al., 2004). Although it was first believed to drive inhibitory synapse formation throughout all the brain, in the brainstem and in cerebellar Purkinje cells NL-2 plays a role in synapse maturation but not in synapse formation (Zhang et al., 2015). Extracellularly it contacts neurexins and MAM domain-containing GPI anchor proteins (MDGAs). Neuroligins contain a short intracellular domain that contains a PDZ domain binding and a tyrosine-based motif; allowing thus to interact with scaffolding proteins (gephyrin, collybistin, and S-SCAM). These interactions allows the further recruitment of inhibitory postsynaptic machineries (Poulopoulos et al., 2009). In hippocampal neurons, NL-2 overexpression leads to increased GABAergic synapse density, while its deletion reduces it (Chih et al., 2005). In the NL2-KO mice, inhibitory synapses are formed although the content of synaptic gephyrin and $GABA_AR$ clusterings is reduced and the inhibitory synaptic transmission is impaired. These deficits are limited to GABAergic synapses in the perisomatic region, as GABAergic synapse density is reduced in somatic, but not the dendritic region of CA1 pyramidal neurons affecting mainly fast-spiking interneurons (Lu et al., 2017).

Neuroligin-3 (NL-3) is present at both excitatory and inhibitory synapse. The R451C mutation has been associated with autism spectrum disorders (ASD) (Etherton et al., 2011). The NL3-R451C knockin mouse displays increased inhibitory transmission in the somatosensitory cortex; however in the hippocampus the picture is more complex, because it has differential effect at inhibitory synapses in parvalbumin- and cholecystokinin- interneurons (Etherton et al., 2011; Krueger-Burg et al., 2017). The mechanism for these circuit-specific effects remains unknown, but likely depends on the precise composition of the individual postsynaptic organizing complexes.

Neuroligin-4 (NL-4) is at inhibitory synapses in retina, hippocampus, spinal cord and brainstem and probably in other regions at low levels (Hoon et al., 2011). Its deletion in the hippocampus impairs the

protein composition and function of perisomatic inhibitory synapses and causes a prominent disruption of hippocampal rhythmogenesis (Jamain et al., 2008).

Neurexins (NRXNs) are present at both excitatory and inhibitory synapses, targeted to the presynaptic terminals. In the mammalian genome 3 NRXN genes exist, each encoding α-protein and a β-protein (Missler et al., 2012). They can undergo alternative splicing to generate thousands of different isoforms of NRXN. They bind to neuroligins and drive the pre-synaptic assembly (Südhof, 2008).

Slitrk3 contains LRR domains. Slitrk3 is selectively localized to inhibitory synapses where it acts as a synapse organizer when binding to its presynaptic partner (PTPδ). Its overexpression in hippocampal neurons leads to increased GABAergic, but not excitatory, synapse formation; while its knockdown reduces selectively GABAergic synapses. Slitrk3-deficient mice exhibit reduced inhibitory synapse density and transmission in hippocampal CA1 (Takahashi et al., 2012).

Protein tyrosine phosphatase δ (PTPδ). Belongs to the immunoglobulin superfamily. Present at both excitatory and inhibitory presynaptic terminals. Binds to Slitrk3 and other Slitrks, as well as other CAMs of the family of immunoglobulins (Takahashi and Craig, 2013).

Dystroglycan is the central component of the dystrophin-glycoprotein complex (DGC) that links the extracellular matrix to the cytoskeleton. Dystroglycan plays a selective role in the formation, maintenance and function of perisomatic CCK- positive presynaptic terminals (Früh et al., 2016).

MAM domain-containing GPI anchor proteins (MDGA1-2) belong to the immunoglobulin superfamily of adhesion molecules. Both of them have been implicated in ASDs and schizophrenia (Pettem et al., 2013b). **MDGA1 is a negative regulator of the formation of inhibitory synapses**, they interact with NL-2 preventing the NL2-neurexin binding (Lee et al., 2013; Pettem et al., 2013b). MDGA2 has been shown to suppress the development of excitatory synapses by blocking the recruitment of glutamatergic synaptic vesicles into VGAT-positive sites (Loh et al., 2016)

Neurofascin 186 (NF186) is a CAM belonging to the immunoglobulin superfamily. NF186 is localized to the axon initial segment (AIS) of neurons and its knock-down in forebrain reduces the density of AIS innervation by parvalbumin-positive chandelier cells (Kriebel et al., 2011), thus reducing inhibitory synaptic transmission, neuron excitability, and long-term potentiation (Saha et al., 2017). In cerebellar Purkinje cells NF186 is necessary to stabilize inhibitory pinceau synapses at the AIS (Lu et al., 2017)

Contactins (CNTNs) belong to the immunoglobulin superfamily of CAMs. They interact with receptor protein tyrosine phosphatases (RPTPs) and L1 family cell adhesion molecules (Lu et al., 2017). CNTNs are involved in synapse development, and CNTN1 and CNTN5 have been implicated in GABAergic synapse development. Genetic deletion of CNTN1 leads to a significant reduction of GABAergic synapse number between Golgi cells and granule cells in cerebellar cortex (Lu et al., 2017). Importantly, genetic deletion of CNTN5 causes a significant reduction of axoaxonic GABAergic synapses in the spinal cord (Ashrafi et al., 2014). This is hypothethised to occur through trans-synaptic adhesion interactions with PTPs and extracellular matrix proteins.

Immunoglobulin superfamily (IgSF) member 9 transmembrane proteins, IgSF9 and IgSF9b, are highly expressed in all the brain and localized to dendrites (Ko et al., 2015) . Both of them are synaptic adhesion molecules but cannot function as a synapse organizer, suggesting that their role is more on synapse specification. **IgSF9** is expressed in pyramidal cells and a subset of interneurons, where it regulates inhibitory synapse development. IgSF9-KO mice slices showed a fewer functional inhibitory synapses and decreases inhibitory synapse markers in hippocampal CA1 region (Mishra et al., 2014). **IgSF9b** is required at inhibitory synapses projecting to inhibitory interneurons. IgSF9b is localized in a subsynaptic domain that is separate from the $GABA_AR$/gephyrin/NL-2 complex and binds to NL-2 indirectly via the scaffolding protein S-SCAM (Woo et al., 2013).

Neuroplastin-65 belongs to the immunoglobulin superfamily. Specifically expressed in the forebrain and enriched in postsynaptic density fractions, regulates excitatory and inhibitory synapse development (Beesley et al., 2014). It directly interacts with $GABA_AR$, and its knockdown decreases GABAA receptors at synaptic sites (Sarto-Jackson et al., 2012). In neuroplastin-65-KO mice, both excitatory and inhibitory synapses are affected in CA1 and the DG of the hippocampus, and $GABA_AR$ composition is altered (Ko et al., 2015).

Calsyntenins are members of the cadherin superfamily of cell adhesion molecules. Two of them have been associated with synapse development. (Pettem et al., 2013a). **Calsyntenin-3** induces inhibitory and excitatory presynaptic differentiation in heterologous synapse-formation assays through contact with α-neurexins (Pettem et al., 2013a; Um et al., 2014). Calsyntenin-3 regulates positively the number of excitatory and inhibitory synapses therefore modulating synaptic transmission (Pettem et al., 2013a). **Calsyntenin-2** is exclusively at inhibitory synapses (Lipina et al., 2016). Deletion of Calsyntenin-2 results in a reduction of the number of parvalbumin interneurons affecting selectively the inhibitory synaptic transmission (Lipina et al., 2016). Interestingly, calsyntenin-2 is not a synapse organizer as compared to calsyntenin-3 (Um et al., 2014). Single knock-down of calsyntenin-2 did not affect synapse

number, but the triple knock-down of all calsyntenins in cultured neurons reduced density for excitatory and inhibitory markers and leads to an impaired inhibitory, but not excitatory synapse transmission (Um et al., 2014). This opens a possibility that he three calsyntenin isoforms may have redundant functions in certain context.

Sema4D is a transmembrane protein, which is cleaved to release its extracellular domain for signalling and this residue will bind to its presynaptic **PlexinB1** to regulate GABAergic synaptogenesis (Lu et al., 2017). Knockdown of Sema4D decreases density of GABAergic synapses, but not of glutamatergic synapses (Raissi et al., 2013). Purified extracellular domain of Sema4D can rapidly induce new GABAergic synapse formation in hippocampal neurons (Kuzirian et al., 2013).

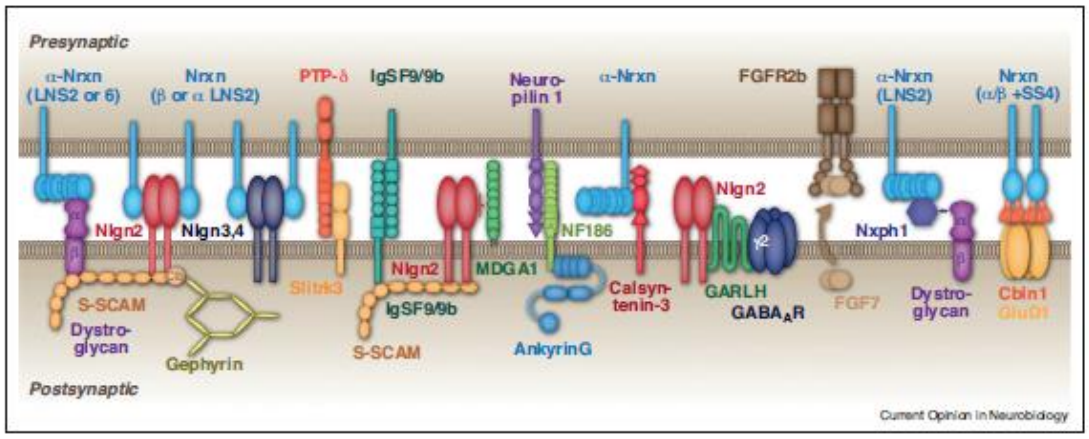

Figure 16: Schematic representation of the trans-synaptic proteins of the GABAergic synapse and their intracellular interactors
From (Krueger-Burg et al., 2017)

2.6.2 Secreted factors

FGF7 member of the fibroblast growth factor (FGF) family. FGF7 acts selectively on the inhibitory synapse to promote the maturation of the presynaptic terminal. FGF7 is secreted postsynaptically to bind the FGFR2b-expressing neurons, promoting the clustering of VGAT (Terauchi et al., 2010). FGF7-KO mice show impairments in the inhibitory innervation to CA3 pyramidal neurons (Ko et al., 2015).

Neurexophilins comprise a family of four secreted glycoproteins (Nxph1-4) that bind specifically to neurexin. The binding of Nxph1 to neurexin, blocks the binding between neurexin and dystroglycan (Reissner et al., 2014). Ectopic expression of Nxph1 at excitatory synapses in cortex leads to ectopic recruitment of both presynaptic $GABA_BR$ and postsynaptic $GABA_AR$ (Born et al., 2014).

Cerebellins (Cblns) are members of the C1q family of secreted proteins. They act as trans-synaptic bridges, binding to presynaptic neurexin and postsynaptic GluRδ2 (in cerebellum) or GluRδ1 (in the forebrain). Nrxn/Cbln/GluRδ1 in cortical neurons stimulates the accumulation of VGAT at inhibitory presynaptic terminals (Yasumura et al., 2012).

Wnt5a would activate the non-canonycal Wnt pathway to increase the number of GABAergic synapses. This evidence was shown in a mice model lacking dystrophin, were the inhibitory is already reduced (Fuenzalida et al., 2016). The possible contribution of Wnt5a in physiological state remains to be elucidated.

BDNF it is synthesized and released by pyramidal neurons to bind its receptor, trkB that is present in interneurons. BDNF signalling promotes GABAergic synapse development, as demonstrated by BDNF gene inactivation leads to reduced inhibitory synapse density and reduced inhibitory synaptic transmission (Hong et al., 2008). Similar results were obtained in a mice depleted for trkB in the cerebellar neurons (Rico et al., 2002). NL-2 was not reduced in this mice suggesting that trkB may act downstream of NL-2 or in a different pathway (Chen et al., 2011). This effects might be mediated by modulation of signalling pathways such as MAPK and Akt (Wuchter et al., 2012).

GABA is the main inhibitory neurotransmitter in the adult brain, but in the developing brain GABA is depolarizing due to the low expression of KCC2 (Rivera et al., 1999; Represa and Ben-Ari, 2005). During the period of synapse formation GABA has been shown to regulate neurite outgrowth in different systems such as the chick cortical and retinal neurons (Spoerri, 1988), rodent hippocampal neurons (Barbin and Pollard, 1993), cerebellar granule cells (Borodinsky et al., 2003), spinal cord cells (Tapia et al., 2001), cortical plate and subplate interneurons (Maric et al., 2001) and raphe nuclei 5-hydroxytrypta- mine (serotonin)-producing neurons (Lauder et al., 1998). Subsequent studies showed that GABA depolarizes the membrane and the effects are exerted by the Ca^{2+} entry via L-type Ca^{2+} channels (Perrot-Sinal et al., 2003). In a model of cerebellar neurons, CAMKII and MAPK where proposed as downstream effectors of this regulation (Borodinsky et al., 2003). More recent studies have shown how $GABA_AR$ is able to induce functional synapse when co-expressed in non-neuronal cells in contact with GABAergic medium spiny neurons in a timescale of hours (Fuchs et al., 2013) and even in a shorter timescale, direct application of **GABA in young neurons lead to formation of functional GABAergic synapses** (Oh et al., 2016).

The trophic roles of GABA *in vivo* in its own synapse have been demonstrated upon conditional knock down of GAD67 in parvalbumin interneurons in the visual cortex, resulted in axonal branching defects in these neurons and a reduction in inhibitory innervation in pyramidal cells. The overexpression of GAD67 in these cells accelerated the maturation of somatic innervation (Chattopadhyaya et al., 2007). In cerebellum, deletion of $GABA_AR$ subunits leads to synapse loss (Fritschy et al., 2006). In immature cultured hippocampal neurons, GABA augment levels of intracellular BDNF mRNA, in a $GABA_AR$ dependent manner (Berninger et al., 1995). **It is thus plausible that the trophic effects of GABA in maturing brain are mediated partly via BDNF and trkB activation**.

2.6.3 Intracellular submembranous scaffold

These array of proteins act as hubs to link the CAMs and the synaptic organizer proteins to the cytoskeleton and downstream signaling pathways.

Gephyrin is the main scaffolding protein of the inhibitory synapse. Essential for glycine and $GABA_AR$ clustering, inhibitory synaptic transmission, and plasticity. Its clustering to the inhibitory synapse is regulated by BDNF, GSK-3β, CDK5 and collybistin-dependent phosphorylation (Choii and Ko, 2015). An array of post-translational modification on gephyrin have been described, most of them influencing the clustering, suggesting that multiple mechanisms could modulate its functions, and inhibitory synapse development (Tyagarajan et al., 2011).

Synaptic scaffolding molecule (S-SCAM) or membrane associated guanylate kinase inverted-2 (**MAGI-2)** is a scaffolding molecule found in both excitatory and inhibitory synapses. In the inhibitory synapses, it interacts with different transynaptic adhesion complex such as NL-2, the DGC, IQSEC3, and IgSF9b (Woo et al., 2013; Krueger-Burg et al., 2017).

GARLH family proteins $GABA_AR$ regulatory Lhfpl (GARLH) family of putative auxiliary subunits of GABAARs. Although it has an extracellular domain, it functions as a submembranous scaffolding protein. GARLH family members LH3 and LH4 form a stable complex with γ2- containing GABAARs and NL-2. Knock-down of GARLH4 resulted in a loss of synaptic GABAAR-γ2 and gephyrin clusters, as well as a reduction in the frequency of inhibitory synaptic transmission in the hippocampus (Yamasaki et al., 2017).

Inhibitory Synapse Protein 1 and 2 (InSyn1-2) Found to colocalize and bind gephyrin and the DGC. In a knockdown approach for both InSyn1 and Insyn2 showed impaired inhibitory transmission in hippocampus (Uezu et al., 2016)

Collybistin, the guanine nucleotide exchange factor collybistin was the first regulator of small GTPases to be identified in inhibitory synapse formation. **Links neuroligin-2 with gephyrin**, being essential for recruitment of gephyrin to GABAergic synapses (Poulopoulos et al., 2009). Only present in hippocampus and basolateral amygdala (Papadopoulos et al., 2007).

BRAG3 (also known as synArfGEF(P0) or IQSEC3) is a guanine nucleotide exchange factor. It is exclusively localized to inhibitory synapses where it associates with the DGC complex and S-SCAM and gephyrin (Fukaya et al., 2011; Um et al., 2016). The knockdown of BRAG3 in hippocampal neurons leads to a decrease in gephyrin puncta size, while its overexpression leads to increased density of gephyrin (Um et al., 2016).

SRGAP2 (Slit-Robo Rho-GTPase activating protein 2) and **WRP** (WASP family veprolin-homologous protein associated Rac GAP, also known as SRGAP3) are Rac1-specific GTPase activating proteins and were first identified as gephyrin-interacting molecules (Okada et al., 2011). In WRP KO mice the density of gephyrin and $GABA_AR$ punctae is decreased (Krueger-Burg et al., 2017). SRGAP2A and SRGAP2C, human paralogs of SRGAP2, were identified as co-regulators of the development of excitatory and inhibitory synapses. SRGAP2A was shown to couple GTPase signaling to postsynaptic scaffold proteins at both excitatory and inhibitory synapses through physical interactions with Homer and gephyrin, respectively. In contrast, SRGAP2C inhibits all functions of SRGAP2A at synapses (Fossati et al., 2016).

PX-RICS (ArhGAP32 isoform 1) is a GTPase activating proteins for Cdc42 and Rac1 (Hayashi et al., 2007). PX-RICS interacts with GABARAP facilitating the trafficking of CAMs (Nakamura et al., 2010). It is hypothesized to control the localization of gephyrin in concert with other guanine exchanging factor such as collybistin and IQSEC3 (Krueger-Burg et al., 2017).

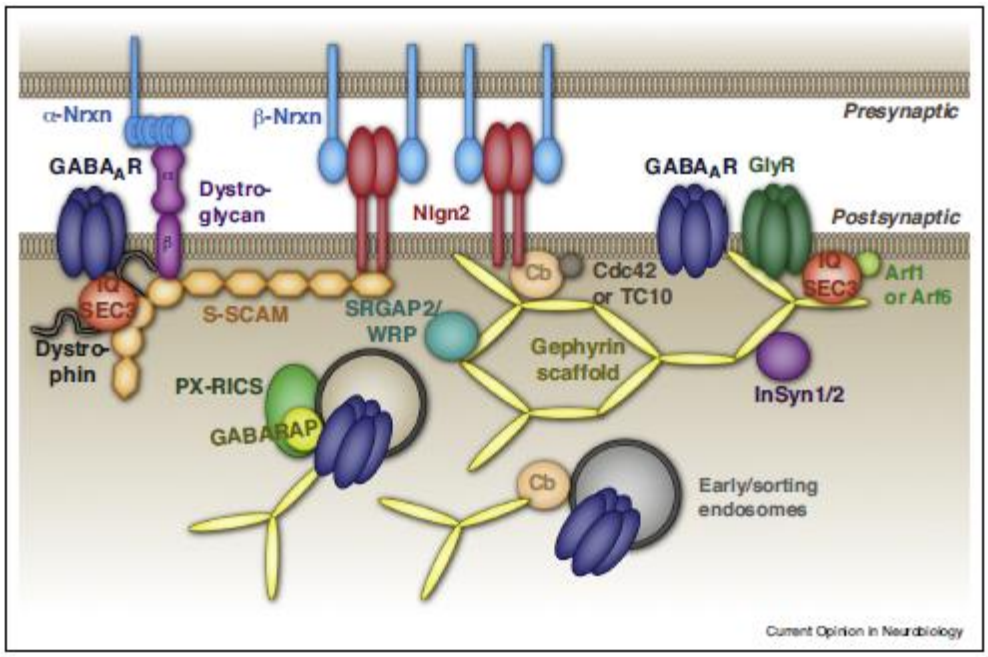

Figure 17: Intracellular scaffolds of the inhibitory synapse

From (Krueger-Burg et al., 2017)

2.6.4 Synapse specificity

This is an extensive list of all the proteins found at inhibitory synapse. However, not all the elements mentioned are at all inhibitory synapses, thus we cannot talk about a single and unique inhibitory synapse, the inhibitory synapse is different from synapse to synapse (Figure 18).

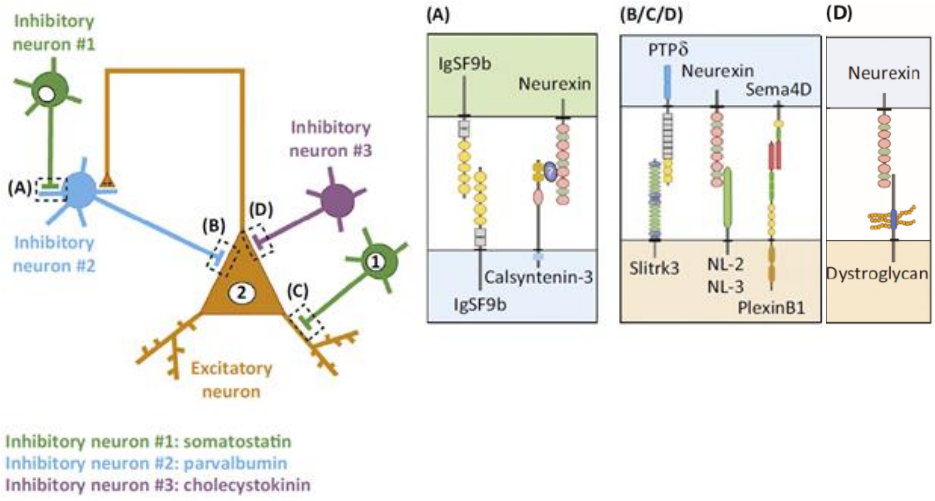

Figure 18: Inhibitory synapse organizers act on different synapses

See a pyramidal neuron (orange) interconnected to interneurons (green, blue or violet). In the boxes, see the inhibitory synaptic pathways based on their subcellular localization. (A) Inhibitory synapse formed on an interneuron. (B–D) Inhibitory synapses formed on the pyramidal neuron (Ko et al., 2015).

In Figure 18 are depicted molecules that are exclusively in the interneuron to interneuron synapse (Box A: IgSF9b-IgSF9b and Neurexin-Calsyntenin-3), while others are in the inhibitory to pyramidal cell (Box B/C/D: PTPδ-Slitrk3, Neurexin-NL2/3, Sema4D-PlexinB1). From these elements it is known that neuroligin-2 synapses form mostly on perisomatic regions from parvalbumin interneurons (Poulopoulos et al., 2009), however the synapse specifity of the rest of elements is lacking. In Box D, find neurexin-dystroglycan which has been showed to occur only in the CCK to pyramidal cell synapse (Früh et al., 2016). All the molecules presented in Figure 18 are present in the hippocampus. However, other molecules present in the inhibitory synapse have region-specific pattern of expression such as the cerebellin, restricted to the cerebellum or forebrain (Krueger-Burg et al., 2017) and neuroplastin-65, only expressed in the forebrain (Beesley et al., 2014)

The information of the content of every synapse will enable a better comprehension of molecular synaptic connectome, which has implications in physiology and pathology (Section 2.7). However, the synapse specificity of many of this proteins is still lacking.

2.7 Defects in synapse formation: implications in pathology

For an appropriate neural circuit function, the formation and specification of synapses is immensely important. The disorders arising from defects in synapse formation, function and/or plasticity have been defined as synaptopathies. There are two groups of pathologies that have been linked to the inhibitory synapse: epilepsy and psychiatric disorders. Epilepsy occurs when the balance excitation/inhibition is perturbed. Psychiatric disorders occur upon alterations in neural circuit structure and function.

2.7.1 Epilepsy

Epilepsy is a brain disorder characterized by the appearance of seizures. Those can be caused by multiple mechanisms, but they all converge in an imbalance between excitation and inhibition resulting anomalous synchronous activities underlying seizures (Reid et al., 2009). Disrupting the mechanisms that inhibit firing or promoting the mechanisms that facilitate excitation can cause seizures.

Many anti-epileptic drugs target $GABA_AR$s to increase inhibitory signalling (Schmidt and Schachter, 2014). The response to the treatment depends on several factors such as the aetiology and severity of the epilepsy, the genetic factors and inflammatory processes amongst others.

Some epilepsies arise due to a single gene mutation, but the majority come from the interaction between genes and environmental factors (Berkovic et al., 2006). Multiple genes have been linked to epilepsy, mainly affecting ion channels either directly or indirectly. Three subunits of the $GABA_AR$ have been linked to epilepsy (Table 7)(Tan et al., 2007; Reid et al., 2009; Bouthour et al., 2012).

Gene (subunit of $GABA_AR$)	Syndrome	Genetic confirmation	Functional *in vitro*	Functional *in vivo*
GABRG2 (γ2)	FS/GEFS+	Yes	Yes	Yes
GABRA1 (α1)	IGE	Yes	Yes	-
GABRD (δ)	IGE/GEFS+	-	Yes	-

Table 7: Mutations in $GABA_AR$ subunits lead to epilepsy

From (Reid et al., 2009) FS=febrile seizures, GEFS=generalized epilepsy with febrile seizures, IGE=idiopathic generalized epilepsy

Different mutations give rise to different epileptogenic mechanisms. The mutation alpha1A322D in GABAARα1 subunit affects mainly the channel gating (Gallagher et al., 2004) while the K289M mutation in GABAARγ2 affects the diffusion and clustering of $GABA_AR$ upon hyperthermia situation

(Bouthour et al., 2012). **Both mutations converge in an impaired inhibitory synaptic transmission and thus lead to epilepsy.**

2.7.2 Psychiatric disorders

Psychiatric disorders are complex multifactorial disorders involving chronic alterations in neural circuit structure and function (Bagot et al., 2014). Here are listed the list of psychiatric disorders linked to inhibitory synapse (Table 8). Defects in the formation of the inhibitory synapse is are correlated often with autism spectrum disorders (ASD) and schizophrenia, but epilepsy, attention deficit hyperactivity disorder (ADHD), depression, anxiety and intellectual disability have also been associated (Table 8).

Molecule	Disease	Reference
Neuroligin-2	Schizophrenia, anxiety, ASD	(Sun et al., 2011; Parente et al., 2017)
Neuroligin-3	ASD	(Kleijer et al., 2014)
Neuroligin-4	ASD	(Kleijer et al., 2014)
S-SCAM	Schizophrenia	(Walsh et al., 2008)
Collybistin	Epilepsy, anxiety, ID	(Kalscheuer et al., 2009; Papadopoulos et al., 2015)
Dystroglycan complex	ID, ASD, ADHD	(Waite et al., 2012)
Gephyrin	ASD, Schizophrenia, Epilepsy	(Lionel et al., 2013)
IgSF9b	Depression	(Shyn et al., 2011)
Iqsec3	ASD, Schizophrenia	(Ellis et al., 2016)
PX-RICS	ASD	(Nakamura et al., 2016)
MDGA1-2	ASD, Schizophrenia	(Kähler et al., 2008; Pettem et al., 2013b)
Neuroplastin-65	ID	(Desrivières et al., 2015)
Alpha-neurexin	Schizophrenia, ASD	(Kenny et al., 2014)

Table 8: Molecules of the inhibitory synapse that have been linked to neuropsychiatric disorders

At the time when mutations in neuroligin were identified as causal for psychiatric disorders (Jamain et al., 2003), it was shown that these molecules are synapse organizers that can induce the recruitment of the pre- and post-synaptic component *in vitro* studies; suggesting a crucial in synapse formation. However, *in vivo* studies in mice lacking NL-1, NL-2 and NL-3 die at birth, but they have nearly normal synapse numbers with an apparently normal ultrastructure. Electrophysiological analyses showed a severe impairment of synaptic transmission (Missler et al., 2003; Varoqueaux et al., 2006). This has led (Südhof, 2008) to suggest that **the trans-synaptic complexes trigger signal transduction events that activate synaptic function essential for the correct functioning of the synapse**. When mutations are

found in these molecules, abnormalities in synaptic transmission in a subset of neural circuits causing the symptomatology of the disease (or at least, partly).

Many works have taken ASD as a matter of study and there are points still to be understood: in families with mutations in SHANK3 (scaffolding molecule of the excitatory synapse) some individuals have ASD symptoms while others not (Südhof, 2008). Another controversial point are the different phenotypes arisen from the same mutation: in two brothers the same mutation in NL-4, one suffered ASD while the other brother showed Tourette's syndrome. In the recent years, genetic studies have identified a large number of mutations that may collectively explain up to 15–20% of all ASD cases (Delorme et al., 2013; Ghosh et al., 2013), while the pathophysiology of the rest of cases in still a matter of debate. **Thus suggesting that the mutations may only increase the chance of ASD and other factors might contribute to the development of the disease.** Recently, some studies have described epigenetics modifications (Bagot et al., 2014) and even in metabolism (Novarino et al., 2012) that can lead to ASD. **These studies prompt the idea that ASDs are multifactorial diseases and only part of the pathophysiology of the ASD could be mediated by defect in synapse function** (Bourgeron, 2015).

MATERIALS AND METHODS

MATERIALS AND METHODS

Neuronal culture

Primary cultures of hippocampal neurons were prepared as previously described (Chamma et al., 2013) with some modifications of the protocol. Briefly, hippocampi were dissected from embryonic day 18 or 19 Sprague-Dawley rats of either sex. Tissue was then trypsinized (0.25% v/v), and mechanically dissociated in 1x HBSS (Invitrogen, Cergy Pontoise, France) containing 10 mM HEPES (Invitrogen). Neurons were plated at a density of 60 or 120 × 103 cells/ml onto 18-mm diameter glass coverslips (Assistent, Winigor, Germany) pre-coated with 50 µg/ml poly-D,L-ornithine (Sigma-Aldrich, Lyon, France) in plating medium composed of Minimum Essential Medium (MEM, Sigma) supplemented with horse serum (10% v/v, Invitrogen), L-glutamine (2 mM) and Na+ pyruvate (1 mM) (Invitrogen). After attachment for 3-4 hours, cells were incubated in culture medium that consists of Neurobasal medium supplemented with B27 (1X), L-glutamine (2 mM), and antibiotics (penicillin 200 units/ml, streptomycin, 200 µg/ml) (Invitrogen), and kept for up to 4 weeks at 37°C in a 5% CO2 humidified incubator. Each week, one fifth of the culture medium volume was renewed. In certain experiments, cytosine d-D-arabinofuranoside (AraC) (5 µM) was added at DIV1 to obtain pure neuronal cell cultures.

DNA constructs

The following constructs were used: *GEPHN* 3'-UTR shRNA and control shRNA-3m (Yu et al., 2007; Tyagarajan et al., 2011), eGFP-gephyrin P1 variant (Lardi-Studler et al., 2007), eGFP-gephyrin S303A and S303D mutants (Tyagarajan et al., 2011, 2013; Flores et al., 2014), shRNA against $A_{2A}R$ (Simões et al., 2016), non-target shRNA coupled to GFP (Gauvain et al., 2011). GABAARγ2-GFP (Eugène et al., 2007), shRNA against $GABA_AR$ γ2 subunit (Li et al., 2005), gephyrin-mRFP (Chamma et al., 2013), shRNA against Neuroligin 2 (kindly provided by Peter Scheiffele, Addgene plasmid # 59358) (Chih et al., 2005), shRNA against slitrk3 coupled to CFP (Takahashi et al., 2012) and a scrambled shRNA sequence "shMock" (kindly provided by Ann Marie Craig, Vancouver, Canada). All the constructs were sequence-verified by Beckman Coulter Genomics.

Neuronal transfection

Transfections were carried out at DIV 6-7 for neurons undergoing synaptogenesis, DIV 14 in adults neurons using Lipofectamine 2000 (Invitrogen) or Transfectin (BioRad, Hercules, USA), according to the manufacturers' instructions (DNA:transfectin ratio 1 µg:3 µl), with 1µg of plasmid DNA per 20 mm well. The following ratios of plasmid DNA were used in co-transfection experiments: 0.5:0.5 µg for eGFP-S303A/eGFP-S303D: GEPHN 3' UTR shRNA, 0.8:0.5 µg for GABAARγ2-GFP: gephyrin-mRFP

Experiments were performed 2-5 days post-transfection in neurons undergoing synaptogenesis, 10 days post-transfection for mature neurons.

Pharmacology

For ICC experiments, SCH58261 (100 nM, Abcam), ADA (4-20U/mL, Roche), AMPCP (100 µM, Sigma) and/or CGS21680 (30nM, Abcam), were directly added to the culture medium and the neurons were returned to a 5% CO2 humidified incubator for 10 min to 1 hour before use. Experiments using tetanus toxin (1-40nM, Alomone Labs) or Nrx1b-Fc peptide (60 µg/mL)(Scheiffele et al., 2000; Levinson et al., 2005), cells were treated for 2 days (from DIV7 to 9) and then the appropriate drugs were added for 30 min to the toxin or the peptide solution. For SPT experiments, neurons were labeled at 37°C in imaging medium (see below for composition) in presence of SCH58261, transferred to a recording chamber and recorded within 45 min at 31°C in imaging medium in presence of SCH58261. The imaging medium consisted of phenol red-free minimal essential medium supplemented with glucose (33 mM; Sigma) and HEPES (20 mM), glutamine (2 mM), Na^+-pyruvate (1 mM), and B27 (1X) from Invitrogen.

Immunocytochemistry

To label and quantify the density of inhibitory synapses, pre-treated neurons were fixed for 15 min at RT in paraformaldehyde (PFA; 4% w/v; Sigma) and sucrose (14% w/v; Sigma) solution in 1X PBS. Cells were then washed and permeabilized with a solution containing Triton X-100 (0.25% w/v, Carl Roth GmbH) diluted in PBS 1X. Cells were then incubated for 1 hour at RT in goat serum (GS; 10% v/v; Invitrogen) and Triton X-100 (0.1% w/v) in PBS to block nonspecific staining. Neurons were then incubated for 1 hour to overnight with a primary antibody mix consisting of rabbit anti-VGAT (1:500, provided by B. Gasnier, Univ. Paris Descartes, Paris), mouse anti-gephyrin (mAb7a, 1:500, Synaptic Systems) and GABAARγ2 subunit (1:2000, provided by J.M. Fristchy, Univ. Zurich) in PBS supplemented with GS (10% v/v, Invitrogen) and Triton (0.1%v/v). After washes, cells were incubated for 45 min at RT with a secondary antibody mix containing donkey anti-guinea pig-cy3 (1:400, Jackson Immunoresearch), goat anti-rabbit-FITC (1:300, Jackson Laboratories) and donkey anti-mouse-cy5 (1:300, Jackson Laboratories) in PBS-GS-Triton blocking solution, washed, and finally mounted on glass slides using Mowiol 4-88 (48 mg/ml, Sigma). Sets of neurons compared for quantification were labeled simultaneously.

For $A_{2A}R$ detection over time in culture, cells were fixed for 15 min at RT in PFA solution (as above), washed in PBS, and permeabilized with Triton as above. After washes, cells were incubated for

1 hour at RT in PBS-GS-Triton blocking solution and incubated for 1 hour with a mouse antibody against GAD 67 (1:500, Chemicon) and rabbit antibody against $A_{2A}R$ (1:100, Alomone labs) in PBS-GS-Triton staining solution. After washes, cells were incubated for 45 min at RT with goat anti-rabbit-cy3 (1:500, Jackson Laboratories) and goat anti-mouse-FITC (1:300, Jackson Laboratories) in PBS-GS-Triton solution, washed, and mounted on glass slides using Mowiol 4-88 (48 mg/ml, Sigma). Sets of neurons compared for quantification were labeled simultaneously.

For STORM imaging of $A_{2A}R$ at inhibitory synapses, cells were fixed for 15 min at RT in PFA solution (as above), washed in PBS, and permeabilized with Triton as above. After washes, cells were incubated for 1 hour at RT in PBS-GS-Triton blocking solution and incubated overnight at 4ºC with a rabbit antibody against $A_{2A}R$ (1:100, Alomone Labs) and mouse anti-gephyrin (mAb7a, 1:500, Synaptic Systems) in PBS-GS-Triton staining solution. After washes, cells were incubated for 45 min at RT with donkey anti-rabbit coupled to Alexa405/Alexa647 and donkey anti-mouse coupled to cy3/A647 and then imaged.

Fluorescence image acquisition and analysis

Image acquisition was performed using a 63 X objective (NA 1.40) on a Leica (Nussloch, Germany) DM6000 upright epifluorescence microscope with a 12-bit cooled CCD camera (Micromax, Roper Scientific) run by MetaMorph software (Roper Scientific, Evry, France). Quantification was performed using MetaMorph software (Roper Scientific). Image exposure time was determined on bright cells to obtain best fluorescence to noise ratio and to avoid pixel saturation. All images from a given culture were then acquired with the same exposure time and acquisition parameters.

For cluster analysis, images were first flatten background filtered (kernel size, 3 X 3 X 2) to enhance cluster outlines, and a user defined intensity threshold was applied to select clusters and avoid their coalescence. Clusters were outlined and the corresponding regions were transferred onto raw images to determine the mean cluster number, area and fluorescence intensity. For quantification of gephyrin or $GABA_AR$ synaptic clusters, gephyrin or receptor clusters comprising at least 3 pixels and colocalized on at least 1 pixel with VGAT clusters were considered. The dendritic length of the region of interest was measured to determine the number of clusters per 10 µm. For each culture, we analyzed ~10 cells per experimental condition and ~20 clusters per cell.

Immunohistochemistry

Brains were perfused with ice-cold aCSF (containing (mM) NaCl 125, KCl 2.5, $CaCl_2$ 2.5, $MgCl_2$ 2, $NaHCO_3$ 26, NaH_2PO_4 1.25, glucose 25], pH 7.4) and brains were dissected and incubated in 4% PFA at 4^oC for 75 minutes. Subsequently brains were cryoprotected in 30% sucrose and parasagittal

free-floating sections were made using a cryotome at a thickness of 35µm. Sections were stored at 4ºC in 0.001% NaN_3.

Standard immunohistochemistry was performed on free-floating sections as previously reported (Notter et al., 2014). For revealing $A_{2A}R$ staining, brain sections were transferred into a buffer containing 50mM sodium citrate preheated to 80°C and heated for 30 mins (Trusel et al., 2015). Slices were permeabilized in 0.5% Triton X-100 for 3 hours at room temperature and subsequently incubated in rabbit anti-$A_{2A}R$ (1/500, AAR-002, Alomone Labs) for 48 hours at 4°C. Slices were rinsed 3 times in 0.1M phosphate buffer (PB) and incubated in goat anti-rabbit CY3 (1/500, from Jackson Labs) for 24 hours at 4ºC. All sections were labelled with DAPI (1/2000) for 20 minutes at room temperature and mounted on slides in Mowiol.

In vivo pentylenetatrazole injection

Adult (postnatal day 84-91) C57bl6 mice (all males from JanvierLabs) were injected subcutaneously with pentylenetatrazole (PTZ, 75 mg/kg, dissolved in saline), and recorded right after injection using video recordings. The procedure was made in accordance with the guidelines of the French Agriculture and Forestry Ministry for handling animals and with the agreement of the Comité National de Réflexion Ethique sur l'Expérimentation Animale (# 4018). The sampling of animals as well as the experimental procedure and analysis of the data were determined based on previous published work. The animals to be used for PTZ vs Control conditions were randomly chosen from the batch of C57bl6 mice delivered from JanvierLabs. After 20-35 min of observation, animals were sacrificed by cervical dislocation, brains were rapidly extracted on ice and the cortex and the hippocampus were dissected, frozen in liquid nitrogen and stored at -80°C until use for biochemistry. The first seizures were observed after 6-7 min of injection and a second sequence of seizures and/or abnormal gait were detected after 14-15 min. Two out of three animals injected with 75 mg/kg of PTZ had tonic-clonic seizures with rigid paw extension followed by death and one animal showed only partial clonus.

Calcium Imaging

GCaMP6-rubi AAV viruses were used to infect hippocampal neurons at DIV3 by addition of 0.3 µl of viral solution in the culture medium. 5 days post infection, cells were imaged at 37°C in an open

chamber mounted on an inverted spinning-disc microscope (Leica DMI4000, Yokogawa CS20 spinning Nipkow disk, 40x/0.6 N.A. objective) in an extracellular solution containing the following in mM: 2 $CaCl_2$, 2 KCl, 3 $MgCl_2$, 10 HEPES, 20 glucose, 120 NaCl, pH7.4. Cells were selected using expression of the reporter protein rubi, and intracellular Ca2+ was imaged using 491nm light from a laser. Emitted light was collected using a 525-39 (±25) nm emission filter. Time lapse (0.33 Hz for 600 s) of confocal stacks (of ~21 images acquired with an interval of 0.3 µm) were acquired with a cooled EM-CCD camera (512 x 512, 16 µm pixel size) using Metamorph. The analysis was performed on a section of the stack where the soma was in focus at different time points. Fluorescence intensities collected in the soma or dendrites before (F0) and following (F) bath addition of the drugs, were background-subtracted before being displayed as F/F0 values. Data were analyzed using Metamorph. Normalization of fluorescence intensity was performed for each cell by dividing the mean fluorescence intensity by the average of fluorescence intensities of the 4 time points before drug application. Statistics (paired t test) were run on the last time point before drug application (120 s) compared to the latest time point after drug application (600 s).

cAMP Imaging

Recombinant Sindbis virus encoding EPAC-sh150 (Polito et al., 2013) were used to infect hippocampal neurons at DIV8 by addition of 1 µl of viral solution in the culture medium ($\sim 5 \times 10^5$ particles per slice). 12h after infection, hippocampal neurons were transferred on the microscope stage and were continuous perfused at 0.5 mL/min with a solution containing the following (in mM): 2 $CaCl_2$, 2 KCl, 3 $MgCl_2$, 10 HEPES, 20 glucose, 120 NaCl, pH7.4 at 32 °C. Two-photon imaging was performed using an upright Leica TCS MP5 microscope with resonant scanning (8 kHz), a Leica 25X/0.95 HCX IRAPO immersion objective and a tunable Ti:sapphire laser (Coherent Chameleon Vision II) with dispersion correction set to 860 nm for CFP excitation. The emission path consisted of an initial 700 nm low-pass filter to remove excess excitation light (E700 SP, Chroma Technologies), 506 nm dichroic mirror for orthogonal separation of emitted signal, 479/40 CFP emission filter, 542/50 YFP emission filter (FF506-Di01-25 × 36; FF01-479/40; FF01-542/50; Brightline Filters; Semrock) and two-channel Leica HyD detector for simultaneous acquisition. Due to the high quantum efficiency and low dark noise of the HyD photodetectors, detector gain was typically set at 10–15% with laser power at 1–5%. Z-stack images (12-bit; 512 × 512) were typically acquired every 15 s. The z-step size was 1–2 µm and total stack size was typically 8–10 sections. Images were processed in ImageJ by using maximum z-projections followed by translation registration correction to reduce x/y movement. However, z-projections were occasionally complicated by movement in the z-axis and were therefore corrected with a custom Matlab script before measurement in ImageJ. After correcting movement in the x/y/z

directions, regions of interest (ROIs) were selected for measurement if they could only be measured for the whole experimental time course.

Statistics

Sample size selection for experiments was based on published experiments, pilot studies as well as in-house expertise. All results were used for analysis except in few cases. Cells with signs of suffering (apparition of blobs, fragmented neurites) were discarded from the analysis. Means are shown ± SEM. Means were compared using the non-parametric Mann-Whitney test (immunocytochemistry) using SigmaPlot 12.5 software (Systat Software). Differences were considered significant for p-values less than 5% (*$p \leq 0.05$; **$p < 0.01$; ***$p < 0.001$).

RESULTS

RESULTS

1. Adenosine A_{2A} receptor: a key sensor of synaptic activity to stabilize/eliminate GABAergic synapses during development

The first study of my PhD aimed at investigating the role of $A_{2A}R$ signalling pathway in the development of GABAergic synapses. Studies in the recent years have shed light on the deleterious consequences of caffeine intake during pre- and peri-natal periods in development of the offspring (Ardais et al., 2016; Mioranzza et al., 2014). This was further confirmed by C. Silva and colleagues that showed that the intake of caffeine or an $A_{2A}R$ antagonist by pregnant dams during the period of gestation and lactation led to deleterious consequences in the offspring: delayed migration of GABA neurons, subsequent hippocampal hyperactivity and increased susceptibility to induced seizures and cognitive deficits (Silva et al., 2013). Furthermore, an *in vitro* study (Ribeiro et al., 2015), showed that $A_{2A}R$ plays a role in axonal elongation and dendritic branching.

These studies question a role for $A_{2A}R$ during synaptogenesis. In this publication, we assess the implication of $A_{2A}R$ during hippocampal GABAergic synaptogenesis. In rat primary hippocampal cultures using pharmacology, shRNA approach, immunocytochemistry and videomicroscopy I observed:

- $A_{2A}R$ is expressed during the period of synaptogenesis and is present in the postsynaptic inhibitory synapse.
- $A_{2A}R$ blockade destabilizes the nascent GABA synapse in a rapid manner.
- The adenosine stabilizing the synapses comes from the neuronal secretion of adenosine *in vitro*
- Implication of the PKA-dependent phosphorylation on gephyrin serine 303 in the $A_{2A}R$-mediated stabilization of GABAergic synapses.
- $A_{2A}R$ regulation does not involve the trans-synaptic system neurexin–neuroligin 2, but PTPδ – Slitrk3.

All this work has been done in collaboration with the lab of Christophe Bernard (Marseille) and Rodrigo Cunha (Coimbra). In the laboratory of Christophe Bernard, they performed mIPSC recordings in hippocampal CA1 acute slices and they showed a reduction in frequency and amplitude when blocking

$A_{2A}R$ in pyramidal cells and interneurons, an effect compatible with the morphological data I obtained. This regulation is operant between P4-12 i.e. during the period of synaptogenesis; is clathrin and AC/PKA-dependent. The laboratory of Rodrigo Cunha showed an increased expression of A2AR in the hippocampus during the period of synaptogenesis. Synaptosome fractionation indicated that A2AR is mainly peri- and post-synaptic at this stage whereas it is mostly presynaptic in the adult. They also showed larger release of adenosine and ATP in P7 compared to P60 brain.

Thus, postsynaptic A2ARs would act as molecular switches, sensing the activity of GABAergic presynaptic terminals to stabilize or trigger the elimination of GABA synapses during a critical developmental period.

Adenosine A_{2A} receptor: a key sensor of synaptic activity to stabilize/eliminate GABAergic synapses during development

Stefania Zappettini[1#], Ferran Gomez-Castro[2,3,4#], Carla G. Silva[1,5], Jessica C. Pressey[2,3,4], Marion Russeau[2,3,4], Emmanuel Eugène[2,3,4], Paula M. Canas[5], Francisco Q. Gonçalves[5], Sofia Alçada-Morais[5], Eszter Szabó[5], Ricardo J. Rodrigues[5], Paula Agostinho[5,6], Angelo R. Tomé[5], Christophe Leterrier[7], Béatrice Tessier[8], Bénédicte Dargent[7], Shiva K. Tyagarajan[9], Olivier Thoumine[8], Rodrigo A. Cunha[5,6], Monique Esclapez[1], Sabine Lévi[2,3,4$], Christophe Bernard[1$*]

# Equally contributing first authors

$ Equally contributing last authors

* Corresponding author

[1] Aix Marseille Univ, INSERM, INS, Inst Neurosci Syst, Marseille, France

[2] INSERM UMR-S 839, 75005, Paris, France

[3] Université Pierre et Marie Curie, 75005, Paris, France

[4] Institut du Fer a Moulin, 75005, Paris, France

[5] CNC-Center for Neuroscience and Cell Biology, University of Coimbra, 3004-517 Coimbra, Portugal

[6] Institute of Biochemistry, Faculty of Medicine, University of Coimbra, 3004-504 Coimbra, Portugal

[7] *CNRS, CRN2M, Aix Marseille University, Marseille, France*

[8] Interdisciplinary Institute for Neuroscience, UMR CNRS 5297- University of Bordeaux, France

[9] Institute of Pharmacology and Toxicology, University of Zürich, 8057 Zurich, Switzerland

Abstract

At GABAergic synapses, GABA release is important to establish synapses, but the mechanisms controlling their fate (stabilization *vs*. elimination) are not well understood. Here, we show that the activation of postsynaptic adenosine 2A receptors (A_{2A}Rs) is necessary and sufficient to stabilize GABAergic synapses in the CA1 region of the mouse hippocampus specifically during synaptogenesis. The molecular mechanism involves adenylyl cyclase/cyclic adenosine monophosphate/protein kinase A dependent phosphorylation of the postsynaptic scaffolding molecule gephyrin and stabilization of the presynaptic terminal through the slitrk3-ptpδ trans-synaptic organizers. Activation of A_{2A}Rs requires the activity-dependent synaptic release of adenosine or of its phosphorylated form adenosine triphosphate (ATP). Absence of activity-dependent release prevents the activation of A_{2A}Rs leading to the destabilization of presynaptic and postsynaptic sites. We propose that, during a key developmental period, postsynaptic A_{2A}Rs act as key detectors, sensing the activity of GABAergic presynaptic terminals to stabilize or trigger the elimination of GABAergic synapses.

One Sentence Summary: Postsynaptic adenosine 2A receptors are key controllers of the stabilization and elimination of GABAergic synapses during synaptogenesis.

Introduction

Stabilization of nascent active synapses and elimination of inactive ones is essential to the adequate wiring of neuronal circuits during development (*1, 2*). The role of GABA in establishing synapses at early stages of development is now clearly established (*3-8*). How active and inactive synapses are stabilized and eliminated, respectively, is less understood. Genetic manipulation of GABA release leads to synapse elimination (*7*), but the underlying mechanisms are not known. In particular, which processes act as detectors of activity/inactivity and which are the molecular downstream effectors for synapse stabilization/elimination? At very early stages of development, both GABA and A_{2A}Rs control axonal elongation and dendrite branching (*9*), as well as neuronal migration (*10*). This led us to propose that A_{2A}Rs may also control stabilization/elimination of GABAergic synapses.

Results

Immunohistochemistry showed a transient increased density of A_{2A}Rs in mouse hippocampi during the peak of synaptogenesis, between postnatal P5 and P16 (figure S1A,B). The analysis of synaptosome preparations showed that A_{2A}Rs were mostly located at synapses in both mature and immature mouse hippocampi (figure S1C). During the first postnatal week, A_{2A}Rs were expressed mostly post- and peri-synaptically (figure S1D). In contrast, they were mostly presynaptic at P30 (figure S1D), as previously reported (*11, 12*). Immunocytochemistry analysis of hippocampal neuronal cultures revealed that A_{2A}Rs were clustered at GABAergic synapses, and that clustering increased during synaptogenesis, between 7 and 14 days in vitro (DIV) (Figure 1A). A_{2A}Rs were not present at all synapses; they accumulated at a subset (39.1 ± 3.7 %, n= 34 cells, 3 independent experiments) of GABAergic synapses. Stochastic optical reconstruction microscopy further confirmed that A_{2A}Rs were located within or near the GABAergic post-synapse (Figure 1B).

In the adult hippocampus, the activation of presynaptic A_{2A}Rs bolsters neurotransmitter release and selectively controls synaptic plasticity (*11*). The transient expression of postsynaptic A_{2A}Rs during a critical period of synaptogenesis at some GABAergic synapses led us to hypothesize that they may play a role in synapse formation and/or stabilization. We thus tested the consequences of antagonizing A_{2A}Rs on GABAergic synapses. In hippocampal cell cultures, single-particle tracking of the $GABA_A$ receptor ($GABA_A$R) γ2 subunit labelled with quantum dots (*13*) revealed that the diffusion of $GABA_A$Rs increased in the presence of the selective A_{2A}R antagonist SCH58261 (figure S2). This was associated with a decrease in the number of postsynaptic clusters of $GABA_A$Rs (Figure 1C), suggesting receptor escape from the synapse. In addition, the number of clusters of the postsynaptic scaffolding protein gephyrin and of the presynaptic vesicular GABA transporter VGAT were decreased (Figure 1C),

demonstrating a destabilization of GABAergic synapses at both pre- and postsynaptic sites. The loss of GABAergic synapses occurred within 30 min (figure S3), suggesting that A_{2A}Rs play a role in synapse stabilization rather than in synapse formation since *de novo* synapse formation requires several hours (*14*). Downregulating A_{2A}R expression with a shRNA led to a loss of synapses (Fig 1D) equivalent to that seen following A_{2A}R activity blockade, demonstrating that the A_{2A}R-mediated synapse stabilization is a cell autonomous process that requires A_{2A}Rs function in the postsynaptic cell. Not all synapses disappeared as only ~25% of GABAergic synapses were destabilized (Figure 1D), in keeping with the finding that not all GABAergic synapses are equipped with A_{2A}Rs (Figure 1D). This may reflect the fact that a given neuron possesses synapses at various stages of stabilization (*i.e.* the already stabilized synapses do not express A_{2A}Rs anymore) or that the A_{2A}R-dependent mechanism is present at specific subsets of GABAergic synapses.

Together these results demonstrate that activation of A_{2A}Rs is necessary to stabilize some GABA synapses during a critical developmental period. Since lack of A_{2A}R activation leads to structural modifications (loss of GABAergic synapses), we investigated the functional consequences, predicting a decrease in the synaptic barrage of GABAergic currents received by neurons. This prediction was tested in hippocampal slices from P6 animals. Single-cell recordings of miniature inhibitory postsynaptic currents (mIPSCs) in CA1 pyramidal cells showed that a 30 min application of SCH58261 decreased the amplitude and frequency of mIPSCs by 30% and 40%, respectively (Figure 2A), in keeping with the previous finding that not all synapses are destabilized. The amplitude and frequency of mIPSCs were also decreased in CA1 interneurons in the presence of SCH58261 (figure S4A). Clathrin-mediated endocytosis of receptors (*15*) accounted for the loss of IPSCs (figure S4A). This result further confirms the postsynaptic action of A_{2A}R and the cell autonomous nature of the process, since the reduction in mIPSCs occurred only in cells in which internalization was still operant (figure S4B).

The fact that A_{2A}R activation is necessary to stabilize a subset of already functional GABAergic synapses raises two questions. Is this mechanism present during a limited developmental period? Is there a minimal time of A_{2A}R inactivity before synapses are destabilized? In keeping with a developmentally-regulated process, the consequences of A_{2A}R blockade on GABAergic transmission were restricted to the period of synaptogenesis (between P4 and P12), with a maximum effect at P6 in slices (Figure 2B). Varying the time of application of SCH58261, we found that the effect on mIPSCs was reversible if A_{2A}R blockade did not exceed 10 min (Figure 2C). Beyond 20 min, the effect was irreversible (Figure 2D). Thus, the A_{2A}R-dependent postsynaptic control of GABAergic synapses is developmentally regulated and a period of at least 20 min of inactivity of A_{2A}Rs is required to trigger the removal of GABAergic synapses *in vitro*.

Based on the previous results, we hypothesized that postsynaptic A_{2A}Rs may act as detectors of active presynaptic terminals. As long as the presynaptic terminal would be active, A_{2A}Rs would be

activated, stabilizing the synapse. The next series of experiments were designed to test this hypothesis. In particular, we addressed three issues: is the adenosine that activates A_{2A}Rs released in an activity-dependent manner? Is the A_{2A}R-mediated synapse stabilization itself an activity-dependent process? What are the molecular mechanisms underlying synapse stabilization?

We first addressed the question of the source of adenosine. Adenosine, the endogenous ligand of A_{2A}Rs, is produced in an activity-dependent manner in adult synapses and can be released as such or results from the extracellular catabolism of released adenine nucleotides through the activity of ecto-5'-nucleotidase or CD73 (*16-18*). If adenosine is responsible for A_{2A}R activation, decreasing its level should have effects similar to antagonizing A_{2A}Rs. Application of adenosine 5-(α,β-methylene)diphosphate (AMPCP), which inhibits CD73, together with adenosine deaminase (ADA), which hydrolyses adenosine into inosine, destabilized synapses in cultures (Figure 3A) and decreased mIPSC amplitude (30%) and frequency (74%) in slices (Figure 3B). Synapse destabilization was prevented by the direct activation of A_{2A}Rs with their agonist CGS21680 (Figure 3A), showing that direct activation of A_{2A}Rs is sufficient to maintain synapse integrity. Using videomicroscopy, we found that removing extracellular adenosine with AMPCP and ADA induced within 20 min the loss of active GABAergic boutons identified by their capacity to uptake the VGAT-Oyster550 recycling dies (figure S5). In AMPCP and ADA conditions, we observed vesicular packets diffusing away from the synapse traveling far along the axon, indicating synapse collapse (figure S5).

Altogether, our results demonstrate that the activation of A_{2A}Rs constitutes a condition that is both necessary and sufficient to stabilize active nascent GABAergic synapses at both pre- and postsynaptic sites.

Two main sources of adenosine can be proposed: a direct activity-dependent release by presynaptic terminals or neighbouring glial cells, and/or the result of the enzymatic conversion of ATP released by neurons or glial cells (*17, 18*). A high concentration of extracellular adenosine was measured following vesicular release from P7 hippocampal synaptosomes (Figure 3C). Blocking CD73 with AMPCP decreased extracellular adenosine by 25% (Figure 3C). Accordingly, we found a large density of CD73 in synapses during the peak of synaptogenesis period (figure S6), in keeping with the tight association of the enzyme with A_{2A}Rs (*19*). Therefore, one fraction of extracellular adenosine comes from local ATP metabolism. We then assessed the possible origin of ATP. Immunohistochemical analysis in the stratum radiatum of the hippocampus of P7 mice indicated a co-localization of the vesicular nucleotide transporter (VNUT) responsible for the accumulation of ATP in synaptic vesicles (*20, 21*) with a subset of VGAT inhibitory terminals (figure S7). This was further confirmed by the direct immunocytochemical analysis of plated hippocampal synaptosomes from P7 mice (figure S7). Therefore, a subset of GABAergic terminals is able to upload GABA and ATP into the same synaptic vesicles. Challenging synaptosomes in high K^+ conditions resulted in a large activity-dependent release

of ATP at P7 (Figure 3C). The secretion of ATP and adenosine was more important at P7 than at P60 (Figure 3C), in support with a key function of the purine system during development. Together, these results confirm that the activation of synaptic terminals at early stage of synaptogenesis bolster the release of adenosine via yet unknown mechanisms and of vesicular ATP, which is efficiently converted into extracellular adenosine by CD73.

In order to assess the neuronal and/or glial origin of the purines, we treated cell cultures with cytosine d-D-arabinofuranoside (AraC) to obtain pure neuronal cell cultures (figure S8A). Neurons established GABAergic synapses in these conditions (figure S8B). In the absence of glial cells, preventing the accumulation of extracellular adenosine with ADA and AMPCP resulted in synapse destabilization, which was prevented by the direct activation of A_{2A}Rs with CGS21680 (figure S8C). The extent of the regulation was comparable in cultures maintained in the absence or presence of glial cells. Therefore, the release of adenosine or ATP from neurons and the local extracellular transformation of ATP into adenosine (Figure 3C; figure S9) are sufficient to activate A_{2A}Rs and to stabilize GABAergic synapses. This result does not rule out a contribution of glial cells *in vivo*.

We then tested the second part of our hypothesis: if A_{2A}Rs act as detectors of active synapses, their activation should be activity-dependent. A 48h treatment with tetanus toxin (to cleave vesicle-associated membrane protein 2 VAMP2, which is essential for activity-dependent vesicular release of neurotransmitters) resulted in the disappearance of 38% of GABAergic synapses (Figure 3D). Since this loss was fully prevented by the direct activation of A_{2A}Rs with CGS21680 (Figure 3D), we conclude that the activity-dependent release of the purines is required to activate A_{2A}Rs in order to stabilize GABAergic synapses.

Having established that A_{2A}Rs act as detectors of active synapses, we then investigated the molecular mechanisms of synapse stabilization downstream of A_{2A}R activation. A_{2A}Rs are G protein-coupled receptors and their prime transducing system is the activation of adenylyl cyclase (AC), which generates the synthesis of cyclic adenosine monophosphate (cAMP). First, we verified that blocking G protein activity inside the recorded cell with guanosine diphosphate-β-S directly led to a decrease in mIPSC frequency and amplitude in slices (figure S10A), reproducing the effect of A_{2A}R blockade (15% and 55% respectively). Second, we verified the involvement of the AC/cAMP signalling cascade. Bath application of IBMX (a non-selective inhibitor of phosphodiesterases that metabolize cAMP) and forskolin (an activator of AC) in the presence of SCH58261 prevented the decrease in mIPSC frequency and amplitude in CA1 pyramidal cells in slices (Figure 4A). Protein kinase A (PKA) is a downstream effector of cAMP. Intracellular inhibition of PKA with the protein kinase inhibitor peptide (PKI) decreased mIPSC amplitude and frequency (figure S10B), in the same proportion as that found with SCH58261 (26% and 50%, respectively). Since PKA-mediated phosphorylation of $GABA_A$Rs and gephyrin is important for their postsynaptic stabilization (*22, 23*), we reasoned that PKA activation via the A_{2A}R-

AC/cAMP activation cascade may insure the phosphorylation of $GABA_A$Rs and gephyrin required to maintain them at the synapse.

Phosphorylation of gephyrin plays a central role in the stabilization of $GABA_A$Rs at synapses (*24*). We thus tested its contribution in cultures, by expressing constructs harbouring mutations of the PKA Ser303 site to aspartate (D) to mimic the gephyrin phosphorylated state (*22*). Decreasing extracellular adenosine with AMPCP and ADA led to synapse destabilization in neurons expressing the wild type gephyrin (Figure 4B). However, expression of gephyrin mutants prevented synapse loss (Figure 4B), demonstrating the involvement of this phosphosite in synapse stabilization. We conclude that the activity-dependent activation of A_{2A}Rs by adenosine leads to AC-cAMP-PKA-mediated phosphorylation of gephyrin at S303 that stabilizes the GABAergic synapse.

Having demonstrated the stabilization mechanism of the postsynaptic site, we focused on the presynaptic site, since our results also show its destabilization after A2AR blockade. Multiple trans-synaptic organizing complexes organize and stabilize pre- and post-synaptic sites at early stages of development (*25-27*). Neurexin-neuroligin-2 and slitrk3-ptpδ are the two main trans-synaptic complexes at GABAergic synapses. Inhibiting NLG2 interaction with presynaptic neurexins using an excess of soluble recombinant neurexin1β-Fc, or knocking-down neuroligin-2 with a specific shRNA bled to a major loss of GABAergic synapses (figure S11, Figure 4C), as shown before (*28, 29*). Activating A_{2A}Rs with CGS21680 rescued synapses (figure S11, Figure 4C), ruling out the contribution of the neurexin-neuroligin-2 complex. In contrast, the synapse loss induced by the shRNA-mediated suppression of slitrk3 could not be rescued by CGS21680 (Figure 4D). We conclude that A_{2A}Rs stabilize GABAergic synapses via the slitrk3-ptpδ trans-synaptic complex.

In conclusion, we propose that at a set of GABAergic synapses, A_{2A}Rs act both as detectors of active presynaptic terminals and as molecular switches to stabilize these synapses via the following functional scheme (figure S12). An active GABAergic terminal releases adenosine or ATP, both contributing to a local activity-dependent increase of extracellular adenosine to activate A_{2A}Rs. Activation of A_{2A}Rs activates the AC/cAMP pathway, leading to PKA-dependent phosphorylation of gephyrin and the stabilization of the postsynaptic element. The adenosine-mediated stabilization of the presynaptic element further involves the slitrk3-ptpδ trans-synaptic complexes. If A_{2A}Rs are not activated during an extended period of time (around 20 min), the whole synapse collapses. This A_{2A}R receptor-dependent mechanism adds to other mechanisms known to control GABAergic synaptogenesis, such as GABA, adhesion molecules or immunoglobulins in establishing synapses, and microglia in pruning of synapses (*3-8, 30*). Many processes rely on parallel pathways or coincidence detection to serve specific purposes. The prototypical case is the activation of NMDA receptor in synaptic plasticity (*31*). Although GABA receptors may also stabilize immature synapses (for example

via the activation of voltage gated calcium channels), we propose that the transient use of the parallel GABAR/A_{2A}R builds a synapse-specific system able to integrate, transiently during development, GABA/adenosine co-signaling at GABA synapses.

References

1. J. R. Sanes, J. W. Lichtman, Development of the vertebrate neuromuscular junction. *Annual review of neuroscience* **22**, 389 (1999).
2. R. C. Paolicelli *et al.*, Synaptic pruning by microglia is necessary for normal brain development. *Science* **333**, 1456 (Sep 9, 2011).
3. B. Chattopadhyaya *et al.*, GAD67-mediated GABA synthesis and signaling regulate inhibitory synaptic innervation in the visual cortex. *Neuron* **54**, 889 (Jun 21, 2007).
4. Z. J. Huang, G. Di Cristo, F. Ango, Development of GABA innervation in the cerebral and cerebellar cortices. *Nat Rev Neurosci* **8**, 673 (Sep, 2007).
5. Z. J. Huang, P. Scheiffele, GABA and neuroligin signaling: linking synaptic activity and adhesion in inhibitory synapse development. *Curr Opin Neurobiol* **18**, 77 (Feb, 2008).
6. Z. J. Huang, Activity-dependent development of inhibitory synapses and innervation pattern: role of GABA signalling and beyond. *J Physiol* **587**, 1881 (May 01, 2009).
7. X. Wu *et al.*, GABA signaling promotes synapse elimination and axon pruning in developing cortical inhibitory interneurons. *J Neurosci* **32**, 331 (Jan 04, 2012).
8. W. C. Oh, S. Lutzu, P. E. Castillo, H. B. Kwon, De novo synaptogenesis induced by GABA in the developing mouse cortex. *Science* **353**, 1037 (Sep 02, 2016).
9. F. F. Ribeiro *et al.*, Axonal elongation and dendritic branching is enhanced by adenosine A receptors activation in cerebral cortical neurons. *Brain structure & function*, (Jun 12, 2015).
10. C. G. Silva *et al.*, Adenosine receptor antagonists including caffeine alter fetal brain development in mice. *Science translational medicine* **5**, 197ra104 (Aug 7, 2013).
11. N. Rebola, R. Lujan, R. A. Cunha, C. Mulle, Adenosine A2A receptors are essential for long-term potentiation of NMDA-EPSCs at hippocampal mossy fiber synapses. *Neuron* **57**, 121 (2008).
12. N. Rebola, P. M. Canas, C. R. Oliveira, R. A. Cunha, Different synaptic and subsynaptic localization of adenosine A2A receptors in the hippocampus and striatum of the rat. *Neuroscience* **132**, 893 (2005).
13. M. Dahan *et al.*, Diffusion dynamics of glycine receptors revealed by single-quantum dot tracking. *Science* **302**, 442 (2003).
14. F. A. Dobie, A. M. Craig, Inhibitory synapse dynamics: coordinated presynaptic and postsynaptic mobility and the major contribution of recycled vesicles to new synapse formation. *J Neurosci* **31**, 10481 (Jul 20, 2011).
15. M. Vithlani, M. Terunuma, S. J. Moss, The dynamic modulation of GABA(A) receptor trafficking and its role in regulating the plasticity of inhibitory synapses. *Physiological reviews* **91**, 1009 (Jul, 2011).
16. B. B. Fredholm, J. F. Chen, R. A. Cunha, P. Svenningsson, J. M. Vaugeois, Adenosine and brain function. *Int.Rev.Neurobiol.* **63**, 191 (2005).

17. B. P. Klyuch, N. Dale, M. J. Wall, Deletion of ecto-5'-nucleotidase (CD73) reveals direct action potential-dependent adenosine release. *The Journal of neuroscience : the official journal of the Society for Neuroscience* **32**, 3842 (Mar 14, 2012).
18. M. J. Wall, N. Dale, Neuronal transporter and astrocytic ATP exocytosis underlie activity-dependent adenosine release in the hippocampus. *The Journal of physiology* **591**, 3853 (Aug 15, 2013).
19. E. Augusto *et al.*, Ecto-5'-nucleotidase (CD73)-mediated formation of adenosine is critical for the striatal adenosine A2A receptor functions. *The Journal of neuroscience : the official journal of the Society for Neuroscience* **33**, 11390 (Jul 10, 2013).
20. M. Hiasa *et al.*, Essential role of vesicular nucleotide transporter in vesicular storage and release of nucleotides in platelets. *Physiological reports* **2**, (Jun 01, 2014).
21. M. Larsson *et al.*, Functional and anatomical identification of a vesicular transporter mediating neuronal ATP release. *Cerebral cortex* **22**, 1203 (May, 2012).
22. C. E. Flores *et al.*, Activity-dependent inhibitory synapse remodeling through gephyrin phosphorylation. *Proceedings of the National Academy of Sciences of the United States of America* **112**, E65 (Jan 6, 2015).
23. S. J. Moss, T. G. Smart, C. D. Blackstone, R. L. Huganir, Functional modulation of GABAA receptors by cAMP-dependent protein phosphorylation. *Science* **257**, 661 (Jul 31, 1992).
24. P. Zacchi, R. Antonelli, E. Cherubini, Gephyrin phosphorylation in the functional organization and plasticity of GABAergic synapses. *Front Cell Neurosci* **8**, 103 (2014).
25. A. M. Craig, Y. Kang, Neurexin-neuroligin signaling in synapse development. *Curr Opin Neurobiol* **17**, 43 (Feb, 2007).
26. T. J. Siddiqui, A. M. Craig, Synaptic organizing complexes. *Curr Opin Neurobiol* **21**, 132 (Feb, 2011).
27. H. Takahashi, A. M. Craig, Protein tyrosine phosphatases PTPdelta, PTPsigma, and LAR: presynaptic hubs for synapse organization. *Trends Neurosci* **36**, 522 (Sep, 2013).
28. J. N. Levinson *et al.*, Neuroligins mediate excitatory and inhibitory synapse formation: involvement of PSD-95 and neurexin-1beta in neuroligin-induced synaptic specificity. *J Biol Chem* **280**, 17312 (Apr 29, 2005).
29. P. Scheiffele, J. Fan, J. Choih, R. Fetter, T. Serafini, Neuroligin expressed in nonneuronal cells triggers presynaptic development in contacting axons. *Cell* **101**, 657 (Jun 9, 2000).
30. V. Sytnyk, I. Leshchyns'ka, M. Schachner, Neural Cell Adhesion Molecules of the Immunoglobulin Superfamily Regulate Synapse Formation, Maintenance, and Function. *Trends in neurosciences* **40**, 295 (May, 2017).
31. R. G. Morris, NMDA receptors and memory encoding. *Neuropharmacology* **74**, 32 (Nov, 2013).

Figures

Figure 1: A_{2A}Rs are postsynaptic and control the stability of GABA synapses during synaptogenesis. **A.** Double-detection of A_{2A}Rs and GAD67 in DIV 14 hippocampal cultures. Some (arrows) but not all (filled arrows) A_{2A}R clusters are detected at GABAergic synapses. Some GABAergic synapses are devoid of A_{2A}Rs (crossed arrows). Mean number of A_{2A}R clusters over time normalized to DIV 3 value. N= 23-46 cells, 4 cultures. **B.** Postsynaptic localization of A_{2A}Rs identified with two-color STORM of gephyrin and A_{2A}Rs. **C**. $GABA_A$Rγ2, gephyrin and VGAT staining and quantification in DIV10 neurons in absence or presence of SCH58261. N= 30-111 cells, 3-7 cultures. **D.** VGAT staining and quantification in DIV 10-11 neurons transfected with non-target (shNT) or on-target A_{2A}R ($shA_{2A}R$) shRNAs. N= 56-60 cells, 5 cultures. Histograms represent means and s.e.m.; Mann-Whitney test (a,c,d): *p≤0.05.

Figure 2: Acute A_{2A}R blockade decreases miniature GABAergic currents during synaptogenesis. A. Top: mIPSC traces before (black) and after (red) SCH58261 in a representative CA1 pyramidal cell (images). Bottom: 30 min of SCH58261 reduces the amplitude and frequency of $GABA_A$R-mediated mIPSCs in CA1 pyramidal cells (12 cells, 12 slices, 6 P6 pups). **B.** Transient SCH58261 action between P4 and P12. N= 4-5 pups, 5-10 slices, 4-11 cells per time point. **C.** The effect of A_{2A}R blockade on GABAergic currents is reversible within 10 min. Ten min application of SCH58261 results in mIPSC amplitude and frequency decrease. Following 30 min of wash out, mIPSCs are back to control values. N= 6 cells, 6 slices, 5 P6 pups. **D.** Twenty min application produces irreversible effects. N= 10 cells, 10 slices, 6 P6 pups. Histograms represent means and s.e.m.; Kolmogorov-Smirnov test: *p≤0.05; **p<0.01; ***p<0.001; NS Not significant.

Figure 3. Source of adenosine stabilizing synapses. A. Immunostaining and quantification of VGAT and $GABA_A$Rγ2 in DIV 10 neurons in absence or presence of the indicated drugs for 30 min. N= 26-41 cells, 3 cultures. **B.** Reduced mIPSCs amplitude and frequency in CA1 pyramidal cells following 30 min treatment with ADA, AMPCP or ADA+AMPCP. N= 12 cells, 12 slices, 6 pups. **C**. Left. Challenging synaptosomes with high K^+ evoked a larger release of adenosine at P7 than at P60. Middle. AMPCP decreased adenosine levels at both ages. N= 6-8 P7 or P60 mice. Right. Larger K^+-evoked release of ATP at P7 than at P60. N=6-8 mice. **D.** $GABA_A$Rγ2 and VGAT staining and quantification in DIV9 neurons treated with tetanus toxin (TeNT) during 48h with or without 30 min CGS21680 application. N= 26-44 cells, 3 cultures. Histograms represent means and s.e.m.; Mann-Whitney test (a, d, c bottom), Kolmogorov-Smirnov test (b), Two-Way ANOVA followed by Bonferroni post hoc test (c, top left): *p≤0.05; **p<0.01; ***p<0.001; NS Not significant.

Figure 4. Molecular mechanisms of synapse stabilization downstream of A_{2A}Rs activation. A. The SCH58261-induced decrease in mIPSC amplitude and frequency was prevented by the activation of the AC/cAMP pathway with IBMX and forskolin. N= 7 cells, 7 slices, 6 P6 pups. **B.** Immunostaining and quantification of $GABA_AR\gamma2$ and VGAT in absence or presence of ADA + AMPCP in DIV10 neurons transfected with 3'-UTR gephyrin shRNA and gephyrin WT or S303D constructs. N= 45-52 cells, 4 cultures. Gephyrin mutants block the ADA+AMPCP effect. **C.** VGAT staining in DIV 10-11 neurons transfected with non-target (shNT) or on-target neuroligin-2 shRNAs (shNLG2) exposed or not to CGS21680 for 30 min. N= 54-58 cells, 4 cultures. **D.** VGAT staining in DIV 10-11 neurons transfected with shMock or shSlitrk3 exposed or not to CGS21680 for 30 min. N= 36-41 cells, 3 cultures. Histograms represent means and s.e.m.; Kolmogorov-Smirnov test (a) and Mann-Whitney test (b-d): *p≤0.05; **p<0.01; ***p<0.001; NS Not significant.

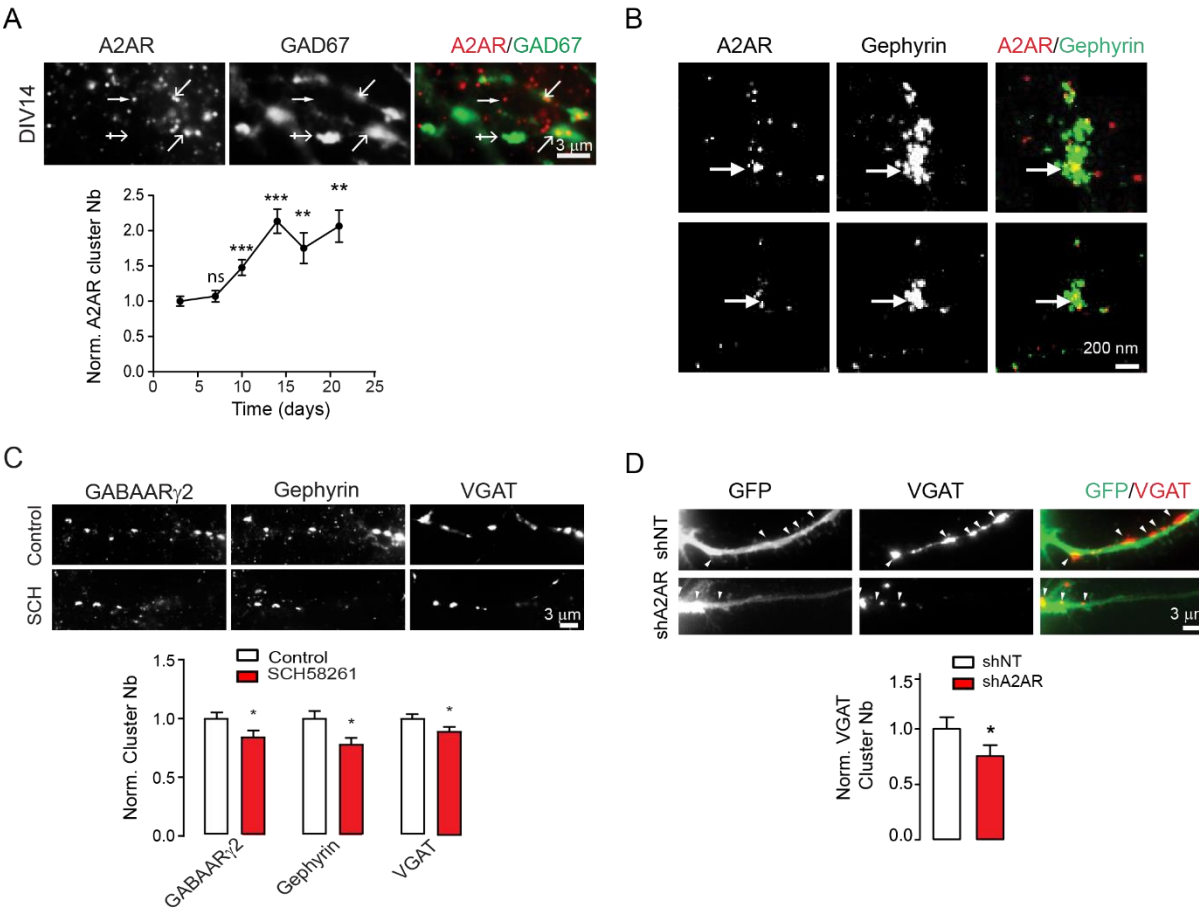
A
A2AR
GAD67
A2AR/GAD67
DIV14
3 µm
Norm. A2AR cluster Nb
Time (days)
ns
***
***
**
**
B
A2AR
Gephyrin
A2AR/Gephyrin
200 nm
C
GABAARγ2
Gephyrin
VGAT
Control
SCH
3 µm
Norm. Cluster Nb
Control
SCH58261
GABAARγ2
Gephyrin
VGAT
D
GFP
VGAT
GFP/VGAT
shNT
shA2AR
3 µm
Norm. VGAT Cluster Nb
shNT
shA2AR

Figure 1

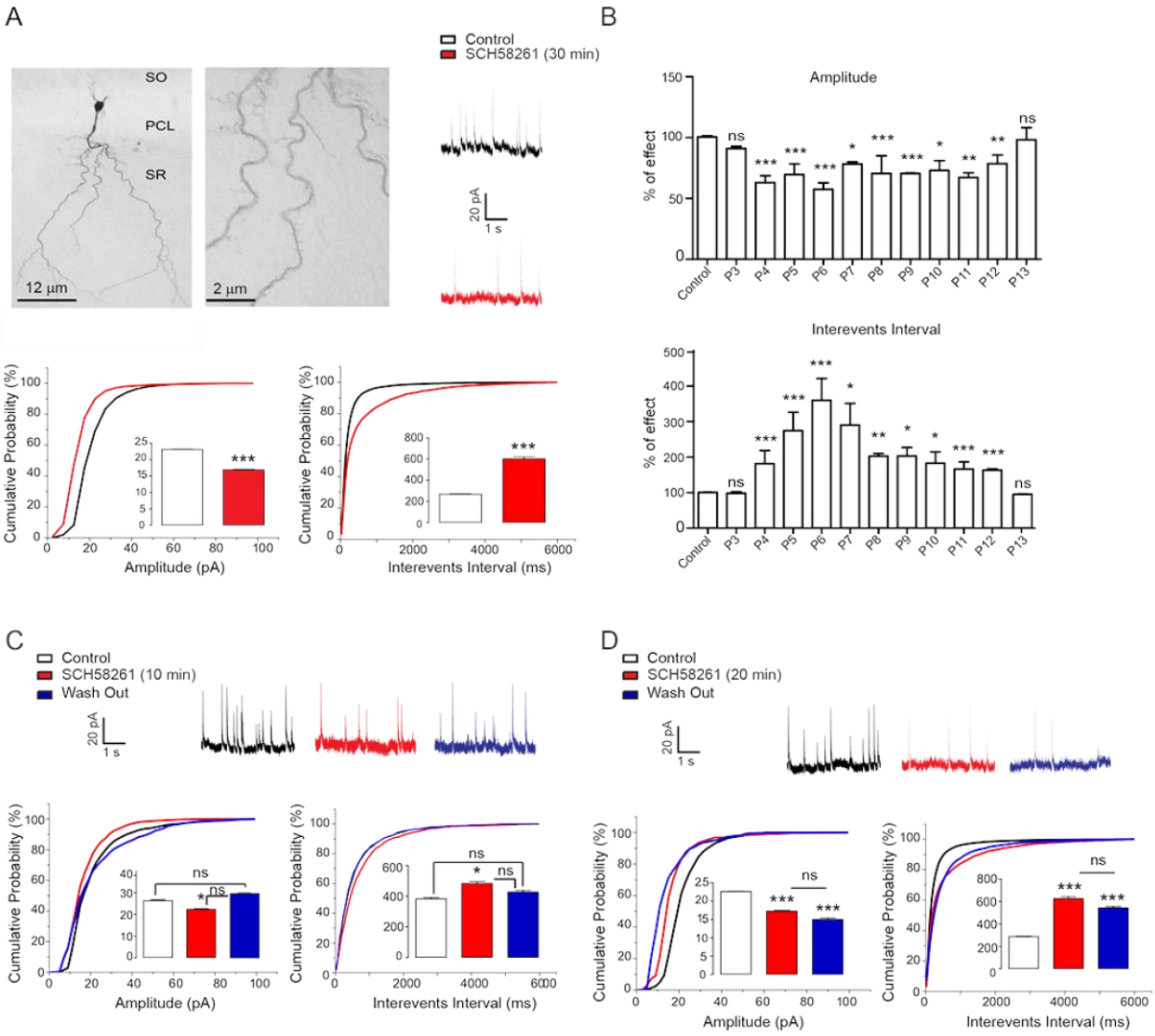
A
SO
PCL
SR
12 µm
2 µm
Control
SCH58261 (30 min)
20 pA
1 s
Cumulative Probability (%)
Amplitude (pA)
Interevents Interval (ms)
B
Amplitude
% of effect
Interevents Interval
Control
P3
P4
P5
P6
P7
P8
P9
P10
P11
P12
P13
C
Control
SCH58261 (10 min)
Wash Out
D
Control
SCH58261 (20 min)
Wash Out

Figure 2

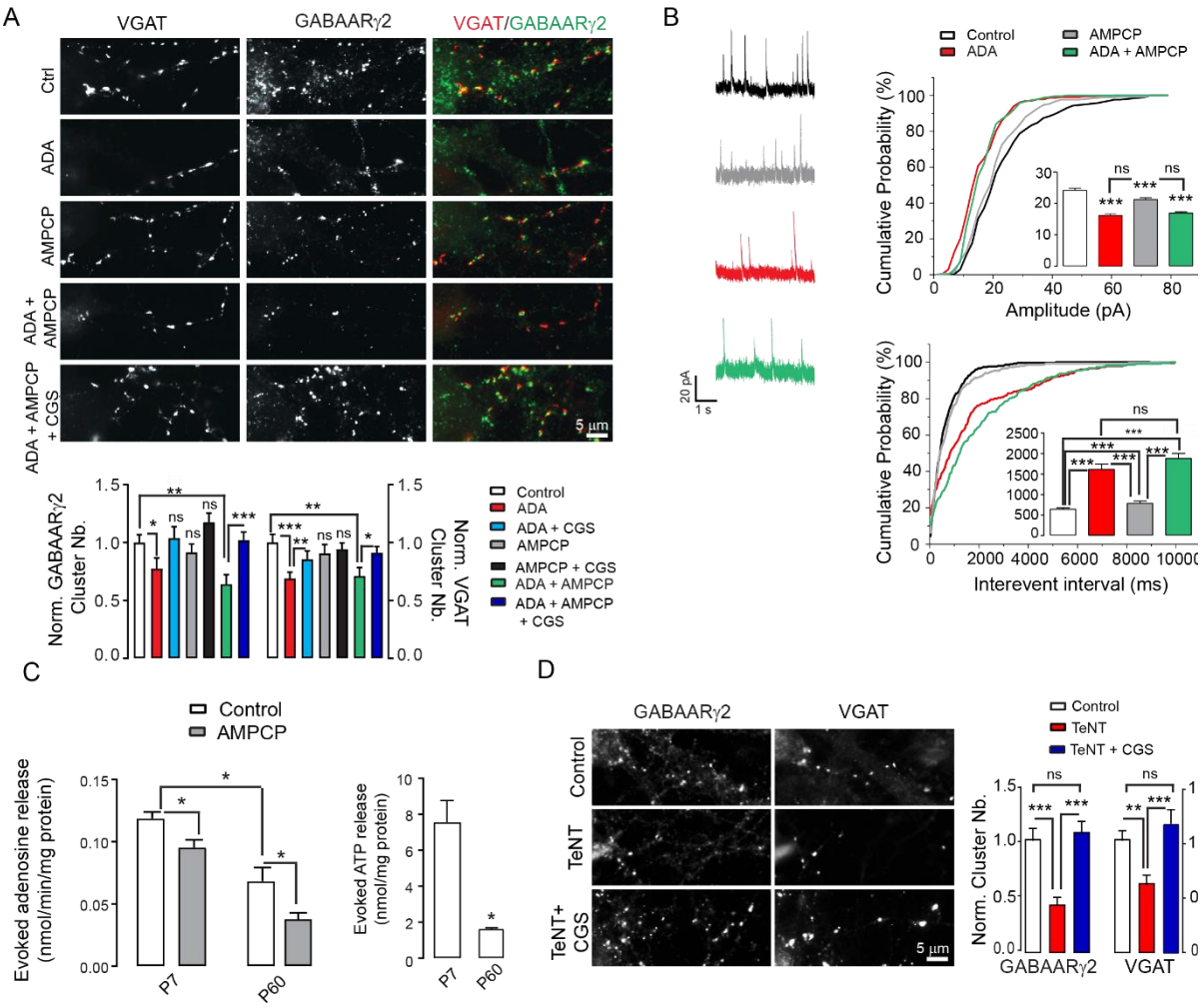
A
VGAT
GABAARγ2
VGAT/GABAARγ2
Ctrl
ADA
AMPCP
ADA + AMPCP
ADA + AMPCP + CGS
5 µm
Norm. GABAARγ2 Cluster Nb.
Norm. VGAT Cluster Nb.
Control
ADA
ADA + CGS
AMPCP
AMPCP + CGS
ADA + AMPCP
ADA + AMPCP + CGS
B
Control
ADA
AMPCP
ADA + AMPCP
20 pA
1 s
Cumulative Probability (%)
Amplitude (pA)
Interevent interval (ms)
C
Control
AMPCP
Evoked adenosine release (nmol/min/mg protein)
Evoked ATP release (nmol/mg protein)
P7
P60
D
GABAARγ2
VGAT
Control
TeNT
TeNT+ CGS
5 µm
Control
TeNT
TeNT + CGS
Norm. Cluster Nb.
GABAARγ2
VGAT

Figure 3

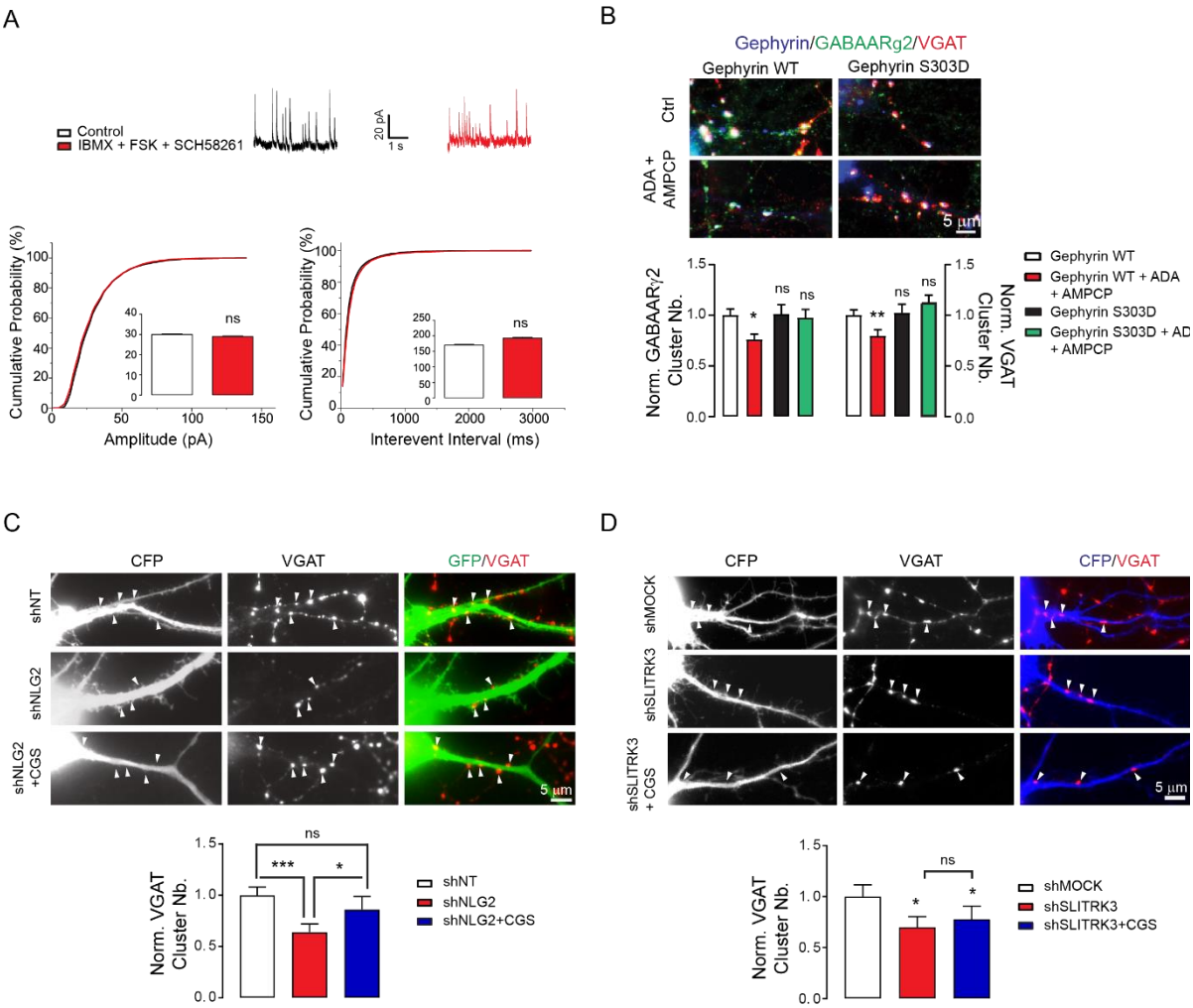
A
Control
IBMX + FSK + SCH58261
20 pA
1 s
Cumulative Probability (%)
Amplitude (pA)
Interevent Interval (ms)
ns
B
Gephyrin/GABAARg2/VGAT
Gephyrin WT
Gephyrin S303D
Ctrl
ADA + AMPCP
5 µm
Norm. GABAARγ2 Cluster Nb.
Norm. VGAT Cluster Nb.
Gephyrin WT
Gephyrin WT + ADA + AMPCP
Gephyrin S303D
Gephyrin S303D + ADA + AMPCP
C
CFP
VGAT
GFP/VGAT
shNT
shNLG2
shNLG2 +CGS
5 µm
Norm. VGAT Cluster Nb.
shNT
shNLG2
shNLG2+CGS
D
CFP
VGAT
CFP/VGAT
shMOCK
shSLITRK3
shSLITRK3 + CGS
5 µm
Norm. VGAT Cluster Nb.
shMOCK
shSLITRK3
shSLITRK3+CGS

Figure 4

Materials and methods

Animals

Adult C57Bl6 mice (3 or 6 weeks old) were purchased from Charles River (Lyon, France) and maintained at CNC animal house facilities under controlled environment (23 ± 2°C; 12 h light/dark cycle and *ad libitum* access to food and water) (both genders pooled). Mice were handled according to European Union guidelines (2010/63) after approval by the Animal's Ethics Committee of the Center for Neuroscience and Cell Biology (Orbea 78-201) and the Portuguese Veterinarian Office. All efforts were made to reduce the number of animals used and to minimize their stress and discomfort, following ARRIVE guidelines.

For all *in vitro* electrophysiological and morphological experiments, GIN male mice (P3-P13) (FVB-Tg(GadGFP)45704Swn/J, Jackson Laboratories) were used. Mice were housed in standard mouse cages under conventional laboratory conditions (12 h/12 h dark-light cycle, constant temperature, constant humidity, and food and water *ad libitum*). Animal care and experimental procedures were conducted in accordance with institutional guidelines and with the European Union guidelines and were approved by the Aix-Marseille University Chancellor's Animal Research Committee, Marseille (France).

Electrophysiology in CA1 hippocampal slices

Coronal hippocampal slices (350 µm) were prepared from male GIN-mice with a vibroslicer Leica VT 1200S in a cold (lower than 4 ºC) cutting solution containing (mM) 140.0 potassium gluconate, 10.0 HEPES, 15.0 sodium gluconate, 0.2 EGTA, 4.0 NaCl, pH 7.2. After recovery for at least one hour in aCSF containing (mM) 126.0 NaCl, 25.0 $NaHCO_3$, 10.0 D-glucose, 3.5 KCl, 2.0 $CaCl_2$, 1.3 $MgCl_2$ and 1.2 NaH_2PO_4 equilibrated with 5% CO_2 in 95% O_2 at room temperature, slices were transferred to a chamber containing the same aCSF and kept at a temperature between 33-35 ºC. Cells were patched under visual control (Nikon FN1 microscope – Scientifica Patch Star manipulators). Currents were recorded with an Axopatch700B amplifier and Digidata 1322 interface (Axon Instruments) using an internal pipette solution containing (mM) 120.0 Cs gluconate, 20.0 CsCl, 1.1 EGTA, 0.1 $CaCl_2$, 10.0 HEPES, 2.0 Mg-ATP, 0.4 Na-GTP, 2 $MgCl_2$, using CsOH to adjust pH (pH 7.3, 280 mOsM). Miniature inhibitory postsynaptic currents (mIPSCs) were recorded at a holding potential of +10mV, the reversal potential for glutamatergic events(*1*), in presence of TTX (1 µM). Average series resistance (RS) in pyramidal cells from P6 were 23.3 ± 1.5 MΩ. When the RS changed during the recording by more than 20%, the recording was terminated. All recorded cells were filled with biocytin for *post-hoc* morphological identification, which was performed according to a previously described protocol (*2*).

Immunohistochemistry

Immunohistochemical analysis was carried out as previously described (*3*). After an overdose of avertin (2.5x 240 µg/g, i.p.), mice were perfused intracardially with a fixative solution containing 4% paraformaldehyde in 0.12 M sodium phosphate buffer (pH 7.4 - PB). Mice received 10 mL of fixative solution for each 10 g of body weight. After perfusion, the brains were removed, post-fixed in the same fixative solution for 2 hours (P12 up to P60) or overnight (pups) and rinsed for 1.5 hours in PB. Blocks of the forebrain were immersed in a cryoprotective solution of 20% sucrose in PB overnight at 4 ºC, quickly frozen on dry ice and sectioned coronally with a thickness of 100 µm (pups up to P9) or 40 µm

(P12 up to P60) with a cryostat (Leica CM3050S, Heidelberg, Germany). The sections were rinsed in 0.01 M of PB saline (pH 7.4 - PBS), collected in anatomical series and stored in 48-well trays as free-floating sections in PBS supplemented with 0.05 µM sodium azide. The trays were stored at 4 ºC until immunohistochemical processing. In each anatomical series, every 8 (pups) or 10 (P12 up to P60) section was stained with cresyl violet (*3*) to determine the general characteristics of the tissue. To stain $A_{2A}R$, sections were rinsed 3 times in PB, incubated for 30 min in 1% H_2O_2 diluted in PB for 30 min and pre-treated for 1 hour in 1:30 normal goat serum (NGS, from Gibco®, Alfagene, Carcavelos, Portugal) diluted in 0.2 M KPBS+0.3% Triton X-100. After washing, sections were incubated overnight at room temperature (RT) with the primary antibody (goat anti-$A_{2A}R$ polyclonal antibody, 1:200, sc-7504 from Santa Cruz Biotechnology, Santa Cruz, CA, USA) diluted in 0.02 M KPBS+0.3% Triton-X100 plus 1:100 NGS. After washing with 0.02 M KPBS, the sections were incubated for 1 hour with the secondary antibody (biotinylated rabbit anti-goat IgG 1:200 from Vector Laboratories, Burlingame, CA, USA) diluted in 0.2 M KPBS plus NGS (1:30). After washing 3x for 30 min in 0.02 M KPBS, the sections were incubated for 1 hour in avidin-biotin-peroxidase complex (ABC Elite; Vector) diluted in 0.02 M KPBS, followed by a 3x 30 min washing step with 0.02 M KPBS and a 15 min incubation with 3,3'-diaminobenzidine (DAB metal concentrate; Pierce, Dagma, Lisboa, Portugal). After washing, sections were mounted on superfrost slides and dried overnight before dehydration and coverslip mounting in Permount medium. Sections were examined under a Zeiss Imager Z2 microscope equipped with AxioCam HR color digital cameras and using the AxioVision 4.7 software (Carl Zeiss, Taper, Sintra, Portugal).

To explore the co-localization of vesicular nucleotide transporter (VNUT) with vesicular GABA transporters (VGAT), the brains from P7 mice were fixed, embedded in 3% agarose and sectioned in 100 µm coronal slices using a Leica VT1200S vibratome. Coronal brain sections were permeabilized and blocked for 1 h in phosphate buffered saline (PBS) containing 1% bovine serum albumin (BSA, from Sigma, Sintra, Portugal), 1% normal donkey serum (NDS, from Millipore, Taper) and 0.3% Triton X-100 at RT. The sections were then incubated with rabbit anti-VNUT (1:50, sc-86312 from Santa Cruz Biotechnology), chicken anti-MAP-2 (1:500, ab92434 from Abcam, Cambridge, UK) and guinea-pig anti-vGAT (1:200, Ref. 131004 from Synaptic Systems, Goettingen, Germany), in PBS with 1% BSA, 1% NDS and 0.1% Triton for 48 h at 4 ºC. After five washing steps with PBS containing 1% BSA, 1% NDS and 0.1% Triton X-100, the brain sections were incubated overnight at 4 ºC with AlexaFluor-488-conjugated donkey anti-guinea-pig, AlexaFluor-555-conjugated donkey anti-rabbit and AlexaFluor-633-conjugated goat anti-chicken (all 1:500, Molecular Probes, Alfagene, Carcavelos, Portugal) in PBS with 1% BSA, 1% NDS and 0.1% Triton X-100. After washing and mounting on slides using Mowiol medium, the sections were visualized in a Zeiss LSM 710 confocal microscope and images processed with ImageJ 1.48v software.

Preparation of total membranes and synaptosomes from the hippocampus

Total membranes and membranes from nerve terminals were prepared as previously described (*4*). After deep anesthesia under halothane atmosphere, mice were killed by decapitation. The hippocampi were quickly removed into ice-cold sucrose (0.32 M) solution containing 1 mM EDTA, 10 mM HEPES, 1 mg/mL BSA, pH 7.4 at 4 ºC, supplemented with a protease inhibitor, phenylmethylsulfonyl fluoride (PMSF 0.1 mM), a cocktail of inhibitors of proteases (CLAP 1%, Sigma) and the antioxidant dithiothreitol (1 µM) and homogenized with a teflon potter elvehjem. The homogenates were centrifuged at 3,000 *g* for 10 min at 4 ºC and the resulting supernatant was divided to prepare total membranes and synaptosomes. To prepare total membranes, the supernatant was further centrifuged at 30,000 *g* for

60 min at 4 ºC; the supernatants were discarded and the pellet, corresponding to total membranes from different brain cell types, was resuspended in appropriate solutions for Western blot or binding assays. To prepare synaptic membranes (membranes from synaptosomes, i.e. purified synapses (*5*), the supernatant was first centrifuged at 14,000 *g* for 12 min at 4 ºC; the resulting pellet (P2 fraction) was resuspended in 1 mL of a 45% (v/v) Percoll solution in HEPES buffer (140 mM NaCl, 5 mM KCl, 25 mM HEPES, 1 mM EDTA, 10 mM glucose; pH 7.4). After centrifugation at 14,000 *g* for 2 min at 4 ºC, the white top layer was collected (synaptosomal fraction), resuspended in 1 mL Krebs-HEPES buffer (140 mM NaCl, 5 mM KCl, 5 mM $NaHCO_3$, 1.2 mM NaH_2PO_4, 1 mM $MgSO_2$, 2 mM $CaCl_2$, 10 mM glucose, and 10 mM HEPES, pH 7.4). Western blot characterization showed that these hippocampal synaptosomes are enriched in presynaptic markers (synaptophysin, SNAP-25, syntaxin-I) with <2% of astrocytic markers (GFAP, GLT-I) (*5, 6*)·(*7*) and virtually no markers of oligodendrocytes (*5*) or of microglia, as gauged by the lack of CD11b immunoreactivity (unpublished data). After homogenization with a micro potter elvehjem, the mixture was centrifuged at 30,000 *g* for 60 min, the supernatant was discarded and the pellet was resuspended in appropriate solutions for Western blot or binding assays.

Subsynaptic fractionation

Membrane fractions representative of the different sub-cellular components of synapses, namely a pre-synaptic active zone, post-synaptic density and extra-synaptic fractions, were obtained using a method previously described (*8*) with some modifications (*9*). Briefly, hippocampi from 10 to 12 mice (or from 30-38 pups, which limited this analysis to 2 experiments) were pooled together and homogenized at 4 ºC in isolation solution (0.32 M sucrose, 0.1 mM $CaCl_2$, 1 mM $MgCl_2$, pH 7.4; 1% CLAP, 0.1 mM PMSF and 1 µM dithiothreitol) and centrifuged at 100,000 *g* for 3 h at 4 ºC. Synaptosomes were collected and centrifuged at 15,000 *g* for 30 min at 4 ºC. The resulting pellets were resuspended and diluted 10x in cold 0.1 mM $CaCl_2$ and then an equal volume of pH 6.0 solubilization buffer 2× concentrated (2% Triton X-100, 40 mM Tris, pH 6.0 at 4 ºC) was added. This suspension of synaptosomal membranes was further incubated for 30 min on ice with mild agitation and the insoluble material (synaptic junctions, comprising the pre-synaptic active zone and the post-synaptic density) was pelleted (40,000 g for 30 min at 4 ºC). The supernatant (non-active zone fraction, corresponding to membranes in the vicinity, but outside the active zone) was decanted and proteins precipitated with 6 volumes of acetone at -20 ºC and recovered by centrifugation (18,000 *g* for 30 min at -15 ºC). The pellet, containing the synaptic junctions, was washed twice in pH 6.0 solubilization buffer and then resuspended in 5 mL of a pH 8.0 solubilization buffer (1% Triton X-100 and 20 mM Tris; pH 8.0 at 4 ºC), incubated for 30 min on ice with mild agitation and centrifuged (40,000 *g* for 30 min at 4 ºC), resulting in a supernatant with the pre-synaptic active zone and a pellet with the post-synaptic density, which were solubilized in 5% SDS for further Western blot analysis. As previously done, the efficiency of each sub-synaptic fractionation was validated by quantifying proteins enriched in the pre-synaptic active zone (SNAP-25), post-synaptic density (PSD95) and in the non-active zone region (synaptophysin) (*9*).

Western blot analysis

The amount of protein in total membranes, synaptosomal, presynaptic, postsynaptic and non-active zone fractions, was determined using the bicinchoninic acid method (Pierce) to carefully dilute all extracts to a final concentration of 2 µg protein/µL in SDS-PAGE buffer. Western blotting was performed as previously described (*4*)·(*10*). Electrophoresis was carried out using a 7.5% SDS-PAGE gel after loading 60 µg of different fractions. Composition of the resolving gel was 7.5% acrylamide, 0.5 M

Tris pH 8.8, 0.2% SDS, 0.2% APS, 6 µL TEMED, water up to 8.7 mL. Composition of stacking gel was 4% acrylamide, 0.125M Tris pH 6.8, 0.1% SDS, 0.05% APS, 10 µL TEMED, water up to 10mL. Proteins were then transferred to polyvinylidene difluoride (PVDF) membranes (GE Healthcare, Carnaxide, Portugal). Membranes were blocked for 1 h at RT with 5% low-fat milk in Tris-buffered saline or 3% BSA (depending on the antibodies used), pH 7.6, and containing 0.1% Tween 20 (TBS-T). Membranes were then incubated overnight at 4 ºC with primary antibodies: we used goat anti-A_{2A}R antibody (1:500, sc-7504 from Santa Cruz Biotechnology) or mouse anti-A_{2A}R antibody (1:1,000, 05-717 from Millipore, Taper), which selectivity was confirmed in tissue from A_{2A}R knockout mice (*4*), diluted in Tris-buffered saline (137 mM NaCl and 20 mM Tris–HCl, pH 7.6) with 0.1% Tween (TBS-T) and 5% BSA (fatty acid free). To validate the effectiveness of the subsynaptic separation, we also used other primary antibodies, namely SNAP-25 (1:10,000; S5187 from Sigma), PSD95 (1:10,000; MAB1596 from Millipore), synaptophysin (1:10,000; ab14692 from Abcam) or syntaxin-I (1:20,000; S0664 from Sigma). After washing twice with TBS-T, the membranes were incubated with appropriate secondary antibody conjugated with alkaline phosphatase (Amersham, Buckinghamshire, UK) for 2 h at RT. After washing, the membranes were revealed using an ECF kit (Amersham) and visualized with an imaging system (VersaDoc 3000, Bio-Rad, Amadora, Portugal) and quantified with the Quantity One software (Bio-Rad). The membranes were then re-probed and tested for β-tubulin immunoreactivity using a mouse anti-β-tubulin-III antibody (1:1000; ab18207 from Abcam), to confirm that similar amounts of protein were applied to the gels (*4*).

Receptor binding

The binding assays were performed as previously described (*4*)·(*10*). Briefly, the total membranes or synaptosomal membranes were resuspended in a preincubation solution (containing 50 mM Tris, 1 mM EDTA, 2 mM EGTA, pH7.4) and a sample was collected to determine the protein concentration using the BCA assay (Pierce). Adenosine deaminase (ADA, 2 U/mL, Roche, Amadora, Portugal) was added and the membranes were incubated for 30 min at 37 ºC to remove endogenous adenosine. The mixtures were centrifuged at 25,000 *g* for 20 min at 4 ºC, and the pelleted membranes were resuspended in Tris-Mg solution (containing 50 mM Tris and 10 mM $MgCl_2$, pH 7.4) with 4 U/mL of ADA. Binding with 3 nM of the selective A_{2A}R antagonist, ^{3}H-SCH58261 (specific activity of 77 Ci/mmol; prepared by GE Healthcare and offered by Dr. E.Ongini, Shering-Plough, Milan, Italy) was performed for 1 h at RT with 140-210 µg of protein, with constant swirling. The binding reactions were stopped by addition of 4 mL of ice-cold Tris-Mg solution and filtration through Whatman GF/C glass microfiber filters (GE Healthcare) in a filtration system (Millipore). The radioactivity was measured after adding 2 mL of scintillation liquid (AquaSafe 500Plus, Zinsser Analytic, Frankfurt, Germany). The specific binding was expressed as fmol/mg protein and was estimated by subtraction of the non-specific binding, which was measured in the presence of 12 µM of xanthine amine congener (Sigma), a mixed A_1R/A_{2A}R antagonist. All binding assays were performed in duplicate.

Release of ATP

The release of ATP was measured on-line using the luciferin-luciferase assay (*11*). Briefly, one aliquot of the synaptosomal suspension (35 µL with circa 40 µg of protein) and 15 µL of ATP assay mix (containing luciferin and luciferase; from Sigma) were added to 150 µL of Krebs-HEPES solution. This suspension was equilibrated at 25 ºC from 3 min (for stimulus-dependent evoked release of ATP) up to 10 min (when testing the impact of most drugs) to ensure the functional recovery of the synaptosomes. The suspension was then transferred to a well of a white 96-well plate, which was

maintained for 1 min at 25 ºC inside a luminometer (Perkin Elmer Victor3) before initiating the recording of the electrical signal generated by the photomultiplier. We first measured the basal outflow of ATP during 60 sec, before triggering the evoked release of ATP with a chemical stimulus consisting of a Krebs-HEPES solution with an isomolar substitution of NaCl by 32 mM of KCl. After this chemical stimulation, the light levels were recorded for an additional 200 sec. The evoked release of ATP was calculated by integration of the area of the peak upon subtraction of the estimated basal ATP outflow and always discounting the (minor) variation of luminescence caused by possible mechanic or osmolarity alterations, which was evaluated in a parallel assay in the same batch of nerve terminals by adding medium with an amount of Krebs-HEPES solution equal to the amount of K^+-rich solution used in the test situation. The levels of ATP were estimated using a calibration curve for ATP, which were linear between $2x10^{-12}$ and $8x10^{-5}$ M (*11*). To test the impact of drugs on ATP release, these drugs were added to the synaptosomes during the 10 min equilibration period at 25 ºC and were present throughout the assays. None of the tested drugs modified the light emission by the luciferin-luciferase assay when testing different concentrations of ATP standards.

Release of adenosine

Adenosine release from hippocampal synaptosomes was carried out as essentially previously described (*12*). Hippocampal synaptosomes (~0.6-0.9 mg protein) were layered over GF-B filters (Whatman, Sigma, Sintra, Portugal), placed in swinney filter holders with 90 μL of volume. They were superfused in a closed-loop manner with 2 mL of Krebs solution containing the adenosine deaminase inhibitor erythro-9-(2-hydroxy-3-nonyl)adenine (EHNA, 10 μM, from Sigma) and the nucleoside transporter inhibitor nitrobenzylthioinosine (NBTI, 1 μM; from Sigma). This solution was maintained at 37 ºC. After 15 min, a sample of 250 μL was collected for HPLC analysis of the basal concentration of adenosine. We immediately added to the remaining superfusion solution 250 μL of Krebs without sodium and with EHNA and NBTI and 240 mM KCl, to obtain a final concentration of 30 mM K^+ to depolarize the synaptosomes and trigger adenosine release (*13*). After 2 min of superfusion in a closed-loop manner, a sample of 250 μL was collected for HPLC analysis of adenosine release. When we tested the effect of the inhibitor of ecto-5'-nucleotidase α,β-methylene ADP (AOPCP, 100 μM, from Sigma), it was present in all solutions used for superfusion of the synaptosomes.

The separation and quantification of adenosine was carried out by High Pressure Liquid Chromatography (HPLC), as previously described (*14*), employing a LiChroCart-RT 125-4 C-18 reverse-phase column (particle size, 5 μm), combined with an UV detector set to 254 nm. The mobile phase consisted of KH_2PO_4 (100 mM; from BDH Aristar, VWR, Carnaxide, Portugal) and methanol (85/15 v/v%) at pH 6.50, with the flow rate of 1 mL/min, and a loop volume of 100 μL. The quantification of adenosine was achieved by calculating the peak areas then converted to concentration values by calibration with known standards ranging from 0.1 to 10 μM. The evoked release was quantified as the total amount of adenosine present after addition of K^+ minus the basal amount of adenosine.

Neuronal culture

Primary cultures of hippocampal neurons were prepared as previously described (*15*) with some modifications of the protocol. Briefly, hippocampi were dissected from embryonic day 18 or 19 Sprague-Dawley rats of either sex. Tissue was then trypsinized (0.25% v/v), and mechanically dissociated in 1x HBSS (Invitrogen, Cergy Pontoise, France) containing 10 mM HEPES (Invitrogen). Neurons were plated at a density of 60 or 120 × 10^3 cells/mL onto 18-mm diameter glass coverslips (Assistent, Winigor, Germany) pre-coated with 50 μg/mL poly-D,L-ornithine (Sigma-Aldrich, Lyon,

France) in plating medium composed of Minimum Essential Medium (MEM, Sigma) supplemented with horse serum (10% v/v, Invitrogen), L-glutamine (2 mM) and Na^+ pyruvate (1 mM) (Invitrogen). After attachment for 3-4 hours, cells were incubated in culture medium that consists of Neurobasal medium supplemented with B27 (1X), L-glutamine (2 mM), and antibiotics (penicillin 200 units/mL, streptomycin, 200 µg/mL) (Invitrogen), and kept for up to 4 weeks at 37 ºC in a 5% CO_2 humidified incubator. Each week, one fifth of the culture medium volume was renewed. In certain experiments, cytosine d-D-arabinofuranoside (AraC) (5 µM) was added at DIV1 to obtain pure neuronal cultures (Extended Data Fig. 8).

DNA constructs

The following constructs were used: *GEPHN* 3'-UTR shRNA and control shRNA-3m (*16*)[,](*17*), eGFP-gephyrin P1 variant (*18*), eGFP-gephyrin S303A and S303D mutants (*16*)[,](*19*)[,](*20*), shRNA against $A_{2A}R$ (*21*) non-target shRNA coupled to GFP (*22*). GABAARγ2-GFP (*23*), gephyrin-mRFP (*15*), shRNA against Neuroligin 2 (kindly provided by Peter Scheiffele, Addgene plasmid # 59358) (*24*), shRNA against slitrk3 coupled to CFP (*25*) and a scrambled shRNA sequence "shMock" (kindly provided by Ann Marie Craig, Vancouver, Canada). All the constructs were sequence-verified by Beckman Coulter Genomics.

Neuronal transfection

Transfections were carried out at DIV 6-7 for neurons undergoing synaptogenesis, DIV 14 in adults neurons using Lipofectamine 2000 (Invitrogen) or Transfectin (BioRad, Hercules, USA), according to the manufacturers' instructions (DNA:transfectin ratio 1 µg:3 µL), with 1µg of plasmid DNA per 20 mm well. The following ratios of plasmid DNA were used in co-transfection experiments: 0.5:0.5 µg for eGFP-S303A/eGFP-S303D: *GEPHN* 3' UTR shRNA, 0.8:0.5 µg for GABAARγ2-GFP: gephyrin-mRFP. Experiments were performed 2-5 days post-transfection in neurons undergoing synaptogenesis, 10 days post-transfection for mature neurons.

Pharmacology

For ICC experiments, SCH58261 (100 nM, Abcam), ADA (4-20 U/mL, Roche), AMPCP (100 µM, Sigma) and/or CGS21680 (30 nM, Abcam), were directly added to the culture medium and the neurons were returned to a 5% CO_2 humidified incubator for 10 min to 1 hour before use. Experiments using tetanus toxin (1-40 nM, Alomone Labs) or Nrx1b-Fc peptide (60 µg/mL) (*26*)[,(27)], cells were treated for 2 days (from DIV 7 to 9) and then the appropriate drugs were added for 30 min to the toxin or the peptide solution . For SPT experiments, neurons were labeled at 37 ºC in imaging medium (see below for composition) in presence of SCH58261, transferred to a recording chamber and recorded within 45 min at 31 ªC in imaging medium in presence of SCH58261. The imaging medium consisted of phenol red-free minimal essential medium supplemented with glucose (33 mM; Sigma) and HEPES (20 mM), glutamine (2 mM), Na^+-pyruvate (1 mM), and B27 (1X) from Invitrogen.

For electrophysiological experiments SCH58261 (100 nM, Abcam), ADA (4-20 U/mL, Roche), AMPCP (100 µM, Sigma) were directly added to the aCSF medium in presence of TTX (1 µM Abcam), equilibrated with 5% CO_2 in 95% O_2 and bath applied with a peristaltic system to the hippocampal slices for 30 min at 30-32 ºC. Dynasore (1 µM, Tocris) GDP□S (10 µM, Tocris), IBMX + FSK (10 µM, Tocris), PKI (10 µM, Tocris) were added in the Cs-gluconate solution in the patch pipet. After the recordings the slices were fixed with paraformaldehyde (PFA 4% w/v; Sigma) overnight, rinsed 3 times with in 0.12 M PB, cryoprotected in a 20% sucrose solution overnight at 4 ºC and quickly frozen on dry ice. The

recorded slices were processed for *post-hoc* morphological identification of the neuron filled with biocytin according to a previously described protocol (*2*).

Immunocytochemistry

To label and quantify the density of inhibitory synapses, pre-treated neurons were fixed for 15 min at RT in 4% PFA and sucrose (14% w/v; Sigma) solution in 1X PBS. Cells were then washed and permeabilized with a solution containing Triton X-100 (0.25% w/v, Carl Roth GmbH) diluted in PBS 1X. Cells were then incubated for 1 hour at RT in goat serum (GS; 10% v/v; Invitrogen) and Triton X-100 (0.1% w/v) in PBS to block nonspecific staining. Neurons were then incubated for 1 hour overnight with a primary antibody mix consisting of rabbit anti-VGAT (1:500, provided by B. Gasnier, Univ. Paris Descartes, Paris), mouse anti-gephyrin (mAb7a, 1:500, Synaptic Systems) and GABAARγ2 subunit (1:2000, provided by J.M. Fristchy, Univ. Zurich) in PBS supplemented with GS (10% v/v, Invitrogen) and Triton (0.1% v/v). After washes, cells were incubated for 45 min at RT with a secondary antibody mix containing donkey anti-guinea pig-cy3 (1:400, Jackson Immunoresearch), goat anti-rabbit-FITC (1:300, Jackson Laboratories) and donkey anti-mouse-cy5 (1:300, Jackson Laboratories) in PBS-GS-Triton blocking solution, washed, and finally mounted on glass slides using Mowiol 4-88 (48 mg/mL, Sigma). Sets of neurons compared for quantification were labeled simultaneously.

For $A_{2A}R$ detection over time in culture, cells were fixed for 15 min at RT in PFA solution (as above), washed in PBS, and permeabilized with Triton as above. After washes, cells were incubated for 1 hour at RT in PBS-GS-Triton blocking solution and incubated for 1 hour with a mouse antibody against GAD 67 (1:500, Chemicon) and rabbit antibody against $A_{2A}R$ (1:100, Alomone labs) in PBS-GS-Triton staining solution. After washes, cells were incubated for 45 min at RT with goat anti-rabbit-cy3 (1:500, Jackson Laboratories) and goat anti-mouse-FITC (1:300, Jackson Laboratories) in PBS-GS-Triton solution, washed, and mounted on glass slides using Mowiol 4-88 (48 mg/mL, Sigma). Sets of neurons compared for quantification were labeled simultaneously.

For STORM imaging of $A_{2A}R$ at inhibitory synapses, cells were fixed for 15 min at RT in PFA solution (as above), washed in PBS, and permeabilized with Triton as above. After washes, cells were incubated for 1 hour at RT in PBS-GS-Triton blocking solution and incubated overnight at 4 ºC with a rabbit antibody against $A_{2A}R$ (1:100, Alomone Labs) and mouse anti-gephyrin (mAb7a, 1:500, Synaptic Systems) in PBS-GS-Triton staining solution. After washes, cells were incubated for 45 min at RT with donkey anti-rabbit coupled to Alexa405/Alexa647 and donkey anti-mouse coupled to cy3/A647 and then imaged.

The immunocytochemical analysis of individual GABAergic was carried out as previously (*28*). P7-mice nerve terminals were obtained through a discontinuous Percoll gradient, as previously described (*6*), placed onto coverslips previously coated with poly-L-lysine for 1 h, fixed with 4% PFA for 15 min and washed twice with PBS medium. The synaptosomes were permeabilized in PBS with 0.2% Triton X-100 for 10 min and then blocked for 1 h in PBS with 3% BSA and 5% normal bovine serum to prevent non-specific binding. The synaptosomes were then immunolabelled with rabbit anti-VNUT (1:50, Santa Cruz Biotechnology), chicken anti-MAP-2 (1:500, Abcam) and guinea-pig anti-VGAT (1:200, Synaptic Systems) antibodies in blocking solution for 1 h at RT. The nerve terminals were then washed three times with PBS with 3% BSA and incubated for 1 h at RT with AlexaFluor-488-conjugated donkey anti-guinea-pig, AlexaFluor-555-conjugated donkey anti-rabbit and AlexaFluor-633-conjugated goat anti-chicken (all 1:500, Molecular Probes) in blocking solution for 1 h at RT. After washing and mounting on slides with Vectashield mounting medium (Vector Laboratories), synaptosomes were visualized and images were acquired in a Zeiss Imager Z2 microscope with a AxioCam HRm and 63x Plan-ApoChromat

oil objective (1.4 numerical aperture), using the Axiovision SE64 Rel. 4.8 software. For each synaptosomal preparation, three coverslips were analyzed by counting 3 different fields and a minimum of 200 individualized elements per field.

Fluorescence image acquisition and analysis

Image acquisition was performed using a 63 X objective (NA 1.40) on a Leica (Nussloch, Germany) DM6000 upright epifluorescence microscope with a 12-bit cooled CCD camera (Micromax, Roper Scientific) run by MetaMorph software (Roper Scientific, Evry, France). Quantification was performed using MetaMorph software (Roper Scientific). Image exposure time was determined on bright cells to obtain best fluorescence to noise ratio and to avoid pixel saturation. All images from a given culture were then acquired with the same exposure time and acquisition parameters.

For cluster analysis, images were first flatten background filtered (kernel size, 3 X 3 X 2) to enhance cluster outlines, and a user defined intensity threshold was applied to select clusters and avoid their coalescence. Clusters were outlined and the corresponding regions were transferred onto raw images to determine the mean cluster number, area and fluorescence intensity. For quantification of gephyrin or $GABA_AR$ synaptic clusters, gephyrin or receptor clusters comprising at least 3 pixels and colocalized on at least 1 pixel with VGAT clusters were considered. The dendritic length of the region of interest was measured to determine the number of clusters per 10 µm. For each culture, we analyzed ~10 cells per experimental condition and ~20 clusters per cell.

Live cell staining for single particle imaging

Neurons were stained as previously described (*15*),(*29*). Briefly, cells were incubated for 3-5 min at 37 ºC with primary antibodies against extracellular epitopes of $GABA_A$ receptor γ2 subunit (guinea pig, 1:750/1:1000 provided by J.M. Fritschy), washed, and incubated for 3-5 min at 37 ºC with biotinylated Fab secondary antibodies (goat anti-guinea pig, 4-12 µg/mL; Jackson Immunoresearch, West Grove, USA) in imaging medium. After washes, cells were incubated for 1 min with streptavidin-coated quantum dots (QDs) emitting at 605 nm (1 nM; Invitrogen) in borate buffer (50 mM) supplemented with sucrose (200 mM) or in PBS (1M; Invitrogen) supplemented with 10% Casein (v/v) (Sigma). Washing and incubation steps were all done in imaging medium.

Single particle tracking and analysis

Cells were imaged as previously described (*15*) using an Olympus IX71 inverted microscope equipped with a 60X objective (NA 1.42; Olympus) and a Lambda DG-4 monochromator (Sutter Instrument). Quantum Dot (QD) real time recordings (integration time of 75 ms over 800 consecutive frames) were acquired with Hamamatsu ImagEM EMCCD camera and MetaView software (Meta Imaging 7.7). Cells were imaged within 45 min following labeling.

QD tracking and trajectory reconstruction were performed with homemade software (Matlab; The Mathworks, Natick, MA) as described in (*15*),(*29*). One to two sub-regions of dendrites were quantified per cell. In cases of QD crossing, the trajectories were discarded from analysis. Values of the mean square displacement (MSD) plot versus time were calculated for each trajectory by applying the relation:

$$MSD(n\tau) = \frac{1}{N-n}\sum_{i=1}^{N-n}\left[\left(x((i+n)\tau) - x(i\tau)\right)^2 + \left(y((i+n)\tau) - y(i\tau)\right)^2\right]$$

(*30*), where τ is the acquisition time, N is the total number of frames, n and i are positive integers with n determining the time increment. Diffusion coefficients (D) were calculated by fitting the first four points without origin of the MSD versus time curves with the equation: $MSD(n\tau) = 4Dn\tau + b$ where b is a constant reflecting the spot localization accuracy.

Videomicroscopy of presynaptic terminals

Cultures were exposed for 30 s to KCl (40 mM) to stimulate synaptic vesicle recycling. Cells were washed and imaged in the presence of the appropriate drugs. All washes, incubation steps, and cell imaging were performed in recording medium. Inhibitory synapses were stained by incubating live neurons for 48 hours at 37 ºC in a 5% CO_2 humidified incubator with a primary VGAT antibody directly coupled to Oyster550 (1:200, Synaptic Systems) diluted in conditioned maintenance medium. Cells were washed and imaged in the presence of the appropriate drugs.

Cells were imaged using an Olympus IX71 inverted microscope equipped with a 60X objective (NA 1.42; Olympus) and a Lambda DG-4 monochromator (Sutter Instrument). Time lapse imaging of FM1-43 or VGAT-Oyster550 (1 image every 5 min) were acquired with Hamamatsu ImagEM EMCCD camera and MetaView software (Meta Imaging 7.7). Cells were imaged for 40 min following labeling.

STORM imaging

STORM imaging on fixed samples was carried out on an inverted N-STORM Nikon Eclipse Ti microscope with a 100x oil-immersion objective (N.A. 1.49) and an Andor iXon Ultra EMCCD camera (image pixel size, 160 nm), using specific lasers for STORM imaging of Alexa dyes (405 and 561 and 647 nm). Movies of 10000 frames were acquired at frame rates of 50 ms. The z position was maintained during acquisition by a Nikon perfect focus system. Single-molecule localization and 2D image reconstruction was conducted as described in (*31*) by fitting the PSF of spatially separated fluorophores to a 2D Gaussian distribution. The positions of fluorophore were corrected by the relative movement of the synaptic cluster by calculating the center of mass of the cluster throughout the acquisition using a partial reconstruction of 2000 frames with a sliding window (*31*). STORM images were rendered by superimposing the coordinates of single-molecule detections, which were represented with 2D Gaussian curves of unitary intensity and SDs representing the localization accuracy (sigma= 20 nm). In order to correct multiple detections coming from the same molecule (*31*), we identified detections occurring in the vicinity of space (2 x sigma) and time (15 s) as belonging to a same molecule.

Statistics

Sample size selection for experiments was based on published experiments, pilot studies as well as in-house expertise. All results were used for analysis except in few cases.

Cells with signs of suffering (apparition of blobs, fragmented neurites) were discarded from the analysis. Means are shown ± SEM. Means were compared using the non-parametric Mann-Whitney test (immunocytochemistry) using SigmaPlot 12.5 software (Systat Software). Diffusion coefficient values having non-normal distributions, a non-parametric Kolmogorov-Smirnov test was run under Matlab (The Mathworks, Natick, MA). Differences were considered significant for p-values less than 5% *(*p≤0.05; **p<0.01; ***p<0.001).*

Clampfit 10.2 and Minianalysis software (Synaptosoft) were used to analyze synaptic events collected from electrophysiological recordings. Cumulative distributions of frequency and amplitude were examined using the same number of events (50) per cell per condition. The statistical analysis was done using a 50 msec binning for the interevent interval and 2.5 pA for the amplitude). Data collected

from electrophysiological recordings, having non-normal distributions, we used a non-parametric two tailed Kolmogorov-Smirnov test with OriginLab 7.5 (OriginLab Corporation). Differences were considered significant for p-values less than 5% *(*p≤0.05; **p<0.01; ***p<0.001).*
For, western blot, receptor binding, release of adenosine and ATP analysis from sysaptosomes, means were compared using the non-parametric Mann-Whitney (ATP release) test or, for multiple comparisons, the one- or two-way ANOVA followed by Dunnet's or Bonferroni post hoc test (Adenosine basal and evoked release, western blots), or and Paired t-test independent means (receptor binding essay) using GraphPad Prim (GraphPad Prim software). Values are expressed as means ± SEM and differences were considered significant for p-values less than 5% *(*p≤0.05; **p<0.01; ***p<0.001).*

References

1. R. Cossart *et al.*, Dendritic but not somatic GABAergic inhibition is decreased in experimental epilepsy. *Nat. Neurosci* **4**, 52 (2001).
2. M. Esclapez, J. C. Hirsch, Y. Ben-Ari, C. Bernard, Newly formed excitatory pathways provide a substrate for hyperexcitability in experimental temporal lobe epilepsy. *J. Comp. Neurol* **408**, 449 (1999).
3. N. Gonçalves, A. T. Simões, R. A. Cunha, L. P. de Almeida, Caffeine and adenosine A(2A) receptor inactivation decrease striatal neuropathology in a lentiviral-based model of Machado-Joseph disease. *Ann Neurol.* **73**, 655 (2013).
4. N. Rebola, P. M. Canas, C. R. Oliveira, R. A. Cunha, Different synaptic and subsynaptic localization of adenosine A2A receptors in the hippocampus and striatum of the rat. *Neuroscience* **132**, 893 (2005).
5. R. A. Cunha, A. M. Sebastião, J. A. Ribeiro, Ecto-5'-nucleotidase is associated with cholinergic nerve terminals in the hippocampus but not in the cerebral cortex of the rat. *J Neurochem.* **59**, 657 (1992).
6. R. J. Rodrigues, P. M. Canas, L. V. Lopes, C. R. Oliveira, R. A. Cunha, Modification of adenosine modulation of acetylcholine release in the hippocampus of aged rats. *Neurobiol Aging* **29**, 1597 (2008).
7. M. Matos *et al.*, Adenosine A2A receptors modulate glutamate uptake in cultured astrocytes and gliosomes. *Glia.* **60**, 702 (2012).
8. G. R. Phillips *et al.*, The presynaptic particle web: ultrastructure, composition, dissolution, and reconstitution. *Neuron* **32** 1(2001).
9. P. M. Canas, R. A. Cunha, in *Receptor and Ion Channel Detection in the Brain,* C. F. Lujan R, Ed. (Springer, New York, 2016), vol. 110, pp. 31-37.
10. G. M. Cunha, P. M. Canas, C. R. Oliveira, R. A. Cunha, Increased density and synapto-protective effect of adenosine A2A receptors upon sub-chronic restraint stress. *Neuroscience* **141**, 1775 (2006).
11. R. A. Cunha, E. S. Vizi, J. A. Ribeiro, A. M. Sebastião, Preferential release of ATP and its extracellular catabolism as a source of adenosine upon high- but not low-frequency stimulation of rat hippocampal slices. *J Neurochem* **67**, 2180 (1996b).
12. P. Garção *et al.*, Functional interaction between pre-synaptic α6β2-containing nicotinic and adenosine A2A receptors in the control of dopamine release in the rat striatum. *Br J Pharmacol* **169**, 1600 (2013).

13. R. A. Cunha, T. Almeida, J. A. Ribeiro, Parallel modification of adenosine extracellular metabolism and modulatory action in the hippocampus of aged rats. *J Neurochem* **76**, 372 (2001).
14. R. A. Cunha, S. A.M., Adenosine and adenine nucleotides are independently released from both the nerve terminals and the muscle fibres upon electrical stimulation of the innervated skeletal muscle of the frog. *Pflugers Arch Eur J Physiol* **424**, 503 (1993).
15. Chamma I. *et al.*, Activity-dependent regulation of the K/Cl transporter KCC2 membrane diffusion, clustering, and function in hippocampal neurons. *J. Neurosci* **33**, 15488 (2013).
16. S. K. Tyagarajan *et al.*, Regulation of GABAergic synapse formation and plasticity by GSK3beta-dependent phosphorylation of gephyrin. . *Proc. Natl. Acad. Sci. U. S. A.* **108**, 379 (2011).
17. W. Yu *et al.*, Gephyrin clustering is required for the stability of GABAergic synapses. *Mol. Cell. Neurosci* **36**, 484 (2007).
18. B. Lardi-Studler *et al.*, Vertebrate-specific sequences in the gephyrin E-domain regulate cytosolic aggregation and postsynaptic clustering. *J. Cell Sci.* **120**, 1371 (2007).
19. C. E. Flores *et al.*, Activity-dependent inhibitory synapse remodeling through gephyrin phosphorylation. *Proc. Natl. Acad. Sci. U. S. A.* , (2014).
20. S. K. Tyagarajan *et al.*, Extracellular signal-regulated kinase and glycogen synthase kinase 3β regulate gephyrin postsynaptic aggregation and GABAergic synaptic function in a calpain-dependent mechanism. *J. Biol. Chem.* **288**, 9634 (2013).
21. A. P. Simões *et al.*, Adenosine A2A receptors in the amygdala control synaptic plasticity and contextual fear memory. *Neuropsychopharmacology* **41**, 2862 (2016).
22. G. Gauvain *et al.*, The neuronal K-Cl cotransporter KCC2 influences postsynaptic AMPA receptor content and lateral diffusion in dendritic spines. *Proc Natl Acad Sci U S A.* **108**, 15474 (2011).
23. E. Eugène *et al.*, GABA(A) receptor gamma 2 subunit mutations linked to human epileptic syndromes differentially affect phasic and tonic inhibition. *J Neurosci* **27**, 14108 (2007).
24. B. Chih, H. Engelman, P. Scheiffele, Control of excitatory and inhibitory synapse formation by neuroligins. *Science* **307**, 1324 (2005).
25. H. Takahashi *et al.*, Selective control of inhibitory synapse development by Slitrk3-PTPδ trans-synaptic interaction. *Nat Neurosci* **15**, S1 (2012).
26. P. Scheiffele, J. Fan, J. Choih, R. Fetter, T. Serafini, Neuroligin Expressed in Nonneuronal Cells Triggers Presynaptic Development in Contacting Axons. *Cell* **101**, 657 (2000).
27. J. N. Levinson *et al.*, Neuroligins mediate excitatory and inhibitory synapse formation: involvement of PSD-95 and neurexin-1beta in neuroligin-induced synaptic specificity. *J Biol Chem* **280**, 17312 (2005).
28. P. M. Canas, A. P. Simões, R. J. Rodrigues, R. A. Cunha, Predominant loss of glutamatergic terminal markers in a β-amyloid peptide model of Alzheimer's disease. *Neuropharmacology* **76**, 51 (2014).
29. H. Bannai, S. Lévi, C. Schweizer, M. Dahan, A. Triller, Imaging the lateral diffusion of membrane molecules with quantum dots. *Nat. Protoc* **1**, 2628 (2006).
30. M. J. Saxton, K. Jacobson, Single-particle tracking: applications to membrane dynamics. *Annu Rev Biophys Biomol Struct* **26**, 373 (1997).
31. C. G. Specht *et al.*, Quantitative nanoscopy of inhibitory synapses: counting gephyrin molecules and receptor binding sites. *Neuron* **79**, 308 (2013).

Supplementary material

Supplementary figure legends.

Figure S1: The density of adenosine A_{2A} receptors (A_{2A}R) is greater during the peak of synaptogenesis in pups than in adult mice. A. Developmental immunohistochemical detection of A_{2A}Rs. **B.** Western Blot showing the developmental A_{2A}R expression on hippocampal synaptosomes. N= 6-8 mice. **C.** Binding assays with the A_{2A}R antagonist ^{3}H-SCH58261 on synaptosomal or total membranes from P7 or P30 hippocampi. P7 n= 8, P30 n= 6 mice. **D**. Subsynaptic fractionation of synaptosomes at P7 and P30. n=2 mice. NAZ: non active zone. Histograms represent means and s.e.m.; One Way Anova followed by Dunnett's post hoc test (b) and Paired t-test (c): *p≤0.05; **p<0.01; NS Not significant.

Figure S2: **A_{2A} receptor blockade rapidly increases the membrane dynamics of $GABA_AR\gamma2$ subunits.** $GABA_AR\gamma2$ trajectories and cumulative probabilities of diffusion coefficient D (±25-75% Interquartile Range) in absence or presence of SCH58261. N≥ 400 trajectories, 3 cultures. Histograms represent means and s.e.m.; Kolmogorov-Smirnov test: *p≤0.05.

Figure S3: Time-course of gephyrin clusters dispersion following blockade of A_{2A}Rs. Detection and quantification of gephyrin-monomeric Red fluorescent protein clusters in DIV10 neurons after application of SCH58261. N= 30-47 cells, 2-3 cultures. Histograms represent means and s.e.m.; Mann-Whitney test: **p<0.01; NS Not significant.

Figure S4: Acute A_{2A}R blockade decreases miniature GABAergic currents in CA1 hippocampal interneurons. A. Left mIPSC traces before (black) and after (red) SCH58261 in a representative CA1 interneuron (images). Note the presence of varicosities (arrowheads), consistent with endocytosis, along the dendritic arborisation. **Right:** Application of SCH58261 during 30 min reduces the amplitude and frequency of $GABA_AR$-mediated mIPSCs in CA1 interneurons (8 cells, 8 slices, 6 P6 pups). **B.** Paired recordings (6 pairs, 6 slices, 6 P6-7 pups) of CA1 interneurons. Once cell was recorded with the standard intracellular solution, while the other was recorded with the same solution containing dynasore to block clathrin-dependent endocytosis. The reduction in mIPSCs amplitude and frequency occurred in the cells recorded with the standard solution (cell 1), but it was fully prevented in cells simultaneously recorded with the dynasore-containing solution (cell 2). Varicosities (arrowheads) consistent with endocytosis were present in cell 1 but not in cell 2. Histograms represent means and s.e.m.; Kolmogorov-Smirnov test: *p≤0.05; **p<0.01***p<0.001.

Figure S5: Adenosine stabilizes active GABA synapses. Live cell imaging in DIV10 neurons of active GABA synaptic terminals visualized by the incorporation of VGAT-Oyster550 antibodies in recycling vesicles, in absence or presence of ADA+AMPCP. **Top,** Images showing a single recording frame of the neuron before drug application and maximum intensity projections of all time points imaged (1000 frames at intervals of 100 ms). Note the loss (yellow arrows) of some active inhibitory boutons (white dots) upon 15 min bath application of ADA+AMPCP and the high mobility of VGAT packets (seen as white lines on the projection) along the axonal processes (blue arrows). **Bottom**, Quantification of the mean number of VGAT puncta in absence or presence of ADA+AMPCP over a 40-min recording. N= 10 cells, 30-39 regions of interest analysed. Unpaired t-test was used to compare time points between them; Paired t-test was used to compare the whole curves.

Figure S6: CD73 expression peaks during the period of synaptogenesis. Western Blot on hippocampal synaptosomes. N= 6-8 mice. One Way Anova followed by Dunnett's post hoc test: *p<0.05.

Figure S7: Vesicular nucleotide transporters are present in GABAergic synapses in the hippocampus at P7. A. Immunostaining of MAP2, VGAT and VNUT in P7 hippocampal slices showing partial colocalization (yellow) of vesicular nucleotide transporters (VNUT) with VGAT in the stratum radiatum (SR) of the CA1 area of P7 mice. Right panel shows an enlargement of the box in the middle panel. **B.** Immunocytochemical analysis of individual hippocampal synaptosomes showing the percentage of synaptosomes expressing both vNUT and vGAT (yellow, arrowheads). N=3-4 mice. Histogram represents mean and s.e.m.

Figure S8: A_{2A}R-dependent stabilization of GABA synapses is still operant in pure neuronal cultures. A. Immunostaining of GFAP and MAP2 in neurons cultured in absence or presence of cytosine arabinoside (ara-C) highlighting the loss of glial cells upon ara-C treatment. **B.** Immunostaining and quantification of VGAT and $GABA_A$Rγ2 in DIV9 neurons cultured in presence of ara-C. N= 42-56 cells, 3 cultures. **C.** Immunostaining and quantification of VGAT and $GABA_A$Rγ2 in neurons cultured in presence (left) or absence (right) of glia and in presence or absence of the indicated drugs for 30 min. –ara-C, n= 66-83 cells, 6 cultures. +ara-C, n=53-56 cells, 3 cultures. Histograms represent means and s.e.m.; Mann-Whitney test: *p<0.05. **p≤0.01; ***p<0.001.

Figure S9. Source of adenosine stabilizing synapses. The basal levels of adenosine in hippocampal synapses tend to be larger in pups (P7) than young adults (P60) and the blockade of CD73 decreased the basal levels of adenosine in pups but not in adults. Data are mean ± SEM of n=6-8; two-way ANOVA followed by Newman-Keuls' post hoc test: *p≤0.05; NS Not significant.

Figure S10: G protein-dependent mechanism of A_{2A}Rs. A-B. Top: mIPSC traces recorded 5 min (control) and 30 min (GDPβS or PKI) after break-in using internal solutions containing GDPβS or PKI in CA1 hippocampal pyramidal cells from P6 hippocampal slices. GDPβS and PKI reduced mIPSCs amplitude and frequency. N= 7 cells, 7 slices, 6 P6 pups. Histograms represent means and s.e.m.; Kolmogorov-Smirnov test: ***p<0.001.

Figure S11: Immunostaining of $GABA_A$Rγ2 and VGAT in neurons exposed for 48 h to a control IgG or neurexin1β Fc peptide and maintained in absence or presence of CGS21680 for 30 min. N= 44-50 cells, 3 cultures. Histograms represent means and s.e.m.; Mann-Whitney **p<0.01; ***p<0.001; NS Not significant.

Figure S12: Proposed functional scheme. An active GABAergic terminal releases adenosine (ADO) or ATP, both contributing to a local activity-dependent increase of extracellular adenosine to activate A_{2A}Rs. Activation of A_{2A}Rs activates the AC/cAMP pathway, leading to PKA-dependent phosphorylation of gephyrin and the stabilization of the postsynaptic element. The adenosine-mediated stabilization of the presynaptic element further involves the slitrk3-ptpδ trans-synaptic complexes. If A_{2A}Rs are not activated during an extended period of time (around 20 min), the whole synapse collapses and $GABA_A$ receptors are internalized.

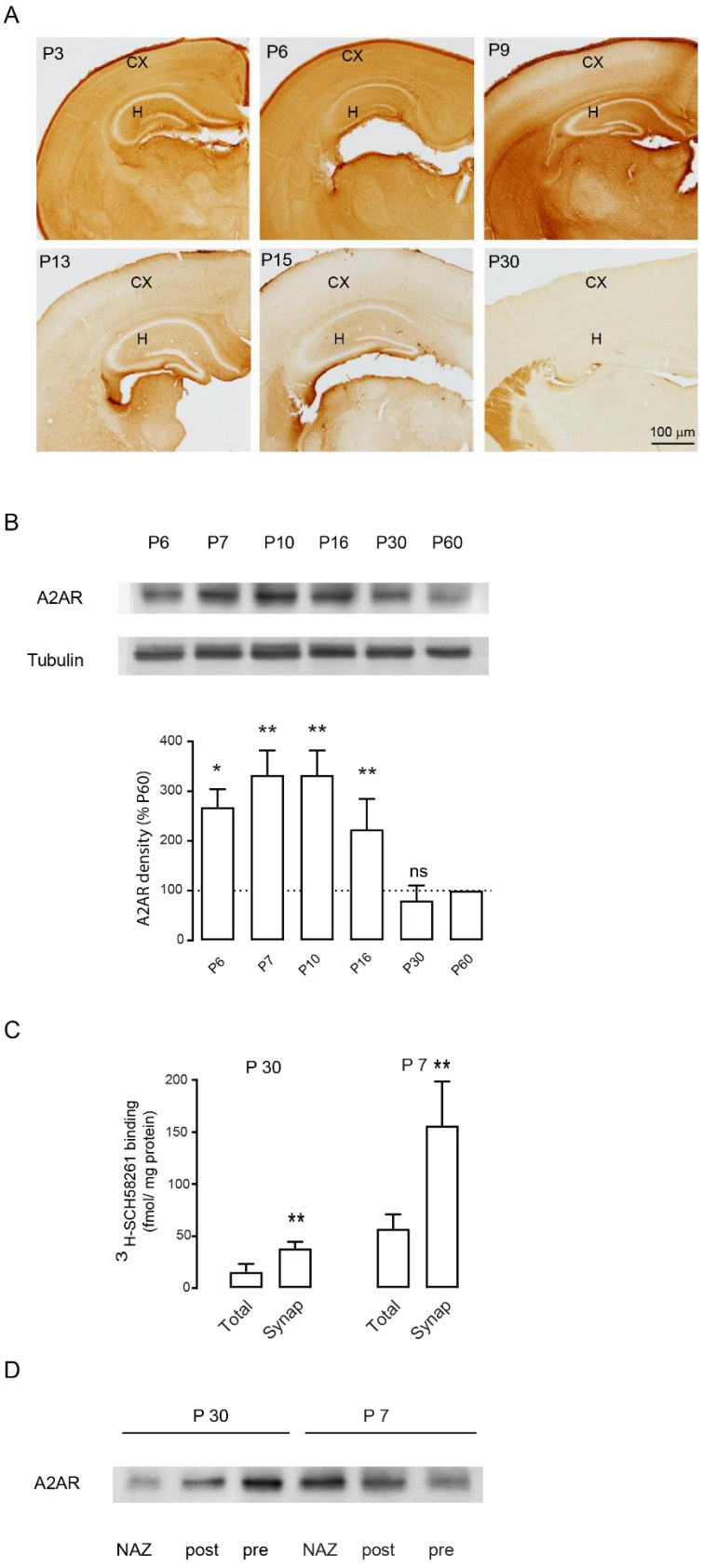
A
P3
CX
H
P6
CX
H
P9
CX
H
P13
CX
H
P15
CX
H
P30
CX
H
100 µm
B
P6 P7 P10 P16 P30 P60
A2AR
Tubulin
A2AR density (% P60)
400
300
200
100
0
*
**
**
**
ns
P6
P7
P10
P16
P30
P60
C
P 30
P 7 **
^{3}H-SCH58261 binding (fmol/ mg protein)
200
150
100
50
0
**
Total
Synap
Total
Synap
D
P 30
P 7
A2AR
NAZ post pre NAZ post pre

Figure S1

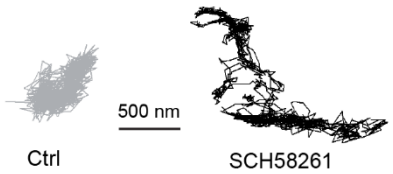

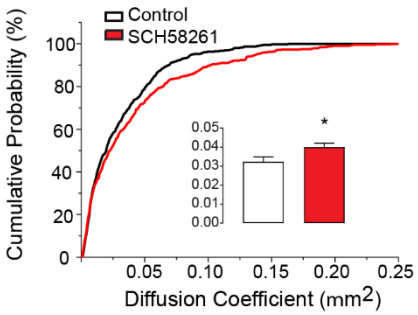

Figure S2

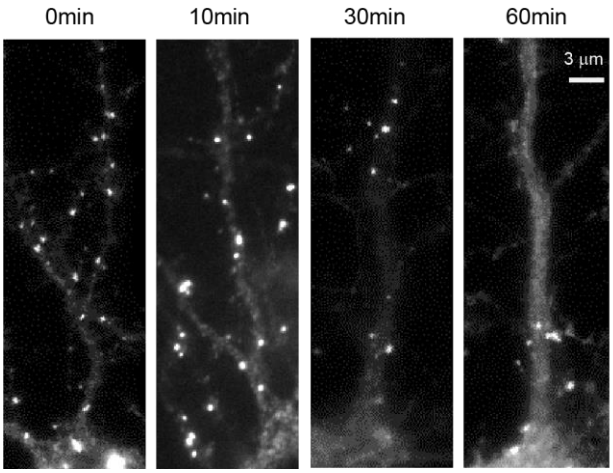

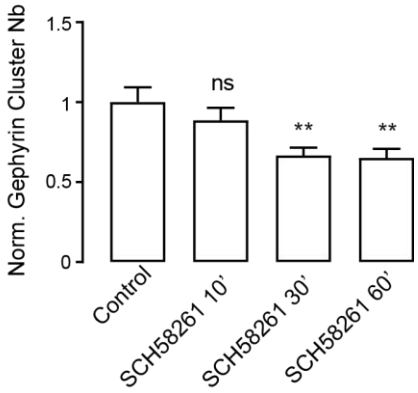

Figure S3

A

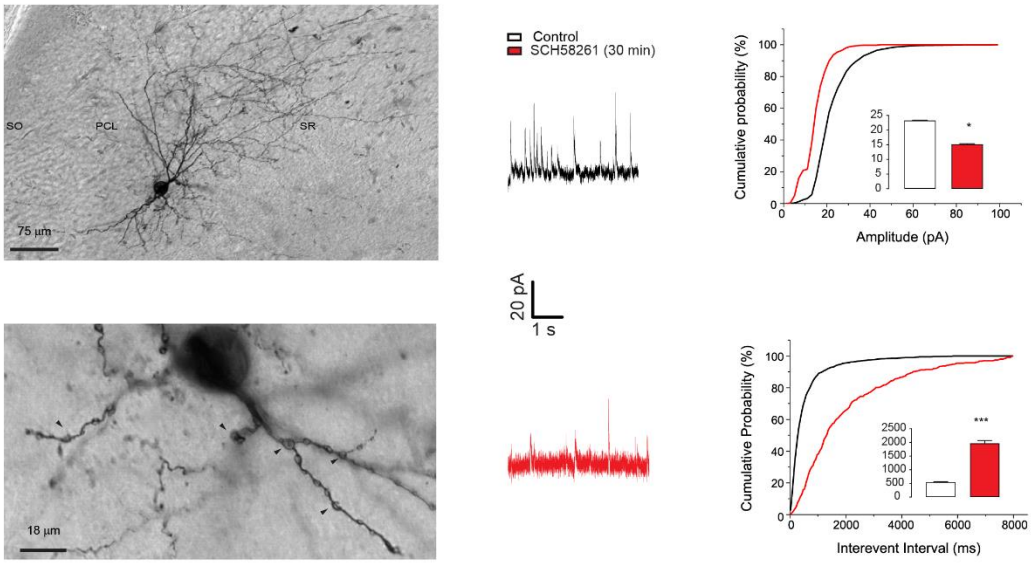
SO
PCL
SR
75 µm
18 µm
Control
SCH58261 (30 min)
20 pA
1 s
Cumulative probability (%)
Amplitude (pA)
Cumulative Probability (%)
Interevent Interval (ms)

B

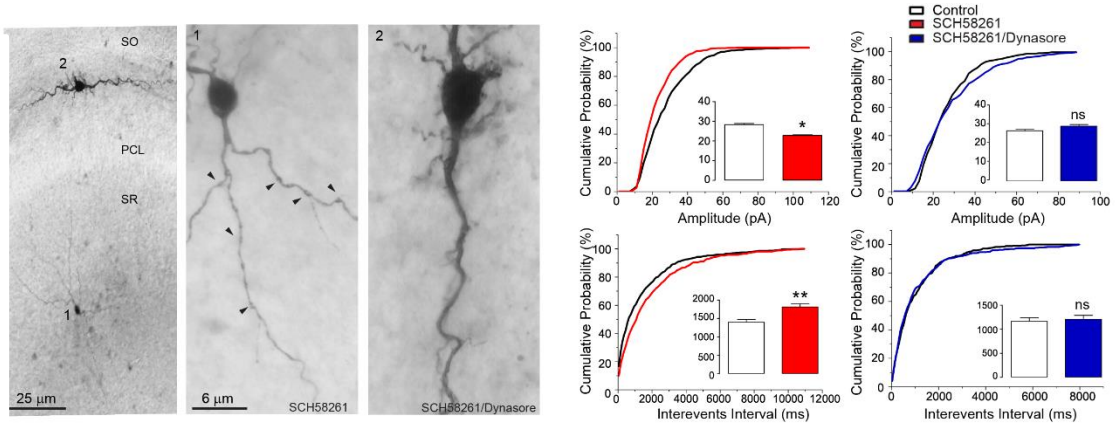
SO
PCL
SR
25 µm
6 µm
SCH58261
SCH58261/Dynasore
Control
SCH58261
SCH58261/Dynasore
Cumulative Probability (%)
Amplitude (pA)
Interevents Interval (ms)

Figure S4

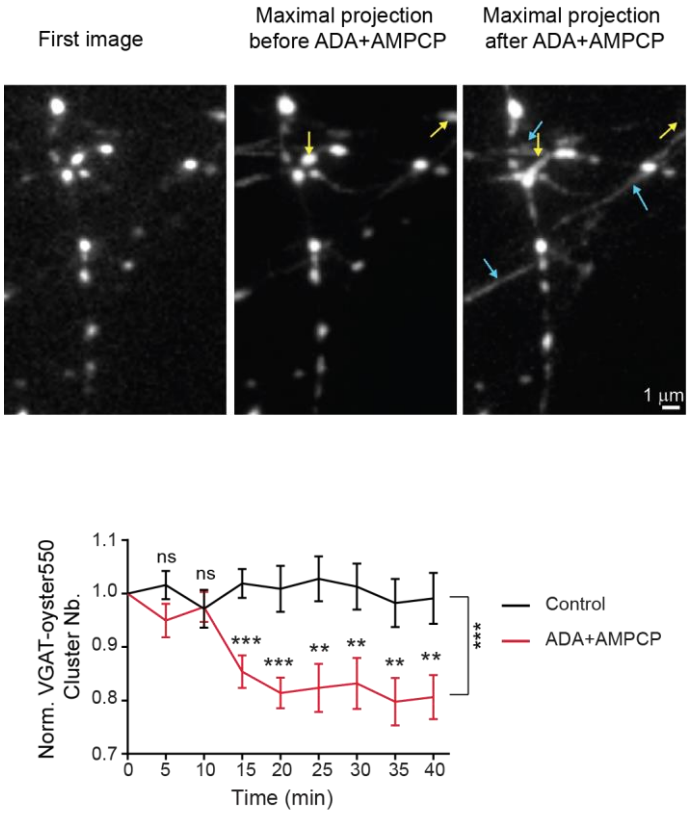

Figure S5

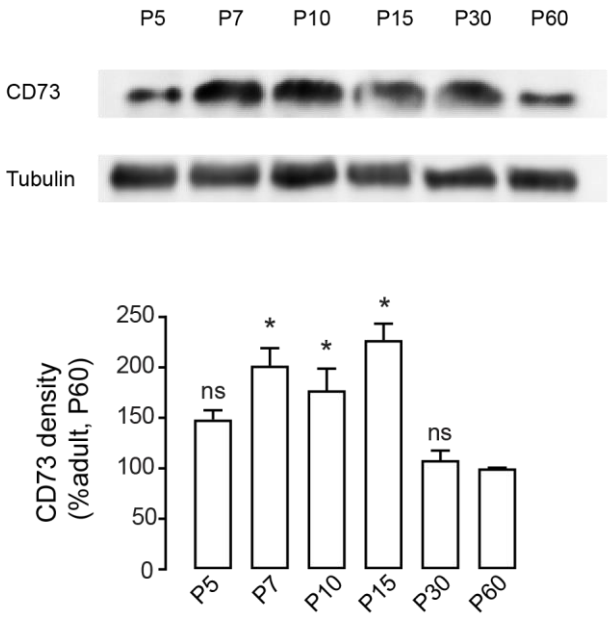

Figure S6

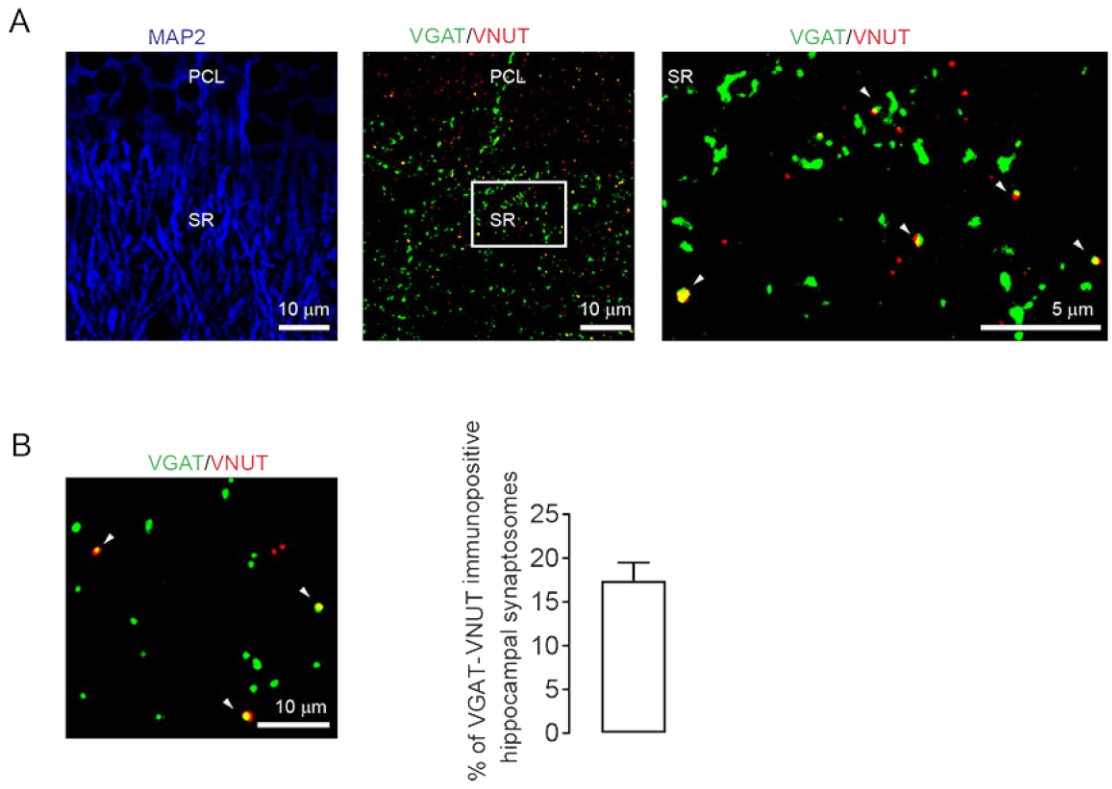
A
MAP2
PCL
SR
10 µm
VGAT/VNUT
PCL
SR
10 µm
VGAT/VNUT
SR
5 µm
B
VGAT/VNUT
10 µm
% of VGAT-VNUT immunopositive hippocampal synaptosomes
25
20
15
10
5
0

Figure S7

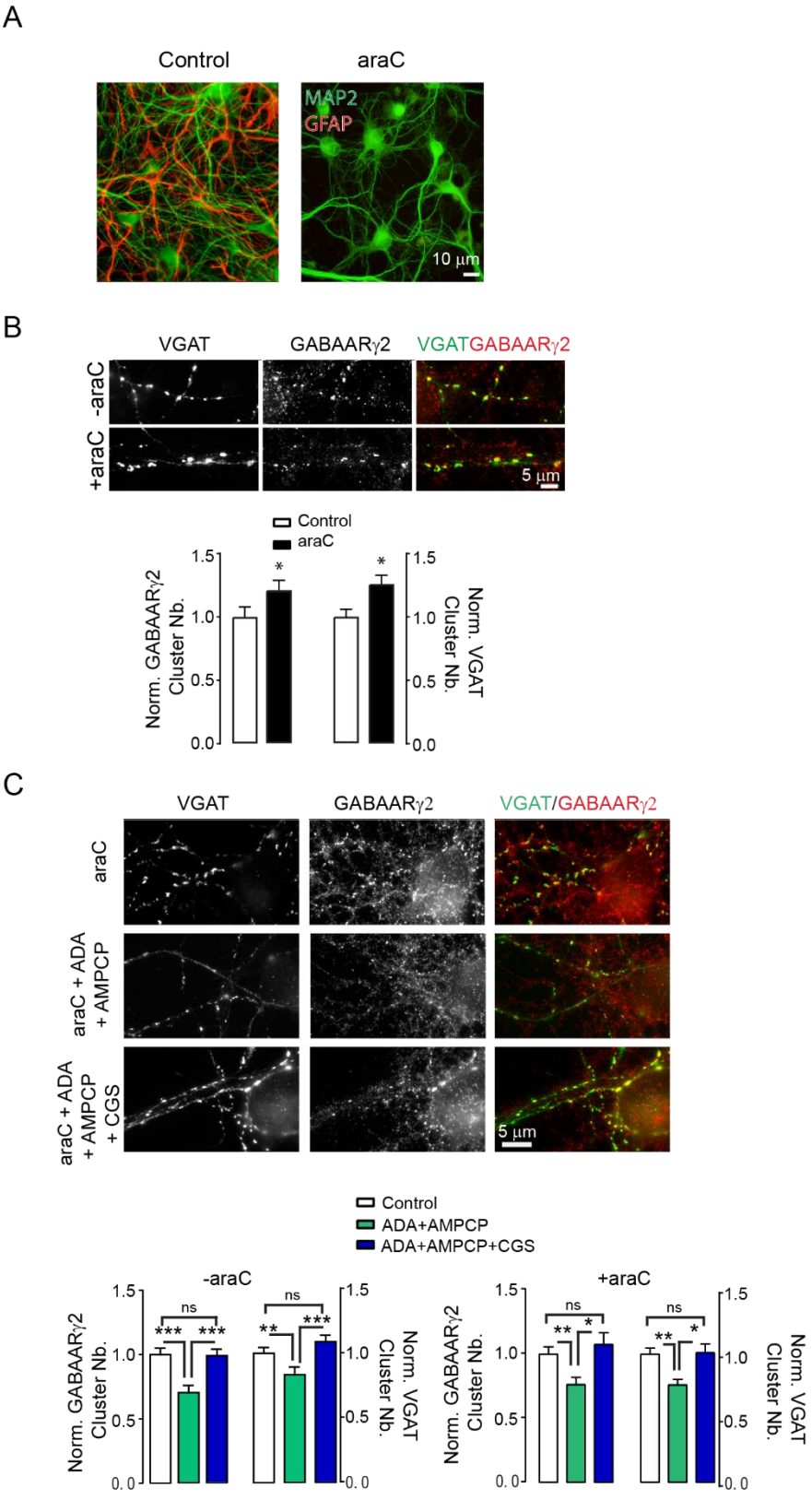
A
Control
araC
MAP2
GFAP
10 µm
B
VGAT
GABAARγ2
VGATGABAARγ2
-araC
+araC
5 µm
Control
araC
Norm. GABAARγ2 Cluster Nb.
Norm. VGAT Cluster Nb.
C
VGAT
GABAARγ2
VGAT/GABAARγ2
araC
araC + ADA + AMPCP
araC + ADA + AMPCP + CGS
5 µm
Control
ADA+AMPCP
ADA+AMPCP+CGS
-araC
+araC
Norm. GABAARγ2 Cluster Nb.
Norm. VGAT Cluster Nb.
ns

Figure S8

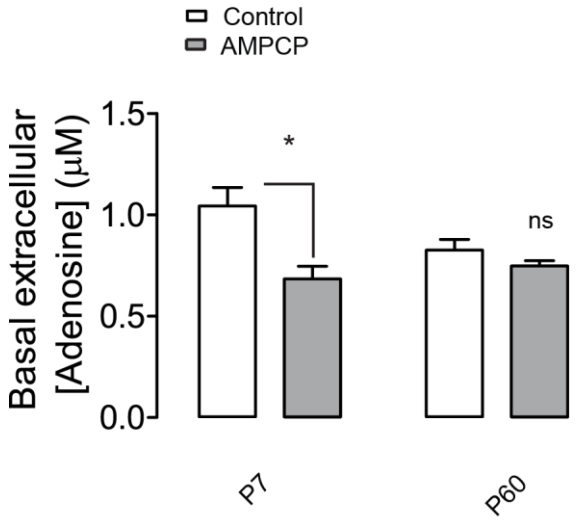

Figure S9

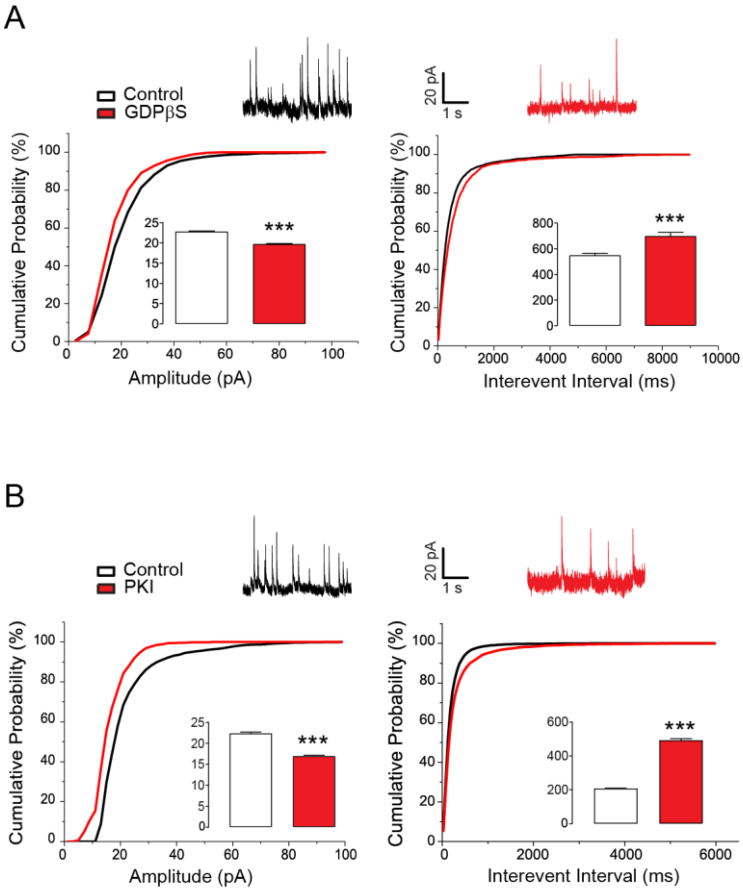

Figure S10

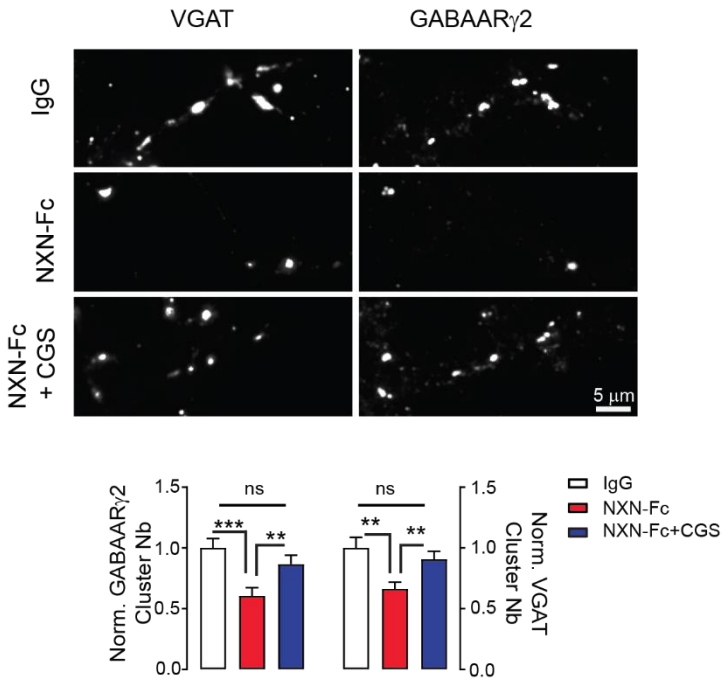

Figure S11

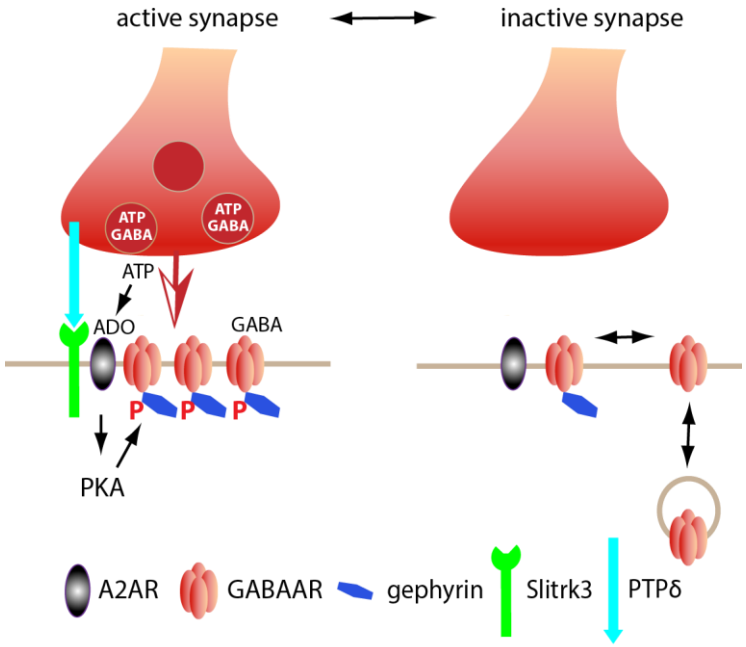

Figure S12

2. Adenosine A_{2A} receptor and $GABA_A$ receptor signaling pathways converge to stabilize nascent GABAergic synapses

In a second study I questioned about the interplay between the adenosine and GABA signalling onto stabilization of GABAergic synapses pathways. Early in development, GABA is depolarizing before the upregulation of KCC2 (Rivera et al., 1999). During this period, GABA modulates neurite outgrowth (Represa and Ben-Ari, 2005) and direct application of GABA in young neurons lead to formation of functional GABAergic synapses (Fuchs et al., 2013; Oh et al., 2016). At immature stage, GABA depolarizes the membrane and the effect is exerted by the Ca^{2+} entry via L-type Ca^{2+} channels (Perrot-Sinal et al., 2003). Since $A_{2A}R$ possibly activates Ca^{2+}-sensitive adenylate cyclases (Jacobson and Gao, 2006), this questions about the role of GABAAR-induced Ca2+ signalling in the adenosine control of GABAergic synapse density. Here I assessed in rat primary hippocampal cultures, using pharmacology, shRNA approach and immunocytochemistry I observed:

- GABA and adenosine release are both activity-dependent.
- The knockdown of either $GABA_AR$ or $A_{2A}R$ reduces the GABAergic innervation. When $A_{2A}R$ is knocked down, direct activation of $GABA_AR$ cannot rescue GABA synapses. Conversely, when $GABA_AR$ is knocked down, $A_{2A}R$ can rescue of GABAergic synapses.
- Both neurexin-neuroligin2 complex and Slitrk3-PTPδ complex are important for the $GABA_AR$-mediated stabilization of synapses, while $A_{2A}R$ can only signal through Slitrk3-PTPδ.
- Direct calmodulin activation seems to rescue the loss of synapses upon GABAARγ2 knockdown.

With the help of Jessica Pressey, we performed calcium imaging to show $GABA_AR$ was indeed increasing intracellular Ca^{2+} in DIV8 neurons. Nicolas Gervasi performed cAMP imaging and showed that $GABA_AR$ or $A_{2A}R$ activation lead to cAMP increase, and when both were activated at the same time, an additive effect was observed. Further experiments are needed to determine if the GABA signalling converges onto the adenosine signalling pathway to activate Ca^{2+}-sensitive adenylate cyclase in order to stabilize GABAergic synapses.

Running title: $A_{2A}R$/$GABA_AR$ stabilization of GABAergic synapses

Adenosine A_{2A} receptor and $GABA_A$ receptor signaling pathways converge to stabilize nascent GABAergic synapses

Ferran Gomez-Castro[1,2,3], Jessica C. Pressey[1,2,3], Nicolas Gervasi[1,2,3], Imane Moutkine[1,2,3], Marion Russeau[1,2,3], and Sabine Lévi[1,2,3*]

[1] INSERM UMR-S 839, 75005, Paris, France

[2] Université Pierre et Marie Curie, 75005, Paris, France

[3] Institut du Fer a Moulin, 75005, Paris, France;

* Corresponding author

Correspondence to:
Sabine Lévi
INSERM-UPMC UMR-S 839
17 rue du Fer a Moulin
75005 Paris, France
Tel. +33 1 45 87 61 13
Fax. +33 1 45 87 61 10
E-mail: sabine.levi@inserm.fr

Author contributions

F.G.C and S.L designed the research. F.G.C performed all the immunocytochemistry experiments and analysed the data. J.C.P performed calcium imaging and S.L. analysed the data. N.G. performed cAMP imaging and analysed the data. I.M., contributed with a new plasmid. F.G.C and S.L prepared the figures. S.L. wrote the paper.

Conflict of interest

The authors declare no conflict of interest.

Abstract

Stabilization of nascent synapses is a key process for the proper development of the central nervous system. Many cellular and molecular mechanisms are at play at GABAergic synapses. Synaptic GABA release and postsynaptic $GABA_AR$ activation have been shown to control this event in a Ca^{2+}-dependent manner via activation of voltage-dependent Ca^{2+} channels (VDCCs). We have recently demonstrated the importance of the adenosine/ATP and of the postsynaptic Adenosine 2A receptors ($A_{2A}Rs$)/adenylyl cyclase (AC)/cyclic adenosine monophosphate (cAMP)/protein kinase A (PKA) signalling pathway in the stabilization of newly formed GABAergic synapses. Here, we investigated the interplay between GABA and adenosine signalling pathways in the stabilization of GABAergic synapses in hippocampal neurons. We showed that the adenosine signalling is sufficient to stabilize GABAergic synapses. The GABA signalling converge onto the adenosine signalling pathway by potentiating Ca^{2+}-dependent ACs via the activation of Calmodulin (CaM). This may in turn impact the stabilization of the slitrk3-PTPδ trans-synaptic organizers.

Introduction

Synapse formation is a crucial step for the development of the central nervous system (CNS) (Shen and Scheiffele, 2010). Many proteins and protein complexes have been described to be exclusively at the inhibitory synapse and to regulate the formation and maintenance of GABAergic synapses (Krueger-Burg et al., 2017; Lu et al., 2017). Among these molecules, two trans-synaptic protein complexes stand out: the neurexin-neuroligin-2 (Varoqueaux et al., 2004; Poulopoulos et al., 2009) and the PTPδ-Slitrk3 (Takahashi and Craig, 2013) complexes. Then, several mechanisms operate to stabilize the newly formed synapses or remove of the unnecessary ones. At GABAergic synapses, GABA release is important to establish synapses(Chattopadhyaya et al., 2007; Huang et al., 2007; Huang and Scheiffele, 2008; Huang, 2009; Wu et al., 2012; Oh et al., 2016). The trophic function of GABA *in vivo* at its own synapse has been demonstrated: the suppression of GABA synthesis enzyme Glutamic Acid Decarboxylase (GAD) of 65 and 67 kD conducts to defects in GABAergic axon branching and synapse formation (Chattopadhyaya et al., 2007). Similarly, deletion of $GABA_AR$ subunits leads to synapse loss (Fritschy et al., 2006). Altogether, this indicates a role of the GABAergic transmission in synapse formation/stabilization. $GABA_AR$ activation can induce functional GABAergic synapses in a timescale of hours (Fuchs et al., 2013) or minutes (Oh et al., 2016). The underlying molecular mechanisms have been studied. Early in development, GABA is depolarizing (Rivera et al., 1999) and this depolarization

regulates neurite outgrowth in different systems such as the chick cortical and retinal neurons (Spoerri, 1988), rodent hippocampal neurons (Barbin and Pollard, 1993), cerebellar granule cells (Borodinsky et al., 2003), spinal cord cells (Tapia et al., 2001), cortical plate and subplate interneurons (Maric et al., 2001) and raphe nuclei 5-hydroxytrypta- mine (serotonin)-producing neurons (Lauder et al., 1998). $GABA_AR$ membrane depolarization induces Ca^{2+} influx via the activation of L-type Ca^{2+} channels (Perrot-Sinal et al., 2003). In a model of cerebellar neurons, Ca^{2+}/Calmodulin-dependent protein kinase II (CAMKII) and Mitogen-activated protein kinase (MAPK) where proposed as downstream effectors of this regulation (Borodinsky et al., 2003).

Recently, we proposed a new role of the adenosine signaling pathway in the stabilization of nascent GABAergic synapses in the hippocampus. The molecular mechanism involves the activity-dependent presynaptic release of adenosine and/or of its phosphorylated form adenosine triphosphate (ATP) followed by the enzymatic ectonucleotidase conversion of ATP into adenosine. Adenosine released in the synaptic cleft activates postsynaptic adenosine A_{2A} receptor ($A_{2A}R$) that in turn activates the downstream adenylyl cyclase (AC)/cyclic adenosine monophosphate (cAMP)/protein kinase A (PKA) signalling pathway. The downstream target of PKA being the postsynaptic scaffolding molecule gephyrin and the slitrk3- PTPδ trans-synaptic organizers.

Here, we studied the interplay between the $GABA_AR$ and the $A_{2A}R$ signaling pathways in the stabilization of nascent GABAergic synapses in hippocampal neurons. We propose that the GABA signaling pathway converge onto the adenosine signaling pathway to stabilize nascent GABAergic synapses. The underlying molecular mechanism may involve $GABA_AR$-mediated Ca^{2+}-Calmodulin (CaM) potentiation of ACs and the stabilization of the slitrk3- PTPδ trans-synaptic organizers.

Material and methods

Neuronal cultures

Primary cultures of hippocampal neurons were prepared as previously described (Chamma et al., 2013) with some modifications of the protocol. Briefly, hippocampi were dissected from embryonic day 18 or 19 Sprague-Dawley rats of either sex. Tissue was then trypsinized (0.25% v/v), and mechanically dissociated in 1x HBSS (Invitrogen, Cergy Pontoise, France) containing 10 mM HEPES (Invitrogen). Neurons were plated at a density of 60 or 120 × 10^3 cells/ml onto 18-mm diameter glass coverslips (Assistent, Winigor, Germany) pre-coated with 50 µg/ml poly-D,L-ornithine (Sigma-Aldrich, Lyon,

France) in plating medium composed of Minimum Essential Medium (MEM, Sigma) supplemented with horse serum (10% v/v, Invitrogen), L-glutamine (2 mM) and Na+ pyruvate (1 mM) (Invitrogen). After attachment for 3-4 hours, cells were incubated in culture medium that consists of Neurobasal medium supplemented with B27 (1X), L-glutamine (2 mM), and antibiotics (penicillin 200 units/ml, streptomycin, 200 µg/ml) (Invitrogen), and kept for 9-11 DIV at 37°C in a 5% CO_2 humidified incubator. One fifth of the culture medium volume was renewed once a week.

DNA constructs

The following constructs were used: shRNA against $A_{2A}R$ (Simões et al., 2016), non-target shRNA coupled to GFP (Gauvain et al., 2011), shRNA against $GABA_AR\gamma2$ subunit (Li et al., 2005)). shRNA against slitrk3 coupled to CFP (Takahashi et al., 2012), shRNA against Neuroligin 2 (kindly provided by Peter Scheiffele, Addgene plasmid # 59358) (Chih et al., 2005) and a scrambled shRNA sequence "shMock" (kindly provided by Ann Marie Craig, Vancouver, Canada). All the constructs were sequence-verified by Beckman Coulter Genomics.

Neuronal transfection

Transfections were carried out at DIV 6-7 for neurons undergoing synaptogenesis, using Transfectin (BioRad, Hercules, USA), according to the manufacturers' instructions (DNA:transfectin ratio 1 µg:3 µl), with 0.5 to 1µg of plasmid DNA per 20 mm well. Experiments were performed 3-5 days post-transfection.

Pharmacology

For ICC experiments, SCH58261 (100 nM, Abcam), CGS21680 (30nM, Abcam), muscimol (10mM, HelloBio) were directly added to the culture medium and the neurons were returned to a 5% CO_2 humidified incubator for 30 min before use. In experiments using tetanus toxin (1-40 nM, Alomone Labs), cells were treated for 2 days (from DIV7 to 9) and then the appropriate drugs were added for 30 min to the toxin solution.

Immunocytochemistry

To label and quantify the density of inhibitory synapses, pre-treated neurons were fixed for 15 min at RT in paraformaldehyde (PFA; 4% w/v; Sigma) and sucrose (14% w/v; Sigma) solution in 1X PBS. Cells

were then washed and permeabilized with a solution containing Triton X-100 (0.25% w/v, Carl Roth GmbH) diluted in PBS 1X. Cells were then incubated for 1 hour at RT in goat serum (GS; 10% v/v; Invitrogen) and Triton X-100 (0.1% w/v) in PBS to block nonspecific staining. Neurons were then incubated for 1 hour to overnight with a primary antibody mix consisting of rabbit anti-VGAT (1:500, provided by B. Gasnier, Univ. Paris Descartes, Paris), and guinea pig anti-$GABA_AR\gamma2$ subunit (1:2000, provided by J.M. Fritschy, Univ. Zurich) in PBS supplemented with GS (10% v/v, Invitrogen) and Triton (0.1%v/v). After washes, cells were incubated for 45 min at RT with a secondary antibody mix containing donkey anti-guinea pig-cy3 (1:400, Jackson Immunoresearch), and goat anti-rabbit-FITC (1:300, Jackson Laboratories) or donkey anti-rabbit-cy5 in PBS-GS-Triton blocking solution, washed, and finally mounted on glass slides using Mowiol 4-88 (48 mg/ml, Sigma). Sets of neurons compared for quantification were labeled simultaneously.

Fluorescence image acquisition and analysis

Image acquisition was performed using a 63X objective (NA 1.40) on a Leica (Nussloch, Germany) DM6000 upright epifluorescence microscope with a 12-bit cooled CCD camera (Micromax, Roper Scientific) run by MetaMorph software (Roper Scientific, Evry, France). Quantification was performed using MetaMorph software (Roper Scientific). Image exposure time was determined on bright cells to obtain best fluorescence to noise ratio and to avoid pixel saturation. All images from a given culture were then acquired with the same exposure time and acquisition parameters.

For cluster analysis, images were first flatten background filtered (kernel size, 3 X 3 X 2) to enhance cluster outlines, and a user defined intensity threshold was applied to select clusters and avoid their coalescence. Clusters were outlined and the corresponding regions were transferred onto raw images to determine the mean cluster number, area and fluorescence intensity. For quantification of $GABA_AR$ synaptic clusters, receptor clusters comprising at least 3 pixels and colocalized on at least 1 pixel with VGAT clusters were considered. The dendritic length of the region of interest was measured to determine the number of clusters per 10 µm. For each culture, we analyzed ~10 cells per experimental condition and ~20 clusters per cell.

Calcium Imaging

GCaMP6-rubi AAV viruses were used to infect hippocampal neurons at DIV3 by addition of 0.3 µl of viral solution in the culture medium. 5 days post infection, cells were imaged at 37°C in an open chamber mounted on an inverted spinning-disc microscope (Leica DMI4000, Yokogawa CS20 spinning

Nipkow disk, 40x/0.6 N.A. objective) in an extracellular solution containing the following in mM: 2 $CaCl_2$, 2 KCl, 3 $MgCl_2$, 10 HEPES, 20 glucose, 120 NaCl, pH7.4. Cells were selected using expression of the reporter protein rubi, and intracellular Ca2+ was imaged using 491nm light from a laser. Emitted light was collected using a 525-39 (±25) nm emission filter. Time lapse (0.33 Hz for 600 s) of confocal stacks (of ~21 images acquired with an interval of 0.3 µm) were acquired with a cooled EM-CCD camera (512 x 512, 16 µm pixel size) using Metamorph. The analysis was performed on a section of the stack where the soma was in focus at different time points. Fluorescence intensities collected in the soma or dendrites before (F0) and following (F) bath addition of the drugs, were background-subtracted before being displayed as F/F0 values. Data were analyzed using Metamorph. Normalization of fluorescence intensity was performed for each cell by dividing the mean fluorescence intensity by the average of fluorescence intensities of the 4 time points before drug application. Statistics (paired t test) were run on the last time point before drug application (120 s) compared to the latest time point after drug application (600 s).

cAMP Imaging

Recombinant Sindbis virus encoding EPAC-sh150 (Polito et al., 2013) were used to infect hippocampal neurons at DIV8 by addition of 1 µl of viral solution in the culture medium (~5×10^5 particles per slice). 12h after infection, hippocampal neurons were transferred on the microscope stage and were continuous perfused at 0.5 mL/min with a solution containing the following (in mM): 2 $CaCl_2$, 2 KCl, 3 $MgCl_2$, 10 HEPES, 20 glucose, 120 NaCl, pH7.4 at 32 °C. Two-photon imaging was performed using an upright Leica TCS MP5 microscope with resonant scanning (8 kHz), a Leica 25X/0.95 HCX IRAPO immersion objective and a tunable Ti:sapphire laser (Coherent Chameleon Vision II) with dispersion correction set to 860 nm for CFP excitation. The emission path consisted of an initial 700 nm low-pass filter to remove excess excitation light (E700 SP, Chroma Technologies), 506 nm dichroic mirror for orthogonal separation of emitted signal, 479/40 CFP emission filter, 542/50 YFP emission filter (FF506-Di01-25 × 36; FF01-479/40; FF01-542/50; Brightline Filters; Semrock) and two-channel Leica HyD detector for simultaneous acquisition. Due to the high quantum efficiency and low dark noise of the HyD photodetectors, detector gain was typically set at 10–15% with laser power at 1–5%. Z-stack images (12-bit; 512 × 512) were typically acquired every 15 s. The z-step size was 1–2 µm and total stack size was typically 8–10 sections. Images were processed in ImageJ by using maximum z-projections followed by translation registration correction to reduce x/y movement. However, z-projections were occasionally complicated by movement in the z-axis and were therefore corrected with a custom Matlab script before measurement in ImageJ. After correcting movement in the x/y/z

directions, regions of interest (ROIs) were selected for measurement if they could only be measured for the whole experimental time course.

Results

ATP/adenosine and GABA are co-released at some GABAergic synapses and can in turn activate the $A_{2A}R$ and $GABA_AR$ signalling pathways to stabilize newly formed GABAergic synapses (Zappettini et al., unpublished observations). This questions about the interplay between these two signalling pathways. To address this question, we first determined in hippocampal primary cultures the activity-dependence of the $A_{2A}R$ and/or $GABA_AR$ pathways on the stabilization of GABAergic synapses. A 48 hours treatment with tetanus toxin to cleave vesicle-associated membrane protein 2 (VAMP2), which is essential for activity-dependent vesicular release of neurotransmitters (Link et al., 1992), resulted in the disappearance of 39% of GABAergic synapses stained for the vesicular inhibitory amino acid transporter VGAT (Fig. 1 A-B). In parallel, the number of $GABA_AR$ γ2 subunit clusters detected at inhibitory synapses was reduced by 58% (Fig. 1 A, C), indicating a loss of both the pre- and the post-synaptic elements in conditions of activity deprivation. The synapse loss was fully prevented by the direct activation of $A_{2A}Rs$ with CGS21680 or $GABA_AR$ with muscimol (Fig. 1 A-C) for 30 minutes. We concluded that the activity-dependent release of adenosine/ATP or GABA is required to activate $A_{2A}Rs$ or $GABA_ARs$ in order to stabilize GABAergic synapses. Since 30 minutes of drug application was sufficient to rescue synapses, this favours a role of GABA and adenosine signalling in synapse stabilization rather than in synapse formation since *de novo* synapse formation requires several hours (Dobie and Craig, 2011). Activating separately $A_{2A}Rs$ or $GABA_ARs$ fully rescue GABAergic synapses suggesting that the two signalling pathways are independent and can replace each other or that they converge. We reasoned that if both pathways converge towards a common mechanism, the simultaneous activation of both pathways will have no additive effect on GABAergic synapses density as compared to the activation of separate mechanisms. On the contrary, if both pathways operate independently of each other, their simultaneous activation may have an additive effect on synapse stabilization. We found that the concomitant activation of $A_{2A}Rs$ and $GABA_ARs$ with CGS21680 and muscimol rescued GABAergic synapses to a similar extent than what was observed when individual receptors were activated at a time (Fig. 1 A-C). This suggests that the $A_{2A}R$ and $GABA_AR$ signalling pathways converge to stabilize GABAergic synapses. Alternatively, the absence of additivity of both pathways could be explained by the fact that the density of GABAergic synapses cannot exceed a

certain density per surface area of dendrite. Further experiments are therefore required to conclude on convergence of mechanisms.

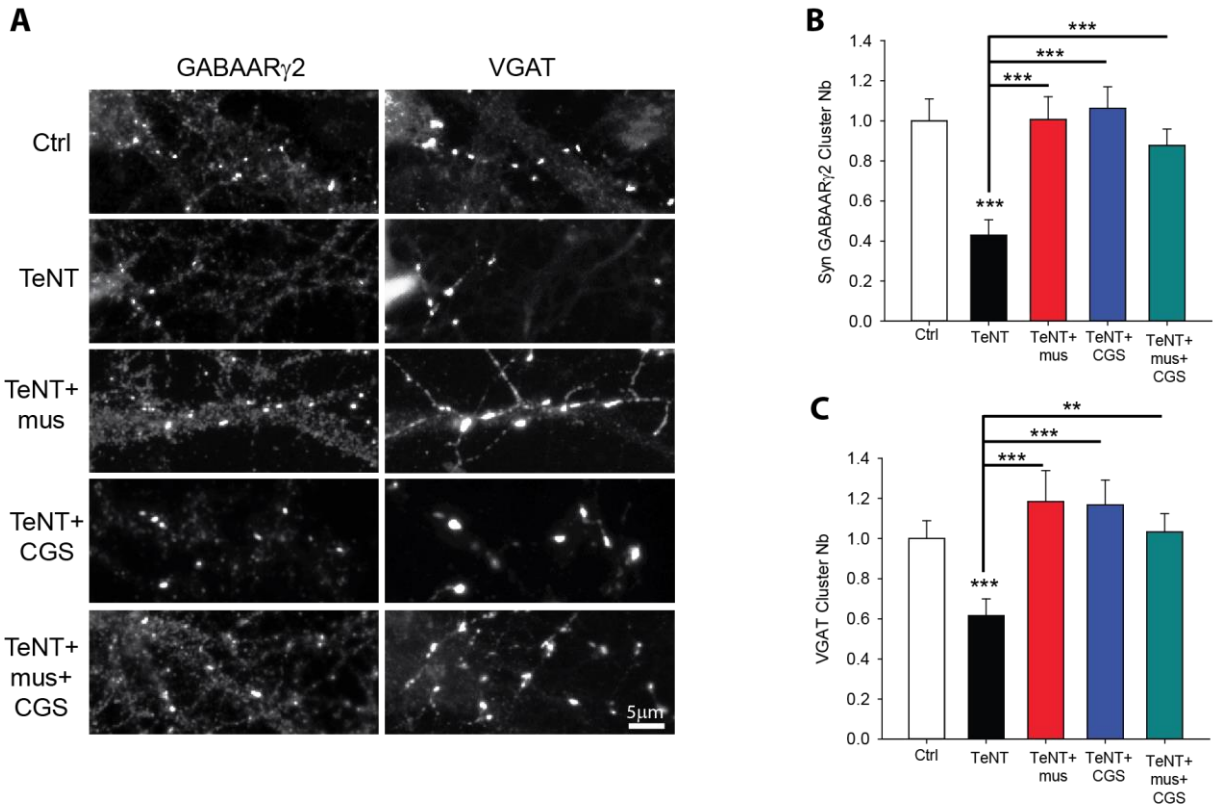

Figure 1. Activity-dependent stabilization of nascent GABAergic synapses requires the activation of $A_{2A}R$ or $GABA_AR$. A. *Representative images of VGAT and $GABA_AR\gamma2$ staining in DIV9 neurons treated with tetanus toxin (TeNT) during 48h with or without 30 min muscimol, CGS21680 or muscimol + CGS21680 application. Scale bar, 5 µm.* ***B-C****. Quantification of VGAT (**B**) and postsynaptic $GABA_AR\gamma2$ (**C**) cluster number per dendrite length showing GABAergic synapses are lost upon activity blockade and can be rescued by the activation of $A_{2A}R$ or $GABA_AR$. Note $A_{2A}R$ and $GABA_AR$ effects on the stabilization of GABAergic synapse is not additive. Ctrl n=44, TeNT n=26, TeNT + muscimol n=29, TeNT + CGS21680 n=37, TeNT + CGS21680 + muscimol n=22 3 cultures, Mann-Whitney test VGAT: ctrl vs TeNT p=0.002, TeNT vs TeNT + muscimol p=<0.001, TeNT vs TeNT + CGS21680 p=<0.001, TeNT vs TeNT + muscimol + CGS21680 p=0.002, TeNT + muscimol vs TeNT + CGS21680 p=0.446, TeNT + muscimol vs TeNT + muscimol + CGS21680 p=0.776, TeNT + CGS21680 vs TeNT + muscimol + CGS21680 p=0.446. Postsynaptic $GABA_AR\gamma2$: Ctrl vs TeNT p=<0.001, TeNT vs TeNT + muscimol p<0.001, TeNT vs TeNT + CGS21680 p=<0.001, TeNT vs TeNT + muscimol + CGS21680 p=<0.001, TeNT + muscimol vs TeNT + CGS21680 p=0.535, TeNT + muscimol vs TeNT + muscimol + CGS21680 p=0.524, TeNT + CGS21680 vs TeNT + muscimol + CGS21680 p=0.196.*

To get further insight in the function of both pathways in GABAergic synapse stabilization, we prevented a given signalling pathway and tested whether the activation of the second pathway could rescue the loss of GABAergic synapses. This was done by knocking-down $A_{2A}R$ or $GABA_AR$ γ2 subunit with specific shRNAs ((Simões et al., 2016)) and by activating either $GABA_ARs$ or $A_{2A}Rs$ signalling pathways with muscimol or CGS21680 treatments respectively. Neurons transfected at DIV 6-7 with shRNAs against $A_{2A}Rs$ or $GABA_AR$ γ2 subunit and labelled at DIV 9-10 with VGAT antibodies showed a significant reduction of 25 % and 43 % in the number of GABAergic synapses (Fig. 2 A-D), as previously reported (Zappettini et al., unpublished observations, Li et al. 2005). Therefore, the rescue of synapses observed after pharmacological activation of $A_{2A}Rs$ or $GABA_ARs$ in conditions of activity deprivation is due to the direct activation of receptors and not to an indirect nonspecific effect of the drugs. Second, the low efficiency of neuron lipotransfection allows to conclude that the $A_{2A}R$ or $GABA_AR$ mediated synapse rescue is a cell-autonomous process that doesn't require network activity changes. Last, this also means that the expression/activation of $A_{2A}Rs$ or $GABA_ARs$ in the postsynaptic cell is sufficient to stabilize GABAergic synapses.

We then asked whether the activation of $A_{2A}R$ or $GABA_AR$ can rescue GABAergic synapse loss in neurons in which $GABA_AR$ or $A_{2A}R$ expression have been supressed. We found that the activation of $GABA_ARs$ with muscimol for 30 minutes could not rescue the GABAergic synapse loss observed in $shA_{2A}Rs$ expressing neurons (Fig. 2 A-B). In contrast, activating $A_{2A}Rs$ with CGS21680 for 30 minutes significantly rescued the loss of GABAergic synapses in neurons lacking the $GABA_AR$ γ2 subunit (Fig. 2 C-D). This indicates that the activation of $A_{2A}Rs$ is required and is sufficient to stabilize newly formed GABAergic synapses.

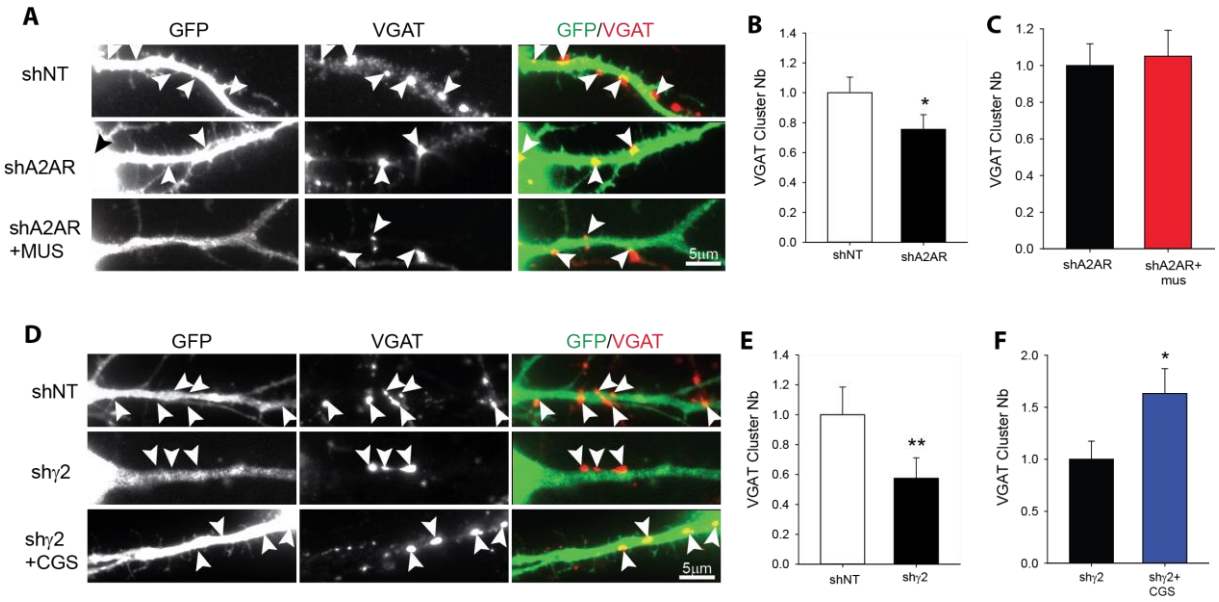

Figure 2. $A_{2A}R$ activity is necessary and sufficient to stabilize GABAergic synapses. A-C, *VGAT staining (**A**) and quantification (**B-C**) in DIV 10-11 neurons transfected with non-target (shNT) or on-target $A_{2A}R$ ($shA_{2A}R$) shRNAs exposed or not to muscimol (MUS) for 30 min. Scale bar, 5 µm. shNT n=56, $shA_{2A}R$ n=60, $shA_{2A}R$ + muscimol n=48, 4-5 cultures. Mann-Whitney test shNT vs $shA_{2A}R$ p=0.03, $shA_{2A}R$ vs $shA_{2A}R$ + muscimol p=0.9. The loss of GABAergic synapses upon suppression of $A_{2A}R$ is not rescued by the activation of $GABA_AR$. **D-F**, VGAT staining (**D**) and quantification (**E-F**) in DIV 10-11 neurons transfected with non-target (shNT) or on-target $GABA_ARγ2$ (shγ2) shRNAs exposed or not to CGS21680 for 30 min. Scale bar, 5 µm. shNT n=41, shγ2 n=35, shγ2 + CGS21680 n=35, 4 cultures. Mann-Whitney test shNT vs shγ2 p=0.004, shγ2 vs shγ2 + CGS21680 p=0.049. The loss of GABAergic synapses upon suppression of $GABA_ARγ2$ is rescued by the activation of $A_{2A}R$.***

Neurexin-neuroligin-2 and slitrk3-PTPδ are the two main trans-synaptic complexes at GABAergic synapses (Varoqueaux et al., 2004; Takahashi et al., 2012). We have previously shown that A_{2A}Rs stabilize GABAergic synapses through PKA-dependent phosphorylation of the scaffolding protein gephyrin and the recruitment of the trans-synaptic slitrk3-PTPδ complex (Zappettini et al., unpublished observations). In young neurons, $GABA_A$Rs induce Ca^{2+} influx via the depolarization-induced activation of the voltage-dependent L-type calcium channels VDCCs (Perrot-Sinal et al., 2003). This in turn may stabilize the synapse through phosphoregulation of key synaptic proteins such as neuroligin-2 (Antonelli et al., 2014). Since we showed that the A_{2A}R signalling pathway stabilizes GABAergic synapses through the slitrk3-PTPδ complex independently of the neurexin-neuroligin-2 complex, we wondered whether the GABA signalling pathway could also regulate GABAergic synapses number through the slitrk3-PTPδ complex, a question still unanswered. This would be in favour of a convergent mechanism of synapse stabilization for the adenosine and GABA signalling pathways.

Knocking-down slitrk3 with a specific shRNA led to a significant loss of GABAergic synapses (Fig. 3 A-C), as shown before (Takahashi et al., 2012). Activating A_{2A}Rs with CGS21680 or $GABA_A$Rs with muscimol could not rescue GABAergic synapses (Fig. 3 A-C). We conclude that both A_{2A}Rs and $GABA_A$Rs stabilize GABAergic synapses via the slitrk3-PTPδ trans-synaptic complex. Knocking-down neuroligin-2 with a specific shRNA both led to a major loss of GABAergic synapses (Fig. 3 D-F), as shown before (Craig and Kang, 2007; Siddiqui and Craig, 2011). Activating A_{2A}Rs with CGS21680 rescued synapses (Fig. 3 D-F), ruling out the contribution of the neurexin-neuroligin-2 complex in the adenosine signalling pathway. In contrast, the synapse loss induced by the shRNA-mediated suppression of neuroligin-2 could not be rescued by muscimol activation of $GABA_A$Rs. Altogether our data indicate that A_{2A}Rs stabilize GABAergic synapses via the slitrk3- PTPδ trans-synaptic complex while $GABA_A$Rs stabilize GABAergic synapses via both the slitrk3- PTPδ trans-synaptic and the neurexin-neuroligin-2 complexes.

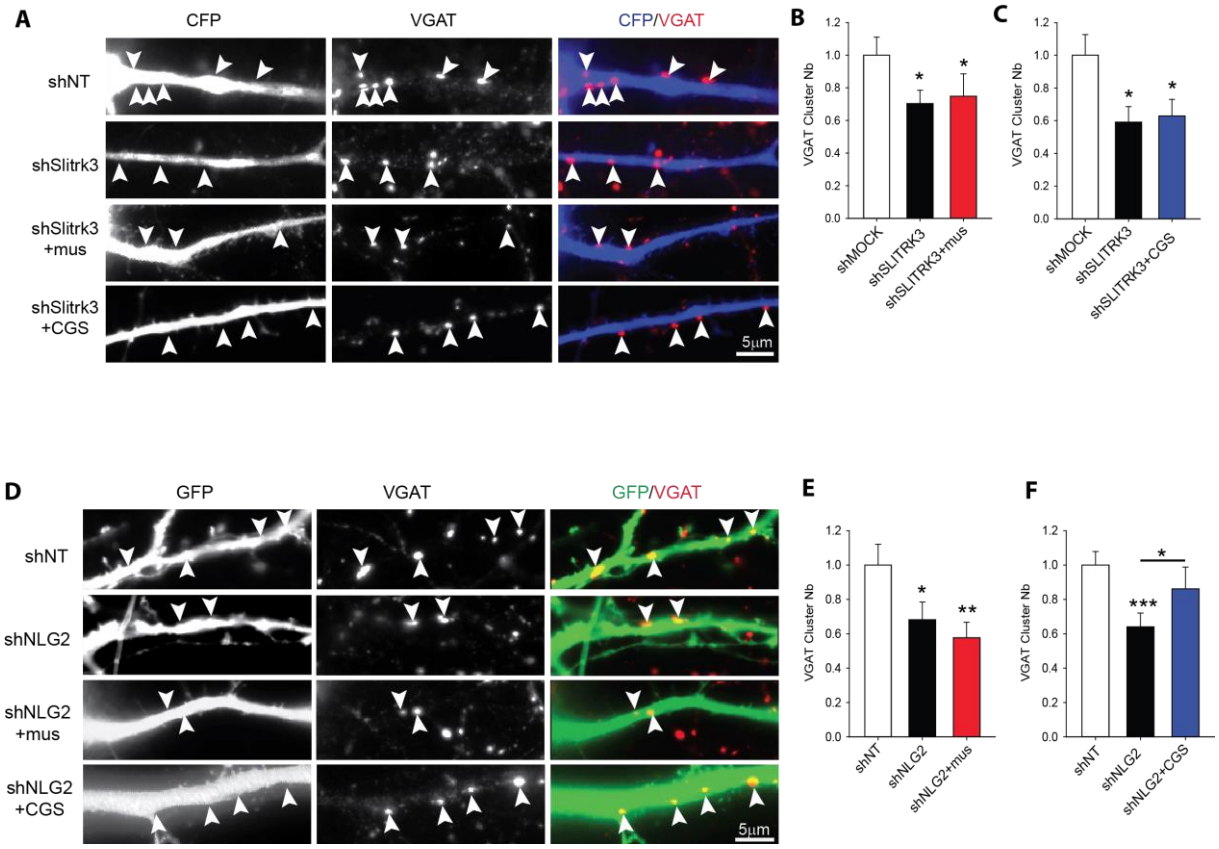

Figure 3. Molecular mechanisms of synapse stabilization downstream of A_{2A}R/$GABA_A$R involve the synaptogenic organizer Slitrk3. A-C, *The loss of GABAergic synapses upon suppression of Slitrk3 is not rescued by the activation of A_{2A}R nor $GABA_A$R. VGAT staining (**A**) and quantification (**B,C**) in DIV 10-11 neurons transfected with shMock or shSlitrk3 exposed or not to muscimol (B) or CGS21680 (C) for 30 minutes. Scale bar, 5 µm. (B)shMock n=42, shSlitrk3 n=34, shSlitrk3 + muscimol n=41, 3 cultures. Mann-Whitney test shMock vs shSlitrk3 p=0.037, shMock vs shSlitrk3+mus p=0.013 shSlitrk3 vs shSlitrk3 +*

muscimol p=0.58. (C) shMock n=41, shSlitrk3 n=37, shSlitrk3 + CGS21680 n=36, 3 cultures. Mann-Whitney test shNT vs shSlitrk3 p=0.019, shMock vs shSlitrk3 + CGS21680 p=0.0347. shSlitrk3 vs shSlitrk3 + CGS21680 p=0.811 ***D-F,*** *The loss of GABAergic synapses upon suppression of NLG2 is rescued by the activation of $A_{2A}R$ but not of $GABA_AR$. VGAT staining (**D**) and quantification (**E,F**) in DIV 10-11 neurons transfected with shNT or shNLG2 exposed or not to muscimol or CGS21680 for 30 minutes. Scale bar, 5 µm. (**E**)Muscimol: shNT n=39, shNLG2 n=36, shNLG2 + muscimol n=33, 3 cultures. Mann-Whitney test shNT vs shNLG2 p=0.0234, shNT vs shNLG2+mus p=0.003 shNLG2 vs shNLG2 + muscimol p=0.58. (**F**) CGS21680: shNT n=56, shNLG2 n=54, shNLG2 + CGS21680 n=58, 4 cultures. Mann-Whitney test shNT vs shNLG2 p=<0.001, shNLG2 vs shNLG2 + CGS21680 p=0.0292, shNT vs shNLG2 + CGS21680 p=0.31*

A_{2A}Rs and $GABA_A$Rs are coupled to cAMP and Ca^{2+} signalling pathways, respectively. A_{2A}Rs are G protein-coupled receptors activating adenylyl cyclase (AC), which generates the synthesis of cyclic adenosine monophosphate (cAMP) responsible for the downstream activation of Protein kinase A (PKA) (Jacobson and Gao, 2006). Hippocampal neurons express type 1 and 8 Ca^{2+} sensitive ACs (Conti et al., 2007). The adenosine control of GABAergic synapse density could therefore be tightly regulated by $GABA_A$R-induced Ca^{2+} signalling. $GABA_A$R elevates Ca^{2+} level early in development (Leinekugel et al., 1995; Perrot-Sinal et al., 2003). Interestingly, adenosine signalling stabilizes GABAergic synapses in neurons undergoing synaptogenesis and not at mature stage (unpublished observations). It could therefore be that the GABA signalling participates in the adenosine regulation of the density of GABAergic synapses. We thus tested the possibility of cAMP tuning by GABA signalling. We first determined whether A_{2A}Rs activation modify $[Ca^{2+}]$i in neurons. Accordingly, as revealed by Ca^{2+} imaging, application of CGS21680 did not lead to a major Ca^{2+} influx in DIV8 or DIV14 neurons (Fig. 4 A-B). This suggests a minor contribution of A_{2A}Rs in Ca^{2+} influx. Alternatively, tonic activation of A_{2A}Rs by ambient adenosine may prevent CGS21680 to elevate intracellular Ca^{2+} level. However, removal of ambient adenosine with adenosine 5-(α,β-methylene)diphosphate (AMPCP), which inhibits the ecto-5'-nucleotidase CD73, the rate-limiting step for the formation of adenosine from extracellular ATP, together with adenosine deaminase (ADA), which hydrolyses adenosine into inosine, did not lead to noticeable changes in $[Ca^{2+}]$I in DIV8 neurons (data not shown). Furthermore, application of CGS21680 in presence of AMPCP and ADA, did not increase $[Ca^{2+}]$i in DIV8 neurons (data not shown), ruling out a direct contribution of Ca^{2+} influx to the A_{2A}R-induced regulation of GABAergic synapses. In contrast, muscimol application increased $[Ca^{2+}]$i in DIV8 hippocampal neurons while it significantly decreased at DIV14 (Fig. 4 A-B). This confirms that GABA elevates intra-neuronal Ca^{2+} level at early developmental stage, a stage corresponding to the period of GABAergic synapse formation i.e. when adenosine stabilizes GABAergic synapses.

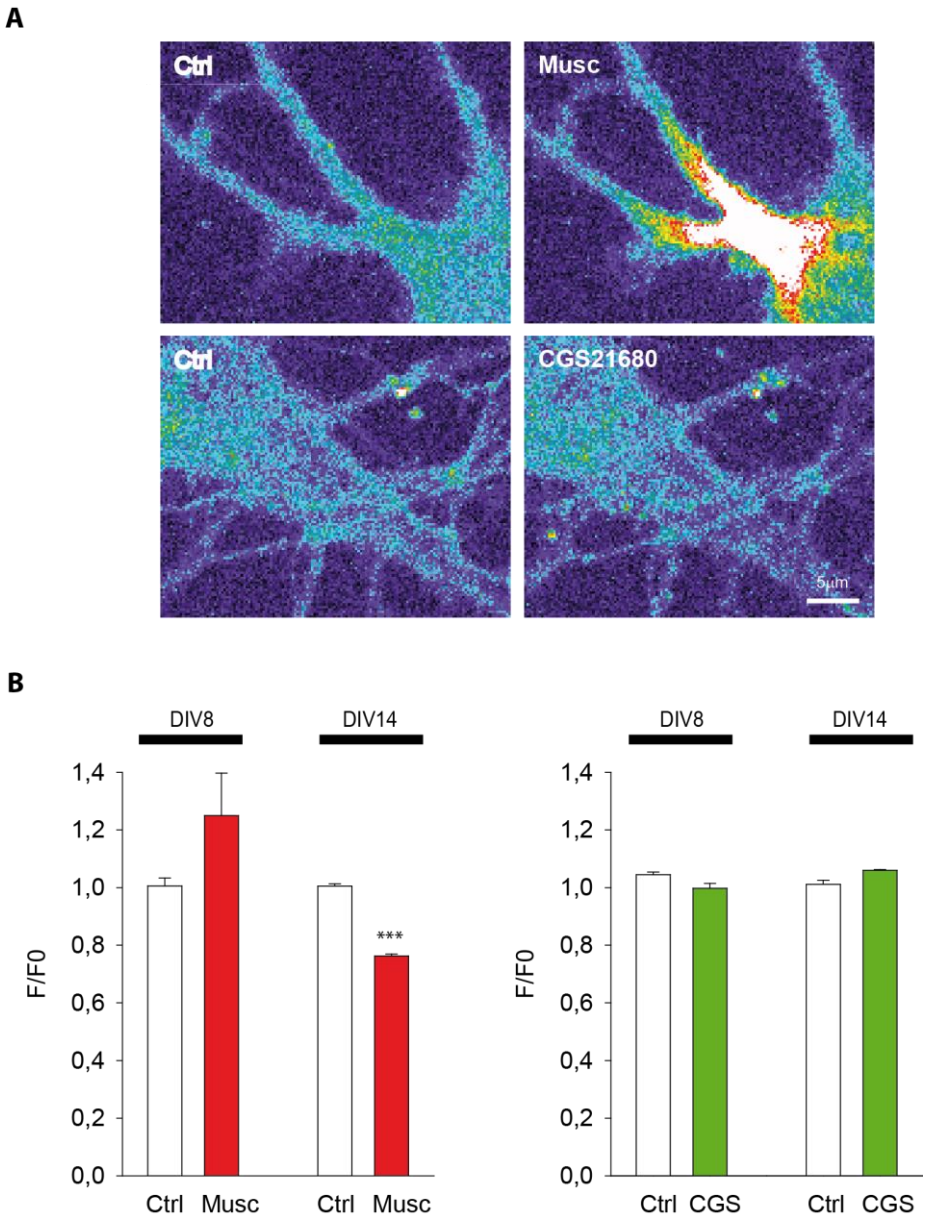

Figure 4. GABA$_A$R but not A$_{2A}$R activation elevates intra-neuronal calcium levels in DIV8 neurons. A*, Pseudocolor images of DIV8 neurons infected with GCaMP6-rubi AAVs, before (left) and after (right) muscimol or CGS21680 treatment, as indicated. Warmer colors correspond to higher GCaMP fluorescence intensities. Scale bar, 5 µm.* ***B****, Calcium levels in proximal dendrites shown as F/F0 ratio (mean ± s.e.m.) before (white bar) and after muscimol (red bar) or CGS21680 (green bar) application. Note an increase and decrease in intracellular calcium levels after muscimol treatment in DIV8 and DIV14 neurons, respectively. In contrast, CGS21680 does not significantly alter intracellular calcium levels regardless of the age of the neurons. Muscimol: DIV8 21 cells, paired t test p=0.087; DIV14 10 cells, P <0,001. CGS21680: DIV8 13 cells, paired t test p=0.12; DIV14 10 cells, p=0.084.*

Since GABA but not adenosine signaling can elevate [Ca^{2+}]i in young neurons and knowing that A_{2A}R activation of ACs can be boosted by CaM (Cooper and Tabbasum, 2014), we asked if GABA signaling

could potentiate the adenosine signaling pathway. To address this question, we performed cAMP imaging in DIV8 hippocampal neurons infected with recombinant Sindbis virus encoding EPAC-S^{H150}, an Epac-based sensor with increased sensitivity for cAMP (Polito et al., 2013). As expected, $A_{2A}R$ activation with CGS21680 led to a rapid and significant increase in intracellular cAMP level (Figure 5 A-B). The increase in neuronal cAMP was however less than what could be detected with forskolin, a direct cell-permeable activator of adenylyl cyclase (Fig. 5 A-B). Interestingly, $GABA_AR$ activation with muscimol elevated cAMP level in a similar range than CGS21680 (Fig. 5 A-B), indicating that the GABA signalling is capable as the $A_{2A}R$ signalling to elevate intracellular cAMP level. Moreover, the application of CGS21680 together with muscimol further elevated the neuronal cAMP level, suggesting $GABA_AR$ activation bolstered $A_{2A}R$-dependent signalling. To show that $GABA_AR$ activation potentiated the $A_{2A}R$-dependent signalling through the activation of CaM-dependent ACs, one need to show that the effect of muscimol on cAMP level is prevented upon AC activity/expression suppression. Unfortunately, application of SQ22536, an inhibitor of ACs did not prevent the forskolin-induced increase in intracellular cAMP level (data not shown). This is coherent with the knowledge that none of the commercially available AC inhibitors can fully counteract Gs protein activity (Polito et al., 2015). One may need to suppress activity/expression of Ca^{2+}- sensitive and -insensitive ACs to conclude on the GABA/adenosine interplay in GABAergic synapse stabilization.

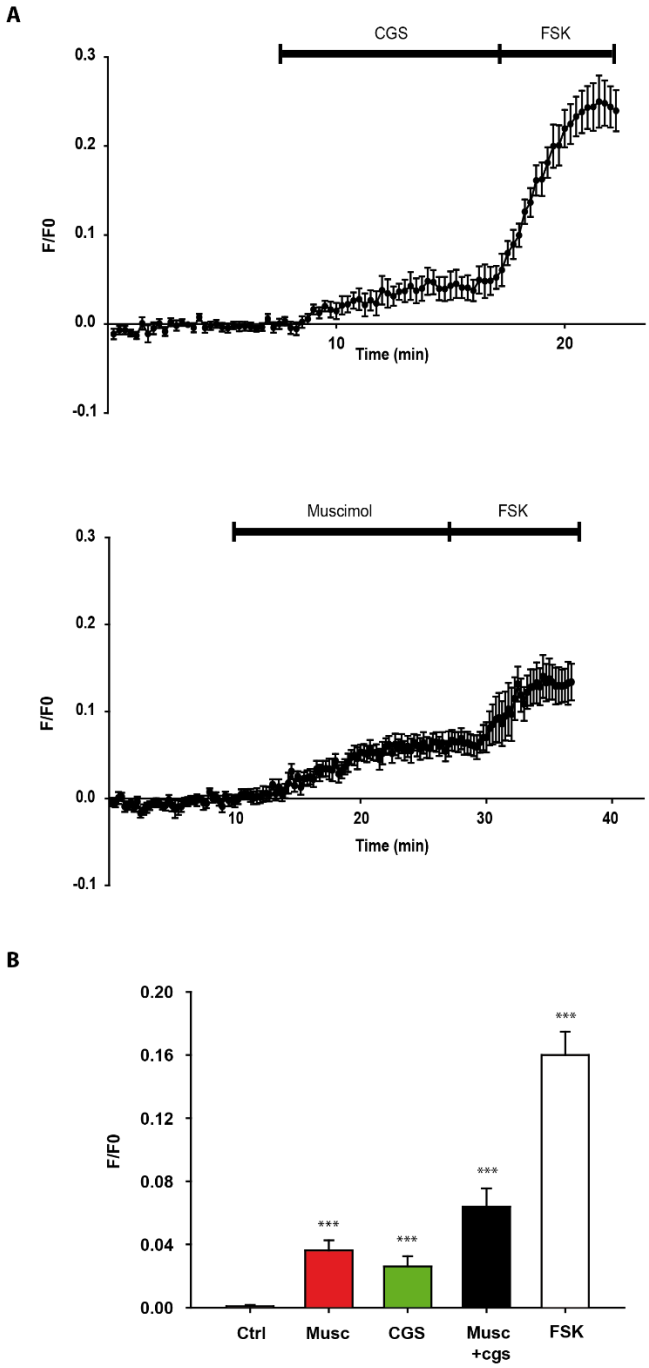

Figure 5. GABA$_A$R activation potentiates A$_{2A}$R-mediated increase in cAMP intracellular level. A*, cAMP level in proximal dendrites of DIV9 neurons infected with recombinant Sindbis virus encoding EPAC-sh150 cAMP sensor. Data are shown as F/F0 ratio (mean ± s.e.m.) measured as a function of time following drug application, as indicated (black bar).* ***B****, Quantitative analysis of the cAMP level as F/F0 ratio (mean ± s.e.m.) in neurons maintained in control conditions (white bar) or after muscimol (red bar), CGS21680 (green bar), muscimol + CGS (black bar) or forskolin (white bar) application. Muscimol and CGS21680 applied separately increase cAMP level and the increase in cAMP is even higher when both drugs are applied simultaneously. One way ANOVA P <0.001.*

Postulating that the GABA signaling bolster the adenosine-mediated stabilization of GABAergic synapses via the activation of CaM dependent ACs, we tested the implication of Ca^{2+}-Calmodulin in GABAergic synapse stabilization. For this purpose, we shut down GABA signalling by supressing expression of the $GABA_AR$ γ2 subunit in DIV10 neurons and we activated Ca^{2+}-Calmodulin with the cell-permeable CaM agonist CALP3 (100µM) for 30 or 60 minutes. Interestingly, CALP3 rescued within 30 minutes the partial loss of GABAergic synapses (Fig. 6 A-B), indicating a role of CaM in the stabilization of GABAergic synapses. Addition of CALP3 for another 30 minutes did not further increase synapse rescue meaning the maximal effect was reached after 30 minutes (data not shown). In agreement with our observation that SQ22356 was not able to inhibit intracellular cAMP elevation in hippocampal neurons, SQ22356 application for 30 minutes could not prevent the CALP3 mediated rescue of GABAergic synapses in neurons lacking the $GABA_AR$ γ2 subunit (data not shown). We thus cannot conclude that CaM stabilizes synapses through the activation of ACs. Experiments are undergoing to directly involve Ca^{2+} -dependent ACs in the CALP3 effect.

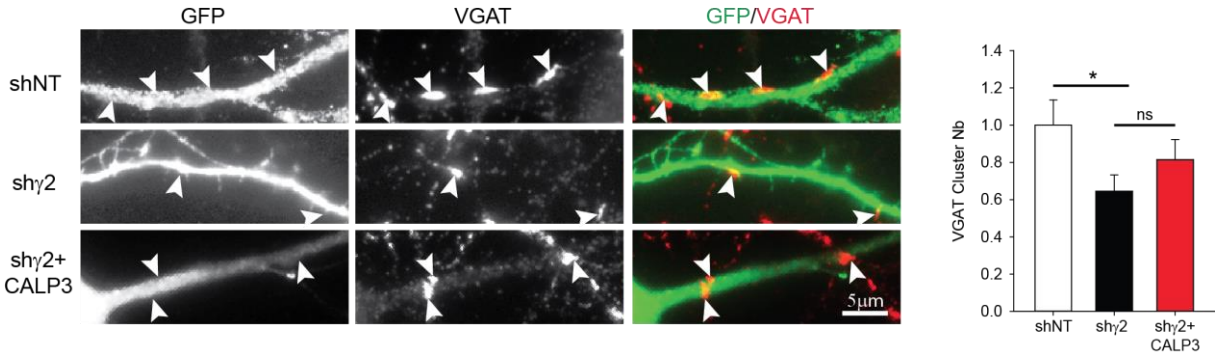

***Figure 6. Calmodulin activation partially rescues the loss of GABAergic synapses induced by $GABA_AR$ γ2 subunit suppression. A-B**, VGAT staining (**A**) and quantification (**B**) in DIV 10-11 neurons transfected with non-target (shNT) or on-target $GABA_AR$γ2 (shγ2) shRNAs exposed or not to CALP3 for 30 minutes. Scale bar, 5 µm. shNT n=25, shγ2 n=28, shγ2 + CGS21680 n=28, 2 cultures. Mann-Whitney test shNT vs shγ2 p=0.049, shγ2 vs shγ2 + CALP3 p=0.23.*

Discussion

Early in development GABA is depolarizing and the induced depolarization has been shown to regulate neurite outgrowth (Represa and Ben-Ari, 2005) through entry of Ca^{2+} via L-type Ca^{2+} channels (Perrot-Sinal et al., 2003), and activation of CAMKII and MAPK (Borodinsky et al., 2003). Later on, a role of GABA in the maturation of the synapse was demonstrated *in vivo* (Chattopadhyaya et al., 2007). Recent studies have shown a synaptogenic activity of GABA in young neurons (Fuchs et al., 2013; Oh et al., 2016).

The notion that adenosine signalling exerts a similar function during development is recent. We have shown that the activation of postsynaptic A_{2A}Rs is necessary and sufficient to stabilize GABAergic synapses in hippocampal neurons during synaptogenesis. The underlying mechanism involves AC activation, cAMP synthesis and PKA-dependent phosphorylation of the postsynaptic scaffolding molecule gephyrin and stabilization of the presynaptic terminal through the slitrk3-PTPδ trans-synaptic organizers. The present work further reports that the GABA signalling converge onto the adenosine signalling pathway to stabilize GABAergic synapses.

In support with a key function of the purine during synaptogenesis, we previously demonstrated: (i) a larger activity-dependent release of ATP and adenosine during the period of synaptogenesis, (ii) a peak of expression of the ecto-5'-nucleotidase, the rate-limiting step for the formation of adenosine from extracellular ATP, in synapses during this critical period, (iii) the peri- and/or post- synaptic expression of A_{2A}R concomitant with the period of synaptogenesis in the hippocampus. Furthermore, cAMP has been involved in the development of CNS connectivity i.e. in neuron specification and polarization, axon guidance and targeting, as well as refinement of synaptic connections. We now propose this key cyclic nucleotide also regulates GABAergic synaptogenesis. Synthesis of cAMP is dependent on the activity of ACs. The developmental expression of Ca^{2+}-sensitive ACs (1 and 8) points to a role of these molecules in synaptogenesis. In particular, AC1 being most broadly distributed in early life, whereas AC8 being most broadly expressed in adulthood, this suggests AC1 controls synaptogenesis in the hippocampus (Nicol et al., 2005).

The role of PKA in synaptogenesis has already been described at the neuromuscular junction (NMJ) (Martinez-Pena y Valenzuela et al., 2013). At central synapses, the pharmacological stimulation of AC (and the subsequent activation of PKA) in hippocampal cultures and slices increases synaptogenesis, an effect that can be prevented by PKA blockade (Tominaga-Yoshino et al., 2002; Yamamoto et al., 2005). Similarly, PKA signalling induces spinogenesis and the formation of functional glutamatergic synapses in the striatum (Kozorovitskiy et al., 2015) and the developing cortex (Kwon and Sabatini,

2011). Our work correspond to the first demonstration of a role of PKA signalling in GABAergic synapse formation.

As reported in earlier work (Essrich et al., 1998; Crestani et al., 1999; Li et al., 2005), knocking-down the $GABA_AR$ γ2 subunit leads to a loss of GABAergic synapses. We demonstrated that GABAergic synapses can be rescued upon $A_{2A}R$ activation in neurons lacking the $GABA_AR$ γ2 subunit. The $GABA_AR$ γ2 null mice display an elevated anxiety (Crestani et al., 1999; Chandra et al., 2005) . If the main defect in the GABAAR γ2 $^{+/-}$ mice is a loss of GABAergic synapses, we predict that facilitating synapse stabilization via $A_{2A}R$ activation may lower anxiety in these animals.

We addressed the underlying mechanism of the $GABA_AR$-mediated stabilization of synapses. We could observe that direct activation of $GABA_AR$ in young neurons leads to a Ca^{2+} increase, as previously reported (Leinekugel et al., 1995; Perrot-Sinal et al., 2003). Ca^{2+} is a second messenger that can modulate many functions. Interestingly, Ca^{2+} can stimulate transmembrane Ca^{2+}-sensitive ACs 1 and 8 via the activation of CaM (Cooper and Tabbasum, 2014). As $A_{2A}R$ is positively coupled to Ca^{2+}-sensitive and insensitive ACs, this suggests that $GABA_AR$ converge onto adenosine signalling via CaM activation of Ca^{2+}-sensitive ACs 1 and 8. cAMP imaging revealed that $GABA_AR$ or $A_{2A}R$ activation increases intracellular cAMP level. Moreover, the simultaneous activation of $GABA_AR$ and $A_{2A}R$ had an additive effect on the production of cAMP. This suggests Ca^{2+} signalling is positively coupled to cAMP production via the activity of $GABA_AR$ in immature neurons. Although the direct demonstration that GABA potentiates cAMP production through activation of Ca^{2+}-sensitive ACs is lacking at the moment, we could show the involvement of CaM in GABAergic synapse stabilization.

The diversity of ACs (10 isoforms) and the diversity of their regulation and localization shape the responses to distinct stimuli (Omori and Kotera, 2007; Willoughby and Cooper, 2007; Kleppisch, 2009). The signal specificity is obtained by the subcellular compartmentalization and temporal regulation of cAMP. Different AC isoforms are targeted to distinct subcellular domains, providing the basis of locally generated cAMP signals. The transmembrane Ca^{2+}-sensitive ACs (AC1, 3, 5, 6 and 8) are tethered to lipid rafts, whereas the Ca^{2+}-independent ACs (AC2, 4, 7 and 9) are excluded from lipid rafts (Willoughby and Cooper, 2007). Interestingly, the delocalization of A2AR from lipids rafts by cholesterol depletion selectively hampers their ability to recruit AC rather than MAPK (Charalambous et al., 2008). This shows the importance of the targeting or exclusion of specific AC isoforms from lipid rafts in regulating the cAMP concentrations and therefore signaling in compartments of the plasma

membrane (Depry et al., 2011). Interactions of cAMP with other second messenger such as Ca^{2+} are involved in the spatiotemporal regulation of cAMP. Therefore, we propose that GABA signaling by activating Ca^{2+}-sensitive ACs may participate in the spatiotemporal regulation of GABAergic synaptogenesis.

Here we show that the GABA signaling operates at synapses containing the neurexin-neuroligin-2 and slitrk3-PTPδ trans-synaptic complexes whereas the adenosine signaling may stabilize GABAergic synapses equipped with the slitrk3-PTPδ trans-synaptic complex only. This suggests that the adenosine signaling stabilizes a subset of GABAergic synapses. Interestingly, the GABAergic innervation is significantly reduced in the middle layer of CA1 stratum pyramidale in Slitrk3$^{-/-}$ mice while it is unaltered in the superficial or deep layers (Takahashi et al., 2012). Additional studies are required to determine the subset of GABAergic synapses stabilized by the adenosine signaling. This may rely on the subset of synapses that express $A_{2A}R$.

References

Antonelli R, Pizzarelli R, Pedroni A, Fritschy J-M, Del Sal G, Cherubini E, Zacchi P (2014) Pin1-dependent signalling negatively affects GABAergic transmission by modulating neuroligin2/gephyrin interaction. Nat Commun 5:5066

Barbin G, Pollard H (1993) Involvement of GABAA receptors in the outgrowth of cultured hippocampal neurons. 152:150–154.

Borodinsky LN, O'Leary D, Neale JH, Vicini S, Coso OA, Fiszman ML (2003) GABA-induced neurite outgrowth of cerebellar granule cells is mediated by GABAA receptor activation, calcium influx and CAMKII and erk1/2 pathways. J Neurochem 84:1411–1420.

Chamma I, Heubl M, Chevy Q, Renner M, Moutkine I, Eugène E, Poncer JC, Lévi S (2013) Activity-dependent regulation of the K/Cl transporter KCC2 membrane diffusion, clustering, and function in hippocampal neurons. J Neurosci 33:15488–15503

Chandra D, Korpi ER, Miralles CP, De Blas AL, Homanics GE (2005) GABAA receptor gamma 2 subunit knockdown mice have enhanced anxiety-like behavior but unaltered hypnotic response to benzodiazepines. BMC Neurosci 6:30

Charalambous C, Gsandtner I, Keuerleber S, Milan-Lobo L, Kudlacek O, Freissmuth M, Zezula J (2008) Restricted collision coupling of the A2A receptor revisited: Evidence for physical separation of two signaling cascades. J Biol Chem 283:9276–9288.

Chattopadhyaya B, Di Cristo G, Wu CZ, Knott G, Kuhlman S, Fu Y, Palmiter RD, Huang ZJ (2007) GAD67-Mediated GABA Synthesis and Signaling Regulate Inhibitory Synaptic Innervation in the Visual Cortex. Neuron 54:889–903

Chih B, Engelman H, Scheiffele P (2005) Control of excitatory and inhibitory synapse formation by neuroligins. Science 307:1324–1328

Conti AC, Maas JW, Muglia LM, Dave BA, Vogt SK, Tran TT, Rayhel EJ, Muglia LJ (2007) Distinct regional and subcellular localization of adenylyl cyclases type 1 and 8 in mouse brain. Neuroscience 146:713–729

Cooper DMF, Tabbasum VG (2014) Adenylate cyclase-centred microdomains. Biochem J 462:199–213

Craig AM, Kang Y (2007) Neurexin–neuroligin signaling in synapse development. Curr Opin Neurobiol 17:43–52

Crestani F, Lorez M, Baer K, Essrich C, Benke D, Laurent JP, Belzung C, Fritschy J-M, L?scher B, Mohler H (1999) Decreased GABAA-receptor clustering results in enhanced anxiety and a bias for threat cues. Nat Neurosci 2:833–839

Depry C, Allen MD, Zhang J (2011) Visualization of PKA activity in plasma membrane microdomains. Mol Biosyst 7:52–58

Dobie F, Craig A (2011) Inhibitory synapse dynamics: coordinated presynaptic and postsynaptic mobility and the major contribution of recycled vesicles to new synapse formation. J Neurosci 31:10481–10493

Essrich C, Lorez M, Benson JA, Fritschy JM, Lüscher B (1998) Postsynaptic clustering of major GABAA receptor subtypes requires the gamma 2 subunit and gephyrin. Nat Neurosci 1:563–571

Fritschy J-M, Panzanelli P, Kralic JE, Vogt KE, Sassoè-Pognetto M (2006) Differential Dependence of Axo-Dendritic and Axo-Somatic GABAergic Synapses on GABAA Receptors Containing the ?1 Subunit in Purkinje Cells. J Neurosci 26:3245–3255

Fuchs C, Abitbol K, Burden JJ, Mercer A, Brown L, Iball J, Anne Stephenson F, Thomson AM, Jovanovic JN (2013) GABAA receptors can initiate the formation of functional inhibitory GABAergic synapses. Eur J Neurosci 38:3146–3158.

Gauvain G, Chamma I, Chevy Q, Cabezas C, Irinopoulou T, Bodrug N, Carnaud M, Lévi S, Poncer JC (2011) The neuronal K-Cl cotransporter KCC2 influences postsynaptic AMPA receptor content and lateral diffusion in dendritic spines. Proc Natl Acad Sci U S A 108:15474–15479.

Huang Z, Scheiffele P (2008) GABA and neuroligin signaling: linking synaptic activity and adhesion in inhibitory synapse development. Curr Opin Neurobiol 18:77–83

Huang ZJ (2009) Activity-dependent development of inhibitory synapses and innervation pattern: role of GABA signalling and beyond. J Physiol 587:1881–1888

Huang ZJ, Di Cristo G, Ango F (2007) Development of GABA innervation in the cerebral and cerebellar cortices. Nat Rev Neurosci 8:673–686

Jacobson K, Gao Z (2006) Adenosine receptors as therapeutic targets. Nat Rev Drug Discov 5:247–264

Kleppisch T (2009) Phosphodiesterases in the Central Nervous System. In: cGMP: Generators, Effectors and Therapeutic Implications, pp 71–92. Berlin, Heidelberg: Springer Berlin Heidelberg.

Kozorovitskiy Y, Peixoto R, Wang W, Saunders A, Sabatini BL (2015) Neuromodulation of excitatory synaptogenesis in striatal development. Elife 4:1–18.

Krueger-Burg D, Papadopoulos T, Brose N (2017) Organizers of inhibitory synapses come of age. Curr Opin Neurobiol 45:66–77

Kwon H-B, Sabatini BL (2011) Glutamate induces de novo growth of functional spines in developing cortex. Nature 474:100–104

Lauder JM, Liu J, Devaud L, Morrow AL (1998) GABA as a trophic factor for developing monoamine neurons. Perspect Dev Neurobiol 5:247–259

Leinekugel X, Tseeb V, Ben-ari Y, Bregestovski P, Port-royal B De (1995) Synaptic GABAA activation induces Ca^{2+} rise in pyramidal cells and interneurons from rat neonatal hippocampal slices. :319–329.

Li R, Yu W, Christie S, Miralles CP, Bai J, Loturco JJ, Blas AL De (2005) Disruption of postsynaptic GABA A receptor clusters leads to decreased GABAergic innervation of pyramidal neurons. :756–770.

Link E, Edelmann L, Chou JH, Binz T, Yamasaki S, Eisel U, Baumert M, Südhof TC, Niemann H, Jahn R (1992) Tetanus toxin action: inhibition of neurotransmitter release linked to synaptobrevin proteolysis. Biochem Biophys Res Commun 189:1017–1023

Lu W, Bromley-Coolidge S, Li J (2017) Regulation of GABAergic synapse development by postsynaptic membrane proteins. Brain Res Bull 129:30–42

Maric D, Liu QY, Maric I, Chaudry S, Chang YH, Smith S V, Sieghart W, Fritschy JM, Barker JL (2001) GABA

expression dominates neuronal lineage progression in the embryonic rat neocortex and facilitates neurite outgrowth via GABA(A) autoreceptor/Cl- channels. J Neurosci 21:2343–2360

Martinez-Pena y Valenzuela I, Pires-Oliveira M, Akaaboune M (2013) PKC and PKA regulate AChR dynamics at the neuromuscular junction of living mice. PLoS One 8:e81311

Nicol X, Muzerelle A, Bachy I, Ravary A, Gaspar P (2005) Spatiotemporal localization of the calcium-stimulated adenylate cyclases, AC1 and AC8, during mouse brain development. J Comp Neurol 486:281–294

Oh WC, Lutzu S, Castillo PE, Kwon H-B (2016) De novo synaptogenesis induced by GABA in the developing mouse cortex. Science 353:1037–1040

Omori K, Kotera J (2007) Overview of PDEs and their regulation. Circ Res 100:309–327

Perrot-Sinal T., Auger A., McCarthy M. (2003) Excitatory actions of GABA in developing brain are mediated by l-type Ca2+ channels and dependent on age, sex, and brain region. Neuroscience 116:995–1003

Polito M, Guiot E, Gangarossa G, Longueville S, Doulazmi M, Valjent E, Hervé D, Girault J-A, Paupardin-Tritsch D, Castro LR V, Vincent P (2015) Selective Effects of PDE10A Inhibitors on Striatopallidal Neurons Require Phosphatase Inhibition by DARPP-32(1,2,3). eNeuro 2

Polito M, Klarenbeek J, Jalink K, Paupardin-Tritsch D, Vincent P, Castro LRV (2013) The NO/cGMP pathway inhibits transient cAMP signals through the activation of PDE2 in striatal neurons. Front Cell Neurosci 7:211

Poulopoulos A, Aramuni G, Meyer G, Soykan T, Hoon M, Papadopoulos T, Zhang M, Paarmann I, Fuchs C, Harvey K, Jedlicka P, Schwarzacher SW, Betz H, Harvey RJ, Brose N, Zhang W, Varoqueaux F (2009) Neuroligin 2 drives postsynaptic assembly at perisomatic inhibitory synapses through gephyrin and collybistin. Neuron 63:628–642

Represa A, Ben-Ari Y (2005) Trophic actions of GABA on neuronal development. Trends Neurosci 28:278–283

Rivera C, Voipio J, Payne JA, Ruusuvuori E, Lahtinen H, Lamsa K, Pirvola U, Saarma M, Kaila K (1999) The K+/Cl- co-transporter KCC2 renders GABA hyperpolarizing during neuronal maturation. Nature 397:251–255

Shen K, Scheiffele P (2010) Genetics and cell biology of building specific synaptic connectivity. Annu Rev Neurosci 33:473–507

Siddiqui TJ, Craig AM (2011) Synaptic organizing complexes. Curr Opin Neurobiol 21:132–143

Simões AP, Machado NJ, Gonçalves N, Kaster MP, Simões AT, Nunes A, Pereira de Almeida L, Goosens KA, Rial D, Cunha RA (2016) Adenosine A2A Receptors in the Amygdala Control Synaptic Plasticity and Contextual Fear Memory. Neuropsychopharmacology 41:2862–2871

Spoerri PE (1988) Neurotrophic effects of GABA in cultures of embryonic chick brain and retina. Synapse 2:11–22

Takahashi H, Craig AM (2013) Protein tyrosine phosphatases PTPδ, PTPσ, and LAR: presynaptic hubs for synapse organization. Trends Neurosci 36:522–534

Takahashi H, Katayama K-I, Sohya K, Miyamoto H, Prasad T, Matsumoto Y, Ota M, Yasuda H, Tsumoto T, Aruga J, Craig AM (2012) Selective control of inhibitory synapse development by Slitrk3-PTPδ trans-synaptic interaction. Nat Neurosci 15:389–398, S1-2

Tapia JC, Mentis GZ, Navarrete R, Nualart F, Figueroa E, Sánchez A, Aguayo LG (2001) Early expression of glycine and GABA(A) receptors in developing spinal cord neurons. Effects on neurite outgrowth. Neuroscience 108:493–506

Tominaga-Yoshino K, Kondo S, Tamotsu S, Ogura A (2002) Repetiti v e acti v ation of protein kinase A induces slow and persistent potentiation associated with synaptogenesis in cultured hippocampus. 44:357–367.

Varoqueaux F, Jamain S, Brose N (2004) Neuroligin 2 is exclusively localized to inhibitory synapses. Eur J Cell Biol 83:449–456

Willoughby D, Cooper DMF (2007) Organization and Ca2+ Regulation of Adenylyl Cyclases in cAMP Microdomains. Physiol Rev 87:965–1010

Wu X, Fu Y, Knott G, Lu J, Di Cristo G, Huang ZJ (2012) GABA signaling promotes synapse elimination and axon pruning in developing cortical inhibitory interneurons. J Neurosci 32:331–343

Yamamoto M, Urakubo T, Tominaga-Yoshino K, Ogura A (2005) Long-lasting synapse formation in cultured rat hippocampal neurons after repeated PKA activation. Brain Res 1042:6–16

DISCUSSION

DISCUSSION

During my PhD work, I focused on the role $A_{2A}R$ in the GABAergic synaptogenesis in hippocampal neurons. This work includes two studies.

In the first study, we showed how adenosine acts through $A_{2A}R$ to stabilize the nascent GABAergic synapses. We found an increase of $A_{2A}R$ expression during the period of synaptogenesis. This developmental expression of $A_{2A}R$ was correlated with a role of $A_{2A}R$ in the stabilization of nascent GABAergic synapses, a regulation restricted between DIV3 and DIV10 in vitro and between P4 and P12. Adenosine can be secreted by both glia and neurons; however, we found that activity-dependent release of neuronal adenosine is sufficient to stabilize newly formed GABAergic synapses in vitro. Our hypothesis is that adenosine activates $A_{2A}R$ and subsequently PKA that in turn phosphorylates the gephyrin serine 303. Moreover, I showed that the $A_{2A}R$-mediated stabilization of the post- and pre-synapse does not require the trans-synaptic neurexin-neuroligin 2 complex but the Slitrk3-PTPδ complex.

In the second study, we studied the interplay between the $A_{2A}R$- and the $GABA_AR$-mediated stabilization of synapses. I observed that both adenosine and GABA role on GABAergic synapse stabilization are activity-dependent. Knocking down $GABA_AR$ or $A_{2A}R$ induced GABAergic synapse loss. Direct activation of $GABA_AR$ cannot rescue GABAergic synapse loss in $A_{2A}R$ knocked down neurons. In contrast, $A_{2A}R$ activation rescued GABAergic synapses in neurons lacking $GABA_AR\gamma2$ subunit. While $A_{2A}R$ can only signal through the trans-synaptic Slitrk3-PTPδ, both neurexin-neuroligin 2 and Slitrk3-PTPδ complexes are important for the $GABA_AR$-mediated stabilization of synapses. Mechanistically, $GABA_AR$ activation leads to an increase in Ca^{2+} and cAMP influx in dendrites. Interestingly, the increase in intracellular cAMP level following the simultaneous activation of $A_{2A}R$ and $GABA_AR$ was additive, suggesting GABA signalling potentiates adenosine-mediated synapse stabilization. We further demonstrated the Ca^{2+}-Calmodulin dependency of GABAergic synapse stabilization. Ca2+-dependent ACs being activated by Ca^{2+}-Calmodulin, this suggests that GABA signalling bolsters adenosine-mediated synapse stabilization by activating Ca^{2+}-Calmodulin.

Here, we will discuss (i) the spatiotemporal expression and synapse stabilization impact of $A_{2A}R$ (ii) the $A_{2A}R$-mediated pathway leading to synaptogenesis (iii) signalling at the developing inhibitory synapse (iv) the pathological implications of the $A_{2A}R$ -mediated stabilisation of synapse.

1. Spatiotemporal expression and synapse stabilization function of $A_{2A}R$

$A_{2A}R$ was first described in the striatum of adult mammals (Jarvis and Williams, 1989; Martinez-Mir et al., 1991), but subsequent studies showed that $A_{2A}R$ expression was broader, being expressed in nucleus accumbens, olfactory tubercles, and areas of amygdala, globus pallidus, nucleus of the solitary tract, cortex, hippocampus, thalamus, cerebellum, and regions of the hindbrain (Rosin et al., 1998).

In the adult hippocampus, presynaptic $A_{2A}R$ plays a role at the excitatory synapse by facilitating the release of glutamate (Dixon et al., 1996; Costenla et al., 2011; Matsumoto et al., 2014). However, less is known about the expression of $A_{2A}R$ early in development. Interestingly, the use of subsynaptic fractionation techniques and superresolution STORM imaging allowed us to show **the peri- and/or post- synaptic expression of $A_{2A}R$ concomitant with the period of synaptogenesis in hippocampal neurons.** Immunohistochemistry showed a transient increased expression of $A_{2A}Rs$ in mouse hippocampi during the peak of synaptogenesis, between postnatal P4 and P16. The analysis of synaptosome preparations showed that $A_{2A}Rs$ were mostly located at synapses in both mature and immature mouse hippocampi. As previously reported (Rebola et al., 2005), $A_{2A}Rs$ were mostly presynaptic at P30. In contrast, they were mostly post- and peri-synaptic during the first postnatal week. Immunocytochemistry analysis of hippocampal neuronal cultures revealed that $A_{2A}Rs$ were clustered at GABAergic synapses, and that clustering increased during the period of synaptogenesis, between 7 and 14 days in vitro (DIV). Stochastic optical reconstruction microscopy (STORM) further confirmed that $A_{2A}Rs$ were located within or near the GABAergic post-synapse, as it colocalizes with gephyrin in the postsynaptic membrane. Our observation that $A_{2A}R$ is present at GABAergic synapses contrasts with mass spectrometry analyses of the inhibitory synapse (Table 9). None of these studies reported $A_{2A}R$ at inhibitory GABAergic synapses. This is probably due to the fact that these analyses were performed in adult tissue/neurons, while we have shown that the $A_{2A}R$ is present at GABAergic synapses in young neurons only. The lack of other spatio-temporal expression studies does not allow to conclude that the $A_{2A}R$ switch from post- to pre- synaptic localization is occurring in other brain regions.

Study	Method	Region	Age	$A_{2A}R$ detected?
(Heller et al., 2012)	Venus- $GABA_AR$ α1 BAC mice	Cortical pyramidal neurons, layer 5-6 and 2-3 (labelled under Otx1 promoter)	Adult	No
(Kang et al., 2014)	His6-FLAG-YFP-tagged NL2 transgenic mice	Broad (Under Thy1 promoter)	2-4 months	No
(Nakamura et al., 2016)	pHluorin/Myc-tagged $GABA_AR$α2 knock-in mice	Hippocampus and cortex	8-10weeks	No
(Loh et al., 2016)	HRP-NL2 HRP-Slitrk3 In primary cultures	Cortex	Rat corticultures prepared from E18 rats, analysis DIV19	No
(Uezu et al., 2016)	BirA-Gephyrin, BirA-CB BirA-InSyn (AAV injection)	Hippocampus and cortex	Injection at P0 Extraction at P40	No

Table 9: Proteomics studies focusing on the inhibitory synapse
Adapted from (Krueger-Burg et al., 2017)

An important question is whether the adenosine signalling is operant at GABAergic synapses only or if it is also active at glutamatergic synapses? In hippocampal cultures, we showed that acute $A_{2A}R$ blockade induced a loss of the pre- and post-synaptic markers of the GABAergic synapse but not of the glutamatergic one (Figure 19). In this preparation, the $A_{2A}R$-mediated stabilization of synapses is restricted to the inhibitory synapse. However, we cannot rule out a role of the adenosine signalling pathway at glutamatergic synapses. In these experiments, we blocked $A_{2A}R$ for 30 minutes only. The destabilization of the glutamatergic synapse may require more time to occur. Alternatively, synaptogenesis occurs later at glutamatergic synapses than at GABAergic synapses. We will first need to analyze the expression profile of $A_{2A}R$ at glutamatergic synapses to determine the time frame to analyse the effect of $A_{2A}R$ blockade on synapse stabilization.

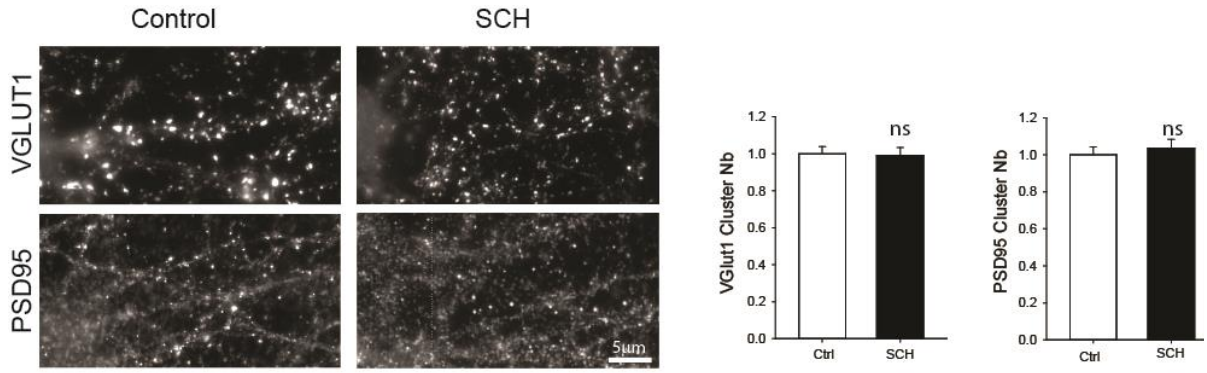

Figure 19: Acute $A_{2A}R$ blockade does not affect VGLUT1 and PSD95 clustering
Immunostaining and quantification of VGLUT1 and PSD95 in DIV 10 neurons in absence or presence of SCH58261 100nM for 30 min. n= 47-55 cells, 3 cultures. Data from Jessica Pressey.

It will be important to determine if the $A_{2A}R$-mediated GABAergic synapse stabilization is synapse specific. Electrophysiology revealed decreased mIPSCs amplitude and frequency upon $A_{2A}R$ blockade with SCH58261 in both pyramidal cells and interneurons of the CA1 region, thus showing that the $A_{2A}R$ is expressed and active in both types of cells. Interneurons are responsible for regulating neuronal inhibition and the synchronization of network activity. Interneurons exert a continuous level of inhibition onto pyramidal neurons and can be generally separated into two types: those targeting cell bodies and those targeting dendrites. Parvalbumin (PV+) and somatostatin (SST+) are two sub-types of interneurons highly expressed in the hippocampus which form synapses at the soma and along the dendrites of pyramidal cells, respectively (Chamberland and Topolnik, 2012).

In hippocampal cultures, we found that $A_{2A}Rs$ were not present at all synapses; they accumulated at a subset (39.1 ± 3.7 %, n= 34 cells, 3 independent experiments) of GABAergic synapses. This could reflect the transitory expression of $A_{2A}R$ and the asynchronous stabilization of synapses or this could mean that the adenosine signalling is operant at synapses formed by given interneuron subtypes. In order to address this point, we perfomed parvalbumin staining to identify GABAergic synapses formed by parvalbumin interneurons. No signal was detected at DIV10. This is coherent with the fact that parvalbumin is expressed only late in development (around P7-10) (Seto-Ohshima et al., 1990; de Lecea et al., 1995). SST is expressed earlier. SST staining did not work in cultures. Immunodetection of SST and VGAT in slices is ongoing. It is probable that the regulation is indeed occurring at SST synapses since C. Bernard's group have shown that in utero exposure to caffeine delay the migration of SST containing GABA neurons in the hippocampus and superficial cortical layers (Silva et al., 2013). To further prove the inhibitory synapse specificity of the $A_{2A}R$ regulation, an optogenetic strategy to identify and manipulate specific PV+ or SST+ interneurons could be used. Using a Cre-inducible channelrhodopsin (ChR2) virus we will perform bilateral stereotaxic hippocampal injections into SST-

Cre or PV-Cre mice lines (Jackson Labs) at P3. This will allow to selectively express ChR2 in either PV+ or SST+ interneurons and directly investigate any alterations in the inhibitory network when the virus is expressed (about one week later). By using this strategy, we will be able to examine the impact of $A_{2A}R$ regulation on synapse using a two-pronged approach. First, patch-clamp recordings of PV+ or SST+ interneurons from acute brain slices could be used to assess any changes in intrinsic neuronal properties after SCH58261 treatment, and second patching pyramidal neurons and activating PV+ or SST+ interneurons via ChR2 will allow to evaluate any changes in inhibitory drive onto the pyramidal cells. Using this approach, it will enable us to determine which type of interneuron (PV+ vs SST+) is impacted by the blockade of $A_{2A}R$ signalling.

It will also be interesting to know if the $A_{2A}R$-mediated stabilization of synapses is restricted to the hippocampus or if this is broader. Experiments by Jessica Pressey show that $A_{2A}R$ is expressed at P16 in hippocampus, cortex and cerebellum (Figure 20), however no morphological analysis has been performed to understand if the $A_{2A}R$ -mediated stabilization of synapses is operant in these brain regions.

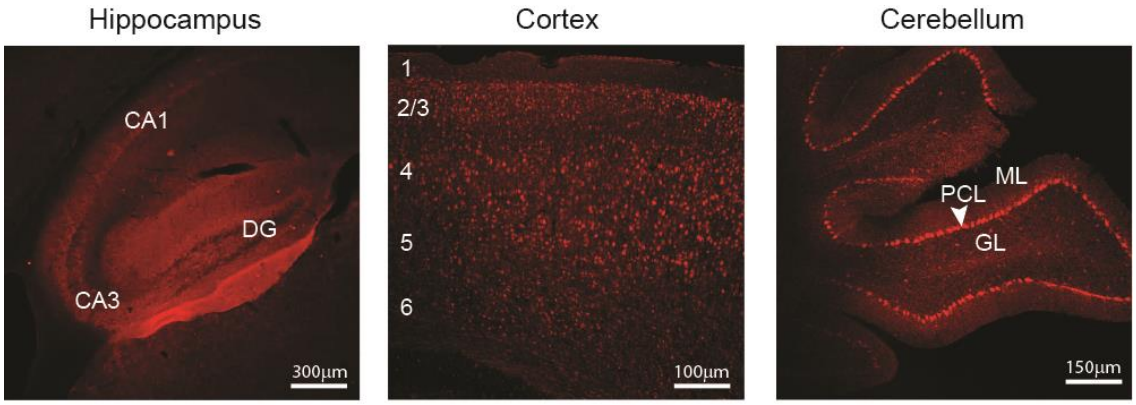

Figure 20: $A_{2A}R$ is expressed is expressed in the hippocampus, cortex and cerebellum at P16
See the expression of A2AR in the different layers of hippocampus, cortex and cerebellum (ML, molecular layer; PCL, Purkinje Cell layer; GL, granular layer).

Adenosine can modulate the number of GABAergic synapses. Yet, is this regulation occurring only through $A_{2A}R$? A_3R and $A_{2B}R$ are poorly expressed in hippocampus, as compared to $A_{2A}R$ and A_1R (Cunha, 2016). A **possible contribution of A1R in synaptogenesis** has never been assessed, thus I used the selective A_1R antagonist DPCPX (100nM), to study a possible modulation of the GABAergic synaptogenesis by this receptor. Acute blockade of A_1R receptor did not affect the clustering of the presynaptic marker VGAT nor the postsynaptic GABAARγ2, showing thus that the **adenosine regulation of synaptogenesis is mediated by $A_{2A}R$** (Figure 21)**.**

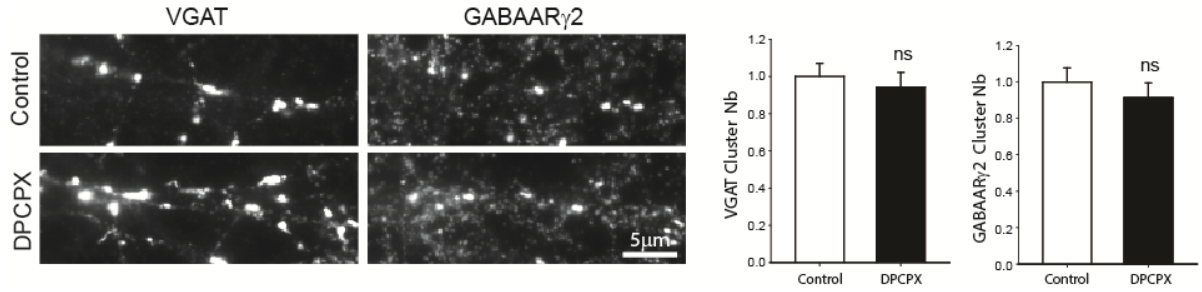

Figure 21: Acute A_1R blockade does not affect VGAT nor GABAARγ2 clustering
Immunostaining and quantification of VGAT and $GABA_AR\gamma2$ DIV 10 neurons in absence or presence of DPCPX 100nM for 30 min. n= 32-34 cells, 3 cultures.

I provide the first report of adenosine via $A_{2A}R$ modulating the number of GABA synapses. However, the purinergic signalling has already been shown to modulate the AMPA receptors in adult hippocampal neurons (Pougnet et al., 2014). ATP released from glia activate P2X2R to trigger dynamin-dependent internalization of AMPARs, leading to reduced surface AMPARs, and subsequent reduction in mEPSC amplitude.

Can the postsynaptic P2 receptors regulate synaptogenesis in hippocampal neurons? All the P2X receptors are expressed in the adult hippocampus, as well as P2Y1, P2Y2, P2Y4, P2Y6 and P2Y12 receptors (Burnstock and Verkhratsky, 2012). Much less is known about their expression early in development. Functional studies demonstrated a role of P2 receptors in neurite outgrowth in hippocampal preparations (Heine et al., 2006) and it was shown recently that P2X2 expression increases during the period of synaptogenesis (Emerit et al., 2016). Furthermore, P2X2 interacts with $GABA_AR$ making it an ideal candidate to modulate GABAergic synaptogenesis (Shrivastava et al., 2011). We studied the role of ATP and P2 receptor in hippocampal synaptogenesis (Figure 22). The blockade of P2 receptors with PPADS tetrasodium salt (100 µM) and TNP-ATP triethylammonium salt (50 µM) didn't impact the pre- and/or the post- synaptic elements of GABAergic synapses. At glutamatergic synapses, the blockade of P2 receptors affected the postsynaptic compartment identified by the accumulation of the scaffolding molecule PSD95 but not presynaptic VGLUT1 positive terminals. Therefore, we conclude that ATP and P2 receptor do not have the same implication in synapse stabilization than the adenosine signalling pathway. The P2 receptor may instead regulate the function of the synapse and in particular of glutamatergic synapses. Our results are opposite to the one of (Pougnet et al., 2014), as they found that ATP application leads to internalization of AMPAR (GluA1 and GluA2 staining) an effect that is blocked by PPADS, thus suggesting different underlying mechanisms. This could be explained by the different timing : DIV10 neurons vs 3-4 weeks old neurons. Further experiments will reveal if the loss of PSD95 is accompanied by a loss of AMPAR and/or NMDAR in the postsynaptic membrane and how would this impact the synaptic transmission.

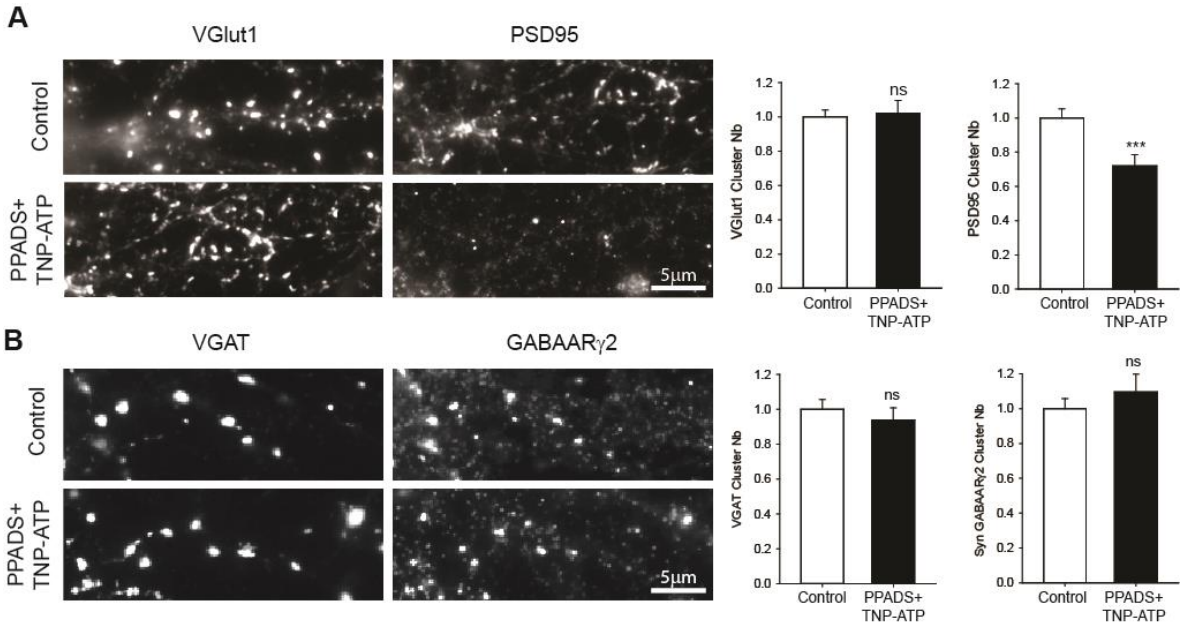

Figure 22: P2 receptors can modulate PSD95 clustering in young neurons

*Immunostaining and quantification of VGLUT1 and PSD95 (A) or VGAT and GABA$_A$Rγ2 (B) in DIV 10 neurons in absence or presence of PPADS (100 µM) and TNP-ATP (50 µM) for 30 min. n=3-5 cultures, 43-63 cells. ***p<0.001. Data from Ferran Gomez Castro and Jessica Pressey.*

2. A$_{2A}$R-mediated molecular pathway leading to the stabilization of synapses

We showed that the stabilization of GABAergic synapses occurs through activation of postsynaptic A$_{2A}$Rs, and subsequent activation of the Adenylyl Cyclase/cAMP/Protein Kinase A (PKA) signaling cascade. This cascade leads to the phosphorylation of the inhibitory postsynaptic scaffolding molecule gephyrin, which stabilizes the major trans-synaptic organizers Slitrk3 and Ptpδ.

A question is whether A$_{2A}$R can act as a synaptogenic organizer. This could be tested by overexpressing A$_{2A}$R in heterologous cells to check its ability to recruit the presynaptic compartment in neuronal co-cultured cells. Knowing that all proteins described as synaptogenic organizers are CAMs with extracellular binding domains (Missler et al., 2012) and that A$_{2A}$R is not (UniProt, 2017), **it is thus highly unlikely that A$_{2A}$R functions as a synapse organizer *per se*.**

If A$_{2A}$R has no synaptogenic activity *per se*, this implies that the A$_{2A}$R-mediated stabilization of inhibitory synapses comes from the activation of intracellular signalling pathways. We have shown that the decreased frequency and amplitude of GABA$_A$R-mediated mIPSC upon the blockade of A$_{2A}$R can be

overcomed by the activation of AC/cAMP/PKA cascade. Therefore, this cascade must be implicated in synapse stabilization.

PKA signalling during synaptogenesis

The observation that PKA signalling could regulate the number of receptor in the postsynaptic membrane has already been done at the neuromuscular junction (NMJ), where PKA activation prevents the removal of pre-existing AChRs and promotes the recycling of internalized AChRs to the postsynaptic membrane. In contrast, PKA inhibition significantly accelerates the removal of postsynaptic AChRs and depresses AChR recycling to the postsynaptic membrane (Martinez-Pena y Valenzuela et al., 2013).

The role of PKA in synaptogenesis has been observed in different systems ranging from invertebrates (Munno et al., 2003) to neuroblastoma cell line from mice (Tojima et al., 2003). In the CNS, works from the Ogura laboratory, have shown that the pharmacological stimulation of AC (and subsequent activation of PKA) in hippocampal cultures and slices increases synaptogenesis, an effect that can be prevented upon PKA blockade (Tominaga-Yoshino et al., 2002; Yamamoto et al., 2005). In this work, they did not distinguish between excitatory and inhibitory synapses. The Sabatini laboratory has shown that PKA signalling induces spinogenesis and the formation of glutamatergic synapses on the newly formed dendritic spines. In the developing cortex, local application of glutamate lead to spinogenesis and formation of functional synapses in a PKA-dependent manner (Kwon and Sabatini, 2011). PKA stimulation by $A_{2A}R$ or dopamine 1 receptor (D_1R) in the striatum also induced spinogenesis and formation of functional synapses (Kozorovitskiy et al., 2015). However, my work corresponds to the first demonstration of a **role of PKA signalling in inhibitory synapse formation.**

At the NMJ, the PKC would act as a negative regulator of the number of AChR clusters in the postsynaptic membrane (Martinez-Pena y Valenzuela et al., 2013). Indeed, stimulation of PKC accelerates the removal of postsynaptic AChRs and depresses AChR recycling to the postsynaptic membrane (Martinez-Pena y Valenzuela et al., 2013). On the contrary, inhibition of PKC prevents the removal of pre-existing AChRs and promotes the recycling of internalized AChRs to the postsynaptic membrane.

In the CNS, PKC regulates the number of receptors in the postsynaptic membrane by different mechanisms: enhancing synapse elimination in cerebellum (Kano et al., 1995; Shuvaev et al., 2011) and decreasing the affinity between glycine receptor and gephyrin (Specht et al., 2011). Although these studies are concordant with the observations made at the NMJ, a role for PKC in glutamatergic

synaptogenesis is emerging as its activation leads to PSD95 accumulation in hippocampus (Mogha et al., 2012; Sen et al., 2016). A possible role for PKC in inhibitory synaptogenesis, has been suggested as in superior colliculus E19 slices, the activation of PKC accelerates the formation of GABAergic synapses (Meier et al., 2003).

Overall, these data point at a **positive role for PKA during synaptogenesis both at the NMJ and at central synapses. Regarding PKC, it regulates negatively the number of AChR clusters in the membrane at the NMJ, but its role at central synapses is less clear**. There are many factors that can regulate PKC activity (Steinberg, 2008), thus the role of this kinase in synaptogenesis is possibly context-dependent.

Activators of PKA

PKA activation depends on the intracellular levels of cyclic AMP. GPCRs coupled to the $G_{\alpha s}$ subunit activate adenylate cyclase that transform ATP into cAMP and cAMP further activates the PKA signalling pathway (Ellis, 2004). An unaddressed question in my work is if other GPCR activators of AC could substitute the $A_{2A}R$ -mediated activation of AC. The GPCR positively coupled expressed in the brain are: 5-HT receptors types 5-HT4 and 5-HT7, Adenosine A_{2A} and A_{2B} receptors, β1, β2 and β3 adrenergic receptors , D1-like family dopamine receptors (D1 and D5) (Ellis, 2004).

As mentioned, in the striatum PKA stimulation by $A_{2A}R$ or D_1R were able to stimulate spinogenesis and formation of excitatory synapses (Kozorovitskiy et al., 2015), showing that **the type of receptor activating PKA is not crucial**. Further experiments are required to show if any of the mentioned receptors are expressed in the hippocampal postsynaptic membrane during this critical period and could activate AC, thus substituting $A_{2A}R$.

Downstream of PKA

Once PKA is activated, it phosphorylates many targets. We restricted our search to key synaptic proteins of the inhibitory synapse. PKA has been shown to phosphorylate different subunits of the $GABA_AR$ receptor as well as the main inhibitory scaffolding molecule gephyrin (Moss et al., 1992; Tyagarajan et al., 2013). Gephyrin carries over 22 phosphorylation sites but i.e. serine 303 is targeted by PKA only (Flores et al., 2014). Since PKA-mediated phosphorylation of gephyrin is important for its postsynaptic stabilization (Tyagarajan and Fritschy, 2014), we tested its contribution, by expressing constructs harbouring mutations of the PKA serine 303 site to aspartate (D) or alanine (A) to mimic the gephyrin phosphorylated or dephosphorylated states (Tyagarajan et al., 2011, 2013; Flores et al., 2014). Decreasing extracellular adenosine with ADA and AMPCP led to synapse destabilization in

neurons expressing the wild type gephyrin. However, expression of both gephyrin mutants prevented synapse loss, demonstrating the involvement of this phosphosite in synapse stabilization. We conclude that the activity-dependent activation of A_{2A}Rs by adenosine leads to AC-cAMP-PKA-mediated phosphorylation of gephyrin at serine 303 that stabilizes the GABAergic synapse. However, this does not rule out the contribution of additional synaptic targets in this regulation such as the $GABA_AR$ itself. Gephyrin is composed of three domains, the G-, C- and E- domains. The C-domain is positioned between the highly conserved G- and E-domains involved in gephyrin multimerization. The C-domain is the most exposed to the surrounding environment, making it a suitable substrate for post-translational modifications (Choii and Ko, 2015). The serine 303 is in the C-domain (Zacchi et al., 2014). Phosphorylation-induced conformational changes of gephyrin could affect the folding of the C-domain and of the neighbouring G- and E- domains, thus altering gephyrin clustering properties (Zacchi et al., 2014) and interactions with synaptic partners such as Slitrk3.

Neurexin-neuroligin-2 and slitrk3-ptpδ are the two main trans-synaptic complexes at the interneuron to pyramidal synapse. Knocking-down neuroligin-2 with a specific shRNA led to a major loss of GABAergic synapse as in (Chih et al., 2005). Activating A_{2A}Rs with CGS21680 rescued synapses ruling out the contribution of the neurexin-neuroligin-2 complex. In contrast, the synapse loss induced by the shRNA-mediated suppression of Slitrk3 (as in(Takahashi et al., 2012)) could not be rescued by CGS21680. However, we cannot rule out the contribution of other yet unknown systems.

The information regarding Slitrk3 is rather scarce. By the use of bioinformatics, we can predict two post-translational modifications of Slitrk3: a phosphorylation in threonine 119 and an acetylation in lysine 277 (Hornbeck et al., 2015). It would be interesting to know if threonine 119 is a target of PKA. Slitrk3 interacts functionally with PTPδ, and bioinformatics tools (Artimo et al., 2012) predict an interaction of human Slitrk3 with: Immunoglobulin mu binding protein 2 (IGHMBP2) and Neurotrophic tyrosine kinase receptor type 1 (NTRK1). Nothing is known about how Slitrk3 recruits the postsynaptic machinery. It is tempting to hypothesize that the interaction with NTRK1, which has been shown to functionally interact with BDNF, would explain how Slitrk3 recruits the postsynaptic machinery.

Kinetics of the A_{2A}R -mediated stabilization of synapses

As mentioned, acute A_{2A}R blockade (30min) leads to a loss of pre- and post-synaptic GABAergic marker. The amplitude and frequency of mIPSCs was also decreased in CA1 pyramidal cells upon 10-minute exposure to the A_{2A}R antagonist. This effect was found to be mediated by clathrin endocytosis. This time-frame is consistent with what has been observed in literature with receptors in the membrane being endocytosed in ten minutes (Oh et al., 2012).

In some experiments, we have observed a loss of GABAergic clustering after exposure to a toxin or an shRNA for long periods (from 48 to 96h) and after 30-minute exposure to an $A_{2A}R$ agonist the loss in synaptic cluster is rescued. Live cell imaging experiments showed us that the time to form a *de novo* synapse is of several hours in different systems (Wierenga et al., 2008; Dobie and Craig, 2011). Therefore, **$A_{2A}R$ plays a role in the stabilization and not *de novo* formation of GABAergic synapses**. In (Schuemann et al., 2013) they show that the locations where transient boutons appeared were often characterized by synaptic markers (VGAT or gephyrin), suggesting that these locations represent potential synaptic sites. Concordant with this observation, inhibitory synapses can be dismantled and formed in the same position (Villa et al., 2016). However, this observation was made on a time-scale of days, and more studies are needed to show the dynamics of the inhibitory synapse in shorter time scales.

Other mechanisms can regulate the GABAergic synapse number in this time frame: Sema4D (Kuzirian et al., 2013) and Wnt5a (Fuenzalida et al., 2016). When activating its pathway, these two mechanisms induce formation of synapses; however, the effect of the blockade was not reported. This contrasts with the adenosine signalling, in which we see no increase in the number of clusters, probably because it is already maximally activated. Conversely, when we impede this signalling we observe a loss of the number of clusters. Thus, and contrasting with other described mechanisms, **the adenosine signalling is maximally activated and plays a role in the stabilization of synapses.**

Source of adenosine

What is the source of adenosine stabilizing the synapses? I have shown in primary hippocampal cultures, the source of adenosine stabilizing the synapses does not come from ATP transformation as the blockade of the CD73 nucletidase (the enzyme that transforms AMP into adenosine) with AMPCP did not affect synapse density. This suggests activity-dependent release of adenosine stabilizes the GABAergic synapse in hippocampal cultured neurons. Contrasting with this observation, we found a significant reduction in $GABA_AR$ -mediated mIPSC amplitude and frequency upon blockade of CD73 nucleotidase in acute hippocampal slices, suggesting an ATP origin of adenosine in integrated systems. Astrocytic release of adenosine is low (Boison et al., 2010). However astrocytes are important for adenosine clearance in the synaptic cleft as they express high levels of adenosine kinase in adult brain, but not on early life (Studer et al., 2006; Boison et al., 2010). To assess the neuronal and/or glial origin of the purines, we treated cell cultures with cytosine-D-arabinofuranoside (AraC) to obtain pure neuronal cell cultures. Neurons established GABAergic synapses in these conditions. In the absence of glial cells, preventing the accumulation of extracellular adenosine with ADA and AMPCP resulted in synapse destabilization, which was prevented by the direct activation of $A_{2A}Rs$ with CGS21680. The

extent of the regulation was comparable in cultures maintained in the absence or presence of glial cells. Therefore, the release of adenosine or ATP from neurons are sufficient to activate A_{2A}Rs and to stabilize GABAergic synapses.

An open question is the mechanism of neuronal secretion of adenosine. In hippocampal CA1 area adenosine can be released by equilibrative transporters (Lovatt et al., 2012) but also via Ca^{2+} dependent exocytic release (Craig and White, 1993). To distinguish between both scenarios, experiments with dipyridamole (a blocker of ENTs (Wall and Dale, 2008) or the use of TTX to block action potential induced release of adenosine could be performed. It will also be of interest to measure adenosine release at a specific synapse.

3. Signalling at the developing inhibitory synapse

Currently, seven secreted factors have been shown to control the formation/stabilization of the inhibitory synapse: FGF7, neuroexophilins, cerebellin, BDNF, GABA, Wnt5a and adenosine (see Introduction Section 2.6.2 for references). Two of them, neuroexphilins and cerebellin, act as bridges in different trans-synaptic systems. FGF7 is secreted postsynaptically to act on the presynaptic counterpart activating its receptor FGFR2b promoting the clustering of VGAT by yet unknown mechanisms (Terauchi et al., 2010). Wnt5a signalling was shown to improve GABAergic clustering and transmission in a pathological mice model lacking dystrophin, a key component of the DGC (Fuenzalida et al., 2016); however it was not assessed in physiological conditions which makes it difficult to conclude the true nature of Wnt5a signalling at the developing inhibitory synapse.

There are thus three presynaptically released molecules than can condition the development of inhibitory synapses: BDNF, GABA and adenosine. Are these three factors acting at the same synapses or at different types of synapses, in different brain regions? Do they use independent signalling pathways or their signalling pathway converge? Are these signalling pathways (partially) redundant? I will now address these questions.

BDNF

BDNF signalling promotes GABAergic synapse development, as shown in the cerebellum (Rico et al., 2002), cortex (Hong et al., 2008) and hippocampus (Marty et al., 2000). The use of antibodies against BDNF reduced inhibitory synapse formation in cerebellar cultures (Drake-Baumann, 2006). BDNF is synthesized and released by pyramidal neurons to bind its receptor trkB present in interneurons (Seil,

2003). Interestingly, the $A_{2A}R$ and the BDNF signalling are tightly linked as the activation of $A_{2A}R$ can regulate BDNF production (Tebano et al., 2008; Jeon et al., 2011), and $A_{2A}R$ can trans-activate trkB even in the absence of BDNF (Lee and Chao, 2001). **This raises the hypothesis that some of the effects of BDNF could be mediated by $A_{2A}R$.** The BDNF and adenosine signalling have some common points. First, both adenosine and BDNF are secreted in an activity-dependent manner, and direct activation of trkB (Drake-Baumann, 2006) or $A_{2A}R$ (See data in Article 1) in absence of activity can overcome the loss of synapses induced by the activity blockade. Second, the $A_{2A}R$ -mediated stabilization of synapses requires PKA signalling, a pathway that can be activated by trkB signalling (Drake-Baumann, 2006; Wuchter et al., 2012). At last, BDNF signalling has been suggested to act in a different pathway than NL-2 (Chen et al., 2011). Thus, the adenosine and the BDNF can crosstalk at different steps. Some of the evidences we found where already described for BDNF/TrkB signalling and could be mediated by transactivation of trkB receptors. Experiments to distinguish if the $A_{2A}R$ -dependent synapse stabilization is mediated (partly) by trkB are undergoing in the laboratory.

GABA

Early in development GABA is depolarizing and can regulate neurite outgrowth (Represa and Ben-Ari, 2005) through entry of Ca^{2+} via L-type Ca^{2+} channels (Perrot-Sinal et al., 2003) and activation of CAMKII and MAPK (Borodinsky et al., 2003). The role of GABA in the maturation of the synapse has also been shown in vivo (Chattopadhyaya et al., 2007). Recent studies have shown a synaptogenic activity of GABA in young neurons (Fuchs et al., 2013; Oh et al., 2016).

In immature cultured hippocampal neurons, GABA augments levels of intracellular BDNF mRNA, in a $GABA_AR$ dependent manner (Berninger et al., 1995). It is thus plausible that the trophic effects of GABA in the maturing brain are mediated partly via BDNF and trkB activation.

We have shown in hippocampus of P7 mice that VNUT (responsible for the accumulation of ATP in synaptic vesicles) colocalizes partly with VGAT. Thus, a subset of GABAergic terminals is able to upload GABA and ATP in the same synaptic vesicles. It would be interesting to know if this particular subset of synapses is facing $A_{2A}R$ clusters, and this can be done by performing a triple immunohistochemistry against VNUT, VGAT and $A_{2A}R$.

In experiments knocking-down the $GABA_AR\gamma2$ subunit I could observe a dramatic loss of GABAergic synapses as reported in literature (Essrich et al., 1998; Crestani et al., 1999; Li et al., 2005). Interestingly, I could show that GABAergic synapses could be rescued upon $A_{2A}R$ activation. The null

mice for $GABA_AR\gamma2$ develop sensorimotor abnormalities (Günther et al., 1995). Life span, social behaviour, motor coordination, memory and reproduction are normal in $GABA_AR\gamma2^{+/-}$ mice but they display an elevated anxiety (Crestani et al., 1999; Chandra et al., 2005). It would be interesting to treat $GABA_AR\gamma2^{+/-}$ mice with $A_{2A}R$ agonists and check their level of anxiety using behavioural tests such as the elevated plus maze test (Belzung and Griebel, 2001). If the main defect in the $GABA_AR\gamma2^{+/-}$ mice is a loss of GABAergic synapses, we predict that facilitating synapse stabilization via $A_{2A}R$ may therefore ameliorates some of the behavioural defects found in these animals.

We addressed the underlying mechanism of the $GABA_AR$-mediated stabilization of synapses. We could observe that direct activation of $GABA_AR$ in young neurons leads to a Ca^{2+} increase, as previously reported (Leinekugel et al., 1995; Perrot-Sinal et al., 2003). Ca^{2+} is a second messenger that can modulate many functions. Interestingly, Ca^{2+} can stimulate adenylate cyclases (AC) 1 and 8 through calmodulin (Cooper and Tabbasum, 2014). As $A_{2A}R$ is positively coupled to AC, this molecule is a putative point of convergence with the $A_{2A}R$ -mediated stabilization of synapses. We performed cAMP imaging to show that activation of either $GABA_AR$ or $A_{2A}R$ lead to cAMP increase. Interestingly, activation of both receptors led to an additive effect in the production of cAMP. Furthermore, direct calmodulin activation seems to rescue the loss of clusters induced by the knockdown of $GABA_AR\gamma2$. This suggests the GABA and adenosine signalling pathways converge onto AC1 or AC8. With the use of genetically-encoded chelator of cAMP (Averaimo et al., 2016) targeted to lipid rafts where AC1 and AC8 are enriched (Nicol and Gaspar, 2014) we will block the signalling downstream of $GABA_AR$ in order to test its implication in the stabilization of GABAergic synapses.

<u>Possible contribution of glia</u>

How the glial cells contribute to the $A_{2A}R$-mediated stabilization of synapses is difficult to assess. We have shown that in pure neuronal cultures, the $A_{2A}R$-mediated stabilization of synapses is still operant. However, this experiment does not rule out a possible contribution of glia. Astrocytes can modulate the extracellular levels of the three signals mediating the inhibitory synapse development: BDNF, GABA and adenosine.

Astrocytic release of adenosine is low and it depends of the adenosine gradient in the synaptic cleft, when intracellular adenosine is lower than extracellular, release of adenosine can occur through ENT (Boison et al., 2010). Alternatively, astrocytes can release ATP that can be locally transformed in adenosine (Pascual et al., 2005). Astrocytes are also important for the removal of adenosine, as adenosine kinase is predominantly expressed in astrocytes and the knockdown of adenosine kinase increases the adenosinergic tone (Boison et al., 2010). Interestingly, the inhibition of adenosine kinase

in hippocampal slices increases endogenous adenosine and depresses neuronal firing, whereas inhibition of adenosine deaminase had no effect (Pak et al., 1994); showing thus that adenosine kinase is critical when regulating extracellular adenosine concentrations. This could explain why in pure neuronal cultures the synapse number is increased as compared to our mixed neuronal cultures.

Interestingly, $A_{2A}R$ in astrocytes can modulate the extracellular levels of GABA by increasing GABA uptake, while A_1R blocks GABA uptake (Matos et al., 2012; Cristóvão-Ferreira et al., 2013). Furthermore, astrocytes can secrete other elements that could be playing a role in the $A_{2A}R$ -mediated stabilization of synapses such as BDNF (Jean et al., 2009).

As discussed, these three signalling molecules can crosstalk at many levels. These different signalling can be (partially) redundant, or regulate the inhibitory signalling development at different synapses or at different time points. It is necessary to perform integrative studies to elucidate these roles.

4. Pathological implications for the $A_{2A}R$-mediated stabilisation of synapse

After the description of this new pathway for the stabilization of the nascent GABAergic synapses, it would be interesting to know if there are pathologies linked to the $A_{2A}R$-mediated stabilization of GABAergic synapses. As mentioned, there are four constitutive, global $A_{2A}R$ knockout mouse lines (gb-$A_{2A}R$ KO) from different genetic backgrounds have been generated, all of them were viable, without gross anatomic abnormalities (Wei et al., 2011).

The behavioural tests performed on these animals have only showed mild phenotypes: elevated anxiety (Ledent et al., 1997), enhanced working memory (Zhou et al., 2009), blunted effect of the caffeine-induced wakefulness (Huang et al., 2005) and they display hypolocomotion as regarding to spontaneous activity (Wei et al., 2011).

Brain regional deletion of $A_{2A}R$ were also generated, a forebrain-specific $A_{2A}R$ KO mice (Bastia et al., 2005) and a striatum-specific $A_{2A}R$ KO mice (Shen et al., 2008). As expected, these mice lines did not have a remarkable phenotype either. The effect on the spontaneous activity was blunted in both lines, and differences in amphetamine sensitization were reported (Wei et al., 2011). However, a molecular

characterization of the excitatory and inhibitory synapses has not been performed in these mice lines nor gb-A_{2A}R KO. However, this mild phenotype is not surprising. As mentioned, the experiments of deletion/overexpression *in vitro* with neuroligins yielded strong effects in terms of synaptic clustering and function (Graf et al., 2004; Chih et al., 2005), however the effect on the KO mice is milder (Varoqueaux et al., 2006). This exemplifies the complexity of the vertebrate system in which there are multiple, partially redundant, parallel trans-synaptic pathways. This redundancy in the synapse assembly in the mammalian brain grants the mammalian brain enough robustness to guarantee functional connectivity.

Some studies in humans have shown genetic linkage between A_{2A}R gene (ADORA2A) and different pathologies, but I will only consider here neurodevelopmental diseases. Interestingly, A_{2A}R is located in a candidate region for bipolar disorder (Berrettini, 2001) and A_{2A}R blockade can produce an antidepressant effect in rodents (El Yacoubi et al., 2001). Genetic linkage between A_{2A}R and panic disorder was found in a SNP coding for silent substitution (1976T>C) in Germanic and Caucasian Western European populations (Deckert et al., 1998; Hamilton et al., 2004). However, this was not replicated in Japanese nor Chinese pedigrees thus suggesting that this association could be ethnicity-dependent (Yamada et al., 2001; Lam et al., 2005). This same SNP did not report association with age of onset of schizophrenia nor Parkinson disease nor mood disorders (Lam et al., 2005; Tsai et al., 2006). Therefore, ADORA2A association with mood disorders might exist, but other determinants are key to the development of these pathologies.

General conclusions

In the adult brain, adenosine acts as a neuromodulator of synaptic transmission via A_1R and $A_{2A}R$. We show that during hippocampal synaptogenesis, $A_{2A}R$ is postsynaptic and has a role in stabilization of the nascent GABAergic synapses. At a set of GABAergic synapses, adenosine signalling through $A_{2A}R$ would sense the presynaptic active terminal and stabilize these terminals. An active GABAergic terminal releases adenosine or ATP, both contributing to a local activity-dependent increase of extracellular adenosine to activate $A_{2A}Rs$. Activation of $A_{2A}Rs$ activates the AC/cAMP/PKA cascade, leading to PKA-dependent phosphorylation of gephyrin and the stabilization of the postsynaptic element. If $A_{2A}Rs$ are not activated during an extended period of time, the synapse will not be stabilized and therefore it will retract.

This $A_{2A}R$-mediated stabilization of synapses adds to the already described BDNF and GABA as signals for the inhibitory synapse. We thus studied the interplay between GABA and adenosine signalling pathways in the stabilization of GABAergic synapses in hippocampal neurons. We showed that the adenosine signalling is sufficient to stabilize GABAergic synapses. The GABA signalling would converge onto the adenosine signalling pathway by potentiating Ca^{2+}-dependent ACs via the activation of Calmodulin (CaM). $A_{2A}Rs$ stabilize GABAergic synapses via the slitrk3-ptpδ trans-synaptic complex while $GABA_ARs$ stabilize GABAergic synapses via both the slitrk3-ptpδ trans-synaptic and the neurexin-neuroligin-2 complexes. All these data allow us to postulate the following functional scheme (Figure 23).

Hence, we have described a novel spatiotemporal location for $A_{2A}R$ that comes with a new role for this signalling, and its relation with the already described role for GABA stabilizing the nascent GABAergic synapses in the hippocampus. Further works must confirm if this regulation occurs in other synapses and brain regions.

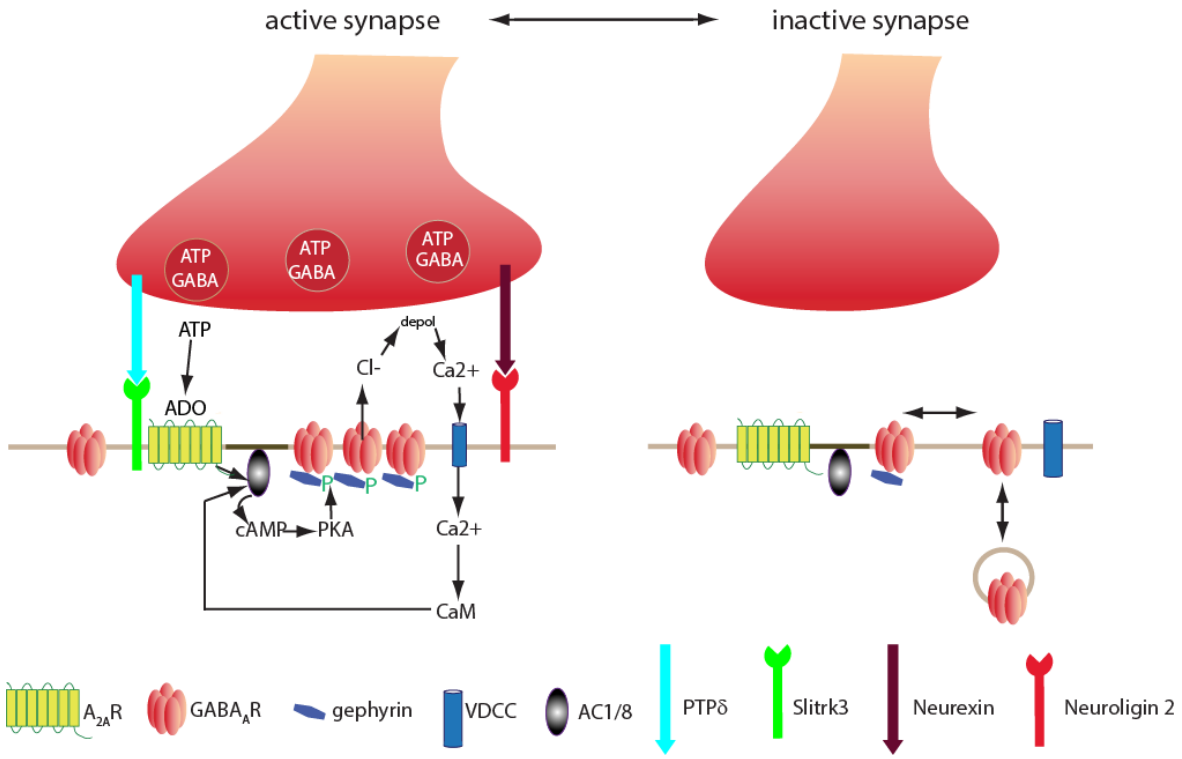

Figure 23: Functional model of adenosine via $A_{2A}R$ stabilizing the nascent GABAergic synapses

ADDITIONAL PUBLICATIONS

ADDITIONAL PUBLICATIONS

1. $GABA_A$ receptor dependent synaptic inhibition rapidly tunes KCC2 activity via the Cl^--sensitive WNK1 kinase

The K_+/Cl_- co-transporter KCC2 determines the efficacy of GABAergic neurotransmission by setting the intraneuronal chloride concentration. KCC2 itself is rapidly regulated on the level of its lateral diffusion, clustering, membrane stability and function by neuronal excitation (Chamma et al., 2013). How GABAergic inhibition can regulate the transporter in mature neurons remains elusive. The aim of this study was to investigate if GABAergic activity can regulate KCC2 in mature hippocampal neurons and to characterize the underlying mechanisms and functional impact. Using single-particle tracking, immunocytochemistry, electrophysiological and biochemical techniques we could show that:

- GABAAR-dependent inhibition can regulate KCC2 very rapidly in a homeostatic manner
- Intracellular chloride can act in this regulation as a second intracellular messenger modifying KCC2 threonine phospho-status via modification of WNK1 kinase activity
- The WNK signaling pathway can get activated under low chloride conditions *in vitro* and *in vivo*

I contributed in this publication by blocking the $GABA_AR$ *in vivo* by pentylenetetrazole (a $GABA_AR$ antagonist) injection and posterior tissue collection. Our results showed for the first time that GABAergic inhibition can tune itself via modifications in WNK1-dependent KCC2 threonine phosphorylation. Rapid modifications of KCC2 lateral diffusion allow hence maintaining functional chloride homeostasis and hyperpolarizing GABA responses in mature neurons.

Running title: GABAergic inhibition regulates KCC2 activity

$GABA_A$ receptor dependent synaptic inhibition rapidly tunes KCC2 activity via the Cl^--sensitive WNK1 kinase

Martin Heubl[1,2,3], Jinwei Zhang[4,5,6], Jessica C. Pressey[1,2,3], Sana Al Awabdh[1,2,3], Marianne Renner[1,2,3], Ferran Gomez-Castro[1,2,3], Imane Moutkine[1,2,3], Emmanuel Eugène[1,2,3], Marion Russeau[1,2,3], Kristopher T. Kahle[6], Jean Christophe Poncer[1,2,3] and Sabine Lévi[1,2,3*]

[1] INSERM UMR-S 839, 75005, Paris, France
[2] Université Pierre et Marie Curie, 75005, Paris, France
[3] Institut du Fer a Moulin, 75005, Paris, France;
[4] MRC Protein Phosphorylation and Ubiquitylation Unit, College of Life Sciences, University of Dundee, Dundee DD1 5EH, Scotland.
[5] Institute of Biomedical and Clinical Sciences, University of Exeter Medical School, Hatherly Laboratory, Exeter, EX4 4PS, UK.[6] Departments of Neurosurgery, Pediatrics, and Cellular & Molecular Physiology; NIH-Yale Centers for Mendelian Genomics; Yale School of Medicine, New Haven, CT 06511 USA
* Corresponding author

Correspondence to:
Sabine Lévi
INSERM-UPMC UMR-S 839
17 rue du Fer a Moulin
75005 Paris, France
Tel. +33 1 45 87 61 13
Fax. +33 1 45 87 61 10
E-mail: sabine.levi@inserm.fr

Abstract

The K^+-Cl^- co-transporter KCC2 (*SLC12A5*) tunes the efficacy of $GABA_A$ receptor-mediated transmission by regulating the intraneuronal concentration of chloride $[Cl^-]_i$ in post-synaptic neurons. KCC2 undergoes activity-dependent regulation in both physiological and pathological conditions. The regulation of KCC2 by synaptic excitation is well documented; however, whether the transporter is regulated by synaptic inhibition is unknown. Here, we reveal a novel mechanism of KCC2 regulation by $GABA_A$ receptor ($GABA_AR$)-mediated transmission in mature hippocampal neurons. Enhancing $GABA_AR$-mediated inhibition confines KCC2 to the plasma membrane, while antagonizing inhibition reduces KCC2 surface expression by increasing the lateral diffusion and endocytosis of the transporter. This mechanism utilizes Cl^- as an intracellular secondary messenger and is dependent on phosphorylation of KCC2 at threonines 906 and 1007 by the Cl^--sensing kinase WNK1. We propose this mechanism contributes to the homeostasis of synaptic inhibition by rapidly adjusting neuronal $[Cl^-]_i$ to $GABA_AR$ activity.

Introduction

Inhibitory GABAergic synaptic neurotransmission in mature neurons depends on a low intracellular chloride concentration $[Cl^-]_i$. Cl^- homeostasis is therefore essential to maintain the polarity and determine the extent of Cl^- fluxes through the ionotropic γ-aminobutyric acid receptor ($GABA_AR$). The hyperpolarizing shift in $GABA_AR$-activated current during development is dependent on a functional up-regulation of the neuronal K^+-Cl^- co-transporter KCC2 (*SLC12A5*), which extrudes Cl^- from neurons using electrochemically-favorable, outwardly-directed K^+ gradient [1]. In addition to its role in maintaining low $[Cl^-]_i$, KCC2 regulates the formation [2], functional maintenance, and plasticity [3,4] of glutamatergic synapses. Consistent with its key role in regulating inhibitory and excitatory neurotransmission, alterations in KCC2 expression and function have been correlated with pathological network activity in a variety of neurological and psychiatric disorders [5–9].

We recently demonstrated that the activity-dependent regulation of KCC2 lateral diffusion and clustering allows for a rapid regulation of Cl^- homeostasis in neurons. Only a few minutes of enhanced glutamatergic synaptic activity is sufficient to increase KCC2 membrane diffusion, leading to transporter escape from clusters located near excitatory and inhibitory synapses and endocytosis from the plasma membrane[10]. This regulation involves the Ca^{2+}-dependent, PP1-mediated, dephosphorylation of KCC2 at serine (S) 940 and the Ca^{2+}-activated, calpain-dependent cleavage of the KCC2 carboxy-terminal domain (CTD) [11,12]. Accordingly, down-regulation of KCC2 has been observed during increased glutamate release [13] and after long term potentiation of glutamatergic synapses [14] that results in a depolarizing shift of the reversal potential of GABA responses (E_{GABA}) [12,15]. GABA itself,

when acting as a depolarizing and sometimes excitatory neurotransmitter early in development, also downregulates KCC2 in a Ca^{2+}-dependent manner via L-type calcium channel activation [16]. While regulation of KCC2 by synaptic *excitation* is well documented, it is still unknown whether synaptic *inhibition* can regulate the membrane expression and/or activity of KCC2 in mature neurons.

Here, we examined whether GABAergic inhibition modulates KCC2 membrane dynamics, clustering, stability, and function in mature hippocampal neurons. We show that acute $GABA_AR$ activation with muscimol stabilizes KCC2 in the plasma membrane. In contrast, suppressing $GABA_AR$-dependent inhibition with gabazine rapidly increases KCC2 membrane dynamics, reducing the membrane clustering, stability, and activity of the transporter. We show that this mechanism is mediated by Cl^- ions acting as a second messenger via the Cl^--sensitive serine/threonine WNK1 kinase-dependent phosphorylation of KCC2 at threonines (T) 906 and 1007, two key regulatory sites of KCC2 activity during brain development [17,18]. Together, our results uncover a novel mechanism that rapidly tunes Cl^- homeostasis and GABA signaling in response to acute changes in synaptic, hyperpolarizing inhibitory transmission. We speculate that antagonizing WNK1 kinase activity may be a promising strategy to restore inhibition by restoring Cl^- homeostasis in diseases like epilepsy, schizophrenia, and neuropathic pain.

Results

$GABA_AR$-dependent inhibition rapidly regulates KCC2 lateral diffusion in the plasma membrane

Increased excitatory activity rapidly down-regulates KCC2 function by promoting its lateral diffusion, reducing its clustering, and increasing its internalization from the neuronal plasma membrane [10,12]. We asked whether pharmacological modulation of neuronal *inhibition* impacts the membrane dynamics of KCC2 using quantum dot-based single particle tracking (QD-SPT) technique in cultures of hippocampal neurons (DIV 21-24). At this stage, $GABA_AR$-mediated responses are hyperpolarizing and inhibitory, as demonstrated by E_{GABA} measurements using gramicidin-perforated patch-clamp and local photolysis of caged GABA (Figure S1). Since changes in neuronal excitation affect KCC2 diffusion and surface expression[10], the impact of inhibitory activity on KCC2 diffusion was explored while blocking neuronal activity and synaptic excitation. Therefore, neurons were analyzed in the presence of the Na^+ channel blocker tetrodotoxin TTX (1 μM), the ionotropic glutamate receptor antagonist kynurenic acid (KYN, 1 mM), and the group I/group II mGluR antagonist R,S-MCPG (500 μM). Herein, the "TTX+KYN+MCPG" condition is referred as the "control" condition (see Methods). To activate or block $GABA_ARs$, neurons were acutely exposed to the agonist muscimol (10 μM) or the competitive antagonist gabazine (10 μM). Whole-cell patch-clamp recording of hippocampal neurons

before, during, and after bath application of the $GABA_AR$ agonist muscimol (10 µM) indicated that muscimol induces a persistent current that desensitizes to less than 50% upon 10 min of agonist application (Figure S1). In contrast, application of gabazine leads to a rapid and complete reduction in mIPSCs throughout application of the drug (Figure S1). Therefore, $GABA_AR$-mediated inhibition in our culture system can be rapidly and significantly stimulated or blocked upon acute bath application of muscimol or gabazine.

We first examined whether activation of GABAergic inhibition by muscimol influences KCC2 diffusion using QD-SPT. For this purpose, neurons were transfected at DIV 14 with a recombinant Flag-tagged KCC2 transporter (KCC2-Flag) and surface labeled at DIV 22-25 with Flag antibodies, and then labeled with specific intermediate biotinylated Fab fragments and streptavidin-coated QDs (see Materials and Methods, and [10]). As shown in Figure 1A, surface exploration of individual QDs was restricted to smaller areas upon muscimol exposure, as compared to control condition. Quantitative analysis performed on the bulk population (extrasynaptic + synaptic) of trajectories revealed no significant effect of muscimol on the diffusion coefficient of KCC2 (Figure 1B). However, the mean-square displacement (MSD) versus time function was steeper for control as compared to muscimol trajectories (Figure 1C), indicative of increased confinement in the muscimol condition. Accordingly, the median explored area (EA) was significantly decreased upon muscimol (Figure 1D; Table S1). Therefore, increased $GABA_AR$ activity leads to an increased confinement of KCC2.

Next, we tested the impact of $GABA_AR$ blockade on KCC2 diffusion in the absence or presence of the competitive antagonist gabazine (10 µM). Bath application of gabazine increased the surface exploration of individual QDs (Figure 1E). When examining the bulk population of QDs, gabazine increased KCC2-Flag diffusion coefficients by 1.4-fold (Figure 1F; Table S1). Furthermore, the MSD versus time function displayed a reduced slope (Figure 1G) and the median value of the explored area was increased by 1.4-fold (Figure 1H; Table S1) upon gabazine application, indicating trajectories were less confined. The regulation of KCC2 diffusion by gabazine was not due to a nonspecific action of the drug, since a similar relief in transporter diffusion constraints was found when neurons were exposed to the $GABA_AR$ pore blocker picrotoxin (100 µM) (Figure S2). Thus, picrotoxin increased the median diffusion coefficient and the median explored area of the bulk population of KCC2-Flag by 1.2-fold (Figure S2; Table S1). We then analyzed the effect of gabazine on the diffusion behavior of KCC2 in the extrasynaptic and synaptic membranes in neurons co-transfected with KCC2-Flag and the excitatory and inhibitory synaptic markers homer1c-GFP and gephyrin-mRFP, respectively. Gabazine application significantly increased the KCC2 diffusion coefficient and the area explored in the extrasynaptic membrane, and near both excitatory and inhibitory synapses (Figure 1I-K; Table S1). Consistent with these observations, gabazine induced a 1.3- and 1.5- fold faster escape of KCC2 from the vicinity of

excitatory and inhibitory synapses, respectively (Figure 1L; Table S1). Thus, KCC2 exhibits reduced diffusion constraints and a faster escape from excitatory and inhibitory synaptic regions upon blockade of $GABA_AR$s.

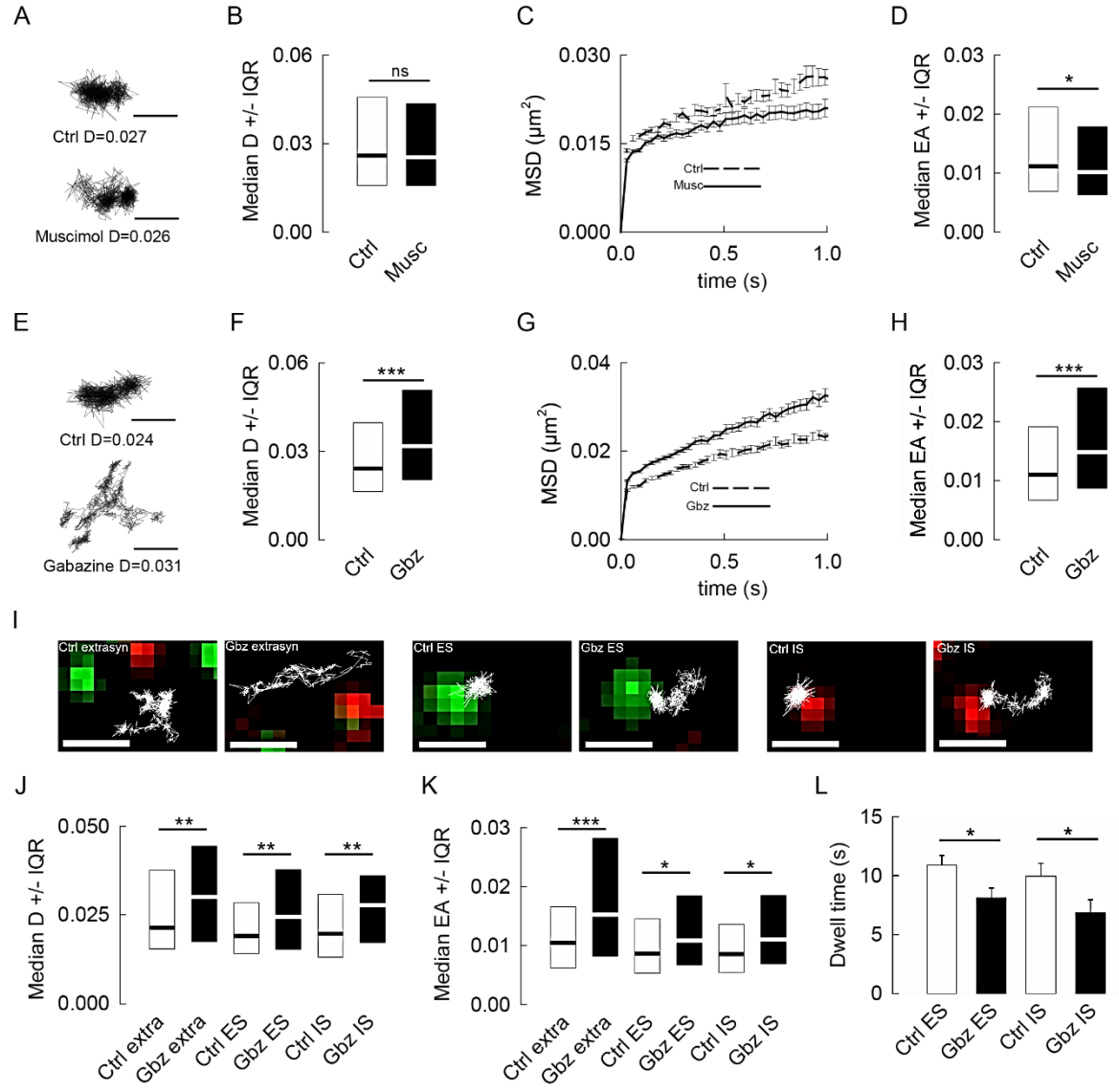

***Figure 1. $GABA_AR$ blockade increases KCC2 membrane diffusion. A**, Examples of KCC2 trajectories showing reduced surface exploration in the presence of muscimol. Scale bars, 0.5 µm. **B,** Median D ± 25%-75% Interquartile Range IQR of diffusion coefficients of KCC2 in control condition (white) or upon application of muscimol (black) showing no significant effect of muscimol on KCC2 diffusion coefficients. n= 416 QDs, 4 cultures, KS test p=0.139. **C-D**, Time-averaged MSD functions (**C**) and median explored area EA ± 25%-75% IQR (**D**) in control (white) vs muscimol (black) conditions show increased confinement upon muscimol application. n= 838 QDs, 4 cultures, KS test p=0.039. **E**, Examples of KCC2 trajectories in the presence or absence of gabazine application showing increase in QD surface exploration in gabazine-treated condition. Scale bars, 0.5 µm. **F,** Median D of KCC2 in control condition (white) are increased upon gabazine application (black). N= 441 QDs, 5 cultures, KS test p<0.001. **G-H**, Time-averaged MSD functions (**G**) and EA (**H**) in control (white) vs gabazine (black) conditions indicate decreased confinement upon $GABA_AR$ blockade. N= 880 QDs, 5 cultures, KS test p<0.001. **I**, QD*

*trajectories (white) overlaid with fluorescent clusters of recombinant homer1c-GFP (green) or gephyrin-mRFP (red) to identify extrasynaptic trajectories (left), trajectories at excitatory (middle) and inhibitory synapses (right). Scale bars, 1 µm. (**J-K**) Median D (**J**) and EA (**K**) of KCC2 are increased in all compartments upon gabazine application (black) as compared to control condition (white). **J**, extra, n= 129 QDs, KS test p=0.009, ES, n= 109 QDs, KS test p=0.004, IS, n= 89 QDs, KS test p=0.001; 4 cultures. **K,** extra, n= 362 QDs, KS test p<0.001; ES, n= 212 QDs, KS test p=0.034; IS, n= 202 QDs, KS test p=0.015, 4 cultures. (**L**) Mean dwell time DT (± s.e.m) of KCC2 at excitatory (ES) and inhibitory (IS) synapses is decreased upon $GABA_AR$ blockade with gabazine (black) as compared to control condition (white). ES, Ctrl n= 207 QDs and Gbz n= 218 QDs, MW test p=0.035; IS, Ctrl n= 162 QDs and Gbz n= 119 QDs, MW test p=0.047, 4 cultures. **B, F, J** D in $\mu m^2 s^{-1}$; **D, H, K** EA in μm^2.*

Synaptic release of GABA may activate synaptic $GABA_A$Rs, as well as extrasynaptic $GABA_A$Rs by spillover. In hippocampal pyramidal cells, tonic currents through extrasynaptic $GABA_A$Rs show a predominant α5 subunit pharmacology [19,20]. Tonic $GABA_A$R currents were virtually undetectable in our cultured hippocampal neurons in absence of GABA application[21] (Figure S1). In agreement, addition of L-655,708 (50 µM), an α5-GABAAR-selective benzodiazepine inverse agonist, had no effect on KCC2 diffusion (Figure 2A-B; Table S2). To check the contribution of tonic $GABA_A$R currents on KCC2 diffusion, we elicited tonic GABA currents with a bath application of GABA (2 µM) 10 min before imaging. Exogenous GABA reduced by 1.2-fold diffusion coefficients of KCC2 and by 1.1-fold its explored area, illustrating higher diffusion constraints onto the transporter as compared to control (Figure 2C-D; Table S2). This is reminiscent of the muscimol-induced confinement of KCC2. Addition of L-655,708 significantly increased the mobility and reduced the confinement of KCC2, relative to GABA alone (Figure 2C-D; Table S2). Therefore, tonic activation of α5-containing $GABA_A$Rs regulates KCC2 diffusion. These results indicate that both phasic and tonic GABA signaling regulate KCC2 diffusion.

$GABA_A$ and $GABA_B$ receptors ($GABA_B$Rs) both contribute to inhibition in the central nervous system. We examined whether metabotropic $GABA_B$ receptor ($GABA_B$R)-mediated inhibition could also alter KCC2 diffusion. Bath application of the $GABA_B$R agonist baclofen (20 µM) hyperpolarized hippocampal neurons by 8.7 ± 2.2 mV (Figure S3). This hyperpolarization was reversible and could be blocked by the selective $GABA_B$R antagonist CGP 52432 (20 µM; Figure S3). We found that up to 45 min exposure to either baclofen or CGP 52432, however, had no apparent effect on diffusion coefficients and explored area (Figure 2E-F; Table S2). Therefore, KCC2 diffusion is specifically regulated by $GABA_A$R but not $GABA_B$R-mediated transmission. Since the activity of $GABA_B$R leads to membrane hyperpolarization, this result further suggests KCC2 diffusion is not directly regulated by hyperpolarization.

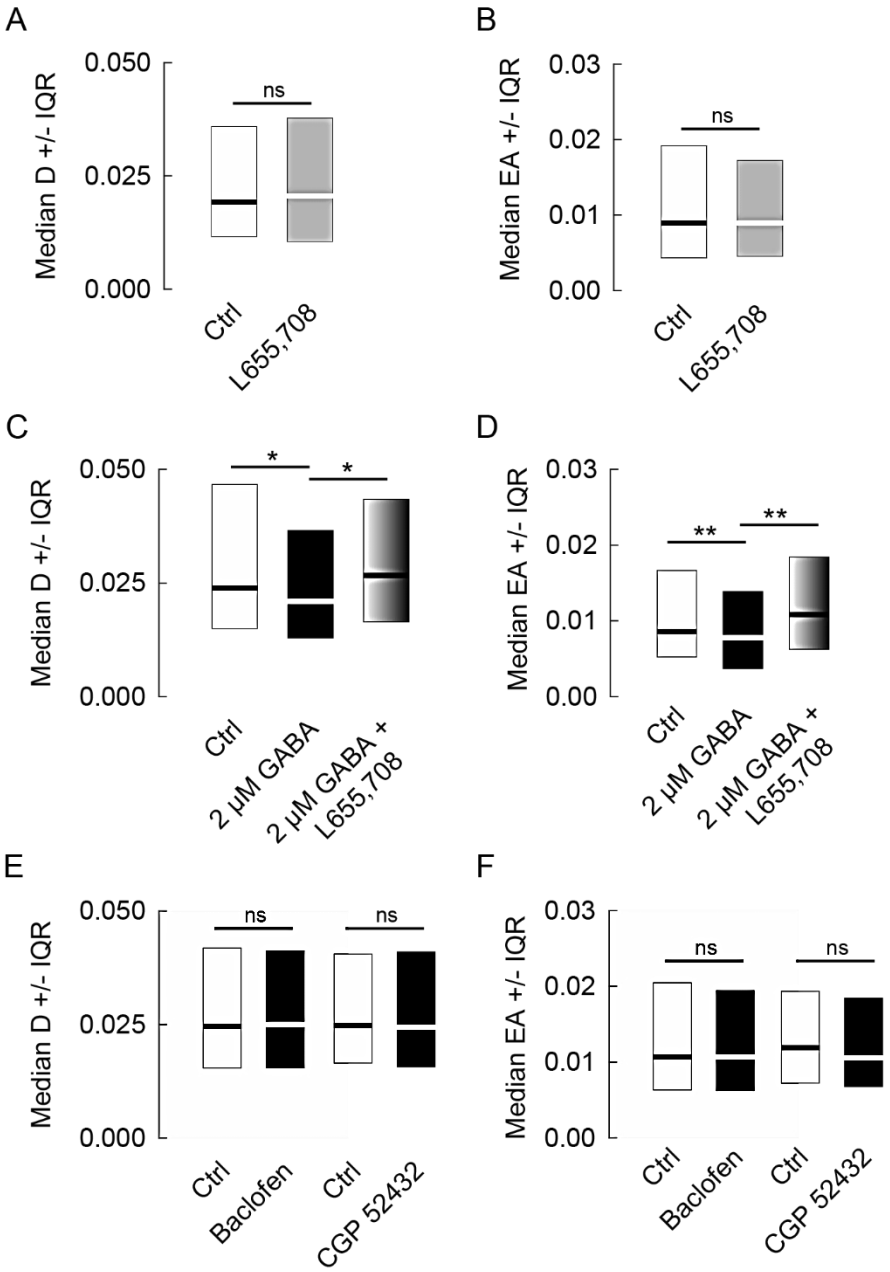

Figure 2. Tonic $GABA_AR$ but not $GABA_BR$ activity regulates the lateral diffusion of KCC2.

A-B, *No contribution of tonic $GABA_AR$-mediated inhibition on KCC2 diffusion under basal conditions. Median diffusion coefficients D ± 25-75% IQR (**A**) and median explored area EA ± 25-75% IQR (**B**) (for bulk population of QDs) of KCC2 measured in absence (white) or presence (gray) of 50 µM L-655,708 in the absence of exogenous GABA.* ***A,*** *n= 320 QDs, 2 cultures, p=0.658;* ***B,*** *n= 640 QDs, 2 cultures, p=0.472.* ***C-D,*** *Tonic activation of $GABA_AR$s by exogenous GABA affects KCC2 diffusion. Application of 2 µM GABA (black) decreased the diffusion and increased the confinement of KCC2 as compared to control condition (white). Addition of L655,708 (pattern) to GABA decreased KCC2 diffusion constraints compared to neurons exposed to GABA only.* ***C,*** *n= 271 QDs, 3 cultures; Ctrl vs GABA p=0.042; GABA vs GABA+L-655,708 p=0.035.* ***D,*** *n= 542 QDs, 3 cultures; Ctrl vs GABA, p<0.001; GABA vs GABA+L-655,708 p<0.001.* ***E-F,*** *No effect of $GABA_BR$ activity on KCC2 diffusion. Median diffusion coefficients (**E**) and median explored area (**F**) (for bulk population of QDs) of KCC2 measured in absence (white) or presence (black) of baclofen or CGP52432.* ***E,*** *baclofen experiment: n= 278 QDs, 3 cultures, p=0.864; CGP52432 experiment: n= 279 QDs, 3 cultures, p=0.425.* ***F,*** *baclofen experiment: n= 555 QDs, 3 cultures, p=0.338; CGP52432 experiment: n= 580 QDs, 3 cultures, p=0.091. In all graphs, KS test was used for data comparison.* ***A, C, E*** *D in $\mu m^2 s^{-1}$;* ***B, D, F*** *EA in μm^2.*

Regulation of KCC2 diffusion by $GABA_AR$-dependent inhibition is independent of Ca^{2+} signaling and S940 dephosphorylation

Rapid, activity-dependent regulation of KCC2 membrane dynamics and stability has been shown to require Ca^{2+} influx through NMDAR and voltage-dependent calcium channels VDCCs [12,15] and Ca^{2+}-dependent S940 dephosphorylation [10]. Our experiments performed in presence of TTX and glutamate receptor antagonists suggest a minor contribution of Ca^{2+} influx in the regulation of KCC2 diffusion by $GABA_ARs$. Accordingly, as revealed by Ca^{2+} imaging, gabazine application in the presence of TTX+KYN+MCPG did not increase $[Ca^{2+}]_i$ in hippocampal neurons (Figure 3A-B). In contrast, application of NMDA (50 µM) in absence of TTX and glutamate receptor antagonists rapidly increased $[Ca^{2+}]_i$ (Figure 3C-D). Therefore, gabazine does not lead to a major Ca^{2+} influx in neurons pre-treated with TTX+KYN+MCPG. Moreover, since our experiments were performed in the presence of the glutamate receptor antagonist kynurenate, a contribution of NMDAR-dependent Ca^{2+} influx to the $GABA_AR$-induced regulation of KCC2 diffusion is ruled out.

We next evaluated the contribution of VDCCs. We tested whether cadmium (100 µM; Cd^{2+}), a non-specific VDCC blocker, may impact the gabazine-induced increase in KCC2 diffusion. In presence of Cd^{2+}, gabazine was still able to increase the diffusion (Figure 3E) and reduce the confinement (Figure 3F) of KCC2 (Table S2). Dephosphorylation of KCC2 S940 is required for the activity-dependent increase in its diffusion [10]. We tested the involvement of this residue in the $GABA_AR$-mediated control of KCC2 diffusion. Over-expression of the phosphomimetic KCC2-S940D transporter[10] did not prevent the gabazine-induced increase in KCC2 diffusion (Figure 3G-H; Table S2). Altogether, these results demonstrate that $GABA_AR$-mediated regulation of KCC2 membrane diffusion does not involve a Ca^{2+} signaling pathway**.**

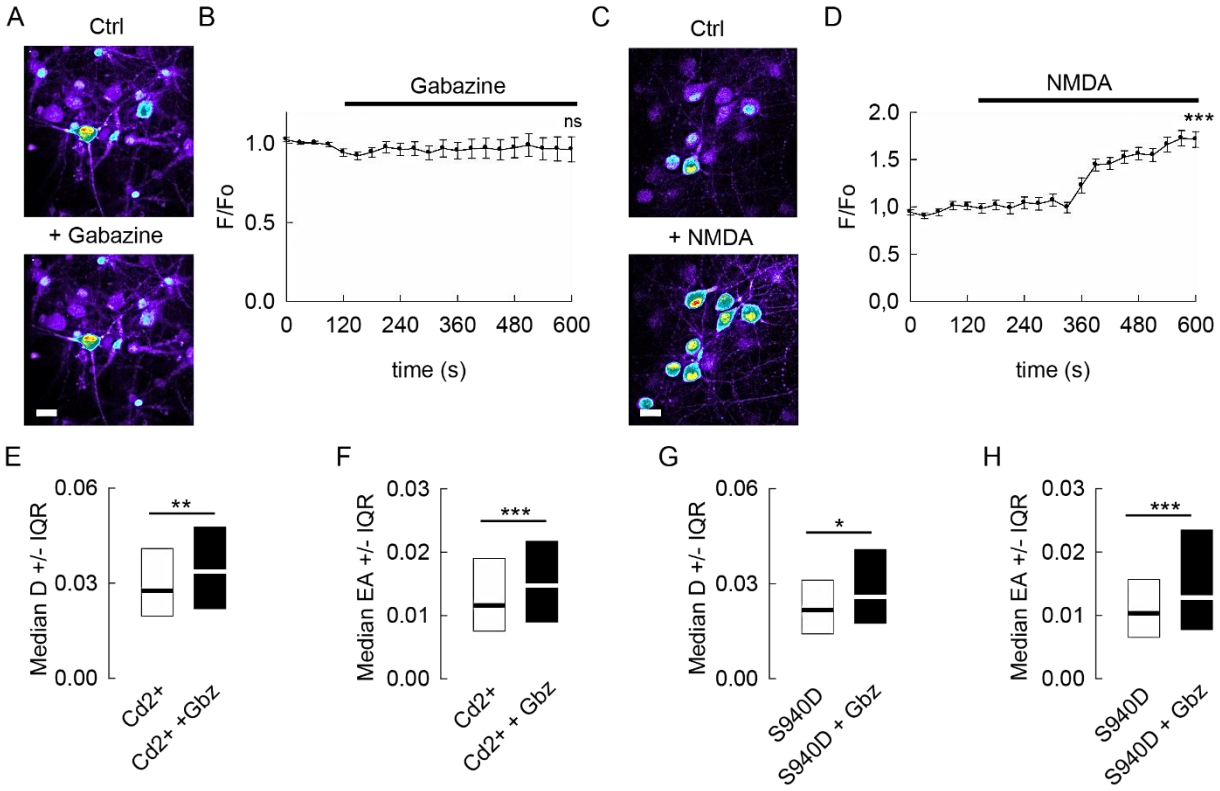

Figure 3. Voltage gated Ca^{2+} channels and S940 dephosphorylation do not contribute to gabazine-induced increase in KCC2 diffusion. A-B, *No effect of gabazine (10 µM) on intracellular calcium level in neurons pre-treated with the Na^{+} channel blocker tetrodotoxin TTX (1 µM), the ionotropic glutamate receptor antagonist kynurenic acid (1 mM), and the group I/group II mGluR antagonist R,S-MCPG (500 µM).* ***A,*** *Pseudocolor images of neurons loaded with Fluo4-AM, before (top) and after (bottom) gabazine treatment. Warmer colors correspond to higher Fluo4-AM fluorescence intensities. Scale bar, 10 µm.* ***B****, Calcium level in proximal dendrites shown as F/F0 ratio (mean ± s.e.m.) measured as a function of time following gabazine application (black bar). 9 cells; 2 cultures; paired t test p=0.691.* ***C-D,*** *NMDA (50 µM) increases intra-neuronal calcium level in absence of other drugs.* ***C****, Pseudocolor images of neurons loaded with Fluo4-AM, before (top) and after (bottom) NMDA treatment. Scale bar, 10 µm.* ***D****, Calcium level shown as F/F0 ratio as in* ***B****. Note the increase in intracellular calcium after NMDA exposure. 19 cells; 2 cultures; paired t test p<0.001.* ***E-F,*** *Median diffusion coefficients D values ± 25-75% IQR (****E****) and median explored area EA ± 25%-75% IQR (****F****) (for bulk population of QDs) of KCC2 measured in presence of the Ca^{2+} channel blocker Cd^{2+} alone (white) or in presence of gabazine (black). Cd^{2+} did not prevent the gabazine-induced reduction in diffusion constraints of KCC2.* ***E****, n= 250 QDs, 3 cultures, p=0.003.* ***F****, n= 500 QDs, 3 cultures, p<0.001.* ***G-H,*** *Median D (****G****) and EA (****H****) (for bulk population of QDs) of KCC2-S940D under control (white) or gabazine (black) conditions. Again, S940D substitution did not prevent the gabazine-induced reduction in diffusion constraints of KCC2.* ***G****, n= 190 QDs, 3 cultures, p=0.021;* ***H****, n= 380 QDs, 3 cultures, p<0.001.* ***E-H****, KS test was used for data comparison.* ***E, G*** *D in $\mu m^2 s^{-1}$;* ***F, H*** *EA in μm^2.*

Molecular mechanisms underlying $GABA_AR$-dependent regulation of KCC2 membrane diffusion

If Ca^{2+} signaling is not involved in $GABA_AR$-mediated regulation of KCC2, what is the underlying signaling mechanism? $GABA_AR$ activation leads to Cl^- influx in mature neurons. Concomitantly, $GABA_AR$ blockade decreases $[Cl^-]_i$. These observations suggest variation in $[Cl^-]_i$ may influence KCC2 membrane diffusion. To test this hypothesis, we first examined whether changes in $GABA_AR$ activity are associated

with changes in $[Cl^-]_i$. We measured the steady-state $[Cl^-]_i$ in neurons using fluorescence resonance energy transfer (FRET) multiphoton imaging of the chloride sensor SuperClomeleon [22]. We calibrated the probe in our system using Neuro2a cells (see Materials end Methods). The FRET ratio of Superclomelon was tightly correlated with $[Cl^-]_I$, with highest sensitivity in the range of 15-100 mM (Figure 4A). However, the probe showed very little sensitivity for concentrations ranging 0-15 mM. We analyzed the effect of muscimol or gabazine on $[Cl^-]_i$ in neurons transfected with SuperClomeleon. As expected, we observed a significant decrease in the FRET ratio of SuperClomeleon signal upon 5 min of muscimol application (-10 ± 3%; Figure 4B), indicating an increase in $[Cl^-]_i$. Blockade of $GABA_AR$ with gabazine is instead expected to decrease $[Cl^-]_i$. However, no detectable change in FRET ratio was observed upon 5' of gabazine application (Figure 4B), likely due to the lack of sensitivity of the probe in the 0-15 mM range in our experimental conditions (Figure 4A). However, prolonged application of gabazine (50 min) led to a reduced FRET ratio of SuperClomeleon (~ 26 ± 8%; Figure 4B), suggestive of an increase in $[Cl^-]_i$, possibly reflecting an active mechanism of chloride homeostasis (see below).

Next, we investigated whether changes in $[Cl^-]_i$ influence the membrane diffusion of KCC2 independently of $GABA_AR$ activity. We increased $[Cl^-]_i$ by exposing neurons to the selective KCC2 inhibitor VU0463271 (10 µM) [23], while $[Cl^-]_i$ was lowered by substituting extracellular Cl^- with methanesulfonate in the imaging medium. As expected for a respective increase and decrease in $[Cl^-]_i$, VU0463271 reduced the FRET ratio of SuperClomeleon signal (-15 ± 5%; Figure 4B), while lowering extracellular Cl^- level increased it (+25 ± 9%; Figure 4B). Using these experimental paradigms, we could then explore the impact of changes in $[Cl^-]_i$ on KCC2 diffusion. Within 10 min and up to 45 min of VU application, we observed a reduction in the surface explored by individual KCC2 transporters (Figure 4C). This did not impact the diffusion coefficient (Figure 4D), but significantly increased KCC2 confinement, as illustrated by the steeper slope of the MSD vs. time function (Figure 4E), and the reduced area explored (Figure 4F; Table S3). Since muscimol or VU had only modest impact on KCC2 confinement, we asked whether increasing $[Cl^-]_I$ via the photostimulation of halorhodopsin eNpHR, the light-driven microbial chloride pump, would influence the diffusion behavior of the transporter. We found that the photostimulation of halorhodopsin eNpHR significantly reduced the diffusion coefficient and increased confinement of KCC2 transporters. This was observed as soon as 10 s after light exposure for matched QDs (Figure 4G) and population of QDs (Figure 4 H-J; Table S3). This effect was robust since it was still detected after 1 min of light exposure. Therefore, increasing $[Cl^-]_I$ increases membrane confinement of the transporter. In contrast, lowering $[Cl^-]_i$ by extracellular Cl^- substitution significantly increased KCC2 surface exploration and mobility for individual trajectories (Figure 4K) and population of QDs (Figure 4L-N; Table S3). Together, these results provide evidence that intracellular Cl^- acts as a second messenger to rapidly modulate KCC2 diffusion downstream of changes in the activity of $GABA_ARs$.

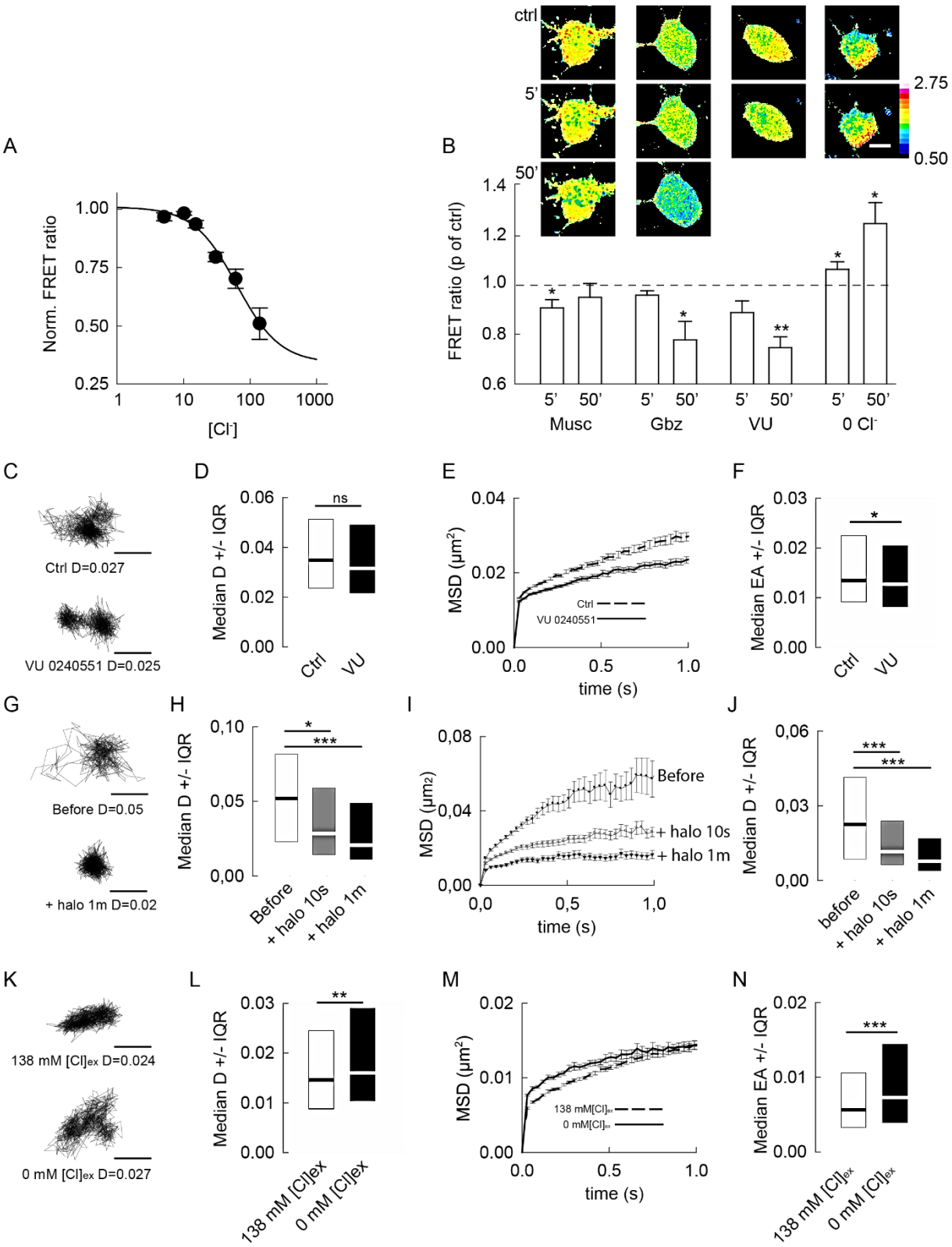

Figure 4. Changes in intracellular $[Cl^-]_i$ concentration tune KCC2 diffusion. A, *Calibration of SuperClomeleon in Neuro2a cells using multiphoton microscopy. Ionophore treatment was used to clamp $[Cl^-]_i$ to 5, 10, 15, 30, 60 and 138 mM. Note the relative lack of sensitivity of the probe in the 5-15 mM range in our experimental conditions.* ***B,*** *Images of Cl^--dependent changes in the FRET ratio (535/483 nm emission) in hippocampal neurons expressing SuperClomeleon, before (ctrl) and after 5*

or 50 min application of muscimol (Musc), gabazine (Gbz), KCC2 blocker (VU) or extracellular Cl^- substitution (0 Cl). The graph shows changes in FRET emission ratio upon treatment relative to control. Muscimol n = 6 cells, p=0.031 at 5 and 0.063 at 50 min; Gabazine n = 5 cells, p= 0.063 at 5 and 0.008 at 50 min; VU n = 4 cells, p=0.125 at 5 and 0.015 at 50 min; 0 Cl n = 4 cells, p=0.047 at 5 and 0.030 at 50 min. Wilcoxon ranked sum test or paired t-test when normality test was passed; 4 cultures. Insets show pseudocolored ratio images of SuperClomeleon fluorescence imaged at 535/483 nm in control and after 5 or 50 min of treatment. Scale bar, 10 µm. ***C****, Examples of KCC2 trajectories in control vs VU application showing a reduction in QD surface exploration with VU. Scale bars, 0.5 µm.* ***D****, Median diffusion coefficient D values ± 25-75% IQR (for bulk population of QDs) of KCC2 in control condition (white) or upon application of VU (black). n= 386 QDs, 3 cultures, KS p=0.228.* ***E-F****, MSD vs time functions (**H**) and median explored area EA ± 25%-75% IQR (**I**) in control (white) vs VU (black) conditions show VU significantly increases KCC2 confinement. N= 712 QDs, 3 cultures, KS test p=0.032.* ***G****, Matched KCC2 trajectories before (t0), and after 10 s or 1 min of light photostimulation of NpHR halorhodospin. Scale bars, 0.5 µm.* ***H-J****, Median diffusion coefficients D (**H**), MSD vs time functions (**I**) and median explored area EA (**J**) for bulk population of QDs showing reduced diffusion and increased confinement of KCC2 upon increase of Cl^-concentration after 10 s or 1 min of NpHR photostimulation.* ***H****, n= 215 QDs, 2 cultures, KS test p=0.011 and p<0.001;* ***J****, n= 469 QDs, 2 cultures, KS test p<0.001.* ***K****, Individual KCC2 trajectories in neurons maintained in high vs low extracellular Cl^- concentration, illustrating increased exploration upon extracellular Cl^- substitution. Scale bars, 0.5 µm.* ***L-N****, Median diffusion coefficients D (**L**), MSD vs time functions (**M**) and median explored area EA (**N**) for bulk population of QDs showing increased diffusion and reduced confinement of KCC2 upon reduction of Cl^-concentration.* ***L****, n= 408 QDs, 3 cultures, KS test p=0.001;* ***N****, n= 816 QDs, 3 cultures, KS test p<0.001.* ***D, H, L*** *D in $\mu m^2 s^{-1}$;* ***F, J, N*** *EA in μm^2.*

How do changes in $[Cl^-]_i$ influence the membrane diffusion of KCC2? The serine-threonine WNK kinases are activated by low $[Cl]_i$ [24,25], and activated WNKs promote KCC2 phosphorylation at T906 and T1007 [26,27]. Dephosphorylation of these residues accompanies the increased functional expression of KCC2 brain development [17,26]. We therefore hypothesized that lowering $[Cl^-]_i$, in mature neurons with gabazine may activate WNK kinase(s) and thereby promote KCC2 T906/T1007 phosphorylation and reduce its membrane confinement.

To test this hypothesis, we utilized real-time quantitative polymerase chain reaction (qRT-PCR) to determine the expression pattern of the four different WNK kinase family members (WNK1-WNK4) [28] in mature hippocampal neurons. As shown in Figure 5A, WNK1 and WNK3 mRNAs are the only WNK family members detected after 28 cycles of PCR amplification in mature hippocampal neurons. qRT-PCR revealed WNK1 is respectively ~500-, 10- and 90- fold more abundant than WNK 2, 3 and 4 transcripts in DIV 21 hippocampal cultures (Figure 5B). The relative abundance of the diverse WNK transcripts did not differ strikingly between DIV 21 hippocampal cultures and hippocampal tissue from adult rat brain (Figure 5B). These results show WNK1, and to a lesser extent WNK3, are the predominant WNK family members expressed in mature hippocampal neurons.

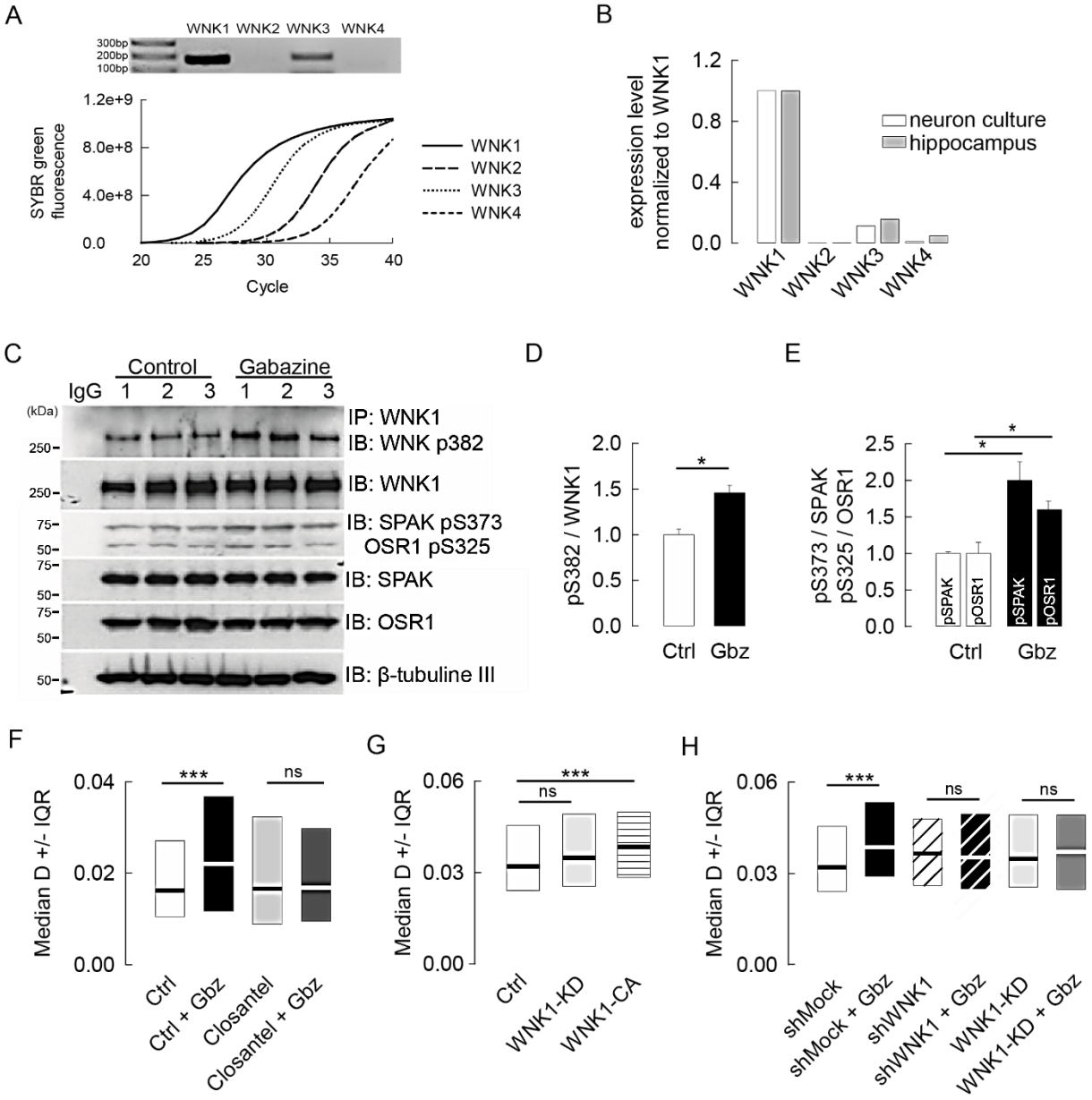

Figure 5. WNK1 is the main WNK kinase family member expressed in the mature hippocampus and is involved in KCC2 regulation by $GABA_AR$-mediated transmission. A*, Top panel, Gel example showing amplification of WNK1 and WNK3 but not of WNK2 and WNK4 cDNAs in DIV 21 hippocampal neurons after 28 cycles of semi-quantitative RT-PCR. Bottom, Quantitative real time polymerase chain reaction qRT-PCR of DIV 21 cultures illustrating amplification first of WNK1 (plain line) transcripts followed by WNK3 (cross), WNK4 (circle) and WNK2 (dash) transcripts.* ***B****, Results of qRT-PCR reactions for WNK1, WNK2, WNK3, and WNK4 from 3-weeks old hippocampal cultures (white) and rat adult hippocampal tissue (gray). Expression levels of WNK2, 3 and 4 were normalized to WNK1 expression level.* ***C-E****, Western Blot and quantification (mean ± s.e.m., three independent experiments 1-3) of the activated kinases WNK1 P-S382, SPAK P-S373, and the SPAK homologue OSR1 P-S325 phosphorylation in control (white) and upon gabazine application (black), showing increased phosphorylation of WNK1 (****C-D****, t-test p=0.011), SPAK (****C-E****, t-test p=0.017) and OSR1 (****C-E****, t-test p=0.035) upon $GABA_AR$ blockade.* ***F,*** *Median diffusion coefficient D values ± 25-75% IQR (for bulk population of QDs) of KCC2 show increased KCC2 diffusion upon gabazine application is completely blocked when gabazine is applied in the presence of the SPAK/OSR1 inhibitor closantel. For each condition n= 405 QDs, 4 cultures. Ctrl (white), Gbz (black), closantel (light gray), closantel+Gbz (dark gray), Ctrl vs Gbz p<0.001, closantel vs closantel*

+ Gbz p=0.55. ***G,*** *Median diffusion coefficients ± 25-75% IQR of KCC2 (for bulk population of QDs) in neurons expressing kinase-dead WNK1 (WNK1-KD, light gray) or constitutively-active WNK1 (WNK1-CA, pattern) vs control plasmid (white). For each condition n= 322 QDs, 5 cultures. Ctrl vs WNK1-KD p=0.234, Ctrl vs WNK1-CA p<0.001.* ***H****, WNK1 suppression by shRNA (shWNK1) and over-expression of WNK1-KD abolished the gabazine-mediated increase in KCC2 diffusion in neurons expressing shMock. For each condition n= 322 QDs, 5 cultures. shMock (white), shMock+Gbz (black); shWNK1 (black stripe), shWNK1+Gbz (white stripe). shMock vs shMock+Gbz p<0.001; shWNK1 vs shWNK1+Gbz p=0.812; WNK1-KD vs WNK1-KD+Gbz p=0.167. In all F-H graphs, the KS test was used for data comparison.* ***F-H****, D in* $\mu m^2 s^{-1}$.

We examined the contribution of WNK1 to the $GABA_A$R-dependent regulation of KCC2 diffusion. Since WNK kinases are activated by auto-phosphorylation of S382 [27], we first tested whether $GABA_A$R blockade induces WNK1 autophosphorylation. Application of gabazine increased WNK1 S382 phosphorylation 1.5-fold, indicating WNK1 activation upon $GABA_A$R blockade (Figure 5C-D). WNK1 stimulates KCC2 phosphorylation via the SPAK/OSR1 kinases [27]. Consistent with WNK1 activation, we found that gabazine application also increased SPAK S373 and OSR1 S325 phosphorylation (Figure 5C-E). Gabazine-induced SPAK S373 and OSR1 S325 phosphorylation could be inhibited by addition of the SPAK/OSR1 inhibitor closantel [29] (Figure S4). In contrast, and consistent with the upstream position of WNK1 in the WNK1-SPAK-KCC2 signaling pathway, closantel had no effect on WNK1 S382 phosphorylation (Figure S4). Given the expression of WNK3 in mature hippocampal neurons (Figure 5A-B), we tested its involvement in the $GABA_A$R-dependent regulation of KCC2 diffusion by over-expressing shRNAs that reduced WNK3 expression by ~80% (Figure S5). WNK3 suppression did not abolish the gabazine-mediated increase in KCC2 diffusion (Figure S5). These results indicate WNK1 is the predominant WNK kinase involved in the $GABA_A$R-dependent regulation of KCC2 diffusion. Next, we assessed the contribution of WNK1/SPAK/OSR1 signaling to KCC2 diffusion by closantel application or over-expression of kinase-dead WNK1 (WNK1-KD) or constitutively-active WNK1 (WNK1-CA) [17]. Inhibition of SPAK/OSR1 with closantel suppressed the gabazine-induced increase in KCC2 mobility (Figure 5F; Table S3). These results demonstrate that the SPAK/OSR1 kinases are essential for the $GABA_A$R-dependent regulation of KCC2 lateral diffusion. Under basal activity, over-expression of WNK1-KD did not influence KCC2 diffusion (Figure 5G; Table S3). In contrast, WNK1-CA significantly enhanced KCC2 diffusion (Figure 5G; Table S3), consistent with previous work showing reduced membrane stability of KCC2 upon WNK1 phosphorylation [17]. We also tested the involvement of WNK1 in the $GABA_A$R-dependent regulation of KCC2 mobility. shRNA-mediated WNK1 knockdown or WNK1-KD over-expression suppressed the gabazine-induced increase in KCC2 mobility (Figure 5H; Table S3). Collectively, these results implicate the activity of the WNK1 and SPAK/OSR1 kinases in the $GABA_A$R-dependent regulation of KCC2 lateral diffusion.

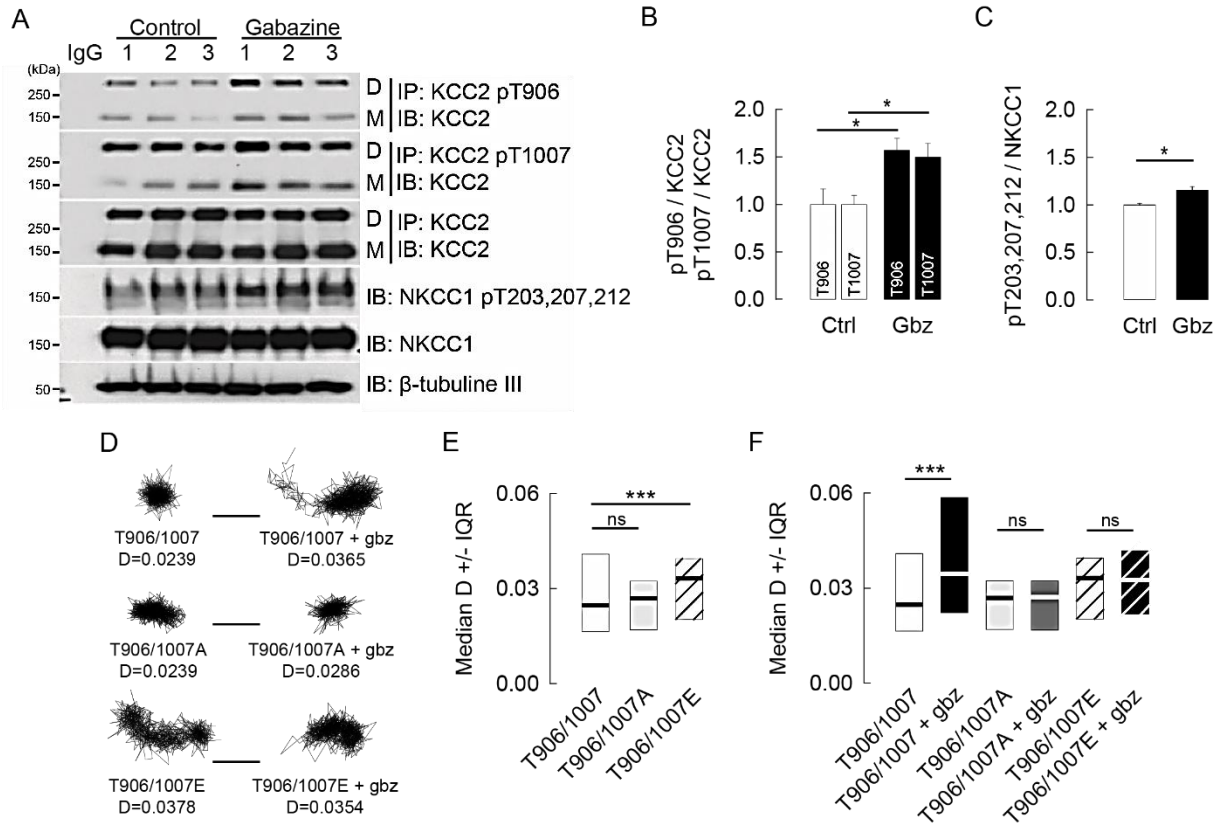

***Figure 6 GABA$_A$R-dependent regulation of KCC2 membrane dynamics is dependent on KCC2 phospohrylation of T906/T1007. A-C**, Western Blot (**A**) and quantification (mean ± s.e.m., three independent experiments 1-3) of KCC2 T906/T1007 (**B**) and NKCC1 T203/T207/T212 (**C**) phosphorylation in control (white) and gabazine (black) conditions showing increased phosphorylation of KCC2 (t-test T906: p=0.050; T1007: p=0.046) and NKCC1 T203/T207/T212 (t-test p=0.020) upon GABA$_A$R blockade. **D**, Examples of KCC2-T906/T1007, KCC2-T906/T1007A and T906/T1007E trajectories in control vs gabazine conditions. Scale bars, 0.5 µm. **E,** Median QD diffusion coefficients D values ± 25-75% IQR (for bulk population of QDs) of KCC2-T906/T1007 (white), KCC2-T906/T1007A (gray), and KCC2-T906/T1007E (black stripe) in resting condition show comparable D values of KCC2-T906/T1007 and KCC2-T906/T1007A transporters. In contrast, the phospho-mimetic KCC2-T906/T1007E was faster than KCC2-T906/T1007. T906/T1007 197 QDs, T906/T1007A 238 QDs, T906/T1007E 241 QDs, 3 cultures ; T906/T1007 vs T906/T1007A p=0.932, T906/T1007 vs T906/T1007E p<0.001. **F**, Median D (for bulk population of QDs) of KCC2-T906/T1007, KCC2-T906/T1007A, and KCC2-T906/T1007E in absence or presence of gabazine. Note that gabazine selectively reduced diffusion constraints of KCC2-T906/T1007 but not of KCC2-T906/T1007A and KCC2-T906/T1007E. T906/T1007 (white) n= 197 QDs, T906/T1007+Gbz (black) n= 197 QDs, T906/T1007A (light gray) n= 238 QDs, T906/T1007A+Gbz (dark gray) n= 238 QDs, T906/T1007E (black stripe) n= 241 QDs, T906/T1007E+Gbz (white stripe) n= 241 QDs, 3 cultures ; T906/T1007 vs T906/T1007+Gbz p<0.001, T906/T1007A vs T906/T1007A+Gbz p=0.916, T906/T1007E vs T906/T1007E+Gbz p=0.648. **E-F**, unless mentioned the KS test was used for all data comparison; D in µm^{2}s^{-1}.*

WNK activity is required for KCC2 T906 and T1007 phosphorylation, which inhibits transporter activity [17,26]. Consistent with increased WNK activation upon GABA$_A$R blockade, gabazine application increased KCC2 T906/T1007 phosphorylation (Figure 6A-B). Interestingly, WNK kinases not only promote KCC2 T906/T1007 but also NKCC1 T203/T207/T212 phosphorylation [30]; this inhibits KCC2 but activates NKCC1-dependent Cl^- transport, respectively [28]. Consistent with this dual modulation of Cl^-

transport by WNK, $GABA_AR$ blockade also induced NKCC1 T203/T207/T212 phosphorylation (Figure 6 A, C). This gabazine-induced phosphorylation of KCC2 and NKCC1 was SPAK/OSR1-dependent, as it was inhibited by closantel (Figure S4). In addition to KCC2, KCC3, and to a lesser extent KCC1 and KCC4, are expressed in hippocampal neurons [31]. We therefore assayed whether KCC3 is phosphorylated following gabazine blockade. Our results show that KCC3 is also phosphorylated upon gabazine application in a SPAK/OSR1-dependent manner (Figure S6). KCC2 may be immuno-precipitated using a phospho-specific KCC2 pT906 antibody that recognizes a phospho-residue highly homologous to other KCCs [27]. We used this antibody to control whether the detection of increased KCC2 T906 phosphorylation is due to a contribution of other KCCs. This was not the case, since KCC1 and KCC4 were not retained after KCC2 T906 immunoprecipitation (Figure S6).

To test the involvement of KCC2 T906/T1007 phosphorylation in the gabazine-induced regulation of KCC2 diffusion, we expressed KCC2 constructs harboring mutation of T906 and T1007 to either glutamate (E) (T906/T1007E) or alanine (T906/T1007A) to mimic the KCC2 T906 and T1007 phosphorylated or dephosphorylated states, respectively [17]. Under basal activity, the diffusion of KCC2 T906/T1007E was enhanced 1.3-fold compared to WT KCC2 (Figure 6D-E; Table S3). In contrast, the mobility of the KCC2 T906/T1007A did not differ significantly from that of WT KCC2 (Figure 6D-E; Table S3). These results indicate that the majority of membrane KCC2 in mature neurons is dephosphorylated on T906/T1007 under basal activity conditions, consistent with previous results [17,26]. Importantly, KCC2 T906/T1007A prevented the gabazine-induced increase in KCC2 lateral diffusion (Figure 6D, F; Table S3). Furthermore, gabazine did not further increase the diffusion of the T906/T1007E transporter (Figure 6D, F; Table S3). Thus, $GABA_AR$-dependent regulation of KCC2 diffusion involves phosphorylation of its T906/T1007 residues.

Functional impact of KCC2 regulation by $GABA_AR$ inhibition

What is the functional impact of $GABA_AR$-mediated regulation of KCC2 diffusion? We previously demonstrated that the regulation of KCC2 lateral diffusion by increased excitation allows for a rapid regulation of the transporter clustering and activity [10].

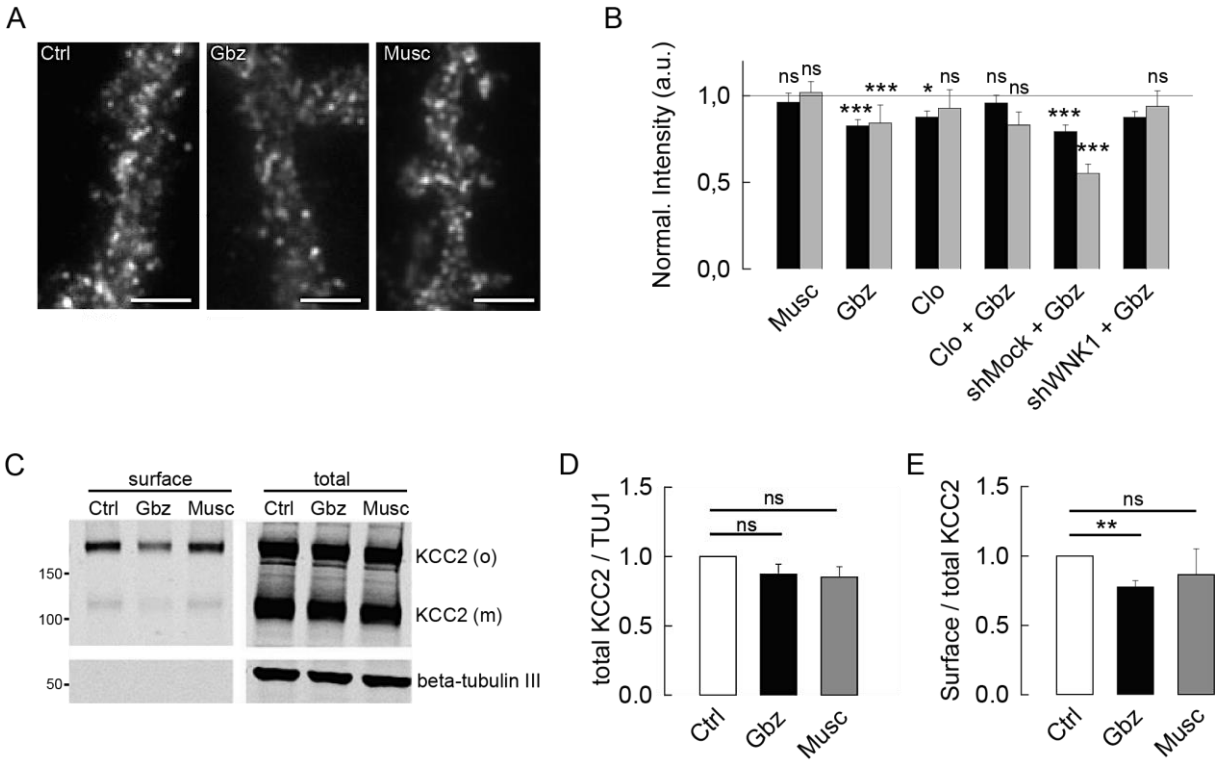

Figure 7. Regulation of KCC2 membrane clustering and stability by GABA$_A$R-mediated inhibition. A*, Flag surface staining in hippocampal neurons (DIV 21-23) expressing recombinant KCC2–Flag in absence (Ctrl) or presence of gabazine (Gbz), or muscimol (Musc) for 30 min. Scale bars, 10 µm. Note the loss of KCC2 immunoreactivity after 30 min exposure to gabazine but not muscimol.* ***B****, Quantifications of KCC2 pixel (black) and cluster (gray) intensity in each experimental condition. Note muscimol had no effect while gabazine decreased KCC2 cluster and pixel intensity. Closantel treatment and WNK1 shRNA (shWNK1) overexpression suppressed the gabazine-induced reduction in KCC2 clustering as compared to control and shMock treated neurons, respectively. Values were normalized to the corresponding control values. The MW test was used for data comparison. Muscimol experiment: Ctrl n= 62 cells, Musc n= 58 cells, cluster intensity p=0.823, pixel intensity p=0.470; 4 cultures. Gabazine and closantel experiment: Ctrl n= 77 cells, Gbz n= 83 cells, cluster intensity p=0.006, pixel intensity p<0.001; Closantel n= 65 cells, cluster intensity p=0.05, pixel intensity p=0.016; Closantel + gabazine n= 57 cells, cluster intensity p=0.441, pixel intensity p=0.448; 4 cultures. ShWNK1 experiment: shMock, n= 48 cells; shMock + gabazine n= 50 cells, cluster intensity p<0.001, pixel intensity p<0.001; shWNK1 n= 40 cells, cluster intensity p=0.38, pixel intensity p=0.957; shWNK1 + gabazine n= 53 cells, cluster intensity p=0.249, pixel intensity p=0.041; 3 cultures.* ***C****, Biotinylated surface fraction and total protein expression of KCC2 after 30-min of gabazine or muscimol treatments.* ***D****, No change of total KCC2 protein level between control (white) and gabazine (black; t test p=0.126) or muscimol (gray; t test p=0.093) conditions (normalized to beta-tubulin III [TUJ1]). N=4.* ***E****, Quantification of the ratio of the surface pool of KCC2 over the total pool of KCC2 in control (white), gabazine (black) and muscimol (gray) conditions showing reduction of surface KCC2 after gabazine (t test p=0.003) but not muscimol (t test p=0.495) treatment (n=4 experiments).*

We therefore examined whether changes in GABA$_A$R-dependent inhibition also resulted in altered KCC2 clustering in hippocampal neurons. In control conditions, KCC2-Flag formed numerous clusters along the dendrites of transfected neurons (Figure 7A). Neither muscimol nor gabazine affected the density of these clusters (Figure 7A, Figure S7). Muscimol did not affect the mean

fluorescence intensity (Figure 7B), or the mean fluorescence intensity per pixel within clusters (Figure 7B), indicating no detectable impact on KCC2 clustering. In contrast, gabazine application reduced membrane-associated KCC2-Flag immunoreactivity (Figure 7A-B). A 30 min exposure to gabazine reduced by 1.2-fold the mean fluorescence intensity of clusters and the mean fluorescence intensity per pixel within clusters (Figure 7B) as compared with untreated cells. Therefore, gabazine-mediated increase in KCC2 membrane dynamics is accompanied by a rapid reduction in the clustering of the transporter. Inhibition of SPAK/OSR1 with closantel (Figure 7B), shRNA knockdown of WNK1 (Figure 7B), or shRNA knockdown of WNK3 (Figure S5) suppressed the gabazine-mediated reduction in the mean fluorescence intensity of clusters and the mean fluorescence intensity per pixel within clusters. These data implicate the WNK1-WNK3/SPAK/OSR1 signaling in the gabazine-dependent regulation of KCC2 clustering.

KCC2 cotransporters that escaped clusters upon gabazine treatment may remain at the cell surface and diffuse freely in the membrane or undergo clathrin-dependent endocytosis. Surface biotinylation experiments revealed that gabazine reduced cell surface KCC2 to 78 ± 9% of control without significantly changing the total protein level of the transporter (Figure 7C-E). In contrast, muscimol did not modify KCC2 surface and total protein level (Figure 7C-E), indicating it does not significantly change the internalization of KCC2. Therefore, gabazine increases the membrane turnover of KCC2, likely due to increased diffusion and cluster dispersal.

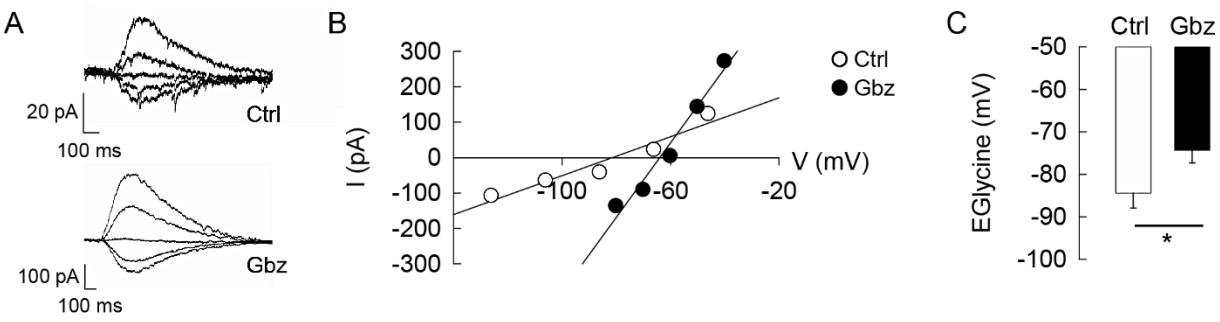

***Figure 8 Loss of KCC2 upon $GABA_AR$ blockade correlates with increased $[Cl^-]_i$. A-B**, Typical gramicidin-perforated patch-clamp recordings of glycine receptor mediated currents induced by short (100 ms) puff of glycine at different membrane potentials in control conditions (**A** upper trace; **B** white) or upon 30 min gabazine application (**A** lower trace; **B** black). $E_{Glycine}$ was determined as the intercept of the I-V curve with the x-axis. **C**, Gabazine application induced $E_{Glycine}$ depolarization (t test p=0.038) indicating increased $[Cl^-]_i$. Data represent the mean ± s.e.m. of 13 cells (Ctrl) and 12 cells (Gbz).*

Reduced expression of membrane-inserted KCC2 is predicted to reduce Cl^- export and impact $GABA_AR$-mediated transmission. In order to evaluate the impact of $GABA_AR$ blockade on $[Cl^-]_i$, we compared the reversal potential of GlyR currents upon application of the $GABA_AR$ antagonist gabazine

in neurons transfected with a recombinant glycine receptor α1 subunit [32]. We found that KCC2 dispersion upon gabazine was accompanied by significant depolarization of the reversal potential of glycine-evoked currents, reflecting an increase in $[Cl^-]_i$ (Figure 8 A-C). This gabazine-induced increase in $[Cl^-]_i$ is reminiscent of the reduced FRET ratio of SuperClomeleon observed in neurons exposed for 50 min to the drug (Figure 4B). Therefore, blocking $GABA_AR$-mediated inhibition results in reduced KCC2-dependent Cl^- extrusion due to increased lateral diffusion, and reduced membrane clustering and membrane expression of the transporter.

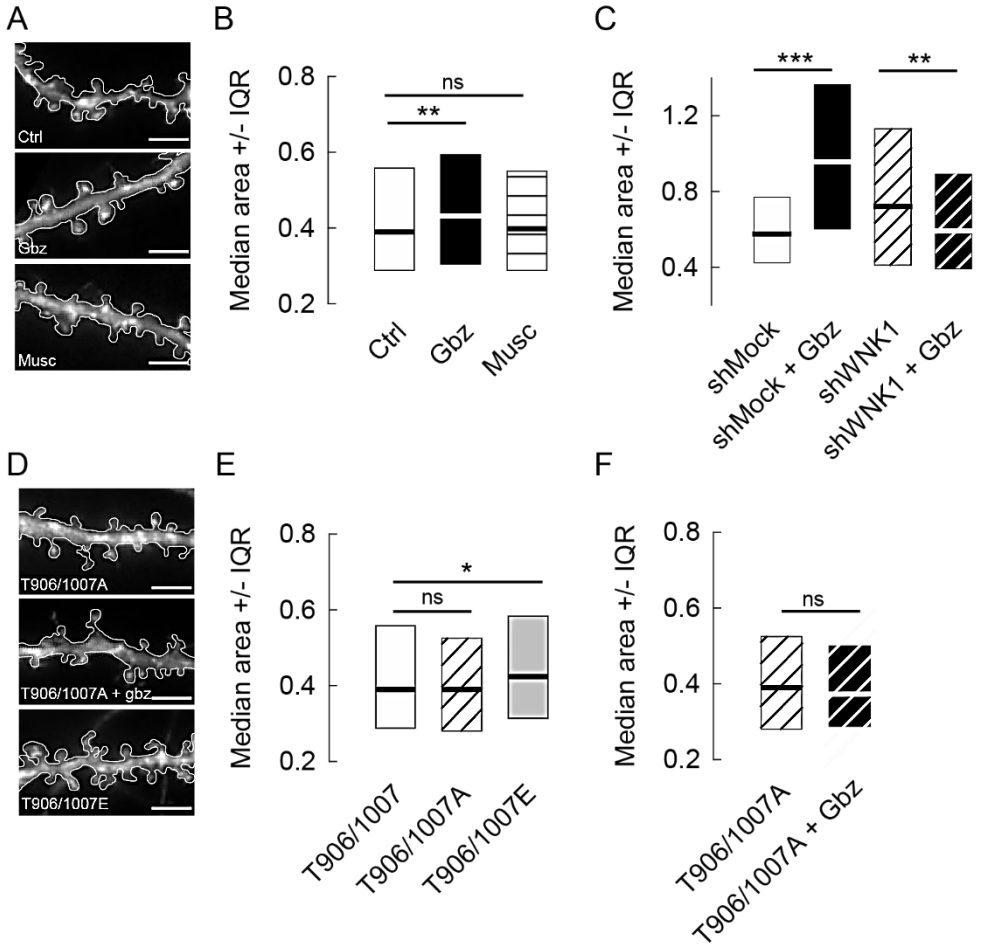

***Figure 9. KCC2-dependent spine volume regulation is modulated by $GABA_AR$-mediated inhibition. A**, Secondary dendrites of eGFP expressing neurons in control conditions or upon application of gabazine or muscimol. Scale bars, 10 µm. **B,** Median values ± 25-75% IQR of spine head area from eGFP expressing neurons in control (white), gabazine (black) or muscimol (pattern). Ctrl n= 1301 spines; Gbz n= 1082 spines; Musc n= 1014 spines, 3 cultures; Ctrl vs Gbz p=0.005, Ctrl vs Musc p=0.978. **C,** Median values ± 25-75% IQR of spine head area from shMock or shWNK1 overexpressing neurons in control (white and black stripes) or gabazine (black and white stripes) conditions, respectively. Note the increase in spine head area upon application of gabazine for shMock (p<0.001) transfected cells and the decrease (p=0.009) in spine head volume for shWNK1 overexpressing neurons. ShMock n= 260 spines; shMock + Gbz n= 232 spines; shWNK1 n= 95 spines, shWNK1 + Gbz n= 166 spines, 2 cultures. **D**, Same as in **A**, for neurons expressing eGFP and KCC2-Flag or KCC2-Flag mutated on T 906/1007 to A (T906/T1007A) or glutamate (T906/T1007E). Scale bars, 10 µm. **E**, Overexpression of T906/T1007E mutant (gray) but not T906/T1007A mutant (fine stripe) increased spine head volume compared to WT (white). **F**, No change in spine head volume could be observed upon gabazine application in cells*

expressing KCC2-Flag T906/T1007A (wide stripe). ***E-F****, T906/T1007 n= 1301 spines, T906/T1007A n= 1224 spines, T906/T1007E n= 983 spines, T906/T1007A+Gbz n= 1093 spines, 3 cultures ; T906/T1007 vs T906/T1007E p=0.014, T906/T1007 vs T906/T1007A p=0.099, T906/T1007A vs T906/T1007A+Gbz p=0.06.* ***B, C, E, F*** *Spine head area in µm². The KS test was used for all data comparison.*

In addition to regulating intraneuronal $[Cl^-]_i$, KCC2 function also controls dendritic spine head volume in mature hippocampal neurons [3]. Thus, KCC2 suppression or chronic pharmacological blockade of its ion transport activity increases spine head diameter [3,4]. We therefore tested whether $GABA_AR$-dependent regulation of KCC2 dynamics and membrane stability may also alter dendritic spines in mature neurons. Up to 30 min of muscimol application had no significant effect on spine head area (Figure 9A-B). Gabazine however caused a 1.4-fold increase in spine head area (Figure 9A-B), consistent with a reduced expression and/or function of the transporter in spines. This gabazine-mediated increase in spine head area required WNK1 but not WNK3 activity, since it was blocked by shRNAs targeting WNK1 (Figure 9C) but not WNK3 (Figure S5). Expression of KCC2 T906/T1007A did not affect dendritic spine morphology (Figure 9D-E). In contrast, spine head size was increased by 1.3-fold upon overexpression of the phospho-mimicking KCC2-T906/T1007E, as compared to WT KCC2 (Figure 9D-E). These results support the notion that most KCC2 is dephosphorylated at T906/T1007 under basal activity conditions in mature neurons and that KCC2 T906/T1007 phosphorylation increases transporter turn-over, thereby leading to spine swelling. Moreover, expression of KCC2-T906/T1007A completely blocked gabazine-induced spine head swelling (Figure 9F). Collectively, these results demonstrate that transient blockade of $GABA_AR$-mediated transmission alters KCC2 surface expression and ion transport function via effects on WNK1 kinase-dependent KCC2 T906/T1007 phosphorylation, thereby affecting both GABA signaling and dendritic spine morphology.

We next asked whether $GABA_AR$-dependent regulation of KCC2 and NKCC1 may occur under physiological and/or pathological conditions. We first tested whether the gabazine-mediated regulation of KCC2 occurred in cultured hippocampal neurons in the absence of sodium channel and glutamate receptor blockers. In such conditions, acute application of gabazine still reduced by ~1.2-fold the mean fluorescence intensity of clusters and the mean fluorescence intensity per pixel within clusters (Figure S8) as compared with untreated cells. Furthermore, this effect was blocked by closantel (Figure S8), thus involving the WNK/SPAK signaling pathway. These results demonstrate that $GABA_AR$-dependent regulation of KCC2 operates under physiological conditions with intact neuronal and synaptic activity.

We then explored the impact of $GABA_AR$ activation in the absence of Na^+ channel and glutamate receptor blockers on the regulation of KCC2 membrane stability in the intact hippocampal network. For this purpose, we performed surface biotinylation experiments in acute hippocampal slices prepared from 5-7 week old C57bl6 mice treated with vehicle or muscimol for 30 min at 35°C.

We found that acute muscimol treatment increased by 1.2 and 1.3 fold the surface expression level of KCC2 monomers and oligomers, respectively (Figure S8). Therefore, we conclude that $GABA_AR$ activation stabilizes KCC2 at the neuronal surface in the intact hippocampal network.

Next, we explored whether the WNK1/SPAK/OSR1 signaling pathway could be activated, and KCC2/NKCC1 threonine phosphoregulation observed, *in vivo*. The activity of the WNK1/SPAK/OSR signaling pathway is elevated in the embryonic and neonatal first postnatal week and significantly decreases with brain maturation into adulthood [17]. We therefore asked whether this pathway could be "reactivated" in the mature brain under pathological conditions. Using subcutaneous injection of the $GABA_AR$ antagonist pentylenetetrazole (PTZ), a commonly used animal model to induce seizures [33], we observed massive changes in both WNK1 and SPAK/OSR1 phosphorylation/activation (by 169-283% and 271-169% respectively) as well as KCC2 T906, KCC2 T1007 and NKCC1 T203/T207/T212 phosphorylation (by 118-318%, 232-203% and 319-307%, Figure 10A-B) in the cortex and hippocampus. These data demonstrate the WNK1/SPAK/OSR1 signaling pathway can be activated in the adult brain in conditions with impaired $GABA_AR$ activity to simultaneously promote the stimulatory and inhibitory phosphorylation of NKCC1 and KCC2, respectively.

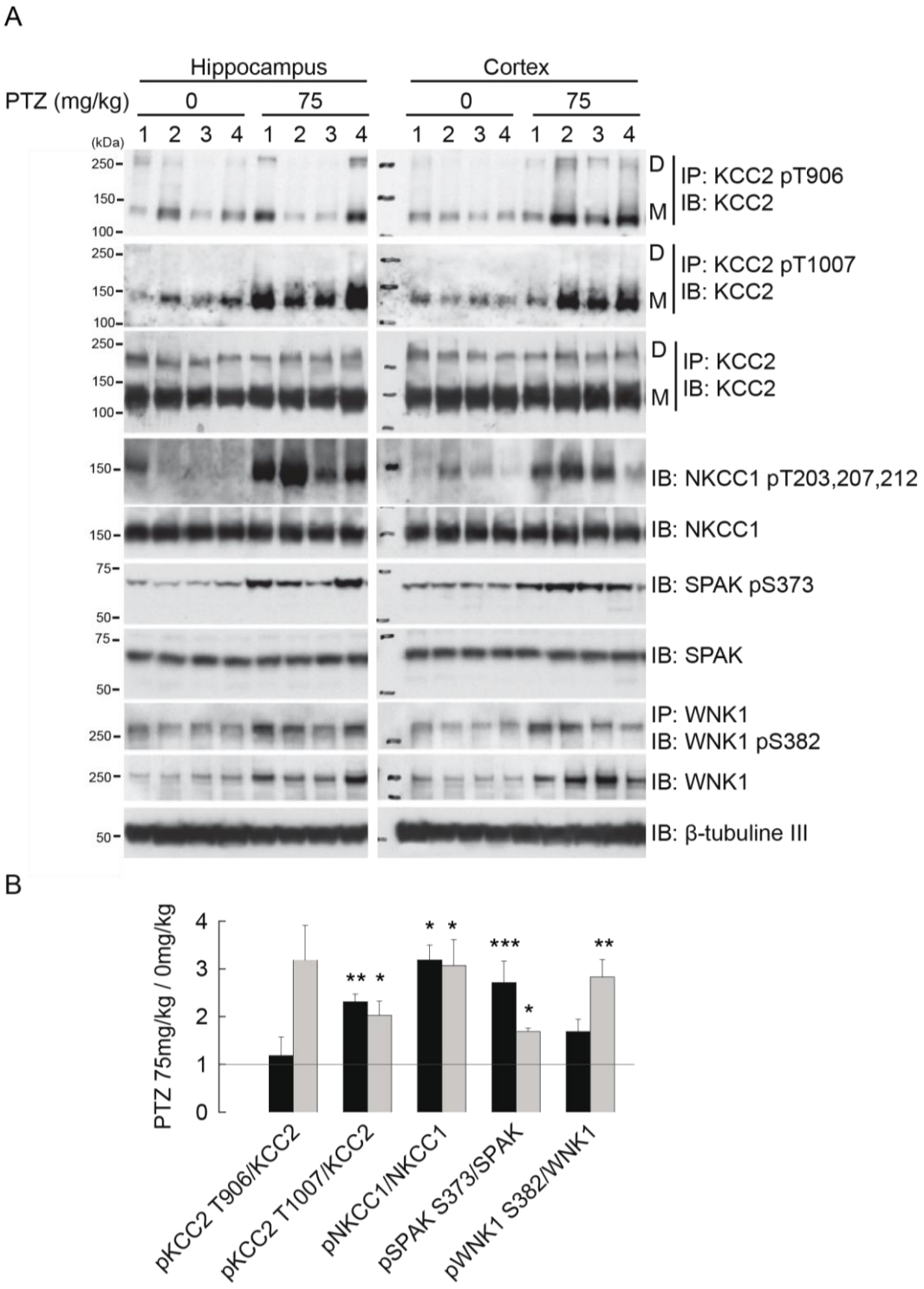

Figure 10. GABA$_A$R-dependent regulation of KCC2 in vivo. A-B, *Activation of the WNK/SPAK signaling pathway in the adult epileptic brain. Western Blot (**A**) and quantification (**B**, mean ± s.e.m., four independent experiments 1-4) showing seizure induction with the GABA$_A$R antagonist pentylenetetrazole (PTZ, 75 mg/kg) led to phosphorylation/activation of WNK1 S382 (t test p= 0.003 and p=0.071) and SPAK S373 (t test p<0.001 and p=0.012) respectively in the cortex (gray) and hippocampus (black) of adult mice. This was accompanied by a net increase in the phosphorylation of NKCC1 T203/T207/T212 (MW test p=0.029) and KCC2T1007 (t test p=0.021 and p=0.002) but not KCC2 T906 (MW test p=0.057 and p=0.686) in the cortex and hippocampus respectively.*

Discussion

Whereas KCC2 is known to be rapidly down-regulated by enhanced neuronal activity and glutamatergic neurotransmission in mature neurons [10,12,14], only one study so far had tested the effect of GABA signaling on KCC2 post-translational regulation. This study showed that increased GABAergic transmission leads to KCC2 downregulation [34]. However, this study was carried out in immature neurons with depolarizing $GABA_AR$-mediated responses and associated activation of VDCC and intracellular Ca^{2+} signaling. In the present study however, we asked whether KCC2 may be regulated by $GABA_AR$-mediated inhibition in mature neurons. Our results reveal a rapid regulation of KCC2 membrane trafficking and transporter function by $GABA_AR$-dependent inhibition. KCC2 lateral diffusion, membrane clustering, and stability are regulated by $GABA_AR$- but not $GABA_BR$- mediated signaling. $GABA_AR$ activation leads to KCC2 confinement, while $GABA_AR$ blockade increases KCC2 membrane dynamics, reducing its membrane aggregation, stability and activity. Our data uncover a novel homeostatic mechanism that may serve for "auto-tuning" of GABAergic signalling via rapid regulation of KCC2-mediated Cl^- export. Our work also demonstrates that Cl^- ions may act as genuine intracellular second messenger in neurons to modulate KCC2 phosphorylation through the WNK signaling pathway.

Different subpopulations of KCC2 exist in the plasma membrane, including freely-moving transporters that are diffusely distributed at the cell surface and slower confined transporters in membrane clusters. Initial data suggesting that clustering may be directly involved in KCC2 function came from the work of Watanabe et al. [35], who showed that KCC2 tyrosine mutation induced cluster loss. This cluster loss was accompanied by a significant reduction in the transporter activity without any significant change in its membrane stability. Our results of activity-dependent regulation of KCC2 favour the hypothesis that rapid changes in KCC2 membrane dynamics and clustering may directly impact KCC2 membrane stability and neuronal Cl^- homeostasis. We have shown that an increase in glutamate receptor mediated excitation [10] or a blockade of GABAergic transmission both lead to an increase in KCC2 lateral diffusion. In both cases, increased KCC2 diffusion was correlated with a change in KCC2 phosphorylation status (S940 dephosphorylation upon increased excitation; T906/T1007 phosphorylation upon $GABA_AR$ blockade). Changes in the diffusion behavior of KCC2 upon phosphorylation are thereby one of the first mechanisms regulating its membrane expression. A working model is that T906/T1007 phosphorylation as well as S940 [10] dephosphorylation may induce conformational changes [36] leading to altered interaction with scaffolding molecules or oligomerization of the transporter that in turn could promote cluster dispersion. Freely-moving transporters may then become available for internalization.

Blockade of $GABA_AR$-mediated transmission and increased neuronal activity both lead to an increase in KCC2 lateral diffusion. While neuronal excitation modulates KCC2 diffusion and membrane stability via Ca^{2+}-dependent dephosphorylation of KCC2 S940 [10,12], we show that neuronal inhibition regulates KCC2 membrane dynamics independently of Ca^{2+} and S940. Instead, Cl^--dependent changes in WNK1 kinase activity link $GABA_AR$ signaling to KCC2 T906/T1007 phosphorylation (Figure 11).

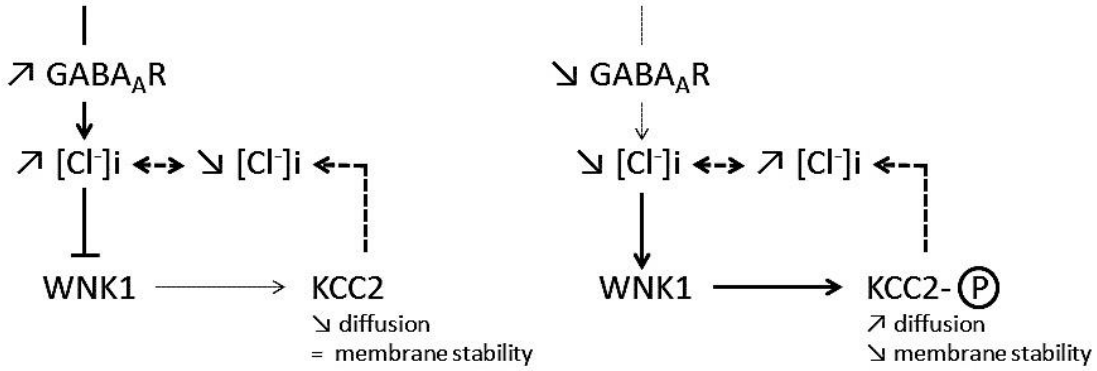

Figure 11. Homeostatic control of intracellular chloride concentration via WNK1-dependent phosphorylation of KCC2. *Upon $GABA_AR$ activation, WNK1 gets inhibited by intracellular chloride leading to stabilization of KCC2 in the membrane and readjustment of $[Cl^-]_i$. In conditions of reduced GABAAR activity, lowering of $[Cl^-]_i$ activates WNK1 and leads to removal of KCC2 from the membrane and elevation of $[Cl^-]_i$.*

Although WNK1 is activated by low $[Cl^-]_i$, it is however more active in immature neurons in which $[Cl^-]_i$ is higher than in mature neurons [17,26,37]. This apparent paradox may reflect the expression pattern of WNK3, which is inversely correlated to that of KCC2 during neuronal development [38]. WNK3 shows weak sensitivity to chloride and is able to activate WNK1 [25,39]. Strong expression of WNK3 in immature neurons and subsequent WNK1 activation may then render WNK1 insensitive to $[Cl]_i$ in immature neurons. Reduced expression of WNK3 in mature neurons would then enable regulation of WNK1 activity by changes in $[Cl]_i$.

Activation of GABAergic synapses leads to changes in $[Cl^-]_i$ [40] . Changes in the activity of GABAergic synapses could hence rapidly alter KCC2 membrane expression through WNK1-dependent KCC2 phosphorylation. Changes in $GABA_AR$ activation and a subsequent increase in KCC2 confinement would maintain KCC2-mediated Cl^- extrusion and help counteract Cl^- influx through $GABA_ARs$.

We proposed gabazine lowers $[Cl]_i$ by decreasing Cl^- influx through $GABA_AR$, and this reduces KCC2 activity via WNK1-dependent regulation of transporter membrane stability. However, we showed an increase rather than a decrease in $[Cl]_i$ (Figure 4B, 8) after neuronal exposure to gabazine. This may be due to the fact that changes in $[Cl]_i$ upon gabazine application occur on different time scales. Although SuperClomeleon imaging could not detect an immediate drop in $[Cl]_i$ upon gabazine

application, we observed a delayed increase in $[Cl]_i$ that is consistent with our electrophysiological recordings. We propose that gabazine application leads to a transient drop in $[Cl-]_i$ that in turn activates the WNK/SPAK/OSR signaling pathway leading to KCC2 phosphorylation on T906 and T1007. This effect is likely to persist well beyond the initial drop in $[Cl]_i$ as it will be reversed through the recruitment of PP1 phosphatase [41,42]. Persistent KCC2 inactivation by threonine phosphorylation would then be expected to translate into a rise in $[Cl-]_i$, consistent with our electrophysiological and chloride imaging data.

$GABA_AR$-dependent regulation of KCC2 may then not only allow neurons to rapidly react to changes in $[Cl^-]_i$ but also permit the neuron to conserve energy. Indeed, for every Cl^- ion extruded by KCC2, the transporter uses the energy of the electrochemical gradient of one K^+ ion. The Na^+/K^+ ATPase that generates the K^+ gradient required for KCC2 function is a main consumer of energy in the brain [43–45]. Even though the highest energetic cost of the Na^+/K^+-ATPase will be used to restore the resting potential of the cell after neuronal firing [44,46], maintaining low $[Cl^-]_i$ is associated with high metabolic cost [31]. Under physiological conditions, rapid redistribution of KCC2 in the membrane might enable neurons to conserve energy by keeping surface KCC2 molecules at the minimum required density to keep E_{GABA} hyperpolarized. Diffusion-trap of KCC2 is hence a very rapid mechanism to adjust the number of KCC2 molecules in the membrane to ensure functional Cl^- homeostasis in neurons.

Finally, our biochemical data indicate that modulation of $GABA_AR$ activity translates not only into a change of KCC2 but also NKCC1 phosphorylation. Given the opposite effect of phosphorylation on KCC2 and NKCC1 activity (activating for NKCC1, inhibitory for KCC2), regulation of the WNK-SPAK pathway is a very efficient mechanism to adjust neuronal Cl^- homeostasis. Impairment of this pathway has been linked to dysregulated Cl^- homeostasis in schizophrenia, autism, and epilepsy [47–50]. We further demonstrate here that this signaling pathway is rapidly and massively activated in an acute epilepsy model. This pathway could therefore be an attractive target to restore Cl^- homeostasis for therapeutic benefit.

Material and Methods

Neuronal culture

Primary cultures of hippocampal neurons were prepared as previously described 10 with some modifications of the protocol. Briefly, hippocampi were dissected from embryonic day 18 or 19 Sprague-Dawley rats of either sex. Tissue was then trypsinized (0.25% v/v), and mechanically dissociated in 1x HBSS (Invitrogen, Cergy Pontoise, France) containing 10 mM HEPES (Invitrogen). Neurons were plated at a density of 120×10^3 cells/ml onto 18-mm diameter glass coverslips (Assistent, Winigor, Germany) pre-coated with 50 µg/ml poly-D,L-ornithine (Sigma-Aldrich, Lyon, France) in

plating medium composed of Minimum Essential Medium (MEM, Sigma) supplemented with horse serum (10% v/v, Invitrogen), L-glutamine (2 mM) and Na^+ pyruvate (1 mM) (Invitrogen). After attachment for 3-4 hours, cells were incubated in culture medium that consists of Neurobasal medium supplemented with B27 (1X), L-glutamine (2 mM), and antibiotics (penicillin 200 units/ml, streptomycin, 200 µg/ml) (Invitrogen) for up to 4 weeks at 37°C in a 5% CO2 humidified incubator. Each week, one fifth of the culture medium volume was renewed.

Neuro2a culture

Neuro2a cells were obtained from DSMZ (ACC-148). Their origin was confirmed by COI DNA barcoding and they have been tested for mycoplasma contamination by DAPI, microbiological culture, RNA hybridization and PCR assays. Neuro2a cells were grown in DMEM GlutaMAX (Invitrogen) supplemented with 1 g/L glucose and 10% fetal bovine serum.

DNA constructs

The KCC2-Flag construct was generated by insertion of three Flag sequences in the second predicted extracellular loop of KCC2 [10]. This recombinant Flag-tagged KCC2 transporter was shown to retain normal traffic and function in transfected hippocampal neurons [10]. KCC2-Flag constructs with Threonine residues 906 and 1007 mutated to glutamate (T906/1007E) or alanine (T906/1007A) were generated by Genscript (Piscataway, USA). Threonine nucleotide sequence was changed to GCA for alanine substitution and to GAG for glutamate substitution. cDNA from E18.5 rat brain was used as a template for the amplification of WNK3 coding transcript. Primers were chosen to amplify three overlapping fragments using Phusion DNA polymerase (Thermofisher Scientific). To obtain N-terminal HA-tagged WNK3, the purified PCR fragments were directionally assembled to a pCAGGS-HA linearized plasmid using In-Fusion HD cloning kit (Clontech) following manufacturer's guidelines. ShRNAs against rat WNK3 were designed and cloned into pGeneclipU1(GFP) (Promega) following manufacturer's protocol. The following target sequences were used: shRNA #1: GAACCTTAAAGACGTACTTAA and shRNA #2: GAACGCCTTCGAGCAACTAAA. All the constructs were sequence-verified by Beckman Coulter Genomics. The following constructs were also used: KCC2-Flag-S940D [10], eGFP (Clontech), glycine receptor α1 subunit [32] (kindly provided by A. Triller, ENS, Paris), gephyrin-mRFP [51] (kindly provided by A. Triller, ENS, Paris), homer1c-GFP [52] (kindly provided by D. Choquet, IIN, Bordeaux, France), WNK1 with "kinase-dead, dominant-negative domain" (WNK1-KD, D368A), "constitutively active" WNK1 (WNK1-CA, S382E), shRNA against rat WNK1 mRNA (shWNK1), a scrambled shRNA sequence "shMock" [17] (kindly provided by I. Medina, INMED, Marseille) and SuperClomeleon [22] (kindly

provided by G.J. Augustine, NTU, Singapore). All constructs were sequenced by Beckman Coulter Genomics (Hope End, Takeley, U.K).

Transfection and transduction

Neuronal transfections were carried out at DIV 13-14 using Lipofectamine 2000 (Invitrogen) or Transfectin (BioRad, Hercules, USA), according to the manufacturers' instructions (DNA:transfectin ratio 1 µg:3 µl), with 1-1.5 µg of plasmid DNA per 20 mm well. The following ratios of plasmid DNA were used in co-transfection experiments: 0.5:0.4:0.3 µg for KCC2-Flag or KCC2-Flag-T906/T1007A or KCC2-Flag-T906/T1007E or KCC2-Flag-S940D together with gephyrin-mRFP and homer1c-GFP; 0.9:0.1 µg for KCC2-Flag or KCC2-Flag-T906/T1007A or KCC2-Flag-T906/T1007E with eGFP or glycine receptor α1 subunit with eGFP; 0.5:0.5 µg for KCC2-Flag or KCC2-Flag-T906/T1007A or KCC2-Flag-T906/T1007E with shWNK1 or shMock or WNK1-KD or WNK1-CA or KCC2-Flag with SuperClomeleon or KCC2-Flag with shNT; 0.5:0.5:0.5 µg for KCC2-Flag with shWNK3 #1 and shWNK3 #2. Experiments were performed 7 to 10 days post-transfection.

Primary hippocampal cultures were infected at 14 div with an AAV1.hSyn.eNpHR3.0-eYFP.WPRE.hGH (Title = 1.6 e^{12}, Upenn Vector Core) at a multiplicity of infection (MOI) of 10. The pAAV-hSyn-eNpHR 3.0-EYFP was a gift from Karl Deisseroth (Addgene plasmid # 26972). Neurons were used 7 days after transduction.

Neuro2a cells were transfected using Transfectin (Biorad) according to the manufacturers' instructions (DNA:transfectin ratio 1 µg:3 µl), with 1-1.5 µg of plasmid DNA per 60 mm well. Cells were transfected with 1ug of SuperClomeleon; 0.5:0.5 µg of KCC2-Flag with shNT or shWNK3 #1 or shWNK3 #2; 0.5:0.5:0.5 µg of KCC2-Flag with shWNK3 #1 and shWNK3 #2. Protein expression was allowed in growth medium for 48-72 h after transfection before use.

Pharmacology

The following drugs were used: TTX (1 µM; Latoxan, Valence, France), R,S-MCPG (500 µM; Abcam, Cambridge, UK), Kynurenic acid (1 mM; Abcam), NBQX (10 µM; Tocris), R,S-APV (100 µM; Tocris), VU0240551 or VU0463271 (10 µM; Sigma), CGP52432 (20 µM; Tocris Bioscience, Lille, France), baclofen (20 µM; Tocris), gabazine (10 µM; Abcam), muscimol (10 µM; Abcam), L655,708 (50 µM; Tocris Bioscience), closantel (10 µM; Sigma), picrotoxin (100 µM; Tocris), Cadmium chloride (100 µM; Sigma). R,S-MCPG and baclofen were prepared in equimolar concentrations of NaOH; TTX in 2% citric acid (v/v); VU0240551, closantel and picrotoxin in DMSO (Sigma). Equimolar DMSO concentrations were used for control experiments in these conditions. For SPT experiments, neurons were transferred to a recording chamber, pre-incubated in presence of drugs at 31°C for 10 min in imaging

medium (see below for composition) and used within 45 min in presence of the appropriate drug for imaging. For calcium imaging in presence of TTX+KYN+MCPG+Cd^{2+}, cells were pre-incubated 5-10 min in presence of these drugs in imaging medium during the Fluo4-AM hydrolysis, and gabazine was applied after a stable fluorescence baseline was obtained. For calcium imaging in absence of TTX+KYN+MCPG+Cd^{2+}, cells were pre-incubated 5-10 min in imaging medium during the Fluo4-AM hydrolysis, and NMDA was applied after a stable fluorescence baseline was obtained. For biochemistry and immunofluorescence experiments, drugs were added directly to the culture medium for 30 min in a CO_2 incubator set at 37°C. The imaging medium consisted of phenol red-free minimal essential medium supplemented with glucose (33 mM; Sigma) and HEPES (20 mM), glutamine (2 mM), Na^+-pyruvate (1 mM), and B27 (1X) from Invitrogen. The 138mM [Cl-] extracellular solution was composed of 2 mM CaCl2, 2 mM KCl, 3 mM MgCl2, 10 mM HEPES, 20 mM Glucose, 126 mM NaCl, 15 mM Na methanesulfonate; the 0 mM [Cl-]extracellular solution was made of 1 mM CaSO4, 2 mM K methanesulfonate, 2 mM MgSO4, 10 mM HEPES, 20 mM Glucose, 144 mM Na methanesulfonate.

Live cell staining for single particle imaging

Neurons were stained as described previously [53]. Briefly, cells were incubated for 3-5 min at 37°C with primary antibodies against Flag (mouse, 1:700, Sigma, cat # F3165), washed, and incubated for 3-5 min at 37°C with biotinylated Fab secondary antibodies (goat anti-mouse: 1:700; Jackson Immunoresearch, cat # 115-067-003, West Grove, USA) in imaging medium. After washes, cells were incubated for 1 min with streptavidin-coated quantum dots (QDs) emitting at 605 nm (1 nM; Invitrogen) in borate buffer (50 mM) supplemented with sucrose (200 mM) or in PBS (1M; Invitrogen) supplemented with 10% Casein (v/v) (Sigma).

Single particle tracking and analysis

Cells were imaged as previously described [10] using an Olympus IX71 inverted microscope equipped with a 60X objective (NA 1.42; Olympus) and a Lambda DG-4 monochromator (Sutter Instrument) or a 120W Mercury lamp (X-Cite 120Q, Lumen Dynamics). Individual images of gephyrin-mRFP and homer1c-GFP, and QD real time recordings (integration time of 30 ms over 1200 consecutive frames) were acquired with an ImagEM EMCCD camera and MetaView software (Meta Imaging 7.7). Cells were imaged within 45 min following appropriate drugs pre-incubation.

QD tracking and trajectory reconstruction were performed with homemade software (Matlab; The Mathworks, Natick, MA) as described in [10,53]. One to two sub-regions of dendrites were quantified per cell. In cases of QD crossing, the trajectories were discarded from analysis. Trajectories were considered synaptic when overlapping with the synaptic mask of gephyrin-mRFP or homer1c-GFP

clusters, or extrasynaptic for spots two pixels (380 nm) away [54]. Values of the mean square displacement (MSD) plot versus time were calculated for each trajectory by applying the relation:

$$MSD(n\tau) = \frac{1}{N-n}\sum_{i=1}^{N-n}\left[\left(x((i+n)\tau) - x(i\tau)\right)^2 + \left(y((i+n)\tau) - y(i\tau)\right)^2\right]$$

(Saxton and Jacobson, 1997), where τ is the acquisition time, N is the total number of frames, n and i are positive integers with n determining the time increment. Diffusion coefficients (D) were calculated by fitting the first four points without origin of the MSD versus time curves with the equation: $MSD(n\tau) = 4Dn\tau + b$ where b is a constant reflecting the spot localization accuracy. Depending on the type of lamp used for imaging, the QD pointing accuracy is ~20-30 nm, a value well below the measured explored areas (at least 1 log difference). Synaptic dwell time was defined as the duration of detection of QDs at synapses on a recording divided by the number of exits as detailed previously [55,56]. The explored area of each trajectory was defined as the MSD value of the trajectory at two different time intervals of at 0.42 and 0.45 s [57]. The number of QDs vary from one cell to another and from one condition to another in a given experiment. To avoid giving too much weight to a condition with larger numbers and in order to compare the conditions between them within the same culture, the number of QDs in each condition was adjusted to the number of QDs of the condition with the smallest number. For conditions with large numbers, values were sorted randomly using the ALEA function of Excel 2013 before data extraction.

Chloride imaging

Calibration of SuperClomeleon was performed in Neuro2a cells. Extra and intracellular chloride were equilibrated using the K^+/H^+ ionophore nigericin and the Cl/OH antiporter tributyltin as described [22]. Cells were perfused with a solution containing nigericin (10 µM, Sigma), tributyltin chloride (10 µM, Sigma) and (in mM) EGTA 2, K-gluconate 2, $MgCl_2$/MgSulfonate 2, HEPES 10, glucose 20 and NaCl/NaGluconate ranging from 0 to 138 (pH 7.4). Neuro2a cells and neurons were imaged at 35°C in a temperature-controlled open chamber (BadController V, Luigs & Neumann, Ratingen, Germany). Two-photon imaging was performed using an upright LeicaTCS MP5 microscope equip with resonant scanner (8 kHz), a Leica 25X/0.95 HCX IRAPO immersion objective and a tunable Ti:sapphire laser (Coherent Chameleon Vision II) with dispersion correction set to 820 nm for CFP excitation. The emission path consisted of an initial 700 nm low-pass filter to remove excess excitation light (E700 SP, Chroma Technologies), 506 nm dichroic mirror for orthogonal separation of emitted signal, 483/32 CFP emission filter, 535/30 YFP emission filter (FF506-Di01-25 36; FF01-479/40; FF01-542/50;

Brightline Filters; Semrock) and two-channel Leica HyD detector for simultaneous acquisition. For Neuro2a imaging, due to the high expression and low dark noise of the HyD photodetectors, detector gain was typically set at 10% with a laser power at 5%. For neurons imaging, due to the expression variability and lower expression of the sensor compared to Neuro2a transfection, detector gain of the HyD photodetectors was typically set at 50-100% with laser power at 7%. Z-stack images (16-bit; 512x512) were typically acquired every 30 s. The z-step size was 1 µm and total stack size was typically 20-30 sections depending on the neurons. Images were processed in ImageJ by using maximum z-projections followed by the correction of minor coverslip drifts using StackReg macro [58]. Regions of interest (ROIs) were selected for measurement if they could only be measured over the whole experiment. Raw CFP and YFP intensity measurements for the entire recording were imported into Microsoft Excel. Background fluorescence (measured from a non-fluorescent area) was subtracted and a fluorescence ratio was calculated for each time point in each ROI series and was normalized to the average baseline ratio for each respective ROI (average of the first 4 frames before treatment). Statistical analysis was performed in SigmaPlot 12.5. Wilcoxon rank sum test (or paired t-test when normality test passed) was used to compare the mean responses before and upon pharmacological treatment.

Calcium Imaging

Neurons at DIV21-25 were loaded with 0.5 mM Fluo-4AM (Invitrogen) for 5 min at 37°C in imaging medium. After washing excess dye, cells were further incubated for 5-10 min to allow hydrolysis of the AM ester. Cells were imaged at 37°C in an open chamber mounted on an inverted spinning-disc microscope (Leica DMI4000, Yokogawa CS20 spinning Nipkow disk, 40x/0.6 N.A. objective). All washes, incubation steps, and cell imaging were performed in imaging medium. Fluo4-AM was illuminated using 491nm light from a diode. Emitted light was collected using a 525-39 (±25) nm emission filter. Time lapse (0.33 Hz for 600 s) of confocal stacks (of ~35 images acquired with an interval of 0.3 µm) were acquired with a cooled EM-CCD camera (512 x 512, 16 µm pixel size) using Metamorph. The analysis was performed on a section of the stack where the soma was in focus at different time points. Fluorescence intensities collected in the soma before (F0) and following (F) bath addition of the drugs, were background-subtracted before being displayed as F/F0 values. Data were analyzed using Metamorph. Normalization of fluorescence intensity was performed for each cell by dividing the mean fluorescence intensity by the average of fluorescence intensities of the 4 time points before drug application. Statistics (paired t test) were run on the last time point before drug application (120 s) compared to the latest time point after drug application (600 s).

Immunocytochemistry

KCC2-Flag membrane clustering was assessed with live cell staining. Pre-treated neurons expressing KCC2-Flag were washed in imaging medium and incubated for 20 min at 4°C with mouse primary antibody against Flag (1:400; Sigma, cat # F3165) in imaging medium in the presence of the appropriate drugs. After washes with imaging medium, cells were fixed for 15 min at room temperature (RT) in paraformaldehyde (PFA; 4% w/v; Sigma) and sucrose (20% w/v; Sigma) solution in 1X PBS. Cells were then washed in PBS and incubated for 30 min at RT in goat serum (GS; 20% v/v; Invitrogen) in PBS to block nonspecific staining. Neurons were then incubated for 45 min at RT with Cy5- conjugated goat anti-mouse antibodies (1.9 g/ml; Jackson ImmunoResearch, cat # 115-175-205) in PBS–GS blocking solution, washed, and mounted on slides. To assess spine morphology pre-treated KCC2-Flag and eGFP co-transfected cells were fixed for 15 min at room temperature (RT) and washed in 1X PBS. Coverslips were mounted on slides with mowiol 844 (48 mg/ml; Sigma).

Fluorescence image acquisition and analysis

Image acquisition was performed using a 100 X objective (NA 1.40) on a Leica (Nussloch, Germany) DM6000 upright epifluorescence microscope with a 12-bit cooled CCD camera (Micromax, Roper Scientific) run by MetaMorph software (Roper Scientific, Evry, France). Quantification was performed using MetaMorph software (Roper Scientific). Image folders were randomized before analysis. For morphological spine analysis exposure time was adjusted for each eGFP image to obtain best fluorescence to noise ratio and to avoid pixel saturation. For each neuron a well-focused dendrite was chosen, spine heads were manually delimited and their area were quantified. To assess KCC2-Flag clusters, exposure time was fixed at a non-saturating level and kept unchanged between cells and conditions. For cluster analysis, images were first flatten background filtered (kernel size, 3 X 3 X 2) to enhance cluster outlines, and a user defined intensity threshold was applied to select clusters and avoid their coalescence. Clusters were outlined and the corresponding regions were transferred onto raw images to determine the mean KCC2–Flag cluster number, area and fluorescence intensity. The dendritic surface area of the region of interest was measured to determine the number of clusters per 10 μm^2. For each culture, we analyzed ~10 cells per experimental condition and ~100 clusters or ~15 spines per cell.

Total RNA extraction and cDNA synthesis

Total RNA extraction was performed on DIV 21 hippocampal cultures using RNeasy Mini kit (Qiagen, Venlo, Netherlands) and on Sprague Dawley rat (13 weeks) hippocampus tissue using RNAsolv (Omega Bio-tek, Norcross, GA) according to manufacturer's instructions. Genomic DNA was removed by digestion with Amplification Grade DNase I (Sigma-Aldrich). First-strand cDNA was synthesized by

reverse transcription of 1 µg of total RNA using Superscript-II and random primers (Invitrogen) according to standard protocols. Reverse transcriptase was absent in some samples as negative control.

Quantitative real-time PCR

Relative expression levels of WNK1-4 mRNA were determined by real time RT-PCR using Absolute SYBR Green Mix (ABgene, Epsom, UK) and the following set of primers: WNK1-for (AAGGTCTGGACACCGAAACC), WNK1-rev (TTCCCTTTTACTGTGGATTCCC), WNK2-for (CATGACATGGAGGCCTCTGG), WNK2-rev (CGGGCTTTTCACTCTCAGGA), WNK3-for (CATCACAGGACCCACTGGAT), WNK3-rev (AGCCATTTCCAACATACACATC), WNK4-for (GCTGCAAACTCACAACAGCA), WNK4-rev (CTCAGGAATCCGTCTCGCTC). Data were analysed with the 2–DCt method, and values normalized to WNK1 expression level.

Surface biotinylation in cultures

Pre-treated neuronal cultures were washed with ice-cold PBS three times, and then incubated in freshly prepared PBS containing 0.5-1 mg/ml EZ-Link Sulfo-NHS-SS-Biotin (Pierce, Rockford, IL, USA) at 4°C for 30 min with gentle agitation. Biotinylation was stopped by addition of Tris-HCl (50 mM; pH 7.4) and cells lysed in in modified RIPA buffer (50 mM Tris-HCl (pH 7.4), 150 mM NaCl, 1% Nonidet P-40, 0.5% DOC, 0.1% SDS, 50 mM NaF, 1 mM Na3VO4 and protease and phosphatase inhibitors, Roche). After thoroughly homogenizing, the samples were centrifuged and the supernatant collected. A small fraction of the lysates was kept for input KCC2 quantification. Lysates were mixed with 50% slurry of Neutravidin beads (Thermo Scientific) and rotated overnight at 4°C. The beads were harvested by centrifugation and washed three times in modified RIPA buffer and one time in modified RIPA buffer without detergents. After the last wash all solution was carefully removed from the beads, and the biotin-bound and input fractions denatured in 6X SDS sample buffer containing DTT at 37°C for 1 h.

Samples were subjected to electrophoresis on polyacrylamide gels and transferred to nitrocellulose membranes. The membranes were incubated for 30 min with TRIS-buffered saline, with 1% Triton (TTBS; Invitrogen) containing 5% (w/v) skim milk. The membranes were then immunoblotted in 5% (w/v) skim milk in TTBS with rabbit anti-KCC2 (Millipore, cat # 07-432) and mouse anti-TUJ1 (R&D Systems, cat # MAB 1195) or anti-actin (SantaCruz, cat # sc-32251) antibodies overnight at 4°C. The blots were then washed 4 times with TTBS and incubated for 1 hour at room temperature with secondary fluorescent antibodies (DyLight700 cat # 610-730-002 or 800 cat # 611-145-002, Rockland) diluted 5000-fold in 5% (w/v) skim milk in TTBS. After repeating the washing steps, fluorescence was detected using Odyssey infrared imaging system (LI-COR Bioscience). The relative intensities of immunoblot bands were determined by densitometry with ImageJ software. Total KCC2

protein expression was determined as the sum of monomeric and oligomeric bands normalized to TUJ1 or actin. Surface expression of KCC2 was determined as the ratio of monomeric + oligomeric biotinylated KCC2 fraction versus total KCC2 fraction.

Surface biotinylation in hippocampal slices

Biotinylation studies were performed as previously described [59] with modifications. Horizontal sections (500 µm) were made from 5-7 week old wild-type animals (C57Bl/6j, Janvier) using a Leica vibratome in NMDG based cutting solution (in mM: NMDG 93, HCl 93, KCl 2.5, NaH2PO4 1.2, NaHCO3 30, HEPES 20, glucose 25, ascorbic acid 5, sodium pyruvate 3, MgCl2 10, CaCl2 0.5, saturated with 95% O2/5% CO2, pH 7.4, 300mOsm). Slices were transferred into an interface chamber at 37°C for 10 min containing ACSF (in mM: CaCl2 1.6, glucose 11, KCl 2.5, MgCl2 1.2, NaCHO3 26.2, NaH2PO4 1, NaCl 124, saturated with 95% O2/5% CO2, pH 7.4, 298mOsm), followed by a 1 hour recovery period at room temperature. The slices were then placed onto a pre-heated recording chamber in either pre-warmed bubbled ACSF or ACSF containing muscimol (10 µM) for 30 min at 35°C. The slices were transferred into bubbled ice-cold ACSF containing 1mg/ml EZ-Link Sulfo-NHSSS-Biotin (21326, Thermo Scientific) with gentle rotation for 45 min at 4°C. Excess biotin was quenched using 1M glycine in ice-cold ACSF for 10 min, and then the slices were rinsed once in ice-cold ACSF and snap frozen on dry ice. The hippocampus was micro-dissected and immediately lysed and homogenized in modified RIPA buffer (50 mM Tris-HCl (pH 7.4), Triton X-100 1%, 150 mM NaCl, 1mM EDTA, DOC 0.5%, NP40 1%, SDS 0.1%, 50 mM NaF, cOmplete protease inhibitor cocktail (Roche)). The samples were centrifuged at 15,000 rpm for 15 min, the supernatant was collected and protein content was determined using a Pierce BCA protein quantification kit (23227, Thermo Scientific). 50 µg of protein was loaded onto 100 µl of 50% slurry of Pierce NeutrAvidin UltraLink Resin (53150, Thermo Scientific), made up to a total volume of 400 µl in modified RIPA buffer and rotated for 2 hours at 4°C. The beads were recuperated by centrifugation and thoroughly washed 4 times in modified RIPA buffer, and after the last wash the beads were incubated in 6X SDS sample buffer containing 10% β-mercaptoethanol at 37°C for 1 hour. The protein samples were run on pre-cast Bis-Tris gels (NuPage 4-12% gradient gels, NP0322, Invitrogen) and immunoblotting was performed. Analysis was performed using ImageJ by normalizing the amount of surface KCC2 to the amount of actin in the non-biotinylated fraction.

Immunoprecipitation and Immunoblotting with phosphorylation site-specific antibodies

Pretreated hippocampal neurons in culture (DIV 23) were lysed in lysis buffer containing 50 mM Tris/HCl, pH 7.5, 1 mM EGTA, 1 mM EDTA, 50 mM sodium fluoride, 5 mM sodium pyrophosphate, 1 mM sodium orthovanadate, 1% (w/v) Nonidet P-40, 0.27 M sucrose, 0.1% (v/v) 2-mercaptoethanol, and protease inhibitors

(Roche). CCCs phosphorylated at the KCC2 T906 and T1007 equivalent residue were immunoprecipitated (centrifuged at 16,000 x g at 4 °C for 20 min) using phosphorylation site-specific antibodies as described [27]. The phosphorylation site-specific antibodies were coupled with protein-G–Sepharose at a ratio of 1 mg of antibody per 1 mL of beads in the presence of 20 µg/mL of lysate to which the corresponding non-phosphorylated peptide had been added. Two mg of clarified cell lysate were incubated with 15 µg of antibody conjugated to 15 µL of protein-G–Sepharose for 2 hours at 4°C with gentle agitation. Beads were washed three times with 1 mL of lysis buffer containing 0.15 M NaCl and twice with 1 mL of wash buffer (50 mM Tris/HCl, pH7.5 and 0.1mM EGTA). Bound proteins were eluted with 1X LDS sample buffer (Invitrogen) containing 1% (v/v) 2-mercaptoethanol.

Cell or tissue lysates (15 µg) in SDS sample buffer were subjected to electrophoresis on polyacrylamide gels and transferred to nitrocellulose membranes. The membranes were incubated for 30 min with TTBS containing 5% (w/v) skim milk. The membranes were then immunoblotted in 5% (w/v) skim milk in TTBS with the indicated primary antibodies overnight at 4°C. Antibodies prepared in sheep [17] were used at a concentration of 1-2 µg/ml. The incubation with phosphorylation site-specific sheep antibodies was performed with the addition of 10 µg/mL of the nonphosphorylated peptide antigen used to raise the antibody. The blots were then washed six times with TTBS and incubated for 1 hour at room temperature with secondary HRP-conjugated antibodies diluted 5000-fold in 5% (w/v) skim milk in TTBS. After repeating the washing steps, the signal was detected with the enhanced chemiluminescence reagent. Immunoblots were developed using a film automatic processor (SRX-101; Konica Minolta Medical) and films were scanned with a 600-dpi resolution on a scanner (PowerLook 1000; UMAX). The relative intensities of immunoblot bands were determined by densitometry with ImageJ software.

Antibodies used for Western blots were raised in sheep and affinity-purified on the appropriate antigen by the Division of Signal Transduction Therapy Unit (DSTT) at the University of Dundee; other antibodies were purchased. KCC1 total antibody [S699C, first bleed; raised against residues 1-118 of human KCC1]; KCC2 total antibody [S700C, first bleed; raised against residues 1-119 of human KCC2A]; KCC3 total antibody [S701C, first bleed; raised against residues 1-175 of human KCC3]; KCC4 total antibody [S801C, first bleed; raised against residues 1-117 of human KCC4]; KCC2a phosphoT906 [S959C, first bleed; raised againstresidues 975-989 of human KCC3a phosphorylated at T991, SAYTYER(T)LMMEQRSRR]; KCC2a phosphoT1007 [S961C, first bleed; raised against residues 1032-1046 or 1041-1055 of human KCC3a phosphorylated at T1048]. NKCC1 total antibody [S022D, second bleed; raised against residues 1-288 of human NKCC1]; NKCC1 phospho-T203/T207/T212 antibody [S763B, third bleed; raised against residues 198-217 of human NKCC1 phosphorylated at T203, T207 and T212, HYYYD(T)HTN(T)YYLR(T)FGHNT]; WNK1-total antibody [S079B, second bleed; raised against residues 2360-2382 of human WNK1]; WNK1phospho-S382 antibody WNK1-phospho-Ser^{382} antibody [S099B, second bleed; raised against residues residues 377-387 of human WNK1

phosphorylated at S382, ASFAK(S)VIGTP]; WNK3-total antibody [S156C, second bleed; raised against residues 1142 – 1461 of human WNK3]; SPAK-total antibody [S551D, third bleed; raised against full-length GST-tagged human SPAK protein]; OSR1-total antibody [S850C, second bleed; raised against RSAHLPQPAGQMPTQPAQVSLR, residues 389 - 408 of mouse OSR1]; SPAK/OSR1 (S-motif) phosphoS373/S325 antibody [S670B, second bleed; raised against 367–379 of human SPAK, RRVPGS(S)GHLHKT, which is highly similar to residues 319–331 of human OSR1 in which the sequence is RRVPGS(S)GRLHKT]. KCC2 total antibody [residues 932-1043 of rat KCC2] was purchased from NeuroMab. The anti-β-Tubulin III (neuronal) antibody (T8578) was purchased from Sigma-Aldrich. Secondary antibodies coupled to horseradish peroxidase used for immunoblotting were obtained from Pierce. IgG used in control immunoprecipitation experiments was affinity-purified from pre-immune serum using Protein G-Sepharose.

Gramicidin perforated patch recordings

Experiments were performed on cells after 20-24 days in culture. Neurons were selected based on their GFP fluorescence indicating co-expression of GFP with glycine receptors. Recordings were made using an Axopatch 200B amplifier (Molecular Devices), filtered at 5 kHz and digitized at 20 kHz. Neurons were perfused with extracellular solution (in mM) 125 NaCl, 20 D-glucose, 10 HEPES, 4 MgCl2, 2 KCl, 1 CaCl2, pH 7.4 containing TTX (1 µM), kynurenate (1 mM) and R,S-MCPG (500µM) in a recording chamber (BadController V; Luigs & Neumann) at 31°C mounted on an upright microscope (BX51WI; Olympus). Gramicidin perforated (50 µg/ml) patch recordings were performed using glass pipettes with a standard internal solution (in mM) 120 K-gluconate, 10 KCl, 10 HEPES, 0.1 EGTA, 4 MgATP 2H20, 0.4 Na3GTP 2H20, pH 7.4. Recordings were made in voltage-clamp mode using an Axopatch 200B amplifier (Molecular Devices) and filtered at 2 kHz and digitized at 20 kHz. The membrane potential was held at -65 mV and depolarizing voltage steps were applied from -30 to +30 mV for 3 s, during which time either 100 µm glycine was puffed onto the soma using a Picospritzer (Parker Hannifin) or Rubi-GABA (15 µM; Tocris) was photolyzed at the soma using a digital modulated diode laser beam at 405 nm (Omicron Deepstar; Photon Lines) as previously described [3]. Glycinergic and GABAergic post-synaptic currents were measured and a linear regression of the current-voltage relationship was used to determine $E_{glycine}$ or E_{GABA}, respectively. Access and input resistance were monitored using a -5 mV step as previously described [3].Voltages were corrected for the liquid junction potential (-16.2 mV) and access resistance was compensated offline.

In vivo pentylenetatrazole injection

Adult (postnatal day 84-91) C57bl6 mice (all males from JanvierLabs) were injected subcutaneously with pentylenetatrazole (PTZ, 75 mg/kg, dissolved in saline), and recorded right after

injection using video recordings. The procedure was made in accordance with the guidelines of the French Agriculture and Forestry Ministry for handling animals and with the agreement of the Comité National de Réflexion Ethique sur l'Expérimentation Animale (# 4018). The sampling of animals as well as the experimental procedure and analysis of the data were determined based on previous published work. The animals to be used for PTZ vs Control conditions were randomly chosen from the batch of C57bl6 mice delivered from JanvierLabs. After 20-35 min of observation, animals were sacrificed by cervical dislocation, brains were rapidly extracted on ice and the cortex and the hippocampus were dissected, frozen in liquid nitrogen and stored at -80°C until use for biochemistry. The first seizures were observed after 6-7 min of injection and a second sequence of seizures and/or abnormal gait were detected after 14-15 min. Two out of three animals injected with 75 mg/kg of PTZ had tonic-clonic seizures with rigid paw extension followed by death and one animal showed only partial clonus.

Data availability

All relevant data are available from the authors.

Statistics

Sampling corresponds to the number of quantum dots for SPT, number of cultures or animals for biochemistry, cells for ICC, chloride and calcium imaging, and electrophysiology experiments. Sample size selection for experiments was based on published experiments, pilot studies as well as in-house expertise. All results were used for analysis except in few cases. For imaging experiments (chloride and calcium imaging, SPT, immunofluorescence), cells with signs of suffering (apparition of blobs, fragmented neurites) were discarded from the analysis. For PTZ-treatment in vivo, one animal with an incorrect injection site was excluded from analysis. Means are shown ± SEM, median values are indicated with their interquartile range (IQR, 25-75%). Means were compared using the non-parametric Mann-Whitney test (immunocytochemistry, dwell time comparison), paired t-test (calcium imaging), Wilcoxon rank sum test or paired t-test when normality test passed (chloride imaging) or two-tailed Student's t-test (biochemistry and gramicidin-perforated patch clamp) using SigmaPlot 12.5 software (Systat Software). Diffusion coefficient and explored area values having non-normal distributions, a non-parametric Kolmogorov-Smirnov test was used. Median values were compared using the Kolmogorov-Smirnov test under Matlab (The Mathworks, Natick, MA). Differences were considered significant for p-values less than 5% *(*p≤0.05; **p<0.01; ***p<0.001; ns, not significant).*

References

1. Rivera, C. *et al.* The K+/Cl- co-transporter KCC2 renders GABA hyperpolarizing during neuronal maturation. *Nature* **397,** 251–255 (1999).

2. Li, H. *et al.* KCC2 Interacts with the Dendritic Cytoskeleton to Promote Spine Development. *Neuron* **56,** 1019–1033 (2007).

3. Gauvain, G. *et al.* The neuronal K-Cl cotransporter KCC2 influences postsynaptic AMPA receptor content and lateral diffusion in dendritic spines. *Proc. Natl. Acad. Sci. U. S. A.* **108,** 15474–15479 (2011).

4. Chevy, Q. *et al.* KCC2 Gates Activity-Driven AMPA Receptor Traffic through Cofilin Phosphorylation. *J. Neurosci.* **35,** 15772–86 (2015).

5. Coull, J. A. M. *et al.* Trans-synaptic shift in anion gradient in spinal lamina I neurons as a mechanism of neuropathic pain. *Nature* **424,** 938–942 (2003).

6. Huberfeld, G. *et al.* Perturbed chloride homeostasis and GABAergic signaling in human temporal lobe epilepsy. *J. Neurosci.* **27,** 9866–9873 (2007).

7. Li, X. *et al.* Long-term expressional changes of Na+-K+-Cl- co-transporter 1 (NKCC1) and K+-Cl- co-transporter 2 (KCC2) in CA1 region of hippocampus following lithium-pilocarpine induced status epilepticus (PISE). *Brain Res.* **1221,** 141–146 (2008).

8. Tyzio, R. & Ben-Ari, Y. Oxytocin-Mediated GABA inhibition During Delivery Attunates Autism Pathogenesis in Rodent Offspring. *Science* **343,** 675–680 (2014).

9. Staley, K. J. The KCC2 Cotransporter and Human Epilepsy : Getting Excited About Inhibition The KCC2 Cotransporter and Human Epilepsy : Getting Excited About Inhibition. (2016). doi:10.1177/1073858416645087

10. Chamma, I. *et al.* Activity-dependent regulation of the K/Cl transporter KCC2 membrane diffusion, clustering, and function in hippocampal neurons. *J. Neurosci.* **33,** 15488–503 (2013).

11. Puskarjov, M., Ahmad, F., Kaila, K. & Blaesse, P. Activity-Dependent Cleavage of the K-Cl Cotransporter KCC2 Mediated by Calcium-Activated Protease Calpain. *Journal of Neuroscience* **32,** 11356–11364 (2012).

12. Lee, H. H. C., Deeb, T. Z., Walker, J. A., Davies, P. A. & Moss, S. J. NMDA receptor activity downregulates KCC2 resulting in depolarizing GABAA receptor-mediated currents. *Nat. Neurosci.* **14,** 736–743 (2011).

13. Kitamura, A. *et al.* Sustained depolarizing shift of the GABA reversal potential by glutamate receptor activation in hippocampal neurons. *Neurosci. Res.* **62,** 270–277 (2008).

14. Wang, W., Gong, N. & Xu, T. Le. Downregulation of KCC2 following LTP contributes to EPSP-spike potentiation in rat hippocampus. *Biochem. Biophys. Res. Commun.* **343,** 1209–1215 (2006).

15. Fiumelli, H., Cancedda, L. & Poo, M. M. Modulation of GABAergic transmission by activity via postsynaptic Ca 2+-dependent regulation of KCC2 function. *Neuron* **48,** 773–786 (2005).

16. Ganguly, K., Schinder, A. F., Wong, S. T. & Poo, M. ming. GABA itself promotes the developmental switch of neuronal GABAergic responses from excitation to inhibition. *Cell* **105,** 521–532 (2001).

17. Friedel, P. *et al.* WNK1-regulated inhibitory phosphorylation of the KCC2 cotransporter maintains the depolarizing action of GABA in immature neurons. *Sci. Signal.* **8,** ra65 (2015).

18. Kahle, K. T. *et al.* Inhibition of the kinase WNK1 / HSN2 ameliorates neuropathic pain by restoring GABA inhibition. **9,** 1–9 (2016).

19. Caraiscos, V. B. *et al.* Tonic inhibition in mouse hippocampal CA1 pyramidal neurons is mediated by alpha5 subunit-containing gamma-aminobutyric acid type A receptors. *Proc. Natl. Acad. Sci. U. S. A.* **101,** 3662–3667 (2004).

20. Glykys, J., Mann, E. O. & Mody, I. Which GABA(A) receptor subunits are necessary for tonic inhibition in the hippocampus? *J. Neurosci.* **28,** 1421–1426 (2008).

21. Eugène, E. *et al.* GABA(A) receptor gamma 2 subunit mutations linked to human epileptic syndromes differentially affect phasic and tonic inhibition. *J. Neurosci.* **27,** 14108–16 (2007).

22. Grimley, J. S. *et al.* Visualization of Synaptic Inhibition with an Optogenetic Sensor Developed by Cell-Free Protein Engineering Automation. *J. Neurosci.* **33,** 16297–16309 (2013).

23. Delpire, E. *et al.* Small-molecule screen identifies inhibitors of the neuronal K-Cl cotransporter KCC2. *Proc. Natl. Acad. Sci. U. S. A.* **106,** 5383–8 (2009).

24. Piala, A. T. *et al.* Chloride sensing by WNK1 involves inhibition of autophosphorylation. *Sci. Signal.* **7,** ra41

(2014).

25. Bazua-Valenti, S. *et al.* The Effect of WNK4 on the Na+-Cl- Cotransporter Is Modulated by Intracellular Chloride. *J. Am. Soc. Nephrol.* **26,** 1781–1786 (2015).

26. Rinehart, J. *et al.* Sites of Regulated Phosphorylation that Control K-Cl Cotransporter Activity. *Cell* **138,** 525–536 (2009).

27. de Los Heros, P. *et al.* The WNK-regulated SPAK/OSR1 kinases directly phosphorylate and inhibit the K+-Cl- co-transporters. *Biochem. J.* **458,** 559–73 (2014).

28. McCormick, J. a & Ellison, D. H. The WNKs: atypical protein kinases with pleiotropic actions. *Physiol. Rev.* **91,** 177–219 (2011).

29. Kikuchi, E. *et al.* Discovery of Novel SPAK Inhibitors That Block WNK Kinase Signaling to Cation Chloride Transporters. *J. Am. Soc. Nephrol.* **26,** 1525–1536 (2015).

30. Kahle, K. T. & Delpire, E. Kinase-KCC2 coupling: Cl - rheostasis, disease susceptibility, therapeutic target. *J. Neurophysiol.* jn.00865.2015 (2015). doi:10.1152/jn.00865.2015

31. Kaila, K., Price, T. J., Payne, J. a, Puskarjov, M. & Voipio, J. Cation-chloride cotransporters in neuronal development, plasticity and disease. *Nat. Publ. Gr.* **15,** 637–654 (2014).

32. Meier, J., Vannier, C., Sergé, A., Triller, A. & Choquet, D. Fast and reversible trapping of surface glycine receptors by gephyrin. *Nat. Neurosci.* **4,** 253–260 (2001).

33. Kandratavicius, L. *et al.* Animal models of epilepsy: Use and limitations. *Neuropsychiatric Disease and Treatment* **10,** 1693–1705 (2014).

34. Woodin, M. a., Ganguly, K. & Poo, M. M. Coincident pre- and postsynaptic activity modifies GABAergic synapses by postsynaptic changes in Cl- transporter activity. *Neuron* **39,** 807–820 (2003).

35. Watanabe, M., Wake, H., Moorhouse, A. J. & Nabekura, J. Clustering of neuronal K+-Cl- cotransporters in lipid rafts by tyrosine phosphorylation. *J. Biol. Chem.* (2009). doi:10.1074/jbc.M109.043620

36. Groban, E. S., Narayanan, A. & Jacobson, M. P. Conformational changes in protein loops and helices induced by post-translational phosphorylation. *PLoS Comput. Biol.* **2,** 238–250 (2006).

37. Berglund, K. *et al.* Imaging synaptic inhibition in transgenic mice expressing the chloride indicator, Clomeleon. *Brain Cell Biol.* **35,** 207–28 (2006).

38. Kahle, K. K. T. *et al.* Modulation of neuronal activity by phosphorylation of the K-Cl cotransporter KCC2. *Trends Neurosci.* **36,** 726–37 (2013).

39. Yang, C. L., Zhu, X. & Ellison, D. H. The thiazide-sensitive Na-Cl cotransporter is regulated by a WNK kinase signaling complex. *J. Clin. Invest.* **117,** 3403–3411 (2007).

40. Doyon, N. *et al.* Efficacy of synaptic inhibition depends on multiple, dynamically interacting mechanisms implicated in chloride homeostasis. *PLoS Comput. Biol.* **7,** e1002149 (2011).

41. Darman, R. B., Flemmer, A. & Forbush, B. Modulation of Ion Transport by Direct Targeting of Protein Phosphatase Type 1 to the Na-K-Cl Cotransporter. *J. Biol. Chem.* **276,** 34359–34362 (2001).

42. Gagnon, K. B. & Delpire, E. Multiple pathways for protein phosphatase 1 (PP1) regulation of Na-K-2Cl cotransporter (NKCC1) function: The N-terminal tail of the Na-K-2Cl cotransporter serves as a regulatory scaffold for Ste20-related proline/alanine-rich kinase (SPAK) and PP1. *J. Biol. Chem.* **285,** 14115–14121 (2010).

43. Arnaiz, G. R. D. L. & Ordieres, M. G. L. Brain Na+, K+-ATPase activity in aging and disease. *Int. J. Biomed. Sci.* **10,** 85–102 (2014).

44. Harris, J. J., Jolivet, R. & Attwell, D. Synaptic Energy Use and Supply. *Neuron* **75,** 762–777 (2012).

45. Buzsaki, G., Kaila, K. & Raichle, M. Inhibition and brain work. *Neuron* **56,** 771–83 (2007).

46. Howarth, C., Gleeson, P. & Attwell, D. Updated energy budgets for neural computation in the neocortex and cerebellum. *J. Cereb. Blood Flow Metab.* **32,** 1222–1232 (2012).

47. Arion, D. & Lewis, D. a. Altered expression of regulators of the cortical chloride transporters NKCC1 and KCC2 in schizophrenia. *Arch. Gen. Psychiatry* **68,** 21–31 (2011).

48. Fernandez-Enright, F., Andrews, J. L., Newell, K. a, Pantelis, C. & Huang, X. F. Novel implications of Lingo-1 and its signaling partners in schizophrenia. *Transl. Psychiatry* **4,** e348 (2014).

49. Ramoz, N., Cai, G., Reichert, J. G., Silverman, J. M. & Buxbaum, J. D. An analysis of candidate autism loci on chromosome 2q24-q33: Evidence for association to the *STK39* gene. *Am. J. Med. Genet. Part B Neuropsychiatr. Genet.* **147B,** 1152–1158 (2008).

50. Yang, L. *et al.* STE20/SPS1-Related Proline/Alanine-Rich Kinase Is Involved in Plasticity of GABA Signaling Function in a Mouse Model of Acquired Epilepsy. *PLoS One* **8,** 1–13 (2013).

51. Hanus, C., Ehrensperger, M.-V. & Triller, A. Activity-dependent movements of postsynaptic scaffolds at inhibitory synapses. *J. Neurosci.* **26,** 4586–4595 (2006).

52. Bats, C., Groc, L. & Choquet, D. The Interaction between Stargazin and PSD-95 Regulates AMPA Receptor Surface Trafficking. *Neuron* **53,** 719–734 (2007).

53. Bannai, H., Lévi, S., Schweizer, C., Dahan, M. & Triller, A. Imaging the lateral diffusion of membrane molecules with quantum dots. *Nat. Protoc.* **1,** 2628–2634 (2006).

54. Dahan, M. *et al.* Diffusion dynamics of glycine receptors revealed by single-quantum dot tracking. *Science* **302,** 442–445 (2003).

55. Charrier, C., Ehrensperger, M.-V., Dahan, M., Lévi, S. & Triller, A. Cytoskeleton regulation of glycine receptor number at synapses and diffusion in the plasma membrane. *J. Neurosci.* **26,** 8502–8511 (2006).

56. Ehrensperger, M.-V., Hanus, C., Vannier, C., Triller, A. & Dahan, M. Multiple association states between glycine receptors and gephyrin identified by SPT analysis. *Biophys. J.* **92,** 3706–3718 (2007).

57. Renner, M., Schweizer, C., Bannai, H., Triller, A. & Lévi, S. Diffusion barriers constrain receptors at synapses. *PLoS One* **7,** e43032 (2012).

58. Thévenaz, P., Ruttimann, U. E. & Unser, M. A pyramid approach to subpixel registration based on intensity. *IEEE Trans. Image Process.* **7,** 27–41 (1998).

59. Mahadevan, V. *et al.* Kainate Receptors Coexist in a Functional Complex with KCC2 and Regulate Chloride Homeostasis in Hippocampal Neurons. *Cell Rep.* **7,** 1762–1770 (2014).

Acknowledgements

We thank J. Nabekura for kindly providing the original pEGFP-IRES-KCC2 full-length construct, D Choquet for the homer1c-GFP construct, A. Triller for gephyrin-mRFP and glycine receptor α1 subunit constructs, I. Medina for WNK1-KD, WNK1-CA, shRNA against rat WNK1 mRNA and a scrambled shRNA sequence. We want to warmly thank M. Mameli, J. Hadchouel and P. Blaesse for critical reading of the manuscript. We are also grateful to the Imaging Facility of Institut du Fer à Moulin. This work was supported by INSERM, the Fondation pour la Recherche Médicale (to JCP and SL), Human Frontiers (to JCP), and the Fondation pour la Recherche sur le Cerveau (to SL). MH was the recipient of a doctoral fellowship from the Université Pierre and Marie Curie as well as from the Bio-Psy LabEx. K.T.K is supported by the National Institutes of Health, the Simons Foundation, and the March of Dimes Foundation Basil O'Connor Award. The Poncer/Levi team is affiliated to Ecole des Neurosciences de Paris and the Bio-Psy LabEx.

Author contributions

S.L. and M.H. designed the research. M.H. and M. Re. performed the single particle tracking experiments and analyzed the data. M.H. and S.L. performed immunofluorescence experiments and M.H., S.L. and M.Ru. analyzed the data. J.P. and J.C.P. performed and analyzed electrophysiological experiments. J.Z. and K.K. designed the biochemical experiments; J.Z. performed the experiments; J.Z. and K.K. analyzed the data. S.A.A. and J.C.P. designed chloride imaging experiments and S.A.A. performed and analyzed the data. FGC performed the epilepsy experiments. E.E. and M. Ru. prepared the hippocampal cultures and I.M. and M. Re. contributed to new reagents and analytical tools. M.H. and S.L. prepared the figures and wrote the paper.

Competing Financial Interests statement

The authors declare no competing commercial interests in relation to the submitted work.

$GABA_A$ receptor dependent synaptic inhibition rapidly tunes KCC2 activity via the Cl^--sensitive WNK1 kinase

Martin Heubl[1,2,3], Jinwei Zhang[4,5,6], Jessica C. Pressey[1,2,3], Sana Al Awabdh[1,2,3], Marianne Renner[1,2,3], Ferran Gomez-Castro[1,2,3], Imane Moutkine[1,2,3], Emmanuel Eugène[1,2,3], Marion Russeau[1,2,3], Kristopher T. Kahle[6], Jean Christophe Poncer[1,2,3] and Sabine Lévi[1,2,3*]

[1] INSERM UMR-S 839, 75005, Paris, France

[2] Université Pierre et Marie Curie, 75005, Paris, France

[3] Institut du Fer a Moulin, 75005, Paris, France;

[4] MRC Protein Phosphorylation and Ubiquitylation Unit, College of Life Sciences, University of Dundee, Dundee DD1 5EH, Scotland.

[5] Institute of Biomedical and Clinical Sciences, University of Exeter Medical School, Hatherly Laboratory, Exeter, EX4 4PS, UK.[6] Departments of Neurosurgery, Pediatrics, and Cellular & Molecular Physiology; NIH-Yale Centers for Mendelian Genomics; Yale School of Medicine, New Haven, CT 06511 USA

* Corresponding author

Correspondence to:

Sabine Lévi
INSERM-UPMC UMR-S 839
17 rue du Fer a Moulin
75005 Paris, France
Tel. +33 1 45 87 61 13
Fax. +33 1 45 87 61 10
E-mail: sabine.levi@inserm.fr

Running title: GABAergic inhibition regulates KCC2 activity

Whole-cell patch clamp recordings

Neurons were recorded at 31°C under superfusion with artificial cerebrospinal fluid containing (in mM) 125 NaCl, 20 D-glucose, 10 HEPES, 4 MgCl2, 2 KCl, 1 CaCl2 (pH = 7.4). Whole-cell recordings measuring GABABR currents were made with glass pipettes containing the following internal solution (in mM): 110 K-methylsulfonate, 20 KCl, 10 HEPES, 10 EGTA, 4 MgATP, 0.4 Na3GTP, 10 Na phosphocreatine, 1.8 MgCl2. Recordings were made in the presence of TTX (1 µM), kynurenate (1 mM), and R,S-MCGP (500 µM), and bicuculline (20 µM). In current-clamp configuration the resting membrane potential (V_m) was monitored for 5 minutes to ensure a stable baseline, followed by the addition of bath applied baclofen (20 µM). Once V_m reached a steady state in the baclofen treatment, the drug was either washed out or the $GABA_BR$ antagonist CGP52132 (20 µM) was added to the bath. The Vm was monitored until it reached a steady state. Whole-cell patch clamp recordings were performed with borosilicate glass micropipettes filled with either (in mM) 135 CsCl, 10 HEPES, 10 EGTA, 4 MgATP and 0.4 Na3GTP (pH = 7.4) for recording tonic, GABAAR-mediated currents or 105 CsMeSO4, 10 CsCl, 10 HEPES, 10 EGTA, 4 MgATP and 0.4 Na3GTP for recording muscimol-evoked currents. Cells were held at -70 mV. GABAAR-mediated currents were recorded in the presence of TTX (1 µM), NBQX (10 µM) and D,L-APV (100 µM). Access and input resistance were regularly monitored with -5 mV voltage steps. All recordings were made using an Axopatch 200B amplifier (Molecular Devices), filtered at 2 kHz and digitized at 25 kHz. All data was collected using the Clampex 10 program and analyzed using Clampfit 10 (Axon). Currents were analyzed offline using Clampfit software.

Supplementary Figures

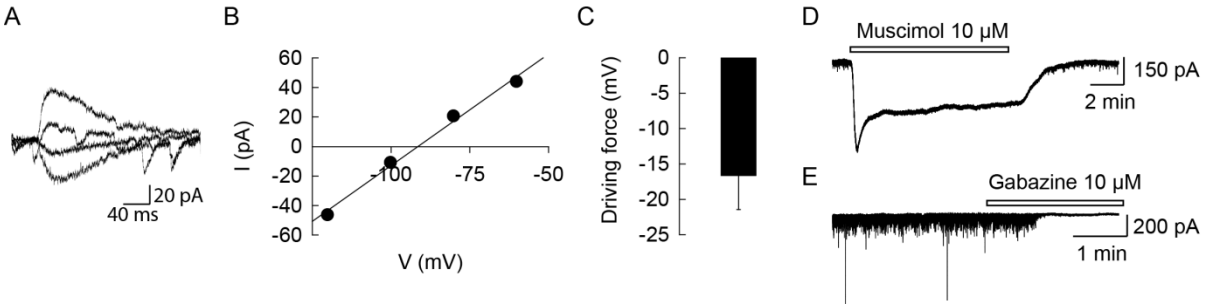

Supplementary figure 1. E_{GABA} and effects of muscimol and gabazine. A-B, *Typical gramicidin-perforated patch-clamp recordings of GABAA receptor mediated currents induced by uncaging of Rubi-GABA at different membrane potentials. E_{GABA} was determined as the intercept of the I-V curve with the x-axis.* ***C****, The driving force for chloride (Cl^-) is hyperpolarizing indicating chloride influx upon $GABA_AR$ activation. N= 11 cells.* ***D****, Whole-cell patch-clamp recording of a hippocampal neuron with a CsMeSO4-based internal solution before, during and after application of the GABAAR agonist muscimol. Muscimol-induced current peaked within approximately 30 s of wash-in and decayed by about 50 % upon 10 minutes of agonist application.* ***E,*** *Whole-cell patch-clamp recording of a hippocampal neuron with a CsCl-based internal solution, before and during application of the GABAAR antagonist gabazine, in the presence of TTX, NBQX and D,L-APV. Gabazine efficiently suppressed mIPSCs with no detectable change in holding current, suggesting it did not affect tonic, GABAAR-mediated currents.*

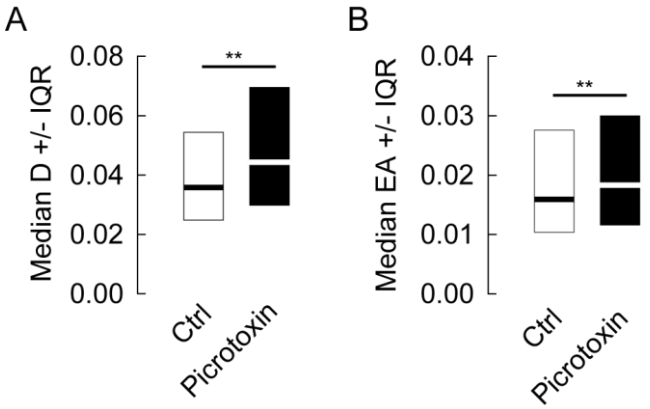

Supplementary figure 2. The pore channel blocker picrotoxin relieves KCC2 diffusion constraints. A-B, *Median diffusion coefficients D values ± 25-75% IQR (**A**) and median explored area EA ± 25%-75% IQR (**B**) (for bulk population of QDs) of KCC2 measured in control (white) vs picrotoxin (black) conditions showing picrotoxin reduces KCC2 diffusion constraints. **A**, n= 227 QDs, 2 cultures; KS test p=0.002. **B**, n= 554 QDs, 2 cultures; KS test p=0.009. **A**, D in $\mu m^2 s^{-1}$; **B**, EA in μm^2.*

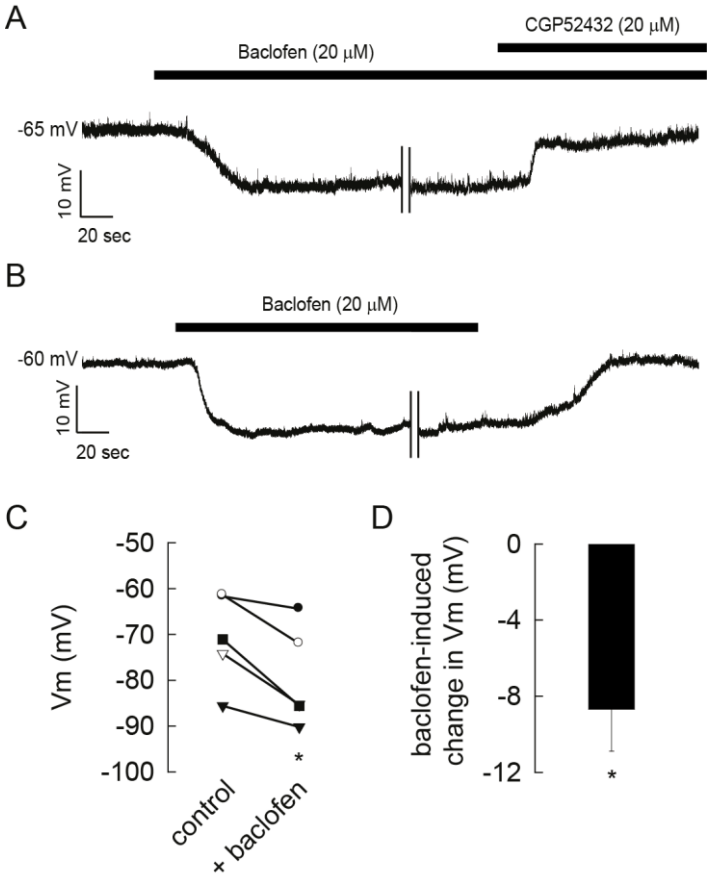

Supplementary figure 3. Activation of $GABA_BR$ hyperpolarizes V_m in cultured hippocampal neurons. A-B, *Representative trace of V_m measured by whole-cell patch clamp recordings in cultured hippocampal neurons (DIV 21-24) bathed in TTX (1 µM), kynurenate (1 mM), and MCPG (500 µM) before and during application of the $GABA_BR$ agonist baclofen (20 µM). Vertical lines depict a break in recording time followed by blocking $GABA_BR$ activity using CGP52432 (20 µM, **A**) or during washout of baclofen (**B**). V_m returns to baseline in response to the addition of CGP52432 and after washing out baclofen. **C**, Scatter plot of V_m measurements before and during the application of baclofen. N= 5 cells; paired t-test p =0.016. **D,** Bar graph summarizing the change in V_m observed during the application of baclofen. Bar represents mean change in V_m ± s.e.m. N= 5 cells, paired t-test, p =0.016.*

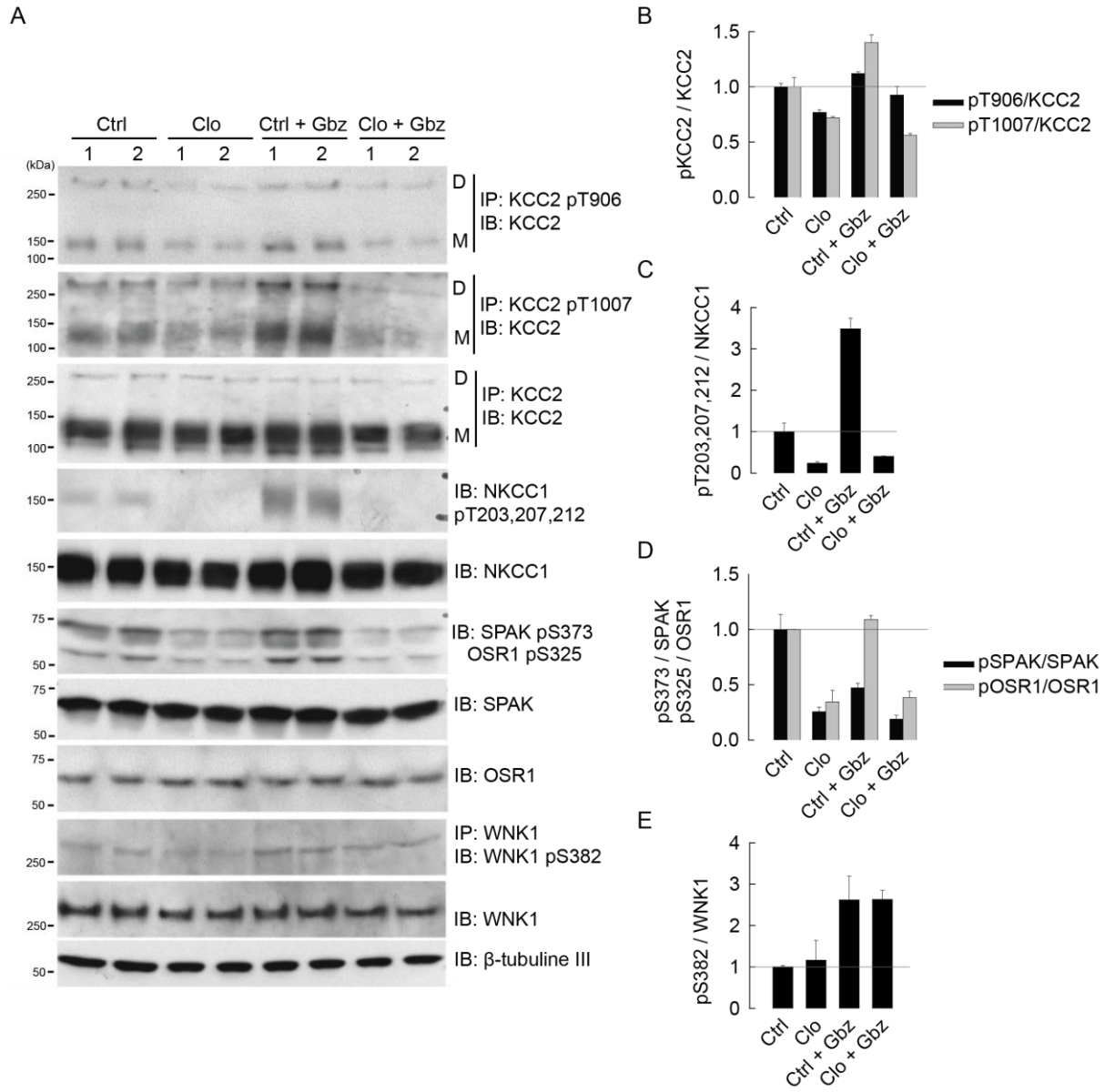

Supplementary figure 4. GABA$_A$R-dependent KCC2 and NKCC1 threonine phosphoregulation require SPAK/OSR1 kinase activity. A-E*, Western Blot (**A**) and quantification (mean ± s.e.m., two independent experiments 1-2) of KCC2 T906/T1007 (**B**), NKCC1 T203/T207/T212 (**C**), SPAK S373 / OSR1 S325 (**D**) and WNK1 S382 (**E**) kinases phosphorylation in control (Ctrl), gabazine (Ctrl+Gbz), closantel (Clo) and closantel+gabazine (Clo+Gbz) conditions. Note closantel inactivates SPAK/OSR kinases but not the upstream kinase WNK1 and blocks the increased phosphorylation of KCC2 and NKCC1 upon GABA$_A$R blockade.*

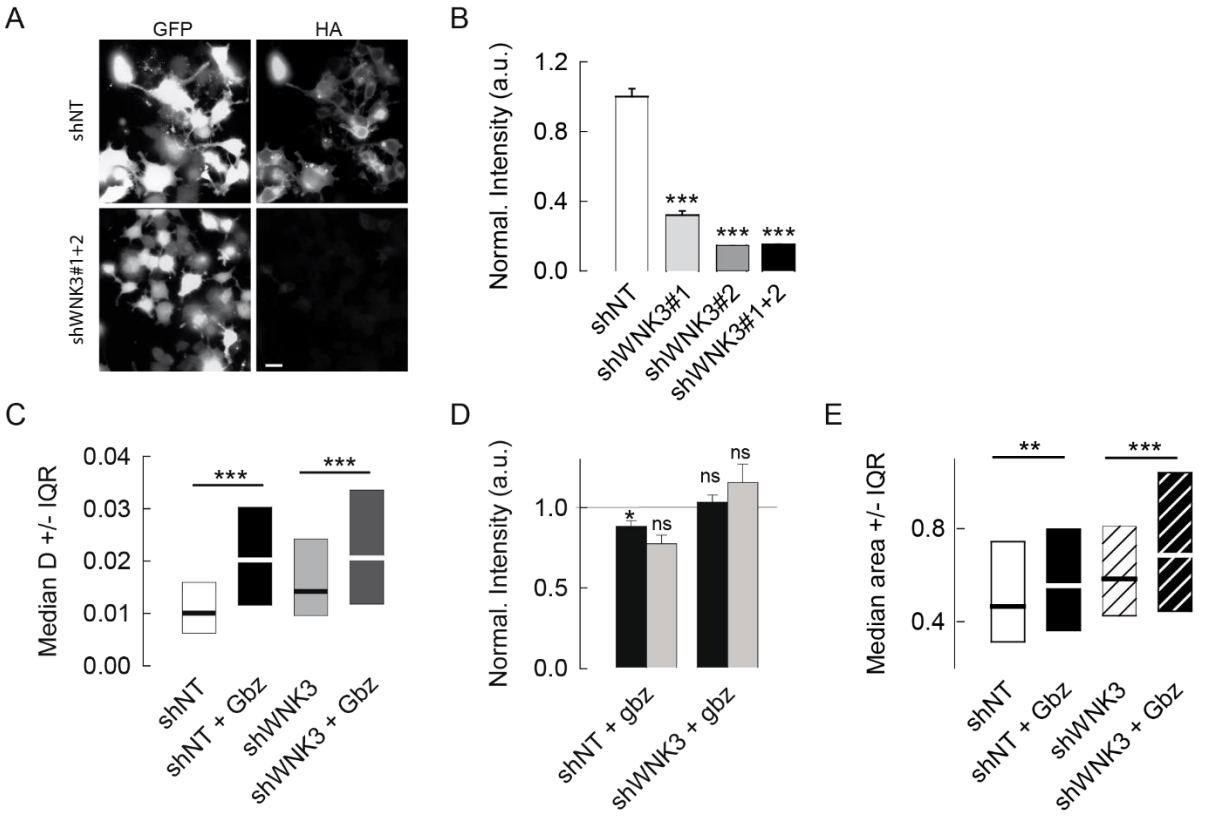

Supplementary figure 5. WNK3 suppression partially blocks gabazine-induced regulation of KCC2. A-B*, Characterization of rat WNK3 shRNAs.* ***A****, HA immunostaining of Neuro2A cells co-transfected with a recombinant HA-tagged rat WNK3 cDNA and either a GFP-tagged non-target shRNA (shNT) or a cocktail of two GFP-tagged shRNAs against WNK3 (shWNK3#1+2). Scale bar, 20 µm.* ***B****, Quantification of the average fluorescence intensity of HA-labeled WNK3 in Neuro2A cells expressing shNT, WNK3 shRNA #1 (shWNK3#1), #2 (shWNK3#2) or a cocktail of #1+2 (shWNK3#1+2). Values were normalized to the shNT mean fluorescence intensity value. The efficiency of shWNK3#1, shWNK3#2 or shWNK3#1+2 is respectively of 68%, 79% and 83%. shNT n= 582 cells, shWNK3#1 n= 539 cells, shWNK3#2 n= 774 cells, shWNK3#1+2 n= 681 cells; MW test p<0.001.* ***C****, WNK3 suppression by shRNA (shWNK3) did not abolish the gabazine-mediated increase in KCC2 diffusion. shNT n= 322 QDs, shNT + Gbz 322 QDs, shWNK3 330 QDs, shWNK3 + Gbz 330 QDs, 2 cultures, shNT vs shNT + Gbz KS test p<0.001, shWNK3 vs shWNK3 + Gbz KS test p<0.001.* ***D****, WNK3 shRNA (shWNK3) overexpression suppressed the gabazine-induced reduction in cluster (gray) and pixel (black) fluorescence intensity as compared to shNT expressing neurons. Values were normalized to the corresponding control values. shNT: Ctrl 70 cells, Gbz n= 73 cells; shWNK3: Ctrl n= 77 cells, Gbz n= 71 cells; 4-5 cultures. shNT vs shNT + Gbz: MW test p=0.018 and p= 0.114 for pixel and cluster intensity respectively; shWNK3 vs shNT: MW test p=0.004 andp=0.004 for pixel and cluster intensity; shWNK3 vs shWNK3 + Gbz: MW test p=0.954 and p=0.797 for pixel and cluster intensity.* ***E,*** *Median values ± 25-75% IQR of spine head area from shNT or shWNK3 overexpressing neurons in control (white and black stripe) or gabazine (black and white stripe) conditions, respectively. Note the increase in spine head area in gabazine condition for shNT (KS test p=0.0011) and shWNK3 (KS test p<0.001) transfected cells. ShNT n= 486 spines; shNT + Gbz n= 244 spines; shWNK3 n= 266 spines, shWNK3 + Gbz n= 291 spines, 2 cultures.* ***C,*** *D in µm^{2}s^{-1};* ***E,*** *spine head area in µm^2.*

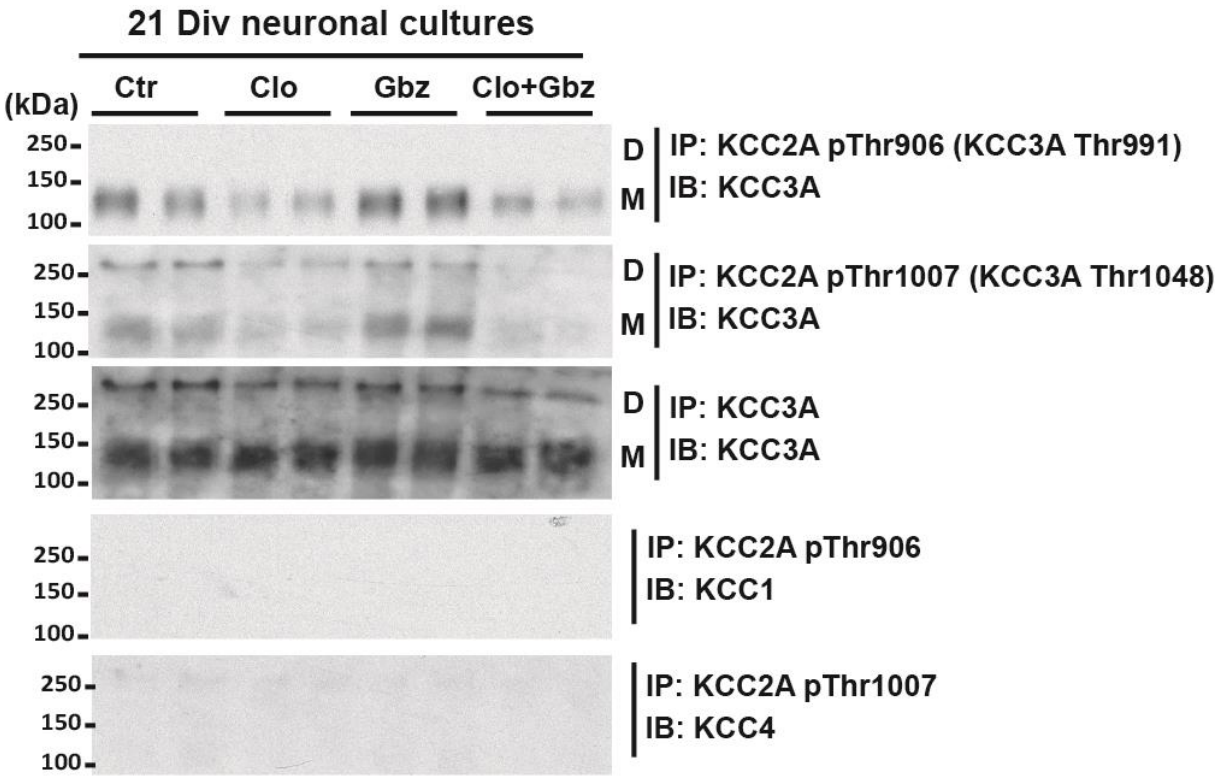

Supplementary figure 6. GABA$_A$R-dependent regulation of KCC3a threonine phosphorylation but not KCC1 or KCC4. *Western Blot of two independent experiments (1-2) of KCC3aT991/T1048 phosphorylation in gabazine (Gbz), closantel (Clo), or closantel+gabazine (clo+Gbz) conditions. Note IP with anti KCC2 pT906/1007 are recognized by an anti KCC3 antibody but not anti- KCC1 or KCC4 antibodies. Gabazine application increased phosphorylation of KCC3 on phospho-sites T991 and T1048 that is blocked by closantel.*

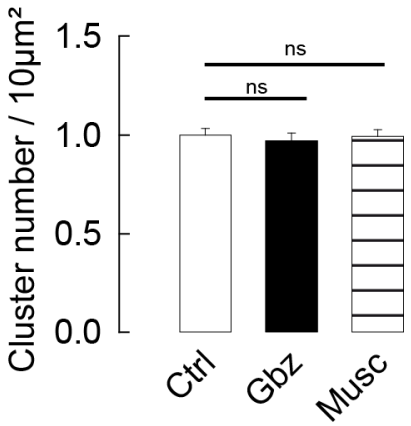

Supplementary figure 7. No effect of GABA$_A$R-mediated inhibition on KCC2 cluster density. *Flag surface staining in hippocampal neurons (DIV 23) expressing recombinant KCC2–Flag in absence (Ctrl) or presence of gabazine (Gbz) or muscimol (Musc) for 30 min. Quantifications showing no effect of gabazine (black, MW test p=0.539) or muscimol (pattern, MW test p=0.856) on KCC2 cluster number per dendritic unit length. Values were normalized to the corresponding control values. Ctrl n= 62 cells; Gbz n= 59 cells; Musc n= 58 cells; 4 cultures.*

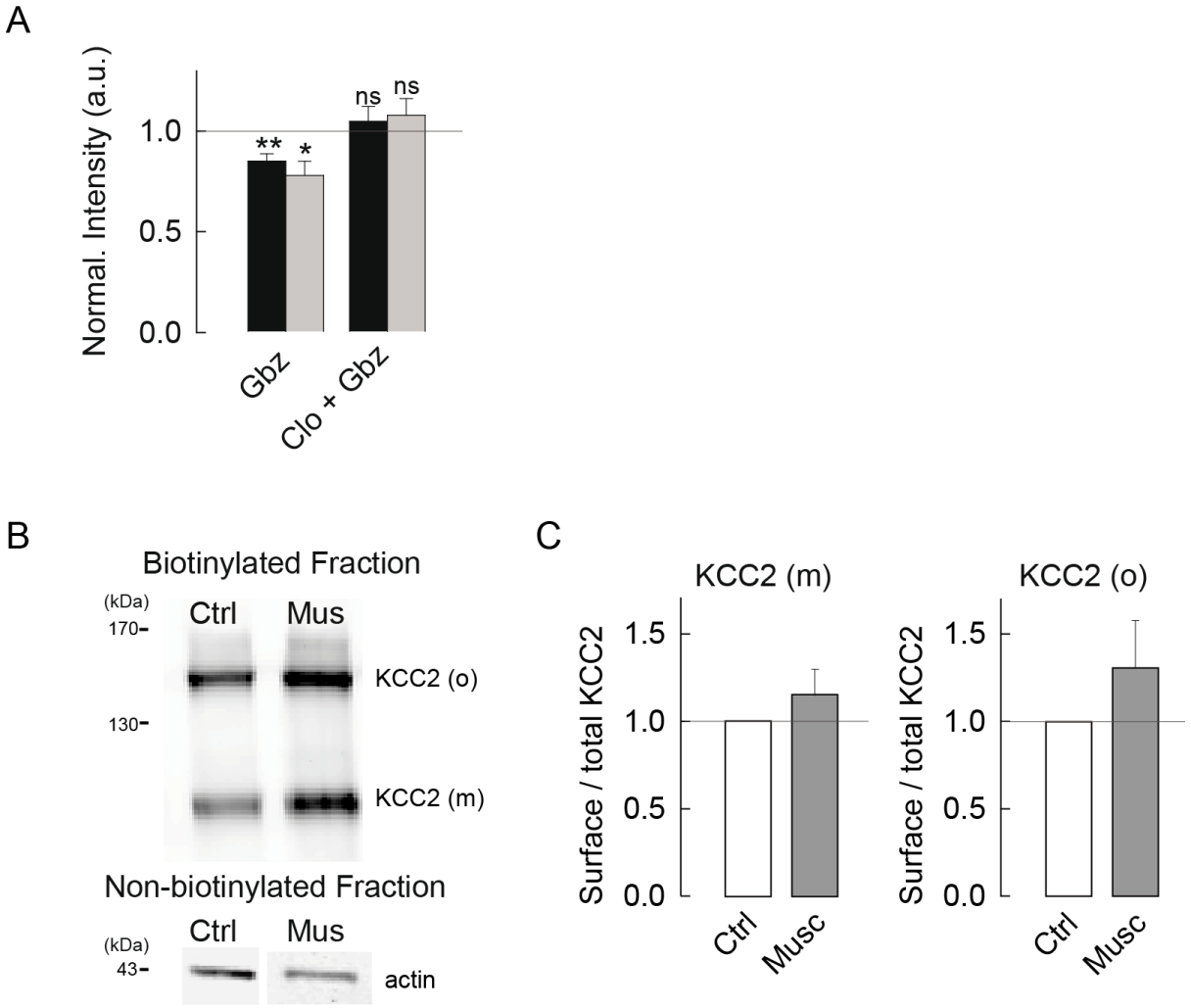

Supplementary figure 8. GABA$_A$R-dependent regulation of KCC2 in intact hippocampal network. ***A,*** *GABA$_A$R-mediated regulation of KCC2 in absence of Na+ channel blocker and glutamate receptors antagonists. Quantifications of KCC2 pixel (black) and cluster (gray) intensity in response to an acute application of gabazine or gabazine + closantel in absence of ttx+kynurenate+mCPG. Note the reduced transporter clustering after gabazine treatment and blockade of gabazine effect by closantel. Ctrl n= 64 cells, Gbz n= 65 cells, Closantel n= 50 cells, Closantel + gabazine n= 43 cells, 4 cultures, ctrl vs Gbz MW test p=0.004 and p=0.02 for pixel and cluster intensity respectively; Clo+Gbz vs Clo MW test p=0.686 and p=0.164 for pixel and cluster intensity.* ***B-C,*** *Acute GABA$_A$R activation increases the membrane stability of KCC2 in acute hippocampal slices.* ***B****, Biotinylation experiments showing an increase in the surface expression of KCC2 monomers (m) and oligomers (o) in 5-7 week old acute hippocampal slices after 30 min of muscimol treatment in absence of sodium channel and glutamate receptor blockers.* ***C****, Quantification of the ratio of the surface pool of KCC2 oligomers and monomers over the total pool of KCC2 in control (white) and muscimol (gray) conditions showing increase of surface KCC2 o and m after muscimol treatment. Values normalized to actin present in the non-biotinylated fraction. N=4 experiments. 3-5 slices per condition and per experiment. Rank sum test, KCC2m p=0.1 and KCC2o p=0.4.*

Experimental conditions	**Fig. Nb**	**Median D (10^{-2} µm²s^{-1})**	**Fig. Nb**	**Median EA (10^{-3} µm²)**	**Fig. Nb**	**Mean DT (s)**
Bulk Ctrl	1B	2.7 (416, 38, 4)	1D	11.1 (838, 38, 4)	n.a.	n.a.
Bulk Muscimol	1B	2.6 (416, 33, 4)	1D	10.2 (838, 33, 4)	n.a.	n.a.
Bulk Ctrl	1F	2.4 (441, 45, 5)	1H	10.9 (880, 45, 5)	n.a.	n.a.
Bulk Gbz	1F	3,2 (441, 39, 5)	1H	14.8 (880, 39, 5)	n.a.	n.a.
Bulk Ctrl	S2A	3.6 (227, 15, 2)	S2B	15.9 (554, 15, 2)	n.a.	n.a.

Bulk Picrotoxin	S2A	4.4 (227, 12, 2)	S2B	18.3 (554, 12, 2)	n.a.	n.a.
Extra Ctrl	1J	2.1 (129, 25, 4)	1K	10.5 (362, 25, 4)	n.a.	n.a.
ES Ctrl	1J	1.9 (109, 33, 4)	1K	8.6 (212, 33, 4)	1L	11,9 (307, 33, 4)
IS Ctrl	1J	2,0 (89, 27, 4)	1K	8.6 (202, 27, 4)	1L	10,1 (162, 27, 4)
Extra Gbz	1J	3,0 (129, 25, 4)	1K	15.2 (362, 25, 4)	n.a.	n.a.
ES Gbz	1J	2,4 (109, 33, 4)	1K	10.9 (212, 33, 4)	1L	8,1 (218, 28, 4)
IS Gbz	1J	2,8 (89, 27, 4)	1K	11.0 (202, 27, 4)	1L	6,8 (119, 29, 4)

Supplementary table 1. $GABA_AR$-dependent control of KCC2 diffusion at synapses and at extrasynaptic sites. *Numbers in parentheses indicate the numbers of QDs, cells, and cultures analyzed. ES, QDs at excitatory synapses; IS, QDs at inhibitory synapses; Extra, QDs at extrasynaptic sites; n.a., not applicable.*

Experimental conditions	**Fig. Nb**	**Median D (10^{-2} µm²s^{-1})**	**Fig. Nb**	**Median EA (10^{-3} µm²)**
Ctrl	2A	1.9 (320, 12, 2)	2B	8.9 (640, 12, 2)
L655,708	2A	2.1 (320, 12, 2)	2B	8.9 (640, 12, 2)
Ctrl	2C	2.4 (271, 24, 3)	2D	8.6 (542, 24, 3)
2 µM GABA	2C	2.1 (271, 19, 3)	2D	7.8 (542, 19, 3)
2 µM GABA + L655,708	2C	2.7 (271, 19, 3)	2D	10.8 (542, 19, 3)
Ctrl	2E	2.5 (278, 19, 3)	2F	10.7 (555, 19, 3)
Baclofen	2E	2.5 (278, 19, 3)	2F	10.7 (555, 19, 3)
Ctrl	2E	2.5 (279, 23, 3)	2F	11.8 (580, 23, 3)
CGP52432	2E	2.4 (279, 20, 3)	2F	10.5 (580, 20, 3)
Cd^{2+}	3E	2.2 (250, 18, 3)	3F	11.6 (500, 18, 3)
Cd^{2+}+Gbz	3E	3.4 (250, 15, 3)	3F	14.7 (500, 15, 3)
S940D	3G	2.2 (190, 16, 3)	3H	10.4 (380, 16, 3)
S940D + Gbz	3G	2.6 (190, 15, 3)	3H	12.8 (380, 15, 3)

Supplementary table 2. Regulation of KCC2 diffusion by tonic $GABA_AR$-mediated inhibition but not by metabotropic $GABA_BR$ and calcium signaling pathway. *Numbers in parentheses indicate the numbers of QDs, cells, and cultures analyzed.*

Experimental conditions	**Fig. Nb**	**Median D (10^{-2} µm²s^{-1})**	**Fig. Nb**	**Median EA (10^{-3} µm²)**
Ctrl	4D	2.8 (368, 22, 3)	4F	13.4 (712, 22, 3)
VU0240551	4D	2.5 (368, 22, 3)	4F	12.7 (712, 22, 3)
eNpHR t 0	4H	5.2 (215, 15, 2)	4J	22.5 (469, 15, 2)
eNpHR t 10s	4H	2.8 (215, 15, 2)	4J	11.5 (469, 15, 2)
eNpHR t 60s	4H	2.1 (215, 15, 2)	4J	7.7 (469, 15, 2)
138mM $[Cl^-]_{ex}$	4L	1.4 (408, 25, 3)	4N	5.6 (816, 25, 3)
0mM $[Cl^-]_{ex}$	4L	1.7 (408, 25, 3)	4N	7.3 (816, 25, 3)
Ctrl	5F	1.6 (405, 24, 4)	n.s.	7.5 (810, 24, 2)
Gbz	5F	2.2 (405, 20, 4)	n.s.	8.9 (810, 20, 2)
Closantel	5F	1.7 (405, 24, 4)	n.s.	8.2 (810, 24, 2)
Closantel + Gbz	5F	1.7 (405, 25, 4)	n.s.	5.7 (810, 25, 2)
shMock	5G,H	3.2 (322, 45, 5)	n.s.	15.8 (644, 45, 5)
shMock + Gbz	5H	3.9 (322, 31, 5)	n.s.	16.7 (644, 31, 5)
shWNK1	5H	3.7 (322, 41, 5)	n.s.	17.3 (644, 41, 5)
shWNK1 + Gbz	5H	3.5 (322, 31, 5)	n.s.	16.1 (644, 31, 5)
WNK1-KD	5G,H	3.5 (322, 34, 5)	n.s.	15.9 (644, 34, 5)
WNK1-KD + Gbz	5H	3.7 (322, 34, 5)	n.s.	15.4 (644, 34, 5)
WNK1-CA	5G	3.8 (322, 33, 5)	n.s.	17.0 (644, 33, 5)
shNT	S5E	1.0 (322, 18, 2)	n.s.	3.3 (644, 18, 2)
shNT + Gbz	S5E	2.1 (322, 16, 2)	n.s.	7.6 (644, 16, 2)
shWNK3	S5E	1.4 (330, 13, 2)	n.s.	5.8 (660, 13, 2)

shWNK3 + Gbz	S5E	2.1 (330, 31, 2)	n.s.	9.8 (660, 31, 2)
T906/T1007	6E,F	2.5 (197, 22, 3)	n.s.	10.9 (394, 22, 3)
T906/T1007 + Gbz	6F	3.4 (197, 15, 3)	n.s.	15.3 (394, 15, 3)
T906/T1007A	6E,F	2.7 (238, 19, 3)	n.s.	11.7 (476, 19, 3)
T906/T1007A + Gbz	6F	2.7 (238, 16, 3)	n.s.	10.7 (476, 16, 3)
T906/T1007E	6E,F	3.3 (241, 23, 3)	n.s.	16.1 (482, 23, 3)
T906/T1007E + Gbz	6F	3.3 (241, 15, 3)	n.s.	15.1 (482, 15, 3)

Supplementary table 3. Molecular mechanisms underlying $GABA_AR$-dependent regulation of KCC2 lateral membrane diffusion. *Numbers in parentheses indicate the numbers of QDs, cells, and cultures analyzed. n.s., not shown.*

REFERENCES

REFERENCES

Abbracchio MP, Burnstock G (1994) Purinoceptors: Are there families of P2X and P2Y purinoceptors? Pharmacol Ther 64:445–475.

Abbracchio MP, Burnstock G, Boeynaemns J., Barnard E., Boyer J., Kennedy C, Knight G, Fumagalli M, Gachet C, Jacobson K, Weisman G (2006) International Union of Pharmacology LVIII: Update on the P2Y G Protein-Coupled Nucleotide Receptors: From Molecular Mechanisms and Pathophysiology to Therapy. Pharmacol Rev 58:281–341

Adén U, Herlenius E, Tang LQ, Fredholm BB (2000) Maternal caffeine intake has minor effects on adenosine receptor ontogeny in the rat brain. Pediatr Res 48:177–183

Ahmad A, Schaack JB, White CW, Ahmad S (2013) Adenosine A2A receptor-dependent proliferation of pulmonary endothelial cells is mediated through calcium mobilization, PI3-kinase and ERK1/2 pathways. Biochem Biophys Res Commun 434:566–571

Akhondzadeh S, Shasavand E, Jamilian H, Shabestari O, Kamalipour A (2000) Dipyridamole in the treatment of schizophrenia: adenosine-dopamine receptor interactions. J Clin Pharm Ther 25:131–137

Allaman I, Lengacher S, Magistretti PJ, Pellerin L (2003) A2B receptor activation promotes glycogen synthesis in astrocytes through modulation of gene expression. Am J Physiol Cell Physiol 284:C696-704

Allison DW, Chervin AS, Gelfand VI, Craig AM (2000) Postsynaptic scaffolds of excitatory and inhibitory synapses in hippocampal neurons: maintenance of core components independent of actin filaments and microtubules. J Neurosci 20:4545–4554

Andreae LC, Burrone J (2014) The role of neuronal activity and transmitter release on synapse formation. Curr Opin Neurobiol 27:47–52

Ango F, Wu C, Van der Want JJ, Wu P, Schachner M, Huang ZJ (2008) Bergmann Glia and the Recognition Molecule CHL1 Organize GABAergic Axons and Direct Innervation of Purkinje Cell Dendrites PLoS Biol 6:e103

Angulo E, Casadó V, Mallol J, Canela EI, Viñals F, Ferrer I, Lluis C, Franco R (2003) A1 adenosine receptors accumulate in neurodegenerative structures in Alzheimer disease and mediate both amyloid precursor protein processing and tau phosphorylation and translocation. Brain Pathol 13:440–451

Antonelli R, Pizzarelli R, Pedroni A, Fritschy J-M, Del Sal G, Cherubini E, Zacchi P (2014) Pin1-dependent signalling negatively affects GABAergic transmission by modulating neuroligin2/gephyrin interaction. Nat Commun 5:5066

Ardais AP, Rocha ASAS, Borges MFMF, Fioreze GT, Sallaberry C, Mioranzza S, Nunes F, Pagnussat N, Botton PHS, Cunha RA, Porciúncula L de O (2016) Caffeine exposure during rat brain development causes memory impairment in a sex selective manner that is offset by caffeine consumption throughout life. Behav Brain Res 303:76–84

Arendash GW, Schleif W, Rezai-Zadeh K, Jackson EK, Zacharia LC, Cracchiolo JR, Shippy D, Tan J (2006) Caffeine protects Alzheimer's mice against cognitive impairment and reduces brain β-amyloid production. Neuroscience 142:941–952

Arion D, Lewis D a (2011) Altered expression of regulators of the cortical chloride transporters NKCC1 and KCC2 in schizophrenia. Arch Gen Psychiatry 68:21–31.

Armentero MT, Pinna A, Ferré S, Lanciego JL, Müller CE, Franco R (2011) Past, present and future of A2A adenosine receptor antagonists in the therapy of Parkinson's disease. Pharmacol Ther 132:280–299

Arnaiz GRDL, Ordieres MGL (2014) Brain Na+, K+-ATPase activity in aging and disease. Int J Biomed Sci 10:85–102.

Artimo P et al. (2012) ExPASy: SIB bioinformatics resource portal. Nucleic Acids Res 40:W597–W603

Ascoli GA et al. (2008) Petilla terminology: nomenclature of features of GABAergic interneurons of the cerebral cortex. Nat Rev Neurosci 9:557–568

Ashrafi S, Betley JN, Comer JD, Brenner-Morton S, Bar V, Shimoda Y, Watanabe K, Peles E, Jessell TM, Kaltschmidt JA (2014) Neuronal Ig/Caspr recognition promotes the formation of axoaxonic synapses in mouse spinal

cord. Neuron 81:120–129
Augusto E, Matos M, Sevigny J, El-Tayeb A, Bynoe MS, Muller CE, Cunha RA, Chen J-F (2013) Ecto-5'-Nucleotidase (CD73)-Mediated Formation of Adenosine Is Critical for the Striatal Adenosine A2A Receptor Functions. J Neurosci 33:11390–11399
Averaimo S, Assali A, Ros O, Couvet S, Zagar Y, Genescu I, Rebsam A, Nicol X (2016) A plasma membrane microdomain compartmentalizes ephrin-generated cAMP signals to prune developing retinal axon arbors. Nat Commun 7:12896.
Avsar E, Empson RM (2004) Adenosine acting via A1 receptors, controls the transition to status epilepticus-like behaviour in an in vitro model of epilepsy. Neuropharmacology 47:427–437
Bagot RC, Labonté B, Peña CJ, Nestler EJ (2014) Epigenetic signaling in psychiatric disorders: stress and depression. Dialogues Clin Neurosci 16:281–295.
Bailey DN, Weibert RT, Naylor AJ (1982) A study of salicylate and caffeine excretion in the breast milk of two nursing mothers. J Anal Toxicol 6:64–68.
Bannai H, Lévi S, Schweizer C, Dahan M, Triller A (2006) Imaging the lateral diffusion of membrane molecules with quantum dots. Nat Protoc 1:2628–2634.
Bannai H, Lévi S, Schweizer C, Inoue T, Launey T, Racine V, Sibarita J-B, Mikoshiba K, Triller A (2009) Activity-Dependent Tuning of Inhibitory Neurotransmission Based on GABAAR Diffusion Dynamics. Neuron 62:670–682.
Bannai H, Niwa F, Mark W, Triller A, Le S, Bannai H, Niwa F, Sherwood MW, Shrivastava AN, Arizono M (2015) Bidirectional Control of Synaptic GABA A R Clustering by Glutamate and Calcium Article Bidirectional Control of Synaptic GABA A R Clustering by Glutamate and Calcium. Cell Reports13:2768–2780.
Barbin G, Pollard H (1993) Involvement of GABAA receptors in the outgrowth of cultured hippocampal neurons. Neuroscience Lett. 152:150–154.
Barraco RA, Clough-Helfman C, Goodwin BP, Anderson GF (1995) Evidence for presynaptic adenosine A2a receptors associated with norepinephrine release and their desensitization in the rat nucleus tractus solitarius. J Neurochem 65:1604–1611
Barraco RA, Helfman CC, Anderson GF (1996) Augmented release of serotonin by adenosine A2a receptor activation and desensitization by CGS 21680 in the rat nucleus tractus solitarius. Brain Res 733:155–161
Barranco-Quintana JL, Allam MF, Del Castillo AS, Navajas RF-C (2007) Alzheimer's disease and coffee: a quantitative review. Neurol Res 29:91–95
Barrie A, Nicholls D (1993) Adenosine A1 receptor inhibition of glutamate exocytosis and protein kinase C-mediated decoupling. J Neurochem 60:1081–1086.
Bastia E, Xu Y-H, Scibelli AC, Day Y-J, Linden J, Chen J-F, Schwarzschild MA (2005) A Crucial Role for Forebrain Adenosine A2A Receptors in Amphetamine Sensitization. Neuropsychopharmacology 30:891–900
Bats C, Groc L, Choquet D (2007) The Interaction between Stargazin and PSD-95 Regulates AMPA Receptor Surface Trafficking. Neuron 53:719–734.
Bech BH, Obel C, Henriksen TB, Olsen J (2007) Effect of reducing caffeine intake on birth weight and length of gestation: randomised controlled trial. BMJ 334:409–409
Beesley PW, Herrera-Molina R, Smalla K-H, Seidenbecher C (2014) The Neuroplastin adhesion molecules: key regulators of neuronal plasticity and synaptic function. J Neurochem 131:268–283
Belzung C, Griebel G (2001) Measuring normal and pathological anxiety-like behaviour in mice: a review. Behav Brain Res 125:141–149
Ben-Ari Y (2001) Developing networks play a similar melody. Trends Neurosci 24:353–360
Berkovic SF, Mulley JC, Scheffer IE, Petrou S (2006) Human epilepsies: interaction of genetic and acquired factors. Trends Neurosci 29:391–397
Berninger B, Marty S, Zafra F, da Penha Berzaghi M, Thoenen H, Lindholm D (1995) GABAergic stimulation switches from enhancing to repressing BDNF expression in rat hippocampal neurons during maturation in vitro. Development 121:2327–2335
Berrettini WH (2001) Molecular linkage studies of bipolar disorders. Bipolar Disord 3:276–283
Bezaire MJ, Soltesz I (2013) Quantitative assessment of CA1 local circuits: knowledge base for interneuron-

pyramidal cell connectivity. Hippocampus 23:751–785
Bialas AR, Stevens B (2012) Glia: regulating synaptogenesis from multiple directions. Curr Biol 22:R833-5.
Bilimoria PM, Stevens B (2015) Microglia function during brain development: New insights from animal models. Brain Res 1617:7–17
Bloodgood BL, Sharma N, Browne HA, Trepman AZ, Greenberg ME (2013) The activity-dependent transcription factor NPAS4 regulates domain-specific inhibition. Nature 503:121–125
Blum AE, Joseph SM, Przybylski RJ, Dubyak GR (2008) Rho-family GTPases modulate Ca(2+) -dependent ATP release from astrocytes. Am J Physiol Cell Physiol 295:C231–C241.
Bogdanov Y, Michels G, Armstrong-Gold C, Haydon PG, Lindstrom J, Pangalos M, Moss SJ (2006) Synaptic GABAA receptors are directly recruited from their extrasynaptic counterparts. EMBO J 25:4381–4389
Boison D, Chen J-F, Fredholm BB (2010) Adenosine signaling and function in glial cells. Cell Death Differ 17:1071–1082
Born G, Breuer D, Wang S, Rohlmann A, Coulon P, Vakili P, Reissner C, Kiefer F, Heine M, Pape H-C, Missler M (2014) Modulation of synaptic function through the α-neurexin–specific ligand neurexophilin-1. Proc Natl Acad Sci 111:E1274–E1283
Borodinsky LN, O'Leary D, Neale JH, Vicini S, Coso OA, Fiszman ML (2003) GABA-induced neurite outgrowth of cerebellar granule cells is mediated by GABAA receptor activation, calcium influx and CAMKII and erk1/2 pathways. J Neurochem 84:1411–1420.
Bourgeron T (2015) From the genetic architecture to synaptic plasticity in autism spectrum disorder. Nat Rev Neurosci 16:551–563
Bouthour W, Leroy F, Emmanuelli C, Carnaud M, Dahan M, Poncer JC, Lévi S (2012) A human mutation in Gabrg2 associated with generalized epilepsy alters the membrane dynamics of GABAA receptors. Cereb Cortex 22:1542–1553
Bouwman J, Maia AS, Camoletto PG, Posthuma G, Roubos EW, Oorschot VMJ, Klumperman J, Verhage M (2004) Quantification of synapse formation and maintenance in vivo in the absence of synaptic release. Neuroscience 126:115–126
Brandon EP, Lin W, D'Amour KA, Pizzo DP, Dominguez B, Sugiura Y, Thode S, Ko C-P, Thal LJ, Gage FH, Lee K-F (2003) Aberrant patterning of neuromuscular synapses in choline acetyltransferase-deficient mice. J Neurosci 23:539–549
Budreck EC, Scheiffele P (2007) Neuroligin-3 is a neuronal adhesion protein at GABAergic and glutamatergic synapses. Eur J Neurosci 26:1738–1748
Buffelli M, Burgess RW, Feng G, Lobe CG, Lichtman JW, Sanes JR (2003) Genetic evidence that relative synaptic efficacy biases the outcome of synaptic competition. Nature 424:430–434
Burnstock G (1972) Purinergic nerves. Pharmacol Rev 24:509–581
Burnstock G (1978) A basis for distinguishing two types of purinergic receptor. Elsevier.
Burnstock G, Krügel U, Abbracchio MP, Illes P (2011) Purinergic signalling: From normal behaviour to pathological brain function. Prog Neurobiol 95:229–274
Burnstock G, Verkhratsky A (2012) Purinergic signalling and the nervous system.
Buzsaki G, Kaila K, Raichle M (2007) Inhibition and brain work. Neuron 56:771–783.
Canals M, Burgueño J, Marcellino D, Cabello N, Canela EI, Mallol J, Agnati L, Ferré S, Bouvier M, Fuxe K, Ciruela F, Lluis C, Franco R (2004) Homodimerization of adenosine A2A receptors: Qualitative and quantitative assessment by fluorescence and bioluminescence energy transfer. J Neurochem 88:726–734.
Canals M, Marcellino D, Fanelli F, Ciruela F, de Benedetti P, Goldberg SR, Neve K, Fuxe K, Agnati LF, Woods AS, Ferré S, Lluis C, Bouvier M, Franco R (2003) Adenosine A_{2A}-Dopamine D_2Receptor-Receptor Heteromerization. J Biol Chem 278:46741–46749
Canas PM, Porciuncula LO, Cunha GMA, Silva CG, Machado NJ, Oliveira JMA, Oliveira CR, Cunha RA (2009) Adenosine A2A Receptor Blockade Prevents Synaptotoxicity and Memory Dysfunction Caused by -Amyloid Peptides via p38 Mitogen-Activated Protein Kinase Pathway. J Neurosci 29:14741–14751
Caraiscos VB, Elliott EM, You-Ten KE, Cheng VY, Belelli D, Newell JG, Jackson MF, Lambert JJ, Rosahl TW, Wafford K a, MacDonald JF, Orser B a (2004) Tonic inhibition in mouse hippocampal CA1 pyramidal neurons is

mediated by alpha5 subunit-containing gamma-aminobutyric acid type A receptors. Proc Natl Acad Sci U S A 101:3662–3667.

Carman AJ, Dacks PA, Lane RF, Shineman DW, Fillit HM (2014) Current evidence for the use of coffee and caffeine to prevent age-related cognitive decline and Alzheimer's disease. J Nutr Health Aging 18:383–392

Carriba P, Ortiz O, Patkar K, Justinova Z, Stroik J, Themann A, Muller C, Woods AS, Hope BT, Ciruela F, Casadó V, Canela EI, Lluis C, Goldberg SR, Moratalla R, Franco R, Ferré S (2007) Striatal Adenosine A2A and Cannabinoid CB1 Receptors Form Functional Heteromeric Complexes that Mediate the Motor Effects of Cannabinoids. Neuropsychopharmacology 32:2249–2259

Chamberland S, Topolnik L (2012) Inhibitory control of hippocampal inhibitory neurons. Front Neurosci 6:1–13.

Chamma I, Heubl M, Chevy Q, Renner M, Moutkine I, Eugène E, Poncer JC, Lévi S (2013) Activity-dependent regulation of the K/Cl transporter KCC2 membrane diffusion, clustering, and function in hippocampal neurons. J Neurosci 33:15488–15503

Chandra D, Korpi ER, Miralles CP, De Blas AL, Homanics GE (2005) GABAA receptor gamma 2 subunit knockdown mice have enhanced anxiety-like behavior but unaltered hypnotic response to benzodiazepines. BMC Neurosci 6:30

Charalambous C, Gsandtner I, Keuerleber S, Milan-Lobo L, Kudlacek O, Freissmuth M, Zezula J (2008) Restricted collision coupling of the A2A receptor revisited: Evidence for physical separation of two signaling cascades. J Biol Chem 283:9276–9288.

Charrier C, Ehrensperger M-V, Dahan M, Levi S, Triller A (2006a) Cytoskeleton Regulation of Glycine Receptor Number at Synapses and Diffusion in the Plasma Membrane. J Neurosci 26:8502–8511

Charrier C, Ehrensperger M-V, Dahan M, Lévi S, Triller A (2006b) Cytoskeleton regulation of glycine receptor number at synapses and diffusion in the plasma membrane. J Neurosci 26:8502–8511.

Charrier C, Machado P, Tweedie-Cullen RY, Rutishauser D, Mansuy IM, Triller A (2010) A crosstalk between β1 and β3 integrins controls glycine receptor and gephyrin trafficking at synapses. Nat Neurosci 13:1388–1395

Chattopadhyaya B, Di Cristo G, Wu CZ, Knott G, Kuhlman S, Fu Y, Palmiter RD, Huang ZJ (2007) GAD67-Mediated GABA Synthesis and Signaling Regulate Inhibitory Synaptic Innervation in the Visual Cortex. Neuron 54:889–903

Che J, Chan ESL, Cronstein BN (2007) Adenosine A2A Receptor Occupancy Stimulates Collagen Expression by Hepatic Stellate Cells via Pathways Involving Protein Kinase A, Src, and Extracellular Signal-Regulated Kinases 1/2 Signaling Cascade or p38 Mitogen-Activated Protein Kinase Signaling Pathway. Mol Pharmacol 72:1626–1636

Chebib M, Johnston GAR (1999) The "ABC" of GABA receptors: a brief review. Clinical and Experimental Pharmacology and Physiology (1999) 26, 937–940

Chen AI, Nguyen CN, Copenhagen DR, Badurek S, Minichiello L, Ranscht B, Reichardt LF (2011) TrkB (tropomyosin-related kinase B) controls the assembly and maintenance of GABAergic synapses in the cerebellar cortex. J Neurosci 31:2769–2780

Chen JF, Huang Z, Ma J, Zhu J, Moratalla R, Standaert D, Moskowitz MA, Fink JS, Schwarzschild MA (1999) A(2A) adenosine receptor deficiency attenuates brain injury induced by transient focal ischemia in mice. J Neurosci 19:9192–9200

Chen JL, Villa KL, Cha JW, So PTC, Kubota Y, Nedivi E (2012) Clustered Dynamics of Inhibitory Synapses and Dendritic Spines in the Adult Neocortex. Neuron 74:361–373

Chetkovich DM, Gray R, Johnston D, Sweatt JD (1991) N-methyl-D-aspartate receptor activation increases cAMP levels and voltage-gated Ca2+ channel activity in area CA1 of hippocampus. Proc Natl Acad Sci U S A 88:6467–6471

Chevy Q, Heubl M, Goutierre M, Backer S, Moutkine I, Eugène E, Bloch-Gallego E, Lévi S, Poncer JC (2015) KCC2 Gates Activity-Driven AMPA Receptor Traffic through Cofilin Phosphorylation. J Neurosci 35:15772–15786.

Chih B, Engelman H, Scheiffele P (2005) Control of excitatory and inhibitory synapse formation by neuroligins. Science 307:1324–1328.

Choii G, Ko J (2015) Gephyrin: a central GABAergic synapse organizer. Exp Mol Med 47:e158 A

Choquet D, Triller A (2013) The dynamic synapse. Neuron 80:691–703

Christopherson KS, Ullian EM, Stokes CCA, Mullowney CE, Hell JW, Agah A, Lawler J, Mosher DF, Bornstein P, Barres BA (2005) Thrombospondins are astrocyte-secreted proteins that promote CNS synaptogenesis. Cell 120:421–433.

Chubykin A a, Atasoy D, Etherton MR, Brose N, Kavalali ET, Gibson JR, Südhof TC (2007) Activity-dependent validation of excitatory versus inhibitory synapses by neuroligin-1 versus neuroligin-2. Neuron 54:919–931

Chung W-S, Clarke LE, Wang GX, Stafford BK, Sher A, Chakraborty C, Joung J, Foo LC, Thompson A, Chen C, Smith SJ, Barres BA (2013) Astrocytes mediate synapse elimination through MEGF10 and MERTK pathways. Nature 504:394–400

Ciruela F, Casadó V, Rodrigues RJ, Luján R, Burgueño J, Canals M, Borycz J, Rebola N, Goldberg SR, Mallol J, Cortés A, Canela EI, López-Giménez JF, Milligan G, Lluis C, Cunha R a, Ferré S, Franco R (2006) Presynaptic control of striatal glutamatergic neurotransmission by adenosine A1-A2A receptor heteromers. J Neurosci 26:2080–2087

Cohen AS, Lin DD, Coulter DA (2000) Protracted postnatal development of inhibitory synaptic transmission in rat hippocampal area CA1 neurons. J Neurophysiol 84:2465–2476

Colgan SP, Eltzschig HK, Eckle T, Thompson LF (2006) Physiological roles for ecto-5'-nucleotidase (CD73). Purinergic Signal 2:351–360.

Comenencia-Ortiz E, Moss SJ, Davies PA (2014) Phosphorylation of GABAA receptors influences receptor trafficking and neurosteroid actions. Psychopharmacology (Berl) 231:3453–3465.

Connolly CN, Wooltorton JR, Smart TG, Moss SJ (1996) Subcellular localization of gamma-aminobutyric acid type A receptors is determined by receptor beta subunits. Proc Natl Acad Sci U S A 93:9899–9904.

Conti AC, Maas JW, Muglia LM, Dave BA, Vogt SK, Tran TT, Rayhel EJ, Muglia LJ (2007) Distinct regional and subcellular localization of adenylyl cyclases type 1 and 8 in mouse brain. Neuroscience 146:713–729

Cooper DMF, Tabbasum VG (2014) Adenylate cyclase-centred microdomains. Biochem J 462:199–213

Coppi E, Cellai L, Maraula G, Dettori I, Melani A, Pugliese AM, Pedata F (2015) Role of adenosine in oligodendrocyte precursor maturation. Front Cell Neurosci 9:155

Coppi E, Cellai L, Maraula G, Pugliese AM, Pedata F (2013) Adenosine A2A receptors inhibit delayed rectifier potassium currents and cell differentiation in primary purified oligodendrocyte cultures. Neuropharmacology 73:301–310

Corodimas KP, Tomita H (2001) Adenosine A1 receptor activation selectively impairs the acquisition of contextual fear conditioning in rats. Behav Neurosci 115:1283–1290.

Costenla AR, Diógenes MJ, Canas PM, Rodrigues RJ, Nogueira C, Maroco J, Agostinho PM, Ribeiro JA, Cunha RA, de Mendonça A (2011) Enhanced role of adenosine A 2A receptors in the modulation of LTP in the rat hippocampus upon ageing. Eur J Neurosci 34:12–21.

Coull JAM, Boudreau D, Bachand K, Prescott SA, Nault F, Sík A, De Koninck P, de Koninck Y (2003) Trans-synaptic shift in anion gradient in spinal lamina I neurons as a mechanism of neuropathic pain. Nature 424:938–942.

Craig AM, Kang Y (2007) Neurexin–neuroligin signaling in synapse development. Curr Opin Neurobiol 17:43–52

Craig CG, White TD (1993) N-Methyl-d-Aspartate- and Non-N-Methyl-d-Aspartate-Evoked Adenosine Release from Rat Cortical Slices: Distinct Purinergic Sources and Mechanisms of Release. J Neurochem 60:1073–1080.

Crestani F, Lorez M, Baer K, Essrich C, Benke D, Laurent JP, Belzung C, Fritschy J-M, L?scher B, Mohler H (1999) Decreased GABAA-receptor clustering results in enhanced anxiety and a bias for threat cues. Nat Neurosci 2:833–839

Cristo G Di, Wu C, Chattopadhyaya B, Ango F, Knott G, Welker E, Svoboda K, Huang ZJ (2004) Subcellular domain-restricted GABAergic innervation in primary visual cortex in the absence of sensory and thalamic inputs. Nat Neurosci 7:1184–1186

Cristóvão-Ferreira S, Navarro G, Brugarolas M, Pérez-Capote K, Vaz SH, Fattorini G, Conti F, Lluis C, Ribeiro JA, McCormick PJ, Casadó V, Franco R, Sebastião AM (2013) A1R-A2AR heteromers coupled to Gs and G i/0 proteins modulate GABA transport into astrocytes. Purinergic Signal 9:433–449

Cunha RA (2016) How does adenosine control neuronal dysfunction and neurodegeneration? J Neurochem.

Cunha RA, Johansson B, Fredholm BB, Ribeiro JA, Sebastião AM (1995) Adenosine A2A receptors stimulate

acetylcholine release from nerve terminals of the rat hippocampus. Neurosci Lett 196:41–44

Cunha RA, Ribeiro JA (2000) Purinergic modulation of [(3)H]GABA release from rat hippocampal nerve terminals. Neuropharmacology 39:1156–1167

Cunha RA, Vizi ES, Ribeiro JA, Sebastião AM (1996) Preferential release of ATP and its extracellular catabolism as a source of adenosine upon high- but not low-frequency stimulation of rat hippocampal slices. J Neurochem 67:2180–2187

Cunha RA, Johansson B, van der Ploeg I, Sebastião A, Ribeiro J, Fredholm B (1994) Evidence for functionally important adenosine A2a receptors in the rat hippocampus. Brain Res 649:208–216.

Dahan M, Lévi S, Luccardini C, Rostaing P, Riveau B, Triller A (2003) Diffusion dynamics of glycine receptors revealed by single-quantum dot tracking. Science 302:442–445.

Danglot L, Triller A, Marty S (2006) The development of hippocampal interneurons in rodents. Hippocampus 16:1032–1060

Darby M, Kuzmiski JB, Panenka W, Feighan D, MacVicar BA (2003) ATP Released From Astrocytes During Swelling Activates Chloride Channels. J Neurophysiol 89

Darcy KJ, Staras K, Collinson LM, Goda Y (2006) Constitutive sharing of recycling synaptic vesicles between presynaptic boutons. Nat Neurosci 9:315–321

Darman RB, Flemmer A, Forbush B (2001) Modulation of Ion Transport by Direct Targeting of Protein Phosphatase Type 1 to the Na-K-Cl Cotransporter. J Biol Chem 276:34359–34362.

De Blas AL (1996) Brain GABAA receptors studied with subunit-specific antibodies. Mol Neurobiol 12:55–71

de Lecea L, del Río JA, Soriano E (1995) Developmental expression of parvalbumin mRNA in the cerebral cortex and hippocampus of the rat. Brain Res Mol Brain Res 32:1–13

de Los Heros P, Alessi DR, Gourlay R, Campbell DG, Deak M, Macartney TJ, Kahle KT, Zhang J (2014) The WNK-regulated SPAK/OSR1 kinases directly phosphorylate and inhibit the K+-Cl- co-transporters. Biochem J 458:559–573.

de Mérici Domingues Paula T, Lioe Teh Shang F, Chiarini-Garcia H, Radicchi Campos Lobato de Almeida F (2017) Caffeine Intake during Pregnancy: What Are the Real Evidences? J Pharm Pharmacol 5:249–260

De Ponti C, Carini R, Alchera E, Nitti MP, Locati M, Albano E, Cairo G, Tacchini L (2007) Adenosine A2a receptor-mediated, normoxic induction of HIF-1 through PKC and PI-3K-dependent pathways in macrophages. J Leukoc Biol 82:392–402

de Wit J, Ghosh A (2014) Control of neural circuit formation by leucine-rich repeat proteins. Trends Neurosci 37:539–550

Deckert J, Nöthen MM, Franke P, Delmo C, Fritze J, Knapp M, Maier W, Beckmann H, Propping P (1998) Systematic mutation screening and association study of the A1 and A2a adenosine receptor genes in panic disorder suggest a contribution of the A2a gene to the development of disease. Mol Psychiatry 3:81–85

Del Río JA, Heimrich B, Borrell V, Förster E, Drakew A, Alcántara S, Nakajima K, Miyata T, Ogawa M, Mikoshiba K, Derer P, Frotscher M, Soriano E (1997) A role for Cajal–Retzius cells and reelin in the development of hippocampal connections. Nature 385:70–74

Delorme R, Ey E, Toro R, Leboyer M, Gillberg C, Bourgeron T (2013) Progress toward treatments for synaptic defects in autism. Nat Med 19:685–694

Delpire E, Days E, Lewis LM, Mi D, Kim K, Lindsley CW, Weaver CD (2009) Small-molecule screen identifies inhibitors of the neuronal K-Cl cotransporter KCC2. Proc Natl Acad Sci U S A 106:5383–5388.

Depry C, Allen MD, Zhang J (2011) Visualization of PKA activity in plasma membrane microdomains. Mol Biosyst 7:52–58

Desrivières S et al. (2015) Single nucleotide polymorphism in the neuroplastin locus associates with cortical thickness and intellectual ability in adolescents. Mol Psychiatry 20:263–274

Dias RB, Ribeiro JA, Sebastião AM (2012) Enhancement of AMPA currents and GluR1 membrane expression through PKA-coupled adenosine A 2A receptors. Hippocampus 22:276–291.

Diógenes MJ, Fernandes CC, Sebastião AM RJ (2004) Activation of Adenosine A2A Receptor Facilitates Brain-Derived Neurotrophic Factor Modulation of Synaptic Transmission in Hippocampal Slices. J Neurosci 24:2905–2913

Dixon AK, Gubitz AK, Sirinathsinghji DJ, Richardson PJ, Freeman TC (1996) Tissue distribution of adenosine receptor mRNAs in the rat. Br J Pharmacol 118:1461–1468

Dobie F, Craig A (2011) Inhibitory synapse dynamics: coordinated presynaptic and postsynaptic mobility and the major contribution of recycled vesicles to new synapse formation. J Neurosci 31:10481–10493

Dou Y, Wu H, Li H, Qin S, Wang Y, Li J, Lou H, Chen Z, Li X, Luo Q, Duan S (2012) Microglial migration mediated by ATP-induced ATP release from lysosomes. Cell Res 22:1022–1033

Doyon N, Prescott S a, Castonguay A, Godin AG, Kröger H, De Koninck Y (2011) Efficacy of synaptic inhibition depends on multiple, dynamically interacting mechanisms implicated in chloride homeostasis. PLoS Comput Biol 7:e1002149.

Drake-Baumann R (2006) Activity-dependent modulation of inhibition in Purkinje cells by TrkB ligands. Cerebellum 5:220–226

Dunwiddie T, Worth T (1982) Sedative and anticonvulsant effects of adenosine analogs in mouse and rat. J Pharmacol Exp Ther 220:70–76

Ehrensperger M-V, Hanus C, Vannier C, Triller A, Dahan M (2007) Multiple association states between glycine receptors and gephyrin identified by SPT analysis. Biophys J 92:3706–3718.

El Yacoubi M, Ledent C, Parmentier M, Bertorelli R, Ongini E, Costentin J, Vaugeois JM (2001) Adenosine A2A receptor antagonists are potential antidepressants: evidence based on pharmacology and A2A receptor knockout mice. Br J Pharmacol 134:68–77

Ellis C (2004) The state of GPCR research in 2004. Nat Rev Drug Discov 3:577–626

Ellis SE, Panitch R, West AB, Arking DE (2016) Transcriptome analysis of cortical tissue reveals shared sets of downregulated genes in autism and schizophrenia. Transl Psychiatry 6:e817

Emerit MB, Baranowski C, Diaz J, Martinez A, Areias J, Alterio J, Masson J, Boué-Grabot E, Darmon M (2016) A New Mechanism of Receptor Targeting by Interaction between Two Classes of Ligand-Gated Ion Channels. J Neurosci 36:1456–1470

Erlander MG, Tillakaratne NJ, Feldblum S, Patel N, Tobin AJ (1991) Two genes encode distinct glutamate decarboxylases. Neuron 7:91–100

Essrich C, Lorez M, Benson JA, Fritschy JM, Lüscher B (1998) Postsynaptic clustering of major GABAA receptor subtypes requires the gamma 2 subunit and gephyrin. Nat Neurosci 1:563–571

Esumi S, Kakazu N, Taguchi Y, Hirayama T, Sasaki A, Hirabayashi T, Koide T, Kitsukawa T, Hamada S, Yagi T (2005) Monoallelic yet combinatorial expression of variable exons of the protocadherin-α gene cluster in single neurons. Nat Genet 37:171–176

Etherton M, Földy C, Sharma M, Tabuchi K, Liu X, Shamloo M, Malenka RC, Südhof TC (2011) Autism-linked neuroligin-3 R451C mutation differentially alters hippocampal and cortical synaptic function. Proc Natl Acad Sci U S A 108:13764–13769

Etzel BA, Guillet R (1994) Effects of neonatal exposure to caffeine on adenosine A1 receptor ontogeny using autoradiography. Dev Brain Res 82:223–230.

Eugène E, Depienne C, Baulac S, Baulac M, Fritschy JM, Le Guern E, Miles R, Poncer JC (2007) GABA(A) receptor gamma 2 subunit mutations linked to human epileptic syndromes differentially affect phasic and tonic inhibition. J Neurosci 27:14108–14116

Fang C, Deng L, Keller CA, Fukata M, Fukata Y, Chen G, Lüscher B (2006) GODZ-mediated palmitoylation of GABA(A) receptors is required for normal assembly and function of GABAergic inhibitory synapses. J Neurosci 26:12758–12768

Fannon AM, Colman DR (1996) A model for central synaptic junctional complex formation based on the differential adhesive specificities of the cadherins. Neuron 17:423–434 A

Farrant M, Nusser Z (2005) Variations on an inhibitory theme: Phasic and tonic activation of GABA A receptors. Nat Rev Neuro6:1–4.

Ferguson GD, Storm DR (2004) Why Calcium-Stimulated Adenylyl Cyclases? Physiology 19 .

Fernandes CC, Pinto-Duarte A, Ribeiro JA, Sebastiao AM (2008) Postsynaptic Action of Brain-Derived Neurotrophic Factor Attenuates 7 Nicotinic Acetylcholine Receptor-Mediated Responses in Hippocampal Interneurons. J Neurosci 28:5611–5618

Fernandez-Alfonso T, Ryan TA (2008) A heterogeneous "resting" pool of synaptic vesicles that is dynamically interchanged across boutons in mammalian CNS synapses. Brain Cell Biol 36:87–100

Fernandez-Enright F, Andrews JL, Newell K a, Pantelis C, Huang XF (2014) Novel implications of Lingo-1 and its signaling partners in schizophrenia. Transl Psychiatry 4:e348.

Ferre S, Karcz-Kubicha M, Hope BT, Popoli P, Burgueno J, Gutierrez MA, Casado V, Fuxe K, Goldberg SR, Lluis C, Franco R, Ciruela F (2002) Synergistic interaction between adenosine A2A and glutamate mGlu5 receptors: Implications for striatal neuronal function. Proc Natl Acad Sci 99:11940–11945

Fink JS, Weaver DR, Rivkees SA, Peterfreund RA, Pollack AE, Adler EM, Reppert SM (1992) Molecular cloning of the rat A2 adenosine receptor: selective co-expression with D2 dopamine receptors in rat striatum. Brain Res Mol Brain Res 14:186–195

Fiumelli H, Cancedda L, Poo MM (2005) Modulation of GABAergic transmission by activity via postsynaptic Ca 2+-dependent regulation of KCC2 function. Neuron 48:773–786.

Flores CE, Nikonenko I, Mendez P, Fritschy J-M, Tyagarajan SK, Muller D (2014) Activity-dependent inhibitory synapse remodeling through gephyrin phosphorylation. Proc Natl Acad Sci U S A

Florio C, Prezioso A, Papaioannou A, Vertua R (1998) Adenosine A1 receptors modulate anxiety in CD1 mice. Psychopharmacol 136:311–319

Fontinha BM, Delgado-García JM, Madroñal N, Ribeiro JA, Sebastião AM, Gruart A (2009) Adenosine A2A Receptor Modulation of Hippocampal CA3-CA1 Synapse Plasticity During Associative Learning in Behaving Mice. Neuropsychopharmacology 34:1865–1874

Fossati M, Pizzarelli R, Schmidt ER, Kupferman J V, Stroebel D, Fossati M, Pizzarelli R, Schmidt ER, Kupferman J V, Stroebel D, Polleux F (2016) Regulate the Development of Excitatory and Inhibitory Synapses SRGAP2 and Its Human-Specific Paralog Co-Regulate the Development of Excitatory and Inhibitory Synapses.Neuron 91 :1–14.

Fredholm BB (1995) Adenosine, Adenosine Receptors and the Actions of Caffeine. Pharmacol Toxicol 76:93–101.

Fredholm BB, Bättig K, Holmén J, Nehlig A, Zvartau EE (1999) Actions of Caffeine in the Brain with Special Reference to Factors That Contribute to Its Widespread Use. Pharmacological reviews 51.

Fredholm BB, Chen JF, Cunha RA, Svenningsson P, Vaugeois JM (2005) Adenosine and Brain Function. Int Rev Neurobiol 63:191–270.

Frias CP, Wierenga CJ (2013) Activity-dependent adaptations in inhibitory axons. Front Cell Neurosci 7

Friedel P, Kahle KT, Zhang J, Hertz N, Pisella LI, Buhler E, Schaller F, Duan J, Khanna AR, Bishop PN, Shokat KM, Medina I (2015) WNK1-regulated inhibitory phosphorylation of the KCC2 cotransporter maintains the depolarizing action of GABA in immature neurons. Sci Signal 8:ra65.

Fritschy J-M, Panzanelli P, Kralic JE, Vogt KE, Sassoè-Pognetto M (2006) Differential Dependence of Axo-Dendritic and Axo-Somatic GABAergic Synapses on GABAA Receptors Containing the ?1 Subunit in Purkinje Cells. J Neurosci 26:3245–3255

Frotscher M (1998) Cajal-Retzius cells, Reelin, and the formation of layers. Curr Opin Neurobiol 8:570–575

Früh S, Romanos J, Panzanelli P, Bürgisser D, Tyagarajan SK, Campbell KP, Santello M, Fritschy J-M (2016) Neuronal Dystroglycan Is Necessary for Formation and Maintenance of Functional CCK-Positive Basket Cell Terminals on Pyramidal Cells. J Neurosci 36:10296–10313

Fuchs C, Abitbol K, Burden JJ, Mercer A, Brown L, Iball J, Anne Stephenson F, Thomson AM, Jovanovic JN (2013) GABAA receptors can initiate the formation of functional inhibitory GABAergic synapses. Eur J Neurosci 38:3146–3158.

Fuenzalida M, Espinoza C, Pérez MÁ, Tapia-Rojas C, Cuitino L, Brandan E, Inestrosa NC (2016) Wnt signaling pathway improves central inhibitory synaptic transmission in a mouse model of Duchenne muscular dystrophy. Neurobiol Dis 86:109–120

Fukaya M, Kamata A, Hara Y, Tamaki H, Katsumata O, Ito N, Takeda S, Hata Y, Suzuki T, Watanabe M, Harvey RJ, Sakagami H (2011) SynArfGEF is a guanine nucleotide exchange factor for Arf6 and localizes preferentially at post-synaptic specializations of inhibitory synapses. J Neurochem 116:1122–1137

Gagnon KB, Delpire E (2010) Multiple pathways for protein phosphatase 1 (PP1) regulation of Na-K-2Cl cotransporter (NKCC1) function: The N-terminal tail of the Na-K-2Cl cotransporter serves as a regulatory

scaffold for Ste20-related proline/alanine-rich kinase (SPAK) and PP1. J Biol Chem 285:14115–14121.
Gallagher MJ (2004) The Juvenile Myoclonic Epilepsy GABAA Receptor 1 Subunit Mutation A322D Produces Asymmetrical, Subunit Position-Dependent Reduction of Heterozygous Receptor Currents and 1 Subunit Protein Expression. J Neurosci 24:5570–5578
Ganguly K, Schinder AF, Wong ST, Poo M ming (2001) GABA itself promotes the developmental switch of neuronal GABAergic responses from excitation to inhibition. Cell 105:521–532.
Garção P, Szabó EC, Wopereis S, Castro AA, Tomé ÂR, Prediger RD, Cunha RA, Agostinho P, Köfalvi A (2013) Functional interaction between pre-synaptic α6β2-containing nicotinic and adenosine A $_{2A}$ receptors in the control of dopamine release in the rat striatum. Br J Pharmacol 169:1600–1611
Gauvain G, Chamma I, Chevy Q, Cabezas C, Irinopoulou T, Bodrug N, Carnaud M, Lévi S, Poncer JC (2011) The neuronal K-Cl cotransporter KCC2 influences postsynaptic AMPA receptor content and lateral diffusion in dendritic spines. Proc Natl Acad Sci U S A 108:15474–15479.
Genovese T, Melani A, Esposito E, Mazzon E, Di Paola R, Bramanti P, Pedata F, Cuzzocrea S (2009) The selective adenosine a2a receptor agonist cgs 21680 reduces jnk mapk activation in oligodendrocytes in injured spinal cord. Shock 32:578–585
George J, Cunha RA, Mulle C, Amédée T (2016) Microglia-derived purines modulate mossy fibre synaptic transmission and plasticity through P2X4 and A1 receptors. Eur J Neurosci 43:1366–1378.
George J, Gonçalves FQ, Cristóvão G, Rodrigues L, Meyer Fernandes JR, Gonçalves T, Cunha R a, Gomes C a (2015) Different danger signals differently impact on microglial proliferation through alterations of ATP release and extracellular metabolism. Glia
Ghosh A, Michalon A, Lindemann L, Fontoura P, Santarelli L (2013) Drug discovery for autism spectrum disorder: challenges and opportunities. Nat Rev Drug Discov 12:777–790
Ghosh H, Auguadri L, Battaglia S, Simone Thirouin Z, Zemoura K, Messner S, Acu?a MA, Wildner H, Y?venes GE, Dieter A, Kawasaki H, O. Hottiger M, Zeilhofer HU, Fritschy J-M, Tyagarajan SK (2016) Several posttranslational modifications act in concert to regulate gephyrin scaffolding and GABAergic transmission. Nat Commun 7:13365
Gimenez-Llort L et al. (2007) Working memory deficits in transgenic rats overexpressing human adenosine A2A receptors in the brain. Neurobiol Learn Mem 87:42–56.
Giménez-Llort L, Fernández-Teruel A, Escorihuela RM, Fredholm BB, Tobeña A, Pekny M, Johansson B (2002) Mice lacking the adenosine A1 receptor are anxious and aggressive, but are normal learners with reduced muscle strength and survival rate. Eur J Neurosci 16:547–550
Glykys J, Mann EO, Mody I (2008) Which GABA(A) receptor subunits are necessary for tonic inhibition in the hippocampus? J Neurosci 28:1421–1426.
Glynn MW, Elmer BM, Garay PA, Liu X-B, Needleman LA, El-Sabeawy F, McAllister AK (2011) MHCI negatively regulates synapse density during the establishment of cortical connections. Nat Neurosci 14:442–451
Gokce O, Südhof TC (2013) Membrane-tethered monomeric neurexin LNS-domain triggers synapse formation. J Neurosci 33:14617–14628
Gracia E, Perez-Capote K, Moreno E, Barkejov J, Mallol J, Lluis C, Franco R, Cortes A, Casado V, Canela E (2011) A $_{2A}$ adenosine receptor ligand binding and signalling is allosterically modulated by adenosine deaminase. Biochem J 435:701–709
Graf ER, Zhang X, Jin S-X, Linhoff MW, Craig AM (2004) Neurexins induce differentiation of GABA and glutamate postsynaptic specializations via neuroligins. Cell 119:1013–1026
Grimley JS, Li L, Wang W, Wen L, Beese LS, Hellinga HW, Augustine GJ (2013) Visualization of Synaptic Inhibition with an Optogenetic Sensor Developed by Cell-Free Protein Engineering Automation. J Neurosci 33:16297–16309.
Groban ES, Narayanan A, Jacobson MP (2006) Conformational changes in protein loops and helices induced by post-translational phosphorylation. PLoS Comput Biol 2:238–250.
Gubitz AK, Widdowson L, Kurokawa M, Kirkpatrick KA, Richardson PJ (1996) Dual signalling by the adenosine A2a receptor involves activation of both N- and P-type calcium channels by different G proteins and protein kinases in the same striatal nerve terminals. J Neurochem 67:374–381

Gundlfinger a, Bischofberger J, Johenning FW, Torvinen M, Schmitz D, Breustedt J (2007) Adenosine modulates transmission at the hippocampal mossy fibre synapse via direct inhibition of presynaptic calcium channels. J Physiol 582:263–277

Günther U, Benson J, Benke D, Fritschy JM, Reyes G, Knoflach F, Crestani F, Aguzzi A, Arigoni M, Lang Y (1995) Benzodiazepine-insensitive mice generated by targeted disruption of the gamma 2 subunit gene of gamma-aminobutyric acid type A receptors. Proc Natl Acad Sci U S A 92:7749–7753.

Hall AC, Lucas FR, Salinas PC (2000) Axonal remodeling and synaptic differentiation in the cerebellum is regulated by WNT-7a signaling. Cell 100:525–535

Hamilton SP, Slager SL, de Leon AB, Heiman GA, Klein DF, Hodge SE, Weissman MM, Fyer AJ, Knowles JA (2004) Evidence for Genetic Linkage Between a Polymorphism in the Adenosine 2A Receptor and Panic Disorder. Neuropsychopharmacology 29:558–565

Hanus C, Ehrensperger M-V, Triller A (2006) Activity-dependent movements of postsynaptic scaffolds at inhibitory synapses. J Neurosci 26:4586–4595.

Harris JJ, Jolivet R, Attwell D (2012) Synaptic Energy Use and Supply. Neuron 75:762–777.

Harris KM, Weinberg RJ (2012) Ultrastructure of synapses in the mammalian brain. Cold Spring Harb Perspect Biol 4:7.

Hashimoto K, Ichikawa R, Takechi H, Inoue Y, Aiba A, Sakimura K, Mishina M, Hashikawa T, Konnerth A, Watanabe M, Kano M (2001) Roles of glutamate receptor delta 2 subunit (GluRdelta 2) and metabotropic glutamate receptor subtype 1 (mGluR1) in climbing fiber synapse elimination during postnatal cerebellar development. J Neurosci 21:9701–9712

Hauser RA, Shulman LM, Trugman JM, Roberts JW, Mori A, Ballerini R, Sussman NM, Istradefylline 6002-US-013 Study Group (2008) Study of istradefylline in patients with Parkinson's disease on levodopa with motor fluctuations. Mov Disord 23:2177–2185

Hausrat TJ, Muhia M, Gerrow K, Thomas P, Hirdes W, Tsukita S, Heisler FF, Herich L, Dubroqua S, Breiden P, Feldon J, Schwarz JR, Yee BK, Smart TG, Triller A, Kneussel M (2015) Radixin regulates synaptic GABAA receptor density and is essential for reversal learning and short-term memory. Nat Commun 6:6872

Hawkes CH (1978) Dipyridamole in migraine. Lancet (London, England) 2:153

Hayano Y, Sasaki K, Ohmura N, Takemoto M, Maeda Y, Yamashita T, Hata Y, Kitada K, Yamamoto N (2014) Netrin-4 regulates thalamocortical axon branching in an activity-dependent fashion. Proc Natl Acad Sci 111:15226–15231

Hayashi T, Okabe T, Nasu-Nishimura Y, Sakaue F, Ohwada S, Matsuura K, Akiyama T, Nakamura T (2007) PX-RICS, a novel splicing variant of RICS, is a main isoform expressed during neural development. Genes to Cells 12:929–939

Heine C, Heimrich B, Vogt J, Wegner a, Illes P, Franke H (2006) P2 receptor-stimulation influences axonal outgrowth in the developing hippocampus in vitro. Neuroscience 138:303–311

Heller EA, Zhang W, Selimi F, Earnheart JC, Slimak MA, Santos-Torres J, Ibañez-Tallon I, Aoki C, Chait BT, Heintz N (2012) The biochemical anatomy of cortical inhibitory synapses. PLoS One 7.

Henkemeyer M, Itkis OS, Ngo M, Hickmott PW, Ethell IM (2003) Multiple EphB receptor tyrosine kinases shape dendritic spines in the hippocampus. J Cell Biol 163:1313–1326

Hennou S, Khalilov I, Diabira D, Ben-Ari Y, Gozlan H (2002) Early sequential formation of functional GABAA and glutamatergic synapses on CA1 interneurons of the rat foetal hippocampus. Eur J Neurosci 16:197–208.

Hong EJ, McCord AE, Greenberg ME (2008) A biological function for the neuronal activity-dependent component of Bdnf transcription in the development of cortical inhibition. Neuron 60:610–624

Hoon M, Soykan T, Falkenburger B, Hammer M, Patrizi A, Schmidt K-FK-F, Sassoe-Pognetto M, Lowel S, Moser T, Taschenberger H, Brose N, Varoqueaux F, Sassoè-Pognetto M, Löwel S, Moser T, Taschenberger H, Brose N, Varoqueaux F (2011) Neuroligin-4 is localized to glycinergic postsynapses and regulates inhibition in the retina. Proc Natl Acad Sci 108:3053–3058

Hornbeck P V., Zhang B, Murray B, Kornhauser JM, Latham V, Skrzypek E (2015) PhosphoSitePlus, 2014: mutations, PTMs and recalibrations. Nucleic Acids Res 43:D512–D520

Howarth C, Gleeson P, Attwell D (2012) Updated energy budgets for neural computation in the neocortex and

cerebellum. J Cereb Blood Flow Metab 32:1222–1232.
Hua JY, Smith SJ (2004) Neural activity and the dynamics of central nervous system development. Nat Neurosci 7:327–332
Huang Z, Scheiffele P (2008) GABA and neuroligin signaling: linking synaptic activity and adhesion in inhibitory synapse development. Curr Opin Neurobiol 18:77–83
Huang ZJ (2009) Activity-dependent development of inhibitory synapses and innervation pattern: role of GABA signalling and beyond. J Physiol 587:1881–1888
Huang ZJ, Di Cristo G, Ango F (2007) Development of GABA innervation in the cerebral and cerebellar cortices. Nat Rev Neurosci 8:673–686
Huang ZL, Qu WM, Eguchi N, Chen JF, Schwarzschild MA, Fredholm BB, Urade Y, Hayaishi O (2005) Adenosine A2A, but not A1, receptors mediate the arousal effect of caffeine. Nat Neurosci 8:858–859
Huberfeld G, Wittner L, Clemenceau S, Baulac M, Kaila K, Miles R, Rivera C (2007) Perturbed chloride homeostasis and GABAergic signaling in human temporal lobe epilepsy. J Neurosci 27:9866–9873.
Hughes EG, Elmariah SB, Balice-Gordon RJ (2010) Astrocyte secreted proteins selectively increase hippocampal GABAergic axon length, branching, and synaptogenesis. Mol Cell Neurosci 43:136–145
Iglesias R, Dahl G, Qiu F, Spray DC, Scemes E (2009) Pannexin 1 The molecular substrate of astrocyte "hemmichannels." J Neurosci 29:7092–7097.
Irie M, Hata Y, Takeuchi M, Ichtchenko K, Toyoda A, Hirao K, Takai Y, Rosahl TW, Südhof TC (1997) Binding of neuroligins to PSD-95. Science 277:1511–1515
Jackisch R, Fehr R, Hertting G (1985) Adenosine: an endogenous modulator of hippocampal noradrenaline release. Neuropharmacology 24:499–507
Jacob TC, Moss SJ, Jurd R (2008) GABAA receptor trafficking and its role in the dynamic modulation of neuronal inhibition. Nat Rev Neurosci 9:331–343
Jacobson KA (2009) Adenosine Receptors in Health and Disease. Hand Exp Pharmacol 193:1–23
Jacobson K, Gao Z (2006) Adenosine receptors as therapeutic targets. Nat Rev Drug Discov 5:247–264
Jamain S et al. (2003) Mutations of the X-linked genes encoding neuroligins NLGN3 and NLGN4 are associated with autism. Nat Genet 34:27–29
Jamain S, Radyushkin K, Hammerschmidt K, Granon S, Boretius S, Varoqueaux F, Ramanantsoa N, Gallego J, Ronnenberg A, Winter D, Frahm J, Fischer J, Bourgeron T, Ehrenreich H, Brose N (2008) Reduced social interaction and ultrasonic communication in a mouse model of monogenic heritable autism. Proc Natl Acad Sci U S A 105:1710–1715
Jarvis MF, Williams M (1989) Direct autoradiographic localization of adenosine A2 receptors in the rat brain using the A2-selective agonist, [3H]CGS 21680. Eur J Pharmacol 168:243–246
Jean YY, Lercher LD, Dreyfus CF (2009) Glutamate elicits release of BDNF from basal forebrain astrocytes in a process dependent on metabotropic receptors and the PLC pathway. Neuron Glia Biol 4:35
Jefferis BJMH, Power C, Hertzman C (2002) Birth weight, childhood socioeconomic environment, and cognitive development in the 1958 British birth cohort study. BMJ 325:305.
Jeon SJ, Rhee SY, Ryu JH, Cheong JH, Kwon K, Yang S-I, Park SH, Lee J, Kim HY, Han S-H, Ko KH, Shin CY (2011) Activation of adenosine A2A receptor up-regulates BDNF expression in rat primary cortical neurons. Neurochem Res 36:2259–2269
Johansson B, Fredholm BB (1995) Further characterization of the binding of the adenosine receptor agonist [3H]CGS 21680 to rat brain using autoradiography. Neuropharmacology 34:393–403
Johansson B, Georgiev V, Fredholm B. (1997) Distribution and postnatal ontogeny of adenosine A2A receptors in rat brain: comparison with dopamine receptors. Neuroscience 80:1187–1207
Johansson B, Halldner L, Dunwiddie T V, Masino SA, Poelchen W, Giménez-Llort L, Escorihuela RM, Fernández-Teruel A, Wiesenfeld-Hallin Z, Xu XJ, Hårdemark A, Betsholtz C, Herlenius E, Fredholm BB (2001) Hyperalgesia, anxiety, and decreased hypoxic neuroprotection in mice lacking the adenosine A1 receptor. Proc Natl Acad Sci U S A 98:9407–9412
Jung J, Shin YH, Konishi H, Lee SJ, Kiyama H (2013) Possible ATP release through lysosomal exocytosis from primary sensory neurons. Biochem Biophys Res Commun 430:488–493

Jungling K, Eulenburg V, Moore R, Kemler R, Lessmann V, Gottmann K (2006) N-Cadherin Transsynaptically Regulates Short-Term Plasticity at Glutamatergic Synapses in Embryonic Stem Cell-Derived Neurons. J Neurosci 26:6968–6978

Kähler AK, Djurovic S, Kulle B, Jönsson EG, Agartz I, Hall H, Opjordsmoen S, Jakobsen KD, Hansen T, Melle I, Werge T, Steen VM, Andreassen OA (2008) Association analysis of schizophrenia on 18 genes involved in neuronal migration: *MDGA1* as a new susceptibility gene. Am J Med Genet Part B Neuropsychiatr Genet 147B:1089–1100

Kaila K, Price TJ, Payne J a, Puskarjov M, Voipio J (2014) Cation-chloride cotransporters in neuronal development, plasticity and disease. Nat Publ Gr 15:637–654.

Kalscheuer VM, Musante L, Fang C, Hoffmann K, Fuchs C, Carta E, Deas E, Venkateswarlu K, Menzel C, Ullmann R, Tommerup N, Dalprà L, Tzschach A, Selicorni A, Lüscher B, Ropers H-H, Harvey K, Harvey RJ (2009) A balanced chromosomal translocation disrupting *ARHGEF9* is associated with epilepsy, anxiety, aggression, and mental retardation. Hum Mutat 30:61–68

Kandratavicius L, Alves Balista P, Lopes-Aguiar C, Ruggiero RN, Umeoka EH, Garcia-Cairasco N, Bueno-Junior LS, Leite JP (2014) Animal models of epilepsy: Use and limitations. Neuropsychiatr Dis Treat 10:1693–1705.

Kang Y, Ge Y, Cassidy RM, Lam V, Luo L, Moon K-M, Lewis R, Molday RS, Wong ROL, Foster LJ, Craig AM (2014) A combined transgenic proteomic analysis and regulated trafficking of neuroligin-2. J Biol Chem 289:29350–29364

Kanno T, Nishizaki T (2012) A2a adenosine receptor mediates PKA-dependent glutamate release from synaptic-like vesicles and Ca2+ efflux from an IP3- and ryanodine-insensitive intracellular calcium store in astrocytes. Cell Physiol Biochem 30:1398–1412.

Kano M, Hashimoto K, Chen C, Abeliovich A, Aiba A, Kurihara H, Watanabe M, Inoue Y, Tonegawa S (1995) Impaired synapse elimination during cerebellar development in PKC gamma mutant mice. Cell 83:1223–1231

Kayser MS, Nolt MJ, Dalva MB (2008) EphB Receptors Couple Dendritic Filopodia Motility to Synapse Formation. Neuron 59:56–69

Keck T, Scheuss V, Jacobsen RI, Wierenga CJ, Eysel UT, Bonhoeffer T, Hübener M (2011) Loss of sensory input causes rapid structural changes of inhibitory neurons in adult mouse visual cortex. Neuron 71:869–882

Kenny EM, Cormican P, Furlong S, Heron E, Kenny G, Fahey C, Kelleher E, Ennis S, Tropea D, Anney R, Corvin AP, Donohoe G, Gallagher L, Gill M, Morris DW (2014) Excess of rare novel loss-of-function variants in synaptic genes in schizophrenia and autism spectrum disorders. Mol Psychiatry 19:872–879

Kepecs A, Fishell G (2014) Interneuron cell types are fit to function. Nature 505:318–326

Kerschensteiner D, Morgan JL, Parker ED, Lewis RM, Wong ROL (2009) Neurotransmission selectively regulates synapse formation in parallel circuits in vivo. Nature 460

Kettenmann H, Hanisch U-K, Noda M, Verkhratsky A (2011) Physiology of Microglia. Physiol Rev 91:461–553

Keuerleber S, Gsandtner I, Freissmuth M (2011) From cradle to twilight: The carboxyl terminus directs the fate of the A 2A-adenosine receptor. Biochim Biophys Acta - Biomembr 1808:1350–1357

Kikuchi E, Mori T, Zeniya M, Isobe K, Ishigami-Yuasa M, Fujii S, Kagechika H, Ishihara T, Mizushima T, Sasaki S, Sohara E, Rai T, Uchida S (2015) Discovery of Novel SPAK Inhibitors That Block WNK Kinase Signaling to Cation Chloride Transporters. J Am Soc Nephrol 26:1525–1536.

Kim CS, Johnston D (2015) A1 adenosine receptor-mediated GIRK channels contribute to the resting conductance of CA1 neurons in the dorsal hippocampus. J Neurophysiol 113:2511–2523

Kirsch J, Kuhse J, Betz H (1995) Targeting of Glycine Receptor Subunits to Gephyrin-Rich Domains in Transfected Human Embryonic Kidney Cells. Mol Cell Neurosci 6:450–461

Kitamura A, Ishibashi H, Watanabe M, Takatsuru Y, Brodwick M, Nabekura J (2008) Sustained depolarizing shift of the GABA reversal potential by glutamate receptor activation in hippocampal neurons. Neurosci Res 62:270–277.

Klausberger T, Somogyi P (2008) Neuronal Diversity and Temporal Dynamics: The Unity of Hippocampal Circuit Operations. Science 321:53–57

Kleijer KTE, Schmeisser MJ, Krueger DD, Boeckers TM, Scheiffele P, Bourgeron T, Brose N, Burbach JPH (2014)

Neurobiology of autism gene products: towards pathogenesis and drug targets. Psychopharmacology (Berl) 231:1037–1062.

Kleppisch T (2009) Phosphodiesterases in the Central Nervous System. In: cGMP: Generators, Effectors and Therapeutic Implications, pp 71–92. Berlin, Heidelberg: Springer Berlin Heidelberg.

Klinger M, Kuhn M, Just H, Stefan E, Palmer T, Freissmuth M, Nanoff C (2002) Removal of the carboxy terminus of the A 2A-adenosine receptor blunts constitutive activity: Differential effect on cAMP accumulation and MAP kinase stimulation. Naunyn Schmiedebergs Arch Pharmacol 366:287–298.

Klishin A, Lozovaya N, Krishtal O (1995) A1 adenosine receptors differentially regulate the N-methyl-d-aspartate and non-N-methyl-d-aspartate receptor-mediated components of hippocampal excitatory postsynaptic current in a Ca2+/Mg2+-dependent manner. Neuroscience 65:947–953.

Klyuch BP, Dale N, Wall MJ (2012) Deletion of ecto-5'-nucleotidase (CD73) reveals direct action potential-dependent adenosine release. J Neurosci 32:3842–3847

Knott GW, Quairiaux C, Genoud C, Welker E (2002) Formation of dendritic spines with GABAergic synapses induced by whisker stimulation in adult mice. Neuron 34:265–273

Ko J, Choii G, Um JW (2015) The balancing act of GABAergic synapse organizers. Trends Mol Med 21:256–268

Kozorovitskiy Y, Peixoto R, Wang W, Saunders A, Sabatini BL (2015) Neuromodulation of excitatory synaptogenesis in striatal development. Elife 4:1–18.

Kriebel M, Metzger J, Trinks S, Chugh D, Harvey RJ, Harvey K, Volkmer H (2011) The cell adhesion molecule neurofascin stabilizes axo-axonic GABAergic terminals at the axon initial segment. J Biol Chem 286:24385–24393

Krishnaswamy A, Yamagata M, Duan X, Hong YK, Sanes JR (2015) Sidekick 2 directs formation of a retinal circuit that detects differential motion. Nature 524:466–470

Krueger-Burg D, Papadopoulos T, Brose N (2017) Organizers of inhibitory synapses come of age. Curr Opin Neurobiol 45:66–77

Krueger SR, Kolar A, Fitzsimonds RM (2003) The presynaptic release apparatus is functional in the absence of dendritic contact and highly mobile within isolated axons. Neuron 40:945–957

Kulesskaya N, Võikar V, Peltola M, Yegutkin GG, Salmi M, Jalkanen S, Rauvala H (2013) CD73 is a major regulator of adenosinergic signalling in mouse brain. PLoS One 8:e66896

Kuzirian MS, Moore AR, Staudenmaier EK, Friedel RH, Paradis S (2013) The Class 4 Semaphorin Sema4D Promotes the Rapid Assembly of GABAergic Synapses in Rodent Hippocampus. J Neurosci 33:8961–8973

Kwon H-B, Sabatini BL (2011) Glutamate induces de novo growth of functional spines in developing cortex. Nature 474:100–104

Lam P, Hong C-J, Tsai S-J (2005) Association study of A2a adenosine receptor genetic polymorphism in panic disorder. Neurosci Lett 378:98–101.

Lange K, Brandt U (1993) Rapid uptake of calcium, ATP, and inositol 1,4,5-trisphosphate via cation and anion channels into surface-derived vesicles from HIT cells containing the inositol 1,4,5-trisphosphate-sensitive calcium store. FEBS Lett 325:205–209.

Lara DR, Brunstein MG, Ghisolfi ES, Lobato MI, Belmonte-de-Abreu P, Souza DO (2001) Allopurinol augmentation for poorly responsive schizophrenia. Int Clin Psychopharmacol 16:235–237

Lardi-Studler B, Smolinsky B, Petitjean CM, Koenig F, Sidler C, Meier JC, Fritschy J-M, Schwarz G (2007) Vertebrate-specific sequences in the gephyrin E-domain regulate cytosolic aggregation and postsynaptic clustering. J Cell Sci 120:1371–1382.

Lauder JM, Liu J, Devaud L, Morrow AL (1998) GABA as a trophic factor for developing monoamine neurons. Perspect Dev Neurobiol 5:247–259

Lazarowski ER, Boucher RC, Harden TK (2000) Constitutive release of ATP and evidence for major contribution of ecto-nucleotide pyrophosphatase and nucleoside diphosphokinase to extracellular nucleotide concentrations. J Biol Chem 275:31061–31068.

Le Vay S, Wiesel TN, Hubel DH (1980) The development of ocular dominance columns in normal and visually deprived monkeys. J Comp Neurol 191:1–51

Ledent C, Vaugeois JM, Schiffmann SN, Pedrazzini T, El Yacoubi M, Vanderhaeghen JJ, Costentin J, Heath JK,

Vassart G, Parmentier M (1997) Aggressiveness, hypoalgesia and high blood pressure in mice lacking the adenosine A2a receptor. Nature 388:674–678

Lee FS, Chao M V (2001) Activation of Trk neurotrophin receptors in the absence of neurotrophins. Proc Natl Acad Sci U S A 98:3555–3560

Lee HHC, Deeb TZ, Walker JA, Davies PA, Moss SJ (2011) NMDA receptor activity downregulates KCC2 resulting in depolarizing GABAA receptor-mediated currents. Nat Neurosci 14:736–743.

Lee K, Kim Y, Lee S-J, Qiang Y, Lee D, Lee HW, Kim H, Je HS, Südhof TC, Ko J (2013) MDGAs interact selectively with neuroligin-2 but not other neuroligins to regulate inhibitory synapse development. Proc Natl Acad Sci U S A 110:336–341

Leinekugel X, Tseeb V, Ben-ari Y, Bregestovski P, Port-royal B De (1995) Synaptic GABAA activation induces Ca2+ rise in pyramidal cells and interneurons from rat neonatal hippocampal slices. Journal of Physiology 487:319–329.

León D, Albasanz JL, Ruíz MA, Iglesias I, Martín M (2005) Effect of chronic gestational treatment with caffeine or theophylline on Group I metabotropic glutamate receptors in maternal and fetal brain. J Neurochem 94:440–451.

Levinson JN, Chéry N, Huang K, Wong TP, Gerrow K, Kang R, Prange O, Wang YT, El-Husseini A (2005) Neuroligins mediate excitatory and inhibitory synapse formation: involvement of PSD-95 and neurexin-1beta in neuroligin-induced synaptic specificity. J Biol Chem 280:17312–17319

Li H, Khirug S, Cai C, Ludwig A, Blaesse P, Kolikova J, Afzalov R, Coleman SK, Lauri S, Airaksinen MS, Keinänen K, Khiroug L, Saarma M, Kaila K, Rivera C (2007a) KCC2 Interacts with the Dendritic Cytoskeleton to Promote Spine Development. Neuron 56:1019–1033.

Li J, Ashley J, Budnik V, Bhat MA (2007b) Crucial role of Drosophila neurexin in proper active zone apposition to postsynaptic densities, synaptic growth, and synaptic transmission. Neuron 55:741–755

Li R, Yu W, Christie S, Miralles CP, Bai J, Loturco JJ, Blas AL De (2005) Disruption of postsynaptic GABA A receptor clusters leads to decreased GABAergic innervation of pyramidal neurons. Journal of Neurochemistry 95:756–770.

Li X, Zhou J, Chen Z, Chen S, Zhu F, Zhou L (2008) Long-term expressional changes of Na+-K+-Cl- co-transporter 1 (NKCC1) and K+-Cl- co-transporter 2 (KCC2) in CA1 region of hippocampus following lithium-pilocarpine induced status epilepticus (PISE). Brain Res 1221:141–146.

Li Y, He Y, Chen M, Pu Z, Chen L, Li P, Li B, Li H, Huang Z-L, Li Z, Chen J-F (2015) Optogenetic Activation of Adenosine A2A Receptor Signaling in the Dorsomedial Striatopallidal Neurons Suppresses Goal-Directed Behavior. Neuropsychopharmacology

Libert F, Schiffmann SN, Lefort A, Parmentier M, Gérard C, Dumont JE, Vanderhaeghen JJ, Vassart G (1991) The orphan receptor cDNA RDC7 encodes an A1 adenosine receptor. EMBO J 10:1677–1682.

Lichtman JW, Colman H (2000) Synapse elimination and indelible memory. Neuron 25:269–278

Lin Y-C, Koleske AJ (2010) Mechanisms of Synapse and Dendrite Maintenance and Their Disruption in Psychiatric and Neurodegenerative Disorders. Annu Rev Neurosci 33:349–378

Lin Y, Bloodgood BL, Hauser JL, Lapan AD, Koon AC, Kim T-K, Hu LS, Malik AN, Greenberg ME (2008) Activity-dependent regulation of inhibitory synapse development by Npas4. Nature 455:1198–1204

Link E, Edelmann L, Chou JH, Binz T, Yamasaki S, Eisel U, Baumert M, Südhof TC, Niemann H, Jahn R (1992) Tetanus toxin action: inhibition of neurotransmitter release linked to synaptobrevin proteolysis. Biochem Biophys Res Commun 189:1017–1023

Lionel AC et al. (2013) Rare exonic deletions implicate the synaptic organizer Gephyrin (GPHN) in risk for autism, schizophrenia and seizures. Hum Mol Genet 22:2055–2066

Lipina T V, Prasad T, Yokomaku D, Luo L, Connor SA, Kawabe H, Wang YT, Brose N, Roder JC, Craig AM (2016) Cognitive Deficits in Calsyntenin-2-deficient Mice Associated with Reduced GABAergic Transmission. Neuropsychopharmacology 41:802–810

Liu X-B, Low LK, Jones EG, Cheng H-J (2005) Stereotyped axon pruning via plexin signaling is associated with synaptic complex elimination in the hippocampus. J Neurosci 25:9124–9134

Liu Y, Rutlin M, Huang S, Barrick CA, Wang F, Jones KR, Tessarollo L, Ginty DD (2012) Sexually Dimorphic BDNF

Signaling Directs Sensory Innervation of the Mammary Gland. Science 338:1357–1360

Loebrich S, Bohring R, Katsuno T, Tsukita S, Kneussel M (2006) Activated radixin is essential for GABAA receptor alpha5 subunit anchoring at the actin cytoskeleton. EMBO J 25:987–999

Loh KH, Stawski PS, Draycott AS, Udeshi ND, Lehrman EK, Wilton DK, Svinkina T, Deerinck TJ, Ellisman MH, Stevens B, Carr SA, Ting AY (2016) Proteomic Analysis of Unbounded Cellular Compartments: Synaptic Clefts. Cell 166:1295–1307.e21

Lopes JP, Morato X, Souza C, Pinhal C, Machado NJ, Canas PM, Silva HB, Stagljar I, Gandia J, Fernandez-Dueñas V, Lujan R, Cunha RA, Ciruela F (2015) The role of parkinson's disease-associated receptor GPR37 in the hippocampus: functional interplay with the adenosinergic system. J Neurochem 134:135–146

Lovatt D, Xu Q, Liu W, Takano T, Smith NA, Schnermann J, Tieu K, Nedergaard M (2012) Neuronal adenosine release, and not astrocytic ATP release, mediates feedback inhibition of excitatory activity. Proc Natl Acad Sci U S A 109:6265–6270

Low LK, Cheng H-J (2006) Axon pruning: an essential step underlying the developmental plasticity of neuronal connections. Philos Trans R Soc Lond B Biol Sci 361:1531–1544

Low LK, Liu X-B, Faulkner RL, Coble J, Cheng H-J (2008) Plexin signaling selectively regulates the stereotyped pruning of corticospinal axons from visual cortex. Proc Natl Acad Sci U S A 105:8136–8141

Lu W, Bromley-Coolidge S, Li J (2017) Regulation of GABAergic synapse development by postsynaptic membrane proteins. Brain Res Bull 129:30–42

Maenhaut C, Van Sande J, Libert F, Abramowicz M, Parmentier M, Vanderhaegen JJ, Dumont JE, Vassart G, Schiffmann S (1990) RDC8 codes for an adenosine A2 receptor with physiological constitutive activity. Biochem Biophys Res Commun 173:1169–1178.

Mahadevan V, Pressey JC, Acton BA, Uvarov P, Huang MY, Chevrier J, Puchalski A, Li CM, Ivakine EA, Airaksinen MS, Delpire E, McInnes RR, Woodin MA (2014) Kainate Receptors Coexist in a Functional Complex with KCC2 and Regulate Chloride Homeostasis in Hippocampal Neurons. Cell Rep 7:1762–1770.

Manzoni OJ, Manabe T, Nicoll RA (1994) Release of Adenosine By Activation of Nmda Receptors in the Hippocampus. Science 265:2098–2101.

Maric D, Liu QY, Maric I, Chaudry S, Chang YH, Smith S V, Sieghart W, Fritschy JM, Barker JL (2001) GABA expression dominates neuronal lineage progression in the embryonic rat neocortex and facilitates neurite outgrowth via GABA(A) autoreceptor/Cl- channels. J Neurosci 21:2343–2360

Markram H, Toledo-Rodriguez M, Wang Y, Gupta A, Silberberg G, Wu C (2004) Interneurons of the neocortical inhibitory system. Nat Rev Neurosci 5:793–807

Martinez-Mir MI, Probst A, Palacios JM (1991) Adenosine A2 receptors: selective localization in the human basal ganglia and alterations with disease. Neuroscience 42:697–706

Martinez-Pena y Valenzuela I, Pires-Oliveira M, Akaaboune M (2013) PKC and PKA regulate AChR dynamics at the neuromuscular junction of living mice. PLoS One 8:e81311

Martire A, Tebano MT, Chiodi V, Ferreira SG, Cunha R a, Köfalvi A, Popoli P (2011) Pre-synaptic adenosine A2A receptors control cannabinoid CB1 receptor-mediated inhibition of striatal glutamatergic neurotransmission. J Neurochem 116:273–280

Marty S, Wehrlé R, Alvarez-Leefmans FJ, Gasnier B, Sotelo C (2002) Postnatal maturation of Na+, K+, 2Cl- cotransporter expression and inhibitory synaptogenesis in the rat hippocampus: an immunocytochemical analysis. Eur J Neurosci 15:233–245

Marty S, Wehrlé R, Fritschy J-M, Sotelo C (2004) Quantitative effects produced by modifications of neuronal activity on the size of GABAA receptor clusters in hippocampal slice cultures. Eur J Neurosci 20:427–440

Marty S, Wehrlé R, Sotelo C (2000) Neuronal activity and brain-derived neurotrophic factor regulate the density of inhibitory synapses in organotypic slice cultures of postnatal hippocampus. J Neurosci 20:8087–8095

Matos M, Augusto E, Santos-Rodrigues A Dos, Schwarzschild M a, Chen J-F, Cunha R a, Agostinho P (2012) Adenosine A2A receptors modulate glutamate uptake in cultured astrocytes and gliosomes. Glia 60:702–716

Matsuda K (2017) Synapse organization and modulation via C1q family proteins and their receptors in the central nervous system. Neurosci Res 116:46–53

Matsuda K, Miura E, Miyazaki T, Kakegawa W, Emi K, Narumi S, Fukazawa Y, Ito-Ishida A, Kondo T, Shigemoto R, Watanabe M, Yuzaki M (2010) Cbln1 Is a Ligand for an Orphan Glutamate Receptor 2, a Bidirectional Synapse Organizer. Science 328:363–368

Matsumoto JPP, Almeida MG, Castilho-Martins EA, Costa MA, Fior-Chadi DR (2014) Protein kinase A mediates adenosine A2a receptor modulation of neurotransmitter release via synapsin I phosphorylation in cultured cells from medulla oblongata. Neurosci Res 85:1–11

Matz J, Gilyan A, Kolar A, McCarvill T, Krueger SR (2010) Rapid structural alterations of the active zone lead to sustained changes in neurotransmitter release. Proc Natl Acad Sci U S A 107:8836–8841

Mauch DH, Nägler K, Schumacher S, Göritz C, Müller EC, Otto A, Pfrieger FW (2001) CNS Synaptogenesis Promoted by Glia-Derived Cholesterol. Science 294:1354–1357

McCormick J a, Ellison DH (2011) The WNKs: atypical protein kinases with pleiotropic actions. Physiol Rev 91:177–219.

Mcdonald BJ, Amato A, Connolly CN, Benke D, Moss SJ, Smart TG (1998) Adjacent phosphorylation sites on GABA A receptor β subunits determine regulation by cAMP-dependent protein kinase. Nature :23–28.

McNaughton N, Morris RG (1987) Chlordiazepoxide, an anxiolytic benzodiazepine, impairs place navigation in rats. Behav Brain Res 24:39–46

Megías M, Emri Z, Freund TF, Gulyás AI (2001) Total number and distribution of inhibitory and excitatory synapses on hippocampal CA1 pyramidal cells. Neuroscience 102:527–540

Meier J, Akyeli J, Kirischuk S, Grantyn R (2003) GABA(A) receptor activity and PKC control inhibitory synaptogenesis in CNS tissue slices. Mol Cell Neurosci 23:600–613

Meier J, Vannier C, Sergé A, Triller A, Choquet D (2001) Fast and reversible trapping of surface glycine receptors by gephyrin. Nat Neurosci 4:253–260.

Micheva KD, Beaulieu C (1995) Neonatal sensory deprivation induces selective changes in the quantitative distribution of GABA-immunoreactive neurons in the rat barrel field cortex. J Comp Neurol 361:574–584

Mievis S, Blum D, Ledent C (2011) A2A receptor knockout worsens survival and motor behaviour in a transgenic mouse model of Huntington's disease. Neurobiol Dis 41:570–576

Miles R, Tóth K, Gulyás AI, Hájos N, Freund TF (1996) Differences between somatic and dendritic inhibition in the hippocampus. Neuron 16:815–823

Miles R, Wong RK (1999) Single neurones can initiate synchronized population discharge in the hippocampus. Nature 306:371–373

Millán JL (2006) Alkaline phosphatases. Purinergic Signal 2:335–341.

Minelli A, Brecha NC, Karschin C, DeBiasi S, Conti F (1995) GAT-1, a high-affinity GABA plasma membrane transporter, is localized to neurons and astroglia in the cerebral cortex. J Neurosci 15:7734–7746

Mioranzza S, Nunes F, Marques DM, Fioreze GT, Rocha AS, Botton PHS, Costa MS, Porciúncula LO (2014) Prenatal caffeine intake differently affects synaptic proteins during fetal brain development. Int J Dev Neurosci 36:45–52

Mishra A, Traut MH, Becker L, Klopstock T, Stein V, Klein R (2014) Genetic Evidence for the Adhesion Protein IgSF9/Dasm1 to Regulate Inhibitory Synapse Development Independent of its Intracellular Domain. J Neurosci 34:4187–4199

Missler M, Südhof TC (1998) Neurexins: Three genes and 1001 products. Trends Genet 14:20–26

Missler M, Südhof TC, Biederer T (2012) Synaptic cell adhesion. Cold Spring Harb Perspect Biol 4:a005694

Missler M, Zhang W, Rohlmann A, Kattenstroth G, Hammer RE, Gottmann K, Südhof TC (2003) Alpha-neurexins couple Ca2+ channels to synaptic vesicle exocytosis. Nature 423:939–948

Mizuno H, Luo W, Tarusawa E, Saito YM, Sato T, Yoshimura Y, Itohara S, Iwasato T (2014) NMDAR-regulated dynamics of layer 4 neuronal dendrites during thalamocortical reorganization in neonates. Neuron 82:365–379.

Mogha A, Guariglia SR, Debata PR, Wen GY, Banerjee P (2012) Serotonin 1A receptor-mediated signaling through ERK and PKCα is essential for normal synaptogenesis in neonatal mouse hippocampus. Transl Psychiatry 2:e66

Monopoli A, Lozza G, Forlani A, Mattavelli A, Ongini E (1998) Blockade of adenosine A2A receptors by SCH 58261

results in neuroprotective effects in cerebral ischaemia in rats. Neuroreport 9:3955–3959

Moriyama K, Sitkovsky M V. (2010) Adenosine A2A Receptor Is Involved in Cell Surface Expression of A2B Receptor. J Biol Chem 285:39271–39288

Moss SJ, Smart TG, Blackstone CD, Huganir RL (1992) Functional modulation of GABAA receptors by cAMP-dependent protein phosphorylation. Science 257:661–665.

Mullner F, Wierenga CJ, Bonhoeffer T (2015) Precision of Inhibition: Dendritic Inhibition by Individual GABAergic Synapses on Hippocampal Pyramidal Cells Is Confined in Space and Time. Neuron 87:576–589

Munno DW, Prince DJ, Syed NI (2003) Synapse number and synaptic efficacy are regulated by presynaptic cAMP and protein kinase A. J Neurosci 23:4146–4155

Murk K, Wittenmayer N, Michaelsen-Preusse K, Dresbach T, Schoenenberger C-A, Korte M, Jockusch BM, Rothkegel M (2012) Neuronal Profilin Isoforms Are Addressed by Different Signalling Pathways Gillingwater TH, ed. PLoS One 7:e34167

Murphy K, Gerzanich V, Zhou H, Ivanova S, Dong Y, Hoffman G, West GA, Winn HR, Simard JM (2003) Adenosine-A2a Receptor Down-Regulates Cerebral Smooth Muscle L-Type Ca2+ Channel Activity via Protein Tyrosine Phosphatase, Not cAMP-Dependent Protein Kinase. Mol Pharmacol 64:640–649

Nägerl UV, Köstinger G, Anderson JC, Martin KAC, Bonhoeffer T (2007) Protracted Synaptogenesis after Activity-Dependent Spinogenesis in Hippocampal Neurons. J Neurosci 27

Nakamura T, Hayashi T, Mimori-Kiyosue Y, Sakaue F, Matsuura K, Iemura S, Natsume T, Akiyama T (2010) The PX-RICS-14-3-3zeta/theta complex couples N-cadherin-beta-catenin with dynein-dynactin to mediate its export from the endoplasmic reticulum. J Biol Chem 285:16145–16154

Nakamura Y, Morrow DH, Modgil A, Huyghe D, Deeb TZ, Lumb MJ, Davies PA, Moss SJ (2016) Proteomic characterization of inhibitory synapses using a novel phluorin-tagged γ-aminobutyric acid receptor, type A alpha2 subunit knock-in mouse. J Biol Chem 291:12394–12407.

Nayeem MA, Pradhan I, Mustafa SJ, Morisseau C, Falck JR, Zeldin DC (2013) Adenosine A2A receptor modulates vascular response in soluble epoxide hydrolase-null mice through CYP-epoxygenases and PPARγ. Am J Physiol Regul Integr Comp Physiol 304:R23-32

Nehlig A, Daval JL, Debry G (1992) Caffeine and the central nervous system: mechanisms of action, biochemical, metabolic and psychostimulant effects. Brain Res Brain Res Rev 17:139–170

Neves G, Chess A (2004) Dscam-mediated self- versus non-self-recognition by individual neurons. Cold Spring Harb Symp Quant Biol 69:485–488

Nicol X, Gaspar P (2014) Routes to cAMP: shaping neuronal connectivity with distinct adenylate cyclases. Eur J Neurosci 39:1742–1751

Nicol X, Hong KP, Spitzer NC (2011) Spatial and temporal second messenger codes for growth cone turning. Proc Natl Acad Sci 108:13776–13781

Nicol X, Muzerelle A, Bachy I, Ravary A, Gaspar P (2005) Spatiotemporal localization of the calcium-stimulated adenylate cyclases, AC1 and AC8, during mouse brain development. J Comp Neurol 486:281–294

Noakes PG, Gautam M, Mudd J, Sanes JR, Merlie JP (1995) Aberrant differentiation of neuromuscular junctions in mice lacking s-laminin/laminin β2. Nature 374:258–262

Nofech-Mozes Y, Blaser SI, Kobayashi J, Grunebaum E, Roifman CM (2007) Neurologic abnormalities in patients with adenosine deaminase deficiency. Pediatr Neurol 37:218–221

Normile HJ, Barraco RA (1991) N6-cyclopentyladenosine impairs passive avoidance retention by selective action at A1 receptors. Brain Res Bull 27:101–104.

North RA (2002) Molecular physiology of P2X receptors. Physiol Rev 82:1013–1067 A

Notter T, Panzanelli P, Pfister S, Mircsof D, Fritschy J-M (2014) A protocol for concurrent high-quality immunohistochemical and biochemical analyses in adult mouse central nervous system. Eur J Neurosci 39:165–175

Novarino G et al. (2012) Mutations in BCKD-kinase lead to a potentially treatable form of autism with epilepsy. Science 338:394–397

O'Connor TP, Cockburn K, Wang W, Tapia L, Currie E, Bamji SX (2009) Semaphorin 5B mediates synapse elimination in hippocampal neurons. Neural Dev 4:18

Oh P, Horner T, Witkiewicz H, Schnitzer JE (2012) Endothelin induces rapid, dynamin-mediated budding of endothelial caveolae rich in ET-B. J Biol Chem 287:17353–17362

Oh WC, Lutzu S, Castillo PE, Kwon H-B (2016) De novo synaptogenesis induced by GABA in the developing mouse cortex. Science 353:1037–1040

Okabe S, Kim H-D, Miwa A, Kuriu T, Okado H (1999) Continual remodeling of postsynaptic density and its regulation by synaptic activity. Nat Neurosci 2:804–811

Okada H, Uezu A, Mason FM, Soderblom EJ, Moseley MA, Soderling SH, Soderling SH (2011) SH3 domain-based phototrapping in living cells reveals Rho family GAP signaling complexes. Sci Signal 4:rs13

Okada M, Kawata Y, Murakami T, Wada K, Mizuno K, Kondo T, Kaneko S (1999) Differential effects of adenosine receptor subtypes on release and reuptake of hippocampal serotonin. Eur J Neurosci 11:1–9

Olsen RW, Sieghart W (2009) GABAA receptors: Subtypes provide diversity of function and pharmacology. Neuropharmacology 56:141–148

Omori K, Kotera J (2007) Overview of PDEs and their regulation. Circ Res 100:309–327

Orr AG, Hsiao EC, Wang MM, Ho K, Kim DH, Wang X, Guo W, Kang J, Yu G-Q, Adame A, Devidze N, Dubal DB, Masliah E, Conklin BR, Mucke L (2015) Astrocytic adenosine receptor A2A and Gs-coupled signaling regulate memory. Nat Neurosci:1–17

Orr AG, Orr AL, Li X-J, Gross RE, Traynelis SF (2009) Adenosine A(2A) receptor mediates microglial process retraction. Nat Neurosci 12:872–878

Oya M, Kitaguchi T, Yanagihara Y, Numano R, Kakeyama M, Ikematsu K, Tsuboi T (2013) Vesicular nucleotide transporter is involved in ATP storage of secretory lysosomes in astrocytes. Biochem Biophys Res Commun 438:145–151

Pak MA, Haas HL, Decking UK, Schrader J (1994) Inhibition of adenosine kinase increases endogenous adenosine and depresses neuronal activity in hippocampal slices. Neuropharmacology 33:1049–1053

Pankratov Y, Lalo U, Krishtal O, Verkhratsky A (2003) P2X receptor-mediated excitatory synaptic currents in somatosensory cortex. Mol Cell Neurosci 24:842–849.

Pankratov Y, Lalo U, Verkhratsky A, North RA (2006) Vesicular release of ATP at central synapses. Pflugers Arch Eur J Physiol 452:589–597.

Paolicelli RC, Bolasco G, Pagani F, Maggi L, Scianni M, Panzanelli P, Giustetto M, Ferreira TA, Guiducci E, Dumas L, Ragozzino D, Gross CT (2011) Synaptic Pruning by Microglia Is Necessary for Normal Brain Development. Science 333:1456–1458

Papadopoulos T, Korte M, Eulenburg V, Kubota H, Retiounskaia M, Harvey RJ, Harvey K, O'Sullivan GA, Laube B, Hülsmann S, Geiger JRP, Betz H (2007) Impaired GABAergic transmission and altered hippocampal synaptic plasticity in collybistin-deficient mice. EMBO J 26:3888–3899

Papadopoulos T, Schemm R, Grubmüller H, Brose N (2015) Lipid binding defects and perturbed synaptogenic activity of a Collybistin R290H mutant that causes epilepsy and intellectual disability. J Biol Chem 290:8256–8270

Parente D, Garriga C, Baskin B (2017) Neuroligin 2 nonsense variant associated with anxiety, autism, intellectual disability, hyperphagia, and obesity. Am J Med Gen

Park H, Poo M (2013) Neurotrophin regulation of neural circuit development and function. Nat Rev Neurosci 14:7–23

Parkinson FE, Damaraju VL, Graham K, Yao SYM, Baldwin SA, Cass CE, Young JD (2011) Molecular biology of nucleoside transporters and their distributions and functions in the brain. Curr Top Med Chem 11:948–972

Parpura V, Zorec R (2010) Gliotransmission: Exocytotic release from astrocytes. Brain Res Rev 63:83–92

Pascual O, Casper KB, Kubera C, Zhang J, Revilla-Sanchez R, Sul J-Y, Takano H, Moss SJ, McCarthy K, Haydon PG (2005) Astrocytic purinergic signaling coordinates synaptic networks. Science 310:113–116

Penn AA, Riquelme PA, Feller MB, Shatz CJ (1998) Competition in Retinogeniculate Patterning Driven by Spontaneous Activity. 316:4–9.

Pereda AE, Bell TD, Chang BH, Czernik AJ, Nairn AC, Soderling TR, Faber DS (1998) Ca2+/calmodulin-dependent kinase II mediates simultaneous enhancement of gap-junctional conductance and glutamatergic transmission. Proc Natl Acad Sci U S A 95:13272–13277

Pereira GS, Mello e Souza T, Vinadé ERC, Choi H, Rodrigues C, Battastini AMO, Izquierdo I, Sarkis JJF, Bonan CD (2002) Blockade of adenosine A1 receptors in the posterior cingulate cortex facilitates memory in rats. Eur J Pharmacol 437:151–154.

Pereira Diniz L, Carvalho Almeida J, Tortelli V, Vargas Lopes C, Setti-Perdigão P, Stipursky J, Assad Kahn S, Ferreira Romão L, de Miranda J, Vieira Alves-Leon S, Marcondes de Souza J, Castro NG, Panizzutti R, Carvalho Alcantara Gomes F (2012) Astrocyte-induced Synaptogenesis Is Mediated by Transforming Growth Factor alpha Signaling through Modulation of D-Serine Levels in Cerebral Cortex Neurons. J Biol Chem.

Perrot-Sinal T., Auger A., McCarthy M. (2003) Excitatory actions of GABA in developing brain are mediated by l-type Ca2+ channels and dependent on age, sex, and brain region. Neuroscience 116:995–1003

Pettem KL, Yokomaku D, Luo L, Linhoff MW, Prasad T, Connor S a, Siddiqui TJ, Kawabe H, Chen F, Zhang L, Rudenko G, Wang YT, Brose N, Craig AM (2013a) The specific α-neurexin interactor calsyntenin-3 promotes excitatory and inhibitory synapse development. Neuron 80:113–128

Pettem KL, Yokomaku D, Takahashi H, Ge Y, Craig AM (2013b) Interaction between autism-linked MDGAs and neuroligins suppresses inhibitory synapse development. J Cell Biol 200:321–336

Piala AT, Moon TM, Akella R, He H, Cobb MH, Goldsmith EJ (2014) Chloride sensing by WNK1 involves inhibition of autophosphorylation. Sci Signal 7:ra41.

Polito M, Guiot E, Gangarossa G, Longueville S, Doulazmi M, Valjent E, Hervé D, Girault J-A, Paupardin-Tritsch D, Castro LR V, Vincent P (2015) Selective Effects of PDE10A Inhibitors on Striatopallidal Neurons Require Phosphatase Inhibition by DARPP-32(1,2,3). eNeuro 2.

Polito M, Klarenbeek J, Jalink K, Paupardin-Tritsch D, Vincent P, Castro LRV (2013) The NO/cGMP pathway inhibits transient cAMP signals through the activation of PDE2 in striatal neurons. Front Cell Neurosci 7:211

Polleux F, Ince-Dunn G, Ghosh A (2007) Transcriptional regulation of vertebrate axon guidance and synapse formation. Nat Rev Neurosci 8:331–340

Pougnet J-T, Toulme E, Martinez A, Choquet D, Hosy E, Boué-Grabot E (2014) ATP P2X receptors downregulate AMPA receptor trafficking and postsynaptic efficacy in hippocampal neurons. Neuron 83:417–430

Poulopoulos A, Aramuni G, Meyer G, Soykan T, Hoon M, Papadopoulos T, Zhang M, Paarmann I, Fuchs C, Harvey K, Jedlicka P, Schwarzacher SW, Betz H, Harvey RJ, Brose N, Zhang W, Varoqueaux F (2009) Neuroligin 2 drives postsynaptic assembly at perisomatic inhibitory synapses through gephyrin and collybistin. Neuron 63:628–642

Prange O, Murphy TH (2001) Modular transport of postsynaptic density-95 clusters and association with stable spine precursors during early development of cortical neurons. J Neurosci 21:9325–9333

Prediger RDS, Batista LC, Takahashi RN (2004) Adenosine A1 receptors modulate the anxiolytic-like effect of ethanol in the elevated plus-maze in mice. Eur J Pharmacol 499:147–154

Prediger RDS, da Silva GE, Batista LC, Bittencourt AL, Takahashi RN (2006) Activation of adenosine A1 receptors reduces anxiety-like behavior during acute ethanol withdrawal (hangover) in mice. Neuropsychopharmacology 31:2210–2220.

Prediger RDS, Takahashi RN (2005) Modulation of short-term social memory in rats by adenosine A1 and A2A receptors. Neurosci Lett 376:160–165.

Pulipparacharuvil S, Renthal W, Hale CF, Taniguchi M, Xiao G, Kumar A, Russo SJ, Sikder D, Dewey CM, Davis MM, Greengard P, Nairn AC, Nestler EJ, Cowan CW (2008) Cocaine Regulates MEF2 to Control Synaptic and Behavioral Plasticity. Neuron 59:621–633

Puskarjov M, Ahmad F, Kaila K, Blaesse P (2012) Activity-Dependent Cleavage of the K-Cl Cotransporter KCC2 Mediated by Calcium-Activated Protease Calpain. J Neurosci 32:11356–11364.

Raissi AJ, Staudenmaier EK, David S, Hu L, Paradis S (2013) Sema4D localizes to synapses and regulates GABAergic synapse development as a membrane-bound molecule in the mammalian hippocampus. Mol Cell Neurosci 57:23–32

Ramoz N, Cai G, Reichert JG, Silverman JM, Buxbaum JD (2008) An analysis of candidate autism loci on chromosome 2q24-q33: Evidence for association to the *STK39* gene. Am J Med Genet Part B Neuropsychiatr Genet 147B:1152–1158.

Rebola N, Canas PM, Oliveira CR, Cunha RA (2005a) Different synaptic and subsynaptic localization of adenosine

A2A receptors in the hippocampus and striatum of the rat. Neuroscience 132:893–903.
Rebola N, Lujan R, Cunha RA, Mulle C (2008) Adenosine A2A Receptors Are Essential for Long-Term Potentiation of NMDA-EPSCs at Hippocampal Mossy Fiber Synapses. Neuron 57:121–134
Rebola N, Rodrigues RJ, Lopes L V., Richardson PJ, Oliveira CR, Cunha RA (2005b) Adenosine A1 and A2A receptors are co-expressed in pyramidal neurons and co-localized in glutamatergic nerve terminals of the rat hippocampus. Neuroscience 133:79–83.
Reid CA, Berkovic SF, Petrou S (2009) Mechanisms of human inherited epilepsies. Prog Neurobiol 87:41–57
Reissner C, Stahn J, Breuer D, Klose M, Pohlentz G, Mormann M, Missler M (2014) Dystroglycan binding to α-neurexin competes with neurexophilin-1 and neuroligin in the brain. J Biol Chem 289:27585–27603
Renner M, Schweizer C, Bannai H, Triller A, Lévi S (2012) Diffusion barriers constrain receptors at synapses. PLoS One 7.
Represa A, Ben-Ari Y (2005) Trophic actions of GABA on neuronal development. Trends Neurosci 28:278–283
Rétey J V, Adam M, Honegger E, Khatami R, Luhmann UFO, Jung HH, Berger W, Landolt H-P (2005) A functional genetic variation of adenosine deaminase affects the duration and intensity of deep sleep in humans. PNAS.
Ribeiro FF, Neves-Tomé R, Assaife-Lopes N, Santos TE, Silva RFM, Brites D, Ribeiro J a, Sousa MM, Sebastião AM (2015) Axonal elongation and dendritic branching is enhanced by adenosine A2A receptors activation in cerebral cortical neurons. Brain Struct Funct
Riccomagno MM, Kolodkin AL (2015) Sculpting Neural Circuits by Axon and Dendrite Pruning. Annu Rev Cell Dev Biol 31:779–805
Rico B, Xu B, Reichardt LF (2002) TrkB receptor signaling is required for establishment of GABAergic synapses in the cerebellum. Nat Neurosci 5:225–233
Rinehart J, Maksimova YD, Tanis JE, Stone KL, Hodson C a., Zhang J, Risinger M, Pan W, Wu D, Colangelo CM, Forbush B, Joiner CH, Gulcicek EE, Gallagher PG, Lifton RP (2009) Sites of Regulated Phosphorylation that Control K-Cl Cotransporter Activity. Cell 138:525–536.
Rivera C, Voipio J, Payne JA, Ruusuvuori E, Lahtinen H, Lamsa K, Pirvola U, Saarma M, Kaila K (1999) The K+/Cl- co-transporter KCC2 renders GABA hyperpolarizing during neuronal maturation. Nature 397:251–255
Robson SC, Sévigny J, Zimmermann H (2006) The E-NTPDase family of ectonucleotidases: Structure function relationships and pathophysiological significance. Purinergic Signal 2:409–430.
Rodrigues RJ, Tomé AR, Cunha RA (2015) ATP as a multi-target danger signal in the brain. Front Neurosci 9:1–11.
Rogel A, Bromberg Y, Sperling O, Zoref-Shani E (2005) Phospholipase C is involved in the adenosine-activated signal transduction pathway conferring protection against iodoacetic acid-induced injury in primary rat neuronal cultures. Neurosci Lett 373:218–221.
Rombo DM, Newton K, Nissen W, Badurek S, Horn JM, Minichiello L, Jefferys JGR, Sebastiao AM, Lamsa KP (2015) Synaptic mechanisms of adenosine A2A> receptor-mediated hyperexcitability in the hippocampus. Hippocampus 25:566–580.
Rosin DL, Robeva A, Woodard RL, Guyenet PG, Linden J (1998) Immunohistochemical localization of adenosine A2A receptors in the rat central nervous system. J Comp Neurol 401:163–186
Saha R, Knapp S, Chakraborty D, Horovitz O, Albrecht A, Kriebel M, Kaphzan H, Ehrlich I, Volkmer H, Richter-Levin G (2017) GABAergic Synapses at the Axon Initial Segment of Basolateral Amygdala Projection Neurons Modulate Fear Extinction. Neuropsychopharmacology 42:473–484
Sarto-Jackson I, Milenkovic I, Smalla K-H, Gundelfinger ED, Kaehne T, Herrera-Molina R, Thomas S, Kiebler MA, Sieghart W (2012) The cell adhesion molecule neuroplastin-65 is a novel interaction partner of γ-aminobutyric acid type A receptors. J Biol Chem 287:14201–14214
Sawada K, Echigo N, Juge N, Miyaji T, Otsuka M, Omote H, Yamamoto A, Moriyama Y (2008) Identification of a vesicular nucleotide transporter. Proc Natl Acad Sci U S A 105:5683–5686
Schafer DP, Lehrman EK, Kautzman AG, Koyama R, Mardinly AR, Yamasaki R, Ransohoff RM, Greenberg ME, Barres BA, Stevens B (2012) Microglia sculpt postnatal neural circuits in an activity and complement-dependent manner. Neuron 74:691–705
Scheiffele P, Fan J, Choih J, Fetter R, Serafini T (2000) Neuroligin Expressed in Nonneuronal Cells Triggers Presynaptic Development in Contacting Axons. Cell 101:657–669

Schmidt D, Schachter SC (2014) Drug treatment of epilepsy in adults. BMJ 348:g254–g254

Schuemann A, Klawiter A, Bonhoeffer T, Wierenga CJ (2013) Structural plasticity of GABAergic axons is regulated by network activity and GABAA receptor activation. Front Neural Circuits 7:1–16

Seil FJ (1999) BDNF and NT-4, but not NT-3, promote development of inhibitory synapses in the absence of neuronal activity. Brain Res 818:561–564

Seil FJ (2003) TrkB receptor signaling and activity-dependent inhibitory synaptogenesis. Histol Histopathol 18:635–646

Seil FJ, Drake-Baumann R (1994) Reduced cortical inhibitory synaptogenesis in organotypic cerebellar cultures developing in the absence of neuronal activity. J Comp Neurol 342:366–377

Sen A, Hongpaisan J, Wang D, Nelson TJ, Alkon DL (2016) Protein Kinase Cϵ (PKCϵ) Promotes Synaptogenesis through Membrane Accumulation of the Postsynaptic Density Protein PSD-95. J Biol Chem 291:16462–16476

Sengpiel V, Elind E, Bacelis J, Nilsson S, Grove J, Myhre R, Haugen M, Meltzer HM, Alexander J, Jacobsson B, Brantsaeter A-L (2013) Maternal caffeine intake during pregnancy is associated with birth weight but not with gestational length: results from a large prospective observational cohort study. BMC Med 11:42

Seress L, Ribak CE (1988) The development of GABAergic neurons in the rat hippocampal formation. An immunocytochemical study. Brain Res Dev Brain Res 44:197–209

Seto-Ohshima A, Aoki E, Semba R, Emson PC, Heizmann CW (1990) Appearance of parvalbumin-specific immunoreactivity in the cerebral cortex and hippocampus of the developing rat and gerbil brain. Histochemistry 94:579–589

Shapiro L, Love J, Colman DR (2007) Adhesion Molecules in the Nervous System: Structural Insights into Function and Diversity. Annu Rev Neurosci 30:451–474

Shen H-Y, Coelho JE, Ohtsuka N, Canas PM, Day Y-J, Huang Q-Y, Rebola N, Yu L, Boison D, Cunha RA, Linden J, Tsien JZ, Chen J-F (2008) A Critical Role of the Adenosine A2A Receptor in Extrastriatal Neurons in Modulating Psychomotor Activity as Revealed by Opposite Phenotypes of Striatum and Forebrain A2A Receptor Knock-Outs. J Neurosci 28:2970–2975

Shen K, Bargmann CI (2003) The immunoglobulin superfamily protein SYG-1 determines the location of specific synapses in C. elegans. Cell 112:619–630

Shen K, Scheiffele P (2010) Genetics and cell biology of building specific synaptic connectivity. Annu Rev Neurosci 33:473–507

Shindou T, Nonaka H, Richardson PJ, Mori A, Kase H, Ichimura M (2002) Presynaptic adenosine A_{2A} receptors enhance GABAergic synaptic transmission *via* a cyclic AMP dependent mechanism in the rat globus pallidus. Br J Pharmacol 136:296–302

Shrivastava AN, Triller A, Sieghart W, Sarto-Jackson I (2011) Regulation of GABA(A) receptor dynamics by interaction with purinergic P2X(2) receptors. J Biol Chem 286:14455–14468

Shuvaev AN, Horiuchi H, Seki T, Goenawan H, Irie T, Iizuka A, Sakai N, Hirai H (2011) Mutant PKCγ in spinocerebellar ataxia type 14 disrupts synapse elimination and long-term depression in Purkinje cells in vivo. J Neurosci 31:14324–14334

Shyn SI et al. (2011) Novel loci for major depression identified by genome-wide association study of Sequenced Treatment Alternatives to Relieve Depression and meta-analysis of three studies. Mol Psychiatry 16:202–215

Sia G-M, Béïque J-C, Rumbaugh G, Cho R, Worley PF, Huganir RL (2007) Interaction of the N-Terminal Domain of the AMPA Receptor GluR4 Subunit with the Neuronal Pentraxin NP1 Mediates GluR4 Synaptic Recruitment. Neuron 55:87–102

Siddiqui TJ, Craig AM (2011) Synaptic organizing complexes. Curr Opin Neurobiol 21:132–143

Silva CG, Métin C, Fazeli W, Machado NJ, Darmopil S, Launay P-S, Ghestem A, Nesa M-P, Bassot E, Szabó E, Baqi Y, Müller CE, Tomé AR, Ivanov A, Isbrandt D, Zilberter Y, Cunha R a, Esclapez M, Bernard C (2013) Adenosine receptor antagonists including caffeine alter fetal brain development in mice. Sci Transl Med 5:197ra104

Simões AP, Machado NJ, Gonçalves N, Kaster MP, Simões AT, Nunes A, Pereira de Almeida L, Goosens KA, Rial D, Cunha RA (2016) Adenosine A2A Receptors in the Amygdala Control Synaptic Plasticity and Contextual Fear

Memory. Neuropsychopharmacology 41:2862–2871 A

Singh SKK, Stogsdill JAA, Pulimood NSS, Dingsdale H, Kim YHH, Pilaz L-JJ, Kim IHH, Manhaes ACC, Rodrigues WSS, Pamukcu A, Enustun E, Ertuz Z, Scheiffele P, Soderling SH, Silver DLL, Ji R-RR, Medina AEE, Eroglu C (2016) Astrocytes Assemble Thalamocortical Synapses by Bridging NRX1alpha and NL1 via Hevin. Cell 164:183–196

Song JY, Ichtchenko K, Südhof TC, Brose N (1999) Neuroligin 1 is a postsynaptic cell-adhesion molecule of excitatory synapses. Proc Natl Acad Sci U S A 96:1100–1105

Specht CG, Grünewald N, Pascual O, Rostgaard N, Schwarz G, Triller A (2011) Regulation of glycine receptor diffusion properties and gephyrin interactions by protein kinase C. EMBO J 30:3842–3853

Spoerri PE (1988) Neurotrophic effects of GABA in cultures of embryonic chick brain and retina. Synapse 2:11–22

Stagi M, Fogel AI, Biederer T (2010) SynCAM 1 participates in axo-dendritic contact assembly and shapes neuronal growth cones. Proc Natl Acad Sci 107:7568–7573

Stefan C, Jansen S, Bollen M (2006) Modulation of purinergic signaling by NPP-type ectophosphodiesterases. Purinergic Signal 2:361–370.

Stehle JH, Rivkees SA, Lee JJ, Weaver DR, Deeds JD, Reppert SM (1992) Molecular cloning and expression of the cDNA for a novel A2- adenosine receptor subtype. MolEndocrinol 6:384–393.

Steinberg SF (2008) Structural basis of protein kinase C isoform function. Physiol Rev 88:1341–1378

Stellwagen D, Shatz CJ (2002) An Instructive Role for Retinal Waves in the Development of Retinogeniculate Connectivity. Neuron 33:357–367

Stout CE, Costantin JL, Naus CCG, Charles AC (2002) Intercellular calcium signaling in astrocytes via ATP release through connexin hemichannels. J Biol Chem 277:10482–10488.

Strecker RE, Morairty S, Thakkar MM, Porkka-Heiskanen T, Basheer R, Dauphin LJ, Rainnie DG, Portas CM, Greene RW, McCarley RW (2000) Adenosinergic modulation of basal forebrain and preoptic/anterior hypothalamic neuronal activity in the control of behavioral state. Behav Brain Res 115:183–204.

Studer FE, Fedele DE, Marowsky A, Schwerdel C, Wernli K, Vogt K, Fritschy JM, Boison D (2006) Shift of adenosine kinase expression from neurons to astrocytes during postnatal development suggests dual functionality of the enzyme. Neuroscience 142:125–137

Suadicani SO, Brosnan CF, Scemes E (2006) P2X 7 Receptors Mediate ATP Release and Amplification of Astrocytic Intercellular Ca. Neuroscience 26:1378–1385.

Südhof TC (2008) Neuroligins and neurexins link synaptic function to cognitive disease. Nature 455:903–911

Suh HW, Song DK, Kim YH (1997) Differential effects of adenosine receptor antagonists injected intrathecally on antinociception induced by morphine and beta-endorphin administered intracerebroventricularly in the mouse. Neuropeptides 31:339–344

Sun C, Cheng M-C, Qin R, Liao D-L, Chen T-T, Koong F-J, Chen G, Chen C-H (2011) Identification and functional characterization of rare mutations of the neuroligin-2 gene (NLGN2) associated with schizophrenia. Hum Mol Genet 20:3042–3051

Sun Y, Vestergaard M, Pedersen CB, Christensen J, Basso O, Olsen J (2008) Gestational age, birth weight, intrauterine growth, and the risk of epilepsy. Am J Epidemiol 167:262–270.

Sytnyk V, Leshchyns'ka I, Nikonenko AG, Schachner M (2006) NCAM promotes assembly and activity-dependent remodeling of the postsynaptic signaling complex. J Cell Biol 174:1071–1085

Takahashi H, Craig AM (2013) Protein tyrosine phosphatases PTPδ, PTPσ, and LAR: presynaptic hubs for synapse organization. Trends Neurosci 36:522–534

Takahashi H, Katayama K-I, Sohya K, Miyamoto H, Prasad T, Matsumoto Y, Ota M, Yasuda H, Tsumoto T, Aruga J, Craig AM (2012) Selective control of inhibitory synapse development by Slitrk3-PTPδ trans-synaptic interaction. Nat Neurosci 15:389–398, S1-2

Tan HO, Reid CA, Single FN, Davies PJ, Chiu C, Murphy S, Clarke AL, Dibbens L, Krestel H, Mulley JC, Jones M V, Seeburg PH, Sakmann B, Berkovic SF, Sprengel R, Petrou S (2007) Reduced cortical inhibition in a mouse model of familial childhood absence epilepsy. PNAS 104:1–6.

Tapia JC, Mentis GZ, Navarrete R, Nualart F, Figueroa E, Sánchez A, Aguayo LG (2001) Early expression of glycine

and GABA(A) receptors in developing spinal cord neurons. Effects on neurite outgrowth. Neuroscience 108:493–506

Tebano MT, Martire A, Potenza RL, Grò C, Pepponi R, Armida M, Domenici MR, Schwarzschild MA, Chen JF, Popoli P (2008) Adenosine A2A receptors are required for normal BDNF levels and BDNF-induced potentiation of synaptic transmission in the mouse hippocampus. J Neurochem 104:279–286.

Terauchi A, Johnson-Venkatesh EM, Toth AB, Javed D, Sutton MA, Umemori H (2010) Distinct FGFs promote differentiation of excitatory and inhibitory synapses. Nature 465:783–787

Thompson BL, Levitt P, Stanwood GD (2009) Prenatal exposure to drugs: effects on brain development and implications for policy and education. Nat Rev Neurosci 10:303–312

Ticho SR, Radulovacki M (1991) Role of adenosine in sleep and temperature regulation in the preoptic area of rats. Pharmacol Biochem Behav 40:33–40.

Tojima T, Kobayashi S, Ito E (2003) Dual role of cyclic AMP-dependent protein kinase in neuritogenesis and synaptogenesis during neuronal differentiation. J Neurosci Res 74:829–837

Tominaga-Yoshino K, Kondo S, Tamotsu S, Ogura A (2002) Repetitive activation of protein kinase A induces slow and persistent potentiation associated with synaptogenesis in cultured hippocampus. Neuroscience Research 44:357–367.

Toni N, Buchs PA, Nikonenko I, Bron CR, Muller D (1999) LTP promotes formation of multiple spine synapses between a single axon terminal and a dendrite. Nature 402:421–425

Tran TS, Rubio ME, Clem RL, Johnson D, Case L, Tessier-Lavigne M, Huganir RL, Ginty DD, Kolodkin AL (2009) Secreted semaphorins control spine distribution and morphogenesis in the postnatal CNS. Nature 462:1065–1069

Trusel M, Cavaccini A, Gritti M, Greco B, Saintot P-P, Nazzaro C, Cerovic M, Morella I, Brambilla R, Tonini R (2015) Coordinated Regulation of Synaptic Plasticity at Striatopallidal and Striatonigral Neurons Orchestrates Motor Control. Cell Rep 13:1353–1365

Tsai S-J, Hong C-J, Hou S-J, Yen F-C (2006) Association study of adenosine A2a receptor (1976C>T) genetic polymorphism and mood disorders and age of onset. Psychiatr Genet 16:185

Tyagarajan SK, Fritschy J-M (2014) Gephyrin: a master regulator of neuronal function? Nat Rev Neurosci 15:141–156

Tyagarajan SK, Ghosh H, Yévenes GE, Imanishi SY, Zeilhofer HU, Gerrits B, Fritschy J-M (2013) Extracellular Signal-regulated Kinase and Glycogen Synthase Kinase 3β Regulate Gephyrin Postsynaptic Aggregation and GABAergic Synaptic Function in a Calpain-dependent Mechanism. J Biol Chem 288:9634–9647

Tyagarajan SK, Ghosh H, Yévenes GE, Nikonenko I, Ebeling C, Schwerdel C, Sidler C, Zeilhofer HU, Gerrits B, Muller D, Fritschy J-M (2011) Regulation of GABAergic synapse formation and plasticity by GSK3beta-dependent phosphorylation of gephyrin. Proc Natl Acad Sci U S A 108:379–384

Tyzio R, Ben-Ari Y (2014) Oxytocin-Mediated GABA inhibition During Delivery Attunates Autism Pathogenesis in Rodent Offspring. Science 343:675–680.

Tyzio R, Represa A, Jorquera I, Ben-Ari Y, Gozlan H, Aniksztejn L (1999) The establishment of GABAergic and glutamatergic synapses on CA1 pyramidal neurons is sequential and correlates with the development of the apical dendrite. J Neurosci 19:10372–10382

Uchida S, Kadowaki-Horita T, Kanda T (2014) Effects of the Adenosine A2A Receptor Antagonist on Cognitive Dysfunction in Parkinson's Disease. In: International review of neurobiology, pp 169–189

Uemura T, Lee S-J, Yasumura M, Takeuchi T, Yoshida T, Ra M, Taguchi R, Sakimura K, Mishina M (2010) Trans-Synaptic Interaction of GluRδ2 and Neurexin through Cbln1 Mediates Synapse Formation in the Cerebellum. Cell 141:1068–1079

Uesaka N, Hirai S, Maruyama T, Ruthazer ES, Yamamoto N (2005) Activity Dependence of Cortical Axon Branch Formation: A Morphological and Electrophysiological Study Using Organotypic Slice Cultures. J Neurosci 25.

Uezu A, Kanak DJ, Bradshaw TWA, Soderblom EJ, Catavero CM, Burette AC, Weinberg RJ, Soderling SH (2016) Identification of an elaborate complex mediating postsynaptic inhibition. Science 353:1123–1129

Ullrich B, Ushkaryov YA, Südhof TC (1995) Cartography of neurexins: more than 1000 isoforms generated by

alternative splicing and expressed in distinct subsets of neurons. Neuron 14:497–507

Um JW, Choii G, Park D, Kim D, Jeon S, Kang H, Mori T, Papadopoulos T, Yoo T, Lee Y, Kim E, Tabuchi K, Ko J (2016) IQ Motif and SEC7 Domain-containing Protein 3 (IQSEC3) Interacts with Gephyrin to Promote Inhibitory Synapse Formation. J Biol Chem 291:10119–10130

Um JW, Pramanik G, Ko JS, Song M-Y, Lee D, Kim H, Park K-S, Südhof TC, Tabuchi K, Ko J (2014) Calsyntenins Function as Synaptogenic Adhesion Molecules in Concert with Neurexins. Cell Rep 6:1096–1109.

Umemori H, Linhoff MW, Ornitz DM, Sanes JR (2004) FGF22 and Its Close Relatives Are Presynaptic Organizing Molecules in the Mammalian Brain. Cell 118:257–270

UniProt (2017) UniProt: the universal protein knowledgebase. Nucleic Acids Res 45:D158–D169

van Calker D, Müller M, Hamprecht B (1978) Adenosine inhibits the accumulation of cyclic AMP in cultured brain cells. Nature 276:839–841

van Calker D, Müller M, Hamprecht B (1979) Adenosine Regulates Via Two Different Types of Receptors, the Accumulation of Cyclic Amp in Cultured Brain Cells. J Neurochem 33:999–1005.

Varoqueaux F, Aramuni G, Rawson RL, Mohrmann R, Missler M, Gottmann K, Zhang W, S?dhof TC, Brose N (2006) Neuroligins Determine Synapse Maturation and Function. Neuron 51:741–754

Varoqueaux F, Jamain S, Brose N (2004) Neuroligin 2 is exclusively localized to inhibitory synapses. Eur J Cell Biol 83:449–456

Varoqueaux F, Sigler A, Rhee J-S, Brose N, Enk C, Reim K, Rosenmund C (2002) Total arrest of spontaneous and evoked synaptic transmission but normal synaptogenesis in the absence of Munc13-mediated vesicle priming. Proc Natl Acad Sci U S A 99:9037–9042

Verhage M, Maia AS, Plomp JJ, Brussaard AB, Heeroma JH, Vermeer H, Toonen RF, Hammer RE, van den Berg TK, Missler M, Geuze HJ, Südhof TC (2000) Synaptic assembly of the brain in the absence of neurotransmitter secretion. Science 287:864–869

Viana da Silva S, Haberl MG, Zhang P, Bethge P, Lemos C, Gonçalves N, Gorlewicz A, Malezieux M, Gonçalves FQ, Grosjean N, Blanchet C, Frick A, Nägerl UV, Cunha RA, Mulle C (2016) Early synaptic deficits in the APP/PS1 mouse model of Alzheimer/'s disease involve neuronal adenosine A2A receptors. Nat Commun 7:11915

Villa KL, Berry KP, Subramanian J, Villa KL, Berry KP, Subramanian J, Cha JW, Oh WC, Kwon H, E Nedivi (2016b) Inhibitory Synapses Are Repeatedly Assembled and Removed at Persistent Sites In Vivo Article Inhibitory Synapses Are Repeatedly Assembled and Removed at Persistent Sites In Vivo. Neuron 89:756–769

Vithlani M, Moss S (2009) The role of GABAAR phosphorylation in the construction of inhibitory synapses and the efficacy of neuronal inhibition. Biochem Soc Trans 37:1355–1358

Vithlani M, Terunuma M, Moss SJ (2011) The Dynamic Modulation of GABAA Receptor Trafficking and Its Role in Regulating the Plasticity of Inhibitory Synapses. Physiol Rev 91:1009–1022

Von Lubitz DK, Beenhakker M, Lin RC, Carter MF, Paul IA, Bischofberger N, Jacobson KA (1996) Reduction of postischemic brain damage and memory deficits following treatment with the selective adenosine A1 receptor agonist. Eur J Pharmacol 302:43–48

Von Lubitz DK, Lin RC, Melman N, Ji XD, Carter MF, Jacobson KA (1994) Chronic administration of selective adenosine A1 receptor agonist or antagonist in cerebral ischemia. Eur J Pharmacol 256:161–167

Waite A, Brown SC, Blake DJ (2012) The dystrophin–glycoprotein complex in brain development and disease. Trends Neurosci 35:487–496

Wall M, Dale N (2008) Activity-dependent release of adenosine: a critical re-evaluation of mechanism. Curr Neuropharmacol 6:329–337

Wall MJ, Dale N (2007) Auto-inhibition of rat parallel fibre-Purkinje cell synapses by activity-dependent adenosine release. J Physiol 581:553–565

Wall MJ, Dale N (2013) Neuronal transporter and astrocytic ATP exocytosis underlie activity-dependent adenosine release in the hippocampus. J Physiol 591:3853–3871

Walsh T et al. (2008) Rare Structural Variants Disrupt Multiple Genes in Neurodevelopmental Pathways in Schizophrenia. Science 320

Wang H, Pineda V V., Chan GCK, Wong ST, Muglia LJ, Storm DR (2003) Type 8 Adenylyl Cyclase Is Targeted to Excitatory Synapses and Required for Mossy Fiber Long-Term Potentiation. J Neurosci 23

Wang W, Gong N, Xu T Le (2006) Downregulation of KCC2 following LTP contributes to EPSP-spike potentiation in rat hippocampus. Biochem Biophys Res Commun 343:1209–1215.

Watanabe M, Wake H, Moorhouse AJ, Nabekura J (2009) Clustering of neuronal K+-Cl- cotransporters in lipid rafts by tyrosine phosphorylation. J Biol Chem.

Wei CJ, Li W, Chen J-FF (2011) Normal and abnormal functions of adenosine receptors in the central nervous system revealed by genetic knockout studies. Biochim Biophys Acta 1808:1358–1379

Weng X, Odouli R, Li DK (2008) Maternal caffeine consumption during pregnancy and the risk of miscarriage: a prospective cohort study. Am J Obstet Gynecol 198:1–8.

Wierenga CJ (2017) Live imaging of inhibitory axons: Synapse formation as a dynamic trial-and-error process. Brain Res Bull 129:43–49

Wierenga CJ, Becker N, Bonhoeffer T (2008) GABAergic synapses are formed without the involvement of dendritic protrusions. Nat Neurosci 11:1044–1052

Willoughby D, Cooper DMF (2007) Organization and Ca2+ Regulation of Adenylyl Cyclases in cAMP Microdomains. Physiol Rev 87:965–1010

Wills ZP, Mandel-Brehm C, Mardinly AR, McCord AE, Giger RJ, Greenberg ME (2012) The Nogo Receptor Family Restricts Synapse Number in the Developing Hippocampus. Neuron 73:466–481

Winberg ML, Mitchell KJ, Goodman CS (1998) Genetic analysis of the mechanisms controlling target selection: complementary and combinatorial functions of netrins, semaphorins, and IgCAMs. Cell 93:581–591

Wit J De, Ghosh A (2015) Specification of synaptic connectivity. Nat Rev Neuro

Woo J, Kwon S-K, Nam J, Choi S, Takahashi H, Krueger D, Park J, Lee Y, Bae JY, Lee D, Ko J, Kim H, Kim M-H, Bae YC, Chang S, Craig AM, Kim E (2013) The adhesion protein IgSF9b is coupled to neuroligin 2 via S-SCAM to promote inhibitory synapse development. J Cell Biol 201

Wu X, Fu Y, Knott G, Lu J, Di Cristo G, Huang ZJ (2012) GABA signaling promotes synapse elimination and axon pruning in developing cortical inhibitory interneurons. J Neurosci 32:331–343

Wuchter J, Beuter S, Treindl F, Herrmann T, Zeck G, Templin MF, Volkmer H (2012) A Comprehensive Small Interfering RNA Screen Identifies Signaling Pathways Required for Gephyrin Clustering. J Neurosci 32:14821–14834

Yamada K, Hattori E, Shimizu M, Sugaya A, Shibuya H, Yoshikawa T (2001) Association studies of the cholecystokinin B receptor and A2a adenosine receptor genes in panic disorder. J Neural Transm 108:837–848

Yamada K, Kobayashi M, Shiozaki S, Ohta T, Mori A, Jenner P, Kanda T (2014) Antidepressant activity of the adenosine A2A receptor antagonist, istradefylline (KW-6002) on learned helplessness in rats. Psychopharmacology (Berl) 231:2839–2849

Yamagata M, Sanes JR (2008) Dscam and Sidekick proteins direct lamina-specific synaptic connections in vertebrate retina. Nature 451:465–469

Yamamoto M, Urakubo T, Tominaga-Yoshino K, Ogura A (2005) Long-lasting synapse formation in cultured rat hippocampal neurons after repeated PKA activation. Brain Res 1042:6–16

Yamasaki T, Hoyos-ramirez E, Martenson JS, Morimoto-tomita M, Yamasaki T, Hoyos-ramirez E, Martenson JS, Morimoto-tomita M, Tomita S (2017) GARLH Family Proteins Stabilize GABA A Receptors Article GARLH Family Proteins Stabilize GABA A Receptors at Synapses. Neuron 93:1138–1152.e6

Yang CL, Zhu X, Ellison DH (2007) The thiazide-sensitive Na-Cl cotransporter is regulated by a WNK kinase signaling complex. J Clin Invest 117:3403–3411.

Yang J-N, Chen J-F, Fredholm BB (2009) Physiological roles of A1 and A2A adenosine receptors in regulating heart rate, body temperature, and locomotion as revealed using knockout mice and caffeine. AJP Hear Circ Physiol 296:H1141–H1149

Yang L, Cai X, Zhou J, Chen S, Chen Y, Chen Z, Wang Q, Fang Z, Zhou L (2013) STE20/SPS1-Related Proline/Alanine-Rich Kinase Is Involved in Plasticity of GABA Signaling Function in a Mouse Model of Acquired Epilepsy. PLoS One 8:1–13.

Yasumura M, Yoshida T, Lee S-J, Uemura T, Joo J-Y, Mishina M (2012) Glutamate receptor ?1 induces preferentially inhibitory presynaptic differentiation of cortical neurons by interacting with neurexins

through cerebellin precursor protein subtypes. J Neurochem 121:705–716

Yu W, Jiang M, Miralles CP, Li R wen, Chen G, de Blas AL (2007) Gephyrin clustering is required for the stability of GABAergic synapses. Mol Cell Neurosci 36:484–500.

Zacchi P, Antonelli R, Cherubini E (2014) Gephyrin phosphorylation in the functional organization and plasticity of GABAergic synapses. Front Cell Neurosci 8:103

Zangrossi H, Leite JR, Graeff FG (1992) Anxiolytic effect of carbamazepine in the elevated plus-maze: possible role of adenosine. Psychopharmacology (Berl) 106:85–89.

Zhang B, Chen LY, Liu X, Maxeiner S, Lee S-J, Gokce O, Südhof TC (2015) Neuroligins Sculpt Cerebellar Purkinje-Cell Circuits by Differential Control of Distinct Classes of Synapses. Neuron 87:781–796

Zhang W, Rajan I, Savelieva K V, Wang C-Y, Vogel P, Kelly M, Xu N, Hasson B, Jarman W, Lanthorn TH (2008) Netrin-G2 and netrin-G2 ligand are both required for normal auditory responsiveness. Genes Brain Behav 7:385–392

Zhou QY, Li C, Olah ME, Johnson RA, Stiles GL, Civelli O (1992) Molecular cloning and characterization of an adenosine receptor: the A3 adenosine receptor. Proc Natl Acad Sci U S A 89:7432–7436

Zhou S-J, Zhu M-E, Shu D, Du X-P, Song X-H, Wang X-T, Zheng R-Y, Cai X-H, Chen J-F, He J-C (2009) Preferential enhancement of working memory in mice lacking adenosine A(2A) receptors. Brain Res 1303:74–83

Ziv NE, Garner CC (2004) Cellular and molecular mechanisms of presynaptic assembly. Nat Rev Neurosci 5:385–399